CO_2 and Isotope Flux Measurements above a Spruce Forest

This dissertation is submitted to the

FACULTY OF BIOLOGY, CHEMISTRY AND GEOSCIENCES

OF THE UNIVERSITY OF BAYREUTH, GERMANY

to attain the academic degree of

DR. RER. NAT.

It is presented by

JOHANNES RUPPERT

Diplom Geoökologe

born July, 1975

in Stuttgart, Germany.

Düsseldorf, July 2008

CO_2 and Isotope Flux Measurements above a Spruce Forest

This doctoral thesis was prepared at the UNIVERSITY OF BAYREUTH at the CHAIR OF HYDROLOGY, DEPARTMENT OF MICROMETEOROLOGY under the supervision of

PROF. DR. THOMAS FOKEN

The research project was part of the framework of the Bayreuth Institute for Terrestrial Ecosystem Research (BITÖK) and funded by the Federal Ministry of Education and Research of Germany (BMBF) (PT BEO51-0339476 D). Important parts of the research were performed in collaboration with the Max-Planck Institute for Biogeochemistry (MPI BGC) in Jena, Germany, and under the supervision of Prof. Dr. Nina Buchmann. The experimental work was partly embedded in the LITFASS-2003 experiment at the Lindenberg Experiment site of the German Meteorological Service (DWD).

Table of Contents

Summary

The measurement of the turbulent carbon dioxide (CO_2) exchange by the eddy covariance (EC) method has become a fundamental tool for the quantitative determination of the atmospheric CO_2 net ecosystem exchange (NEE) and the investigation of the carbon mass balances of ecosystems. Such measurements require a high degree of quality control in order to prevent systematic errors. The determination of the annual sum of NEE and filling of data gaps is complicated by characteristic diurnal and seasonal variation in the governing gross flux components of assimilation, i.e. photosynthetic uptake of CO_2, and respiration.

In this dissertation, a set of criteria is suggested for the identification of high quality NEE data. They are applied to data obtained above a spruce forest in the Fichtelgebirge Mountains in Germany. The application of the quality criteria resulted in less systematic distribution of data gaps compared to a commonly applied criterion based on the friction velocity u_* measured above the canopy. The suggested method is therefore able to reduce the risk of double accounting of nighttime respiration fluxes and systematic error in the annual sum of NEE.

The isotopic flux partitioning method can be applied to quantify the assimilation and respiration flux components. Especially above forest ecosystems, it requires isotope flux measurements with high analytical precision in order to resolve small gradients in the isotopic signature of the turbulent exchange. A conditional sampling instrument was developed and tested in laboratory and field experiments. By combining the hyperbolic relaxed eddy accumulation method (HREA), whole-air sampling and high precision isotope ratio mass spectrometry (IRMS), $^{13}CO_2$ and $CO^{18}O$ isotopic flux densities (isofluxes) could be measured with an estimated uncertainty of 10-20% during a three day intensive measuring campaign of the field experiment WALDATEM-2003 (Wavelet Detection and Atmospheric Turbulent Exchange Measurements 2003).

Thorough quality control was applied at all stages of the experiment, including the data evaluation. The sampling process and the assumption of similarity in the turbulent exchange characteristics of different scalars (scalar similarity) were assessed by simulation of HREA sampling based on high temporal resolution data of the turbulent energy and gas exchange. Above three different vegetation types, distinct diurnal changes of scalar similarity were observed and attributed to events on time scales longer than 60 s, which most likely represent changes in the source/sink strength or convective or advective processes. Poor scalar-scalar correlations indicate the risk of systematic underestimation of fluxes measured by HREA. There is some evidence for good scalar similarity and a generally linear relation between bulk CO_2 mixing ratios and its isotopic signatures in the turbulent exchange. However, the slope of that relation was observed to change temporarily so that especially for the EC/flask method temporal and spatial scales represented in flask samples must carefully be considered. HREA isoflux measurements have a footprint similar to the footprint of EC measurements and are therefore able to integrate small-scale heterogeneity in ecosystems.

CO_2 mixing ratios and $\delta^{13}C$ and $\delta^{18}O$ isotopic signatures measured in updraft and downdraft whole-air samples allowed determining ecosystem integrated and truly flux weighted isotopic signatures of the atmospheric ecosystem gas exchange and ecosystem isotope discrimination Δ_e and Δ_E on half-hourly timescales. The observed diurnal variability demonstrates the need for their repeated high precision measurement at ecosystem scale for the evaluation of isotopic mass balances. For the isotopic flux partitioning method, additional data on the integrated canopy isotope discrimination Δ'_{canopy} from independent measurements or validated models is

indispensable. An observed fast equilibration of isotopic disequilibria $\Delta^{13}C$ and $\Delta^{18}O$ between the assimilation and respiration fluxes may indicate that the successful application of the isotopic flux partitioning method is limited to short periods after significant environmental changes on the scale of few days.

Zusammenfassung

Die Messung des turbulenten Kohlendioxidaustausches mit der Eddy Kovarianzmethode (eddy covariance, EC) ist eine wichtige Methode für die quantitative Bestimmung des CO_2 Netto-Ökosystem-Austausches (net ecosystem exchange, NEE) und die Untersuchung von Kohlenstoffbilanzen von Ökosystemen geworden. Derartige Messungen erfordern intensive Qualitätskontrollen, um systematische Fehler zu vermeiden. Erschwert wird die Bestimmung der Jahressumme des NEE und das Füllen von Datenlücken durch die charakteristischen täglichen und jahreszeitlichen Schwankungen in den ausschlaggebenden Brutto-Flusskomponenten der Assimilation, d.h. der Aufnahme von CO_2 durch die Photosynthese, und der Respiration.

In dieser Dissertation werden Kriterien vorgeschlagen nach denen NEE Daten mit hoher Qualität identifiziert werden können. Diese Kriterien werden auf NEE Daten angewendet, die über einem Fichtenwald im Fichtelgebirge in Deutschland gesammelt wurden. Die Anwendung der Qualitätskriterien ergab eine weniger systematische Verteilung der Datenlücken im Vergleich zur Anwendung eines häufig genutzten Kriteriums, das auf der Messung der Schubspannungsgeschwindikeit u_* über dem Bestand beruht. Die vorgeschlagene Methode ist deshalb in der Lage, das Risiko für eine doppelte Berücksichtigung nächtlicher Respirationsflüsse zu verringern und systematische Fehler in der Jahressumme des NEE zu vermeiden.

Durch die Anwendung der Methode der Isotopenflusstrennung (isotopic flux partitioning method) können die Flusskomponenten der Assimilation und Respiration quantifiziert werden. Sie bedarf insbesondere in Waldökosystemen einer hohen analytischen Genauigkeit, damit kleine Gradienten der Isotopensignaturen im turbulenten Luftaustausch aufgelöst werden können. Für die austauschspezifische Probenahme (conditional sampling) wurde ein Instrument entwickelt und im Labor- und Freilandexperiment getestet. Durch die Kombination der hyperbolischen vereinfachten Eddy-Akkumulationsmethode (hyperbolic relaxed eddy accumulation, HREA) mit konservativer Luftprobenahme (whole-air sampling) und hochgenauer Isotopenverhältnis-Massenspektrometrie (isotope ratio mass spectrometry, IRMS) konnten $^{13}CO_2$- und $CO^{18}O$-Isotopenflussdichten (isofluxes) gemessen werden. Die geschätzte Messunsicherheit während einer dreitägigen Intensivmesskampagne des Freilandexperimentes WALDATEM-2003 (Wavelet Detection and Atmospheric Turbulent Exchange Measurements 2003) betrug 10-20%.

Bei dem Experiment wurde auf allen Ebenen eine sorgfältige Qualitätskontrolle durchgeführt, die sich auch auf die Auswertung der Daten erstreckte. Durch Simulationen der HREA Probenahme auf der Grundlage zeitlich hochauflösender Daten des turbulenten Energie- und Gasaustausches wurde der Probenahmeprozess und die Annahme der Ähnlichkeit verschiedener Skalare bezüglich ihres turbulenten Austausches (scalar similarity) überprüft. Oberhalb von drei unterschiedlichen Vegetationstypen wurden ausgeprägte Änderungen der skalaren Ähnlichkeit beobachtet und mit Austauschprozessen in Verbindung gebracht, die länger als 60 s andauern und höchstwahrscheinlich auf Änderungen in der Quellen- und Senkenstärke oder auf konvektive oder advektive Prozesse zurückzuführen sind. Eine Geringe Korrelation zwischen den Skalaren (scalar-scalar correlation) deutet auf das Risiko einer systematischen Unterschätzung der Flüsse durch HREA Messungen hin. Es wurden Hinweise auf eine gute skalare Ähnlichkeit und eine grundsätzlich lineare Beziehung zwischen CO_2-Mischungsverhältnissen und -isotopensignaturen im turbulenten Austausch gefunden. Jedoch unterlag die Steigung dieser linearen Beziehung zeitlichen Veränderungen. Deshalb müssen

insbesondere für die EC/Flaschen-Methode (EC/flask method) die zeitlichen und räumlichen Skalen, die durch die Flaschenproben wiedergegeben werden, sorgfältig berücksichtigt werden. HREA Messungen der Isotopenflussdichte (isoflux) haben ein der EC Messung entsprechendes Quellgebiet (footprint) und sind deshalb geeignet, um kleinskalige Heterogenität in Ökosystemen zu integrieren.

Die Messung von CO_2-Mischungsverhältnissen und $\delta^{13}C$- und $\delta^{18}O$-Isotopensignaturen in konservativen Proben (whole-air samples) der aufwärtsbewegten und abwärtsbewegten Luft hat es ermöglicht, die Isotopensignaturen des Gasaustausches zwischen Ökosystem und Atmosphäre in richtiger Weise flussgewichtet und für das gesamte Ökosystem integrierend zu bestimmen. Dementsprechend konnte die Ökosystem-Isotopendiskriminierung Δ_e und Δ_E auf einer halbstündlichen Zeitskala bestimmt werden. Schwankungen der Werte im Tagesverlauf zeigen, dass es notwendig ist, diese wiederholt und mit hoher Messgenauigkeit auf Ökosystemebene zu bestimmen, um Isotopen-Massenbilanzen auswerten zu können. Für die Methode der Isotopenflusstrennung sind zusätzliche Daten der integralen Isotopendiskriminierung Δ'_{canopy} der Baumkrone erforderlich, die durch unabhängige Messungen oder validierte Modelle bestimmt werden müssen. Die Beobachtungen deuten auf eine schnelle Angleichung der Unterschiede der Isotopensignaturen (isotopic disequilibria) $\mathcal{D}^{13}C$ und $\mathcal{D}^{18}O$ des Assimilations- und Respirationsflusses hin. Die Anwendbarkeit der Methode der Isotopenflusstrennung scheint dadurch auf kurze Zeiträume von wenigen Tagen nach signifikanten Veränderungen in den Umweltbedingungen beschränkt zu sein.

Acknowledgments

Many people have contributed to this work and supported me during my PhD. I first want to thank my supervisors Thomas Foken and Nina Buchmann for the original concept, which provided the basis for the entire research project, for critical discussions on the experiment design and results and encouragement. I acknowledge and also want to thank all my coauthors and my colleagues at the Department of Micrometeorology at the University of Bayreuth. They contributed significantly to the achievement of the results presented in the research papers and improved the manuscripts with their critical review. The company of Christoph Thomas and our open exchange and collaboration on all aspects of our research and during the WALDATEM-2003 field experiment was essential. Matthias Mauder, Teresa Bertolini, Johannes Lüers, Johannes Olesch and the staff of the Bayreuth Institute for Terrestrial Ecosystem Research (BITÖK) of the University of Bayreuth provided important technical expertise and practical support during the GRASATEM-2003 and WALDATEM-2003 experiments. Anthony C. Delany, Dave R. Bowling and Willi A. Brand shared information on conditional sampling and isotope analysis, which was the basis for the successful instrument development and laboratory experiments. The final assembly of rugged sampling instruments for the field experiments relied on the technical support of Johannes Olesch. The effort of Michael Rothe and Armin Jordan allowed the high precision analysis of a large number of air samples in the gas- and isotope laboratories of the Max-Planck Institute for Biogeochemistry in Jena. This research project was supported by the German Federal Ministry of Education and Research (PT BEO51-0339476 D). I especially wish to thank my fiancée Christine Reißenweber and my parents for their continuous support and encouragement during the finalization of this dissertation.

List of publications and manuscripts

This dissertation in cumulative form consists of a synopsis and four individual publications or manuscripts, which are presented in Appendices 1 to 4. Two research papers are already published in international peer reviewed scientific journals. Two manuscripts are prepared for their subsequent submission.

Published[1] research papers

Ruppert, J., C. Thomas, and T. Foken (2006), Scalar similarity for relaxed eddy accumulation methods, *Boundary-Layer Meteorology, 120*, 39-63, doi:10.1007/s10546-005-9043-3.

Ruppert, J., M. Mauder, C. Thomas, and J. Lüers (2006), Innovative gap-filling strategy for annual sums of CO_2 net ecosystem exchange, *Agricultural and Forest Meteorology, 138*, 5-18, doi:10.1016/j.agrformet.2006.03.003.

Manuscripts prepared for submission

Ruppert, J., W. A. Brand, N. Buchmann, and T. Foken (2008), Whole-air relaxed eddy accumulation for the measurement of isotope and trace-gas fluxes, manuscript prepared for submission to *Journal of Geophysical Research, D: Atmospheres.*

Ruppert, J., C. Thomas, J. Lüers, T. Foken, and N. Buchmann (2008), Ecosystem $^{13}CO_2$ and $CO^{18}O$ isotope discrimination measured by hyperbolic relaxed eddy accumulation, manuscript prepared for submission to *Global Biogeochemical Cycles*.

[1] With respect to the copyright of the publisher, the format (layout and typesetting) of the already published research papers is according to the journals preprint format, i.e. the format of the authors submission of the finally reviewed and accepted manuscript. The preprint format is allowed for self publication by the corresponding publishers and identical in content to the finally published version. The copyright of the published print or online format remains with the publisher, as denoted in Appendix 1 and 2.

List of additional publications from the research project

References of additional publications are listed here as the outcome of the research project for completeness. They are no integral part of the dissertation, but where appropriate, references are made in Appendices 1 to 4.

Foken, T., C. Thomas, J. Ruppert, J. Lüers, and M. Göckede (2004), Turbulent exchange processes in and above tall vegetation, paper presented at 16th Symposium on Boundary Layers and Turbulence, American Meteorological Society, Portland, ME, USA, 8-13 August 2004.

Ruppert, J. (2004), Woher kommt das CO_2? ^{13}C und ^{18}O Isotopenflüsse über Ökosystemen in bisher unerreichter Präzision, in *Spektrum - Umweltforschung*, edited, pp. 34-35.

Ruppert, J., and T. Foken (2004), Messung turbulenter Flüsse von Kohlendioxid und stabilem Kohlenstoffisotop ^{13}C über Pflanzenbeständen mit Hilfe der Relaxed Eddy Accumulation Methode, in *BITÖK Forschungsbericht 2002*, edited, Bayreuther Institut für Terrestrische Ökosystemforschung (BITÖK), Bayreuth.

Ruppert, J., and T. Foken (2004), Messung turbulenter Flüsse von Kohlendioxid und stabilem Kohlenstoffisotop ^{13}C über Pflanzenbeständen mit Hilfe der Relaxed Eddy Accumulation Methode, in *BITÖK Forschungsbericht 2003*, edited, Bayreuther Institut für Terrestrische Ökosystemforschung (BITÖK), Bayreuth.

Ruppert, J., M. Rothe, A. Jordan, W. A. Brand, A. C. Delany, N. Buchmann, and T. Foken (2004), Whole-air relaxed eddy accumulation for the measurement of isotope and trace-gas fluxes, poster presented at SIBAE-BASIN Conference, Interlaken, Switzerland, April 1-3, 2004. (The poster presentation was honorably mentioned at the conference)

Ruppert, J. (2005), ATEM software for atmospheric turbulent exchange measurements using eddy covariance and relaxed eddy accumulation systems + Bayreuth whole-air REA system setup, *Arbeitsergebnisse 28*, 29 pp, Universität Bayreuth, Abt. Mikrometeorologie, Bayreuth, Germany. Print, ISSN 1614-8916.

Ruppert, J., and T. Foken (2005), Messung turbulenter Flüsse von Kohlendioxid und stabilem Kohlenstoffisotop ^{13}C über Pflanzenbeständen mit Hilfe der Relaxed Eddy Accumulation Methode, in Klimatologische und mikrometeorologische Froschungen im Rahmen des Bayreuther Institutes für terrestrische Ökosystemforschung (BITÖK) 1998 - 2004, edited by T. Foken, *Arbeitsergebnisse 29*, 81-104, Universität Bayreuth, Abt. Mikrometeorologie, Bayreuth, Germany. Print, ISSN 1614-8916.

Thomas, C., J. Ruppert, J. Lüers, J. Schröter, J. C. Mayer, and T. Bertolini (2004), Documentation of the WALDATEM-2003 experiment, 28.4.-3.8.2003, *Arbeitsergebnisse 24*, 59 pp, Universität Bayreuth, Abt. Mikrometeorologie, Bayreuth, Germany. Print, ISSN 1614-8916.

Wichura, B., J. Ruppert, A. C. Delany, N. Buchmann, and T. Foken (2004), Structure of carbon dioxide exchange processes above a spruce forest, in *Biogeochemistry of Forested Catchments in a Changing Environment: A german case study*, edited by E. Matzner, pp. 161-176, Springer, Berlin.

1. Introduction

Predictions of the global climate change due to the greenhouse warming effect [*IPCC*, 2007] ask for the investigation of the global carbon balance and its sensitivity. The carbon flux into the atmosphere from fossil fuel burning can be determined of human activity data. The uptake of atmospheric carbon dioxide (CO_2) by upper ocean waters and consequential acidification of ocean waters can be described by a diffusion process and the formation of carbonic acid. A second important sink for atmospheric CO_2 is the terrestrial biosphere. The determination of CO_2 net ecosystem exchange (NEE) using the eddy-covariance method (EC) has therefore become a fundamental tool for the investigation of the carbon balance of terrestrial ecosystems. This method is commonly applied to measure the atmospheric CO_2 exchange of different ecosystems around the globe [*Aubinet et al.*, 2000; *Baldocchi et al.*, 2001]. The derivation of the turbulent flux density from EC data requires certain corrections, transformations and quality control [*Aubinet et al.*, 2003; *Foken et al.*, 2004].

The derivation of the annual sum of NEE and filling of data gaps is complicated by characteristic diurnal and seasonal variation in the governing gross flux components of assimilation, i.e. photosynthetic uptake of CO_2, and respiration. Consequently, a high potential for systematic errors exist [*Goulden et al.*, 1996; *Moncrieff et al.*, 1996]. Careful assessment of the data is therefore required, including criteria for rejecting invalid data and gap-filling strategies to replace rejected and missing data with modeled values. A study by *Falge, et al.* [2001] showed small differences in the accuracy of the gap-filling models but that the accuracy of annual sums of NEE is sensitive to the criteria applied to rate the data quality and reject certain data.

The NEE is the result of the two relatively large flux components of assimilation as a sink and respiration as a source of CO_2. Photosynthesis and respiration processes are sensitive to multiple environmental factors, e.g. temperature, soil moisture availability and changes in global radiation. In the face of global and regional climate changes, consequential changes in ecosystem carbon balances may therefore form significant positive and negative feedbacks to the greenhouse warming effect [*Flanagan and Ehleringer*, 1998]. The analysis of sensitivities in the net carbon balance requires better understanding of the contribution and sensitivity of the individual gross flux components. The determination of the assimilation flux, i.e. the carbon dioxide consumption by photosynthesis, and the respiration flux of terrestrial ecosystems has therefore become an important research interest [e.g. *Reichstein et al.*, 2003; *Reichstein et al.*, 2005]. The parameterization of NEE and the validation of models for the component fluxes ask for constrain by multiple measurement methods.

Problems with upscaling (bottom-up approach) resulting from small scale heterogeneity in ecosystems could be avoided by partitioning the NEE into its component fluxes (top-down approach). This however requires the existence and measurement of a tracer, which can identify the individual contributions to the net flux at ecosystem scale. A method that assesses typical scalar correlations for taking conditional samples of the turbulent gas exchange is suggested by *Thomas, et al.* [2008]. The isotopic signature of CO_2, i.e. the CO_2 isotope ratios with respect to $^{13}CO_2$ and $CO^{18}O$, can serve as tracer, because photosynthetic uptake discriminates against the heavier isotopes [*Farquhar et al.*, 1989; *Yakir and da S. L. Sternberg*, 2000]. Based on specific and different isotopic signatures of the assimilation flux and the respiration flux, the combination of the bulk CO_2 and the isotope mass balances can facilitate the flux partitioning at local ecosystem scale [*Bowling et al.*, 2001; *Lloyd et al.*, 1996; *Wichura et al.*, 2000; *Yakir and Wang*, 1996] (Appendix 4, Figure 1, ED-37). On regional and global scale isotopic mass

balance analysis and flux partitioning requires the determination of the isotope discrimination of the terrestrial biosphere [*Bakwin et al.*, 1998; *Ciais et al.*, 1995; *Flanagan and Ehleringer*, 1998; *Fung et al.*, 1997; *Miller et al.*, 2003; *Randerson et al.*, 2002]. The isotopic signatures of fluxes and isotope discrimination are commonly determined at the leaf and branch scale [e.g. *Barbour et al.*, 2007; *Cernusak et al.*, 2004; *Flanagan et al.*, 1994; *Seibt et al.*, 2006; *Wingate et al.*, 2007]. Better understanding of the dynamic and absolute values of isotopic signatures in the atmospheric turbulent exchange at ecosystem scale is highly needed to constrain isotope partitioning approaches [*Lai et al.*, 2004; *Phillips and Gregg*, 2001]. A method for the determination of the ecosystem isotope discrimination Δ_e is suggested by *Buchmann, et al.* [1998]. It evaluates the isotopic signature δ_R of the respiration flux as integral signature of the ecosystem. This method was applied to a number of different ecosystems and to global scale modeling in studies by *Buchmann and Kaplan* [2001] and *Kaplan, et al.* [2002].

The success of isotopic flux partitioning methods applied at ecosystem scale depends on the precise information on isotopic signatures and isotope discrimination. Therefore, the following aspects should be considered in this study:

(i) A significant difference of the isotopic signatures of component fluxes must exist for successful application of the isotopic flux partitioning method.

(ii) Small isotopic gradients in the turbulent exchange ask for high precision measurements of the isotopic flux density (isoflux), especially above tall vegetation.

(iii) Conditions of well-mixed air are normally an inherent assumption of the mass balance analysis.

(iv) The analysis of the mixing of sources with different isotopic signatures by mass balances requires that isotopic parameters are weighted by the size of the flux, which is also required for up and downscaling.

(v) The appropriateness of spatial and temporal scales of isotopic parameters and their temporal variability must be considered.

High demand for increased measurement precision of the $\delta^{13}C$ and $\delta^{18}O$ isotopic signatures of atmospheric turbulent CO_2 exchange and of the ecosystem isotope discrimination and for the investigation of their temporal variability is expressed in a number of recent studies on the measurement of isotope fluxes by tunable diode laser (TDL) [*Bowling et al.*, 2003b; *Griffis et al.*, 2004; *Griffis et al.*, 2005; *Saleska et al.*, 2006; *Zhang et al.*, 2006] and in studies on modeling of ecosystem/atmosphere isotope exchange [*Aranibar et al.*, 2006; *Chen et al.*, 2006; *Fung et al.*, 1997; *Lai et al.*, 2004; *Ogée et al.*, 2003; *Ogée et al.*, 2004]. The current level of analytical precision, the need for relatively long integration times and problems with stability of TDL measurements leave uncertainty with respect to potential systematic errors, which cannot be eliminated by integration of continuous data. High precision isotope ratio analysis is therefore required in order to prevent systematic errors and to determine the isotopic signature of the atmospheric turbulent exchange and related parameters of isotope discrimination with high precision. Precisely measured values are required for the validation of soil-vegetation-atmosphere transfer models for the CO_2, $^{13}CO_2$ and $CO^{18}O$ isotopic gas exchange and for the analysis of isotopic mass balances at ecosystem, regional or global scale.

2. Objective of the thesis

The objective of this thesis is to contribute to an improved quantitative analysis of carbon mass balances of ecosystems. More specific objectives are the following:

To facilitate quantitative methods for the investigation of the atmospheric $^{13}CO_2$ and $CO^{18}O$ isotope exchange and the bulk carbon CO_2 of ecosystems with special regard to forest ecosystems,

to minimize the uncertainty of such methods by identifying and as far as possible eliminating potential sources of systematic error,

to extend the bulk CO_2 and $^{13}CO_2$ isotope mass balance analysis by measuring also $CO^{18}O$ isotope fluxes,

to increase and subsequently determine the precision of isotopic flux measurements above forest ecosystems,

to assess the potential for the application of the isotopic flux partitioning method at ecosystem scale for the partitioning of the commonly determined net ecosystem exchange (NEE) into its gross flux components of assimilation and respiration,

to determine ecosystem integrated and flux weighted parameters of the isotopic exchange and their diurnal variability.

3. Instrument and software development

3.1. Development of high precision isotope sampling systems

In order to achieve the high analytical precision required for isotope flux measurements, a special air sampling system had to be developed. Consultations with Anthoni C. Delany, Dave R. Bowling and Willi A. Brand and results of cryo-trap hyperbolic relaxed eddy accumulation (HREA) systems presented by *Bowling, et al.* [1999a] and *Wichura, et al.* [2001] led to the decision for the development of a whole-air relaxed eddy accumulation (REA) sampling system for isotope flux measurements (Appendix 3, Figure 1, REA-25). The hyperbolic sampling characteristic is implemented by a certain method of online data evaluation as suggested by *Bowling et al.* [1999b]. The design of the whole-air REA system goes back to the principles of conditional sampling of trace gases [*Businger and Oncley*, 1990; *Delany et al.*, 1991; *Desjardins*, 1977; *Oncley et al.*, 1993; *Pattey et al.*, 1993] and is based on a design idea suggested for isotope sampling by *Bowling et al.* [2003a]. In this sampling system, foil balloon bags serve as intermediate storage for updraft and downdraft air samples at ambient pressure. The conservation of whole-air samples allows for high precision of the sampling procedure with respect to the subsequent isotope analysis by minimizing potential effects that could alter the isotope ratio of the sample: The Mylar® multi-layer material of the foil balloon bags is flexible, robust and air tight also for very small molecules. It effectively prevents the diffusion of CO_2 molecules due to a nylon layer coated with aluminum flakes. It provides a sufficiently inert inner surface of polyethylene (PE). The pre-drying of updraft and downdraft air samples, and the collection and conservation of large volumes of whole-air samples with minimum pressure changes minimized any subsequent sample fractionation at orifices or surfaces and furthermore allowed to extend the analysis on $CO^{18}O$ isotope fluxes.

The investigation of complex air exchange processes and isotopic signatures in the forest ecosystem additionally required an isotope and trace gas profile air sampling system. It was designed for continuous CO_2 mixing ratio measurements and for collecting flask samples for subsequent high precision isotope laboratory analysis. The instrument development of both sampling systems was performed at the University of Bayreuth. More details are presented in Appendix 3 [*Ruppert et al.*, 2008a].

3.2. Software developments

The HREA method requires the fast online evaluation of turbulence data and precise timing of sample segregation. This required the development of special software and data input and output interfaces for data recording and the exact monitoring and control of the whole-air sampling process. Furthermore, high precision isotope data asked for automation of the in-field air sample treatment and storage in glass flasks. For these purposes, the software ATEM [*Ruppert*, 2005] was developed at the Department of Micrometeorology, University of Bayreuth. A second software ATEM_PROFILE is an adaptation of ATEM and was developed for the control of the isotope and trace gas profile system. A third software package ATEM_EVAL allowed for the evaluation of data of both systems and a variety of simulations of REA and HREA sampling on turbulence time series. The simulations were required for the quality control and determination of the *b*-factors used in the REA and HREA method [*Ruppert et al.*, 2008a]. The software development was performed with the software LabView®.

4. Experiments and data evaluation

The individual research papers presented in this thesis use data from several micrometeorological field experiment campaigns conducted by the Department of Micrometeorology of the University of Bayreuth, which were supervised by Prof. Thomas Foken. Three field experiments with isotope flux measurements were supervised by Prof. Thomas Foken and Prof. Nina Buchmann. Laboratory experiments and all analysis of flask air samples were performed in co-operation with and at the Isotope- and Gas-Laboratory of the Max-Planck Institute of Biogeochemistry in Jena under the supervision of Willi A. Brand.

The predominant part of the data and samples was collected during the WALDATEM-2003 field experiment, which was performed in co-operation with my colleague Christoph Thomas and as an intensive field measurement campaign of the Department of Micrometeorology of the University of Bayreuth. The second research paper is based on CO_2 flux measurements and additional environmental data collected at the FLUXNET station Waldstein/Weidenbrunnen (GE1-Wei), which is supervised by Prof. Thomas Foken and Johannes Lüers of the Department of Micrometeorology of the University of Bayreuth.

4.1. Laboratory experiments

The foil balloon bags and the complete whole-air REA sampling system were thoroughly tested for potential sources of contamination, isotope fractionation and the overall measurement precision in laboratory experiments, which were performed in co-operation with the Isotope- and Gas-Laboratory of the Max-Planck Institute in Jena. The first test of new foil balloons as intermediate storage container showed significant contamination of isotope samples. The tests were repeated after cleaning the balloon bags by flushing with dried ambient air and nitrogen and exposure to direct sunlight for several days. After this treatment, no signs of contamination were found during the aspired intermediate storage times of up to one hour.

Before the experiments GRASATEM-2003 and WALDATEM-2003 small leaks in the fittings of the complete whole-air REA sampling system were identified by applying high vacuum and removed. Subsequently the whole-air REA system was tested for its overall measurement precision by repeated sampling from a compressed air tank and high precision isotope analysis of the flask samples. During the third test individual sections of the sampling system including the foil balloons were analysed. In the forth laboratory experiment the complete whole-air REA system was tested with the same sampling protocol that was later used during the field experiments but sampling air from the compressed air tank. The results of the laboratory experiments are presented in Appendix 3 [*Ruppert et al.*, 2008a].

4.2. GRASATEM-2002

The GRASATEM-2002 (Grassland Atmospheric Turbuelnt Exchange Measurements 2002) experiment was performed by Johannes Ruppert and Matthias Mauder at the Ecological-Botanical Gardens of the University of Bayreuth in August 2002 and was supervised by Prof. Foken. It served as a field test of a preliminary design of the whole-air REA sampling system and the isotope flux measurement strategy. The results of this experiment allowed to improve the design and precision of the sampling system and to gain first insights in the turbulent isotope exchange of a grassland ecosystem.

4.3. GRASATEM-2003

Measurements of the experiment GRASATEM-2003 (Grassland Atmospheric Turbulent Exchange Measurements 2003) were performed over short cut grassland (canopy height h_c=0.12 m) during the LITFASS-2003 experiment [*Beyrich et al.*, 2004; *Mauder et al.*, 2003] at the Falkenberg experimental site of the German Meteorological Service (Meteorological Observatory Lindenberg), Germany (52°10'04" N, 14°07'03" E, 71 m a.s.l.). The turbulent CO_2 flux was measured at 2.25 m above ground by a sonic anemometer (USA-1, METEK, Meteorologische Messtechnik GmbH, Elmshorn, Germany) and a CO_2/H_2O open path sensor (LI-7500, LI-COR Inc., Lincoln, NE, USA) from 14th of May 2003 to 1st of June 2003. The isotopic exchange was measured with the whole-air REA system by analyzing updraft and downdraft air samples. In parallel biomass samples of the vegetation were collected, dried in a microwave, milled and analyzed for the isotope ratios of starch and sugars, in order to determine the isotopic signature of fresh assimilate. However, the data of this experiment did not provide the precision required for isotope flux analysis. The main reason was a very low rate of photosynthesis of the short cut grass layer under very dry conditions during the experiment. Consequently, only very small isotopic differences were observed in updraft and downdraft air samples. During two of the five days with isotope REA sampling, the failure of a backpressure valve caused a lack of overpressure of the air samples stored in the glass flasks, which resulted in less precise isotope analysis. Furthermore, for nearly all wind directions the mean air flow was disturbed by a hedge with small trees 30 m north of the measuring position. This led to a asymmetric pattern of the observed mean vertical wind velocities, which could not be corrected by the planar fit method [*Wilczak et al.*, 2001]. Due to the small isotopic differences and the additional sampling problems, the data from the GRASATEM-2003 experiment was not suitable for isotopic flux analysis.

4.4. WALDATEM-2003 and continuous EC flux data

The whole-air REA system was used to collect updraft and downdraft air during the field experiment WALDATEM-2003 (Wavelet Detection and Atmospheric Turbulent Exchange Measurements 2003, [*Thomas et al.*, 2004]) in June and July 2003. Samples were collected above a spruce forest (*Picea abies, L.*) with a plant area index (PAI) of 5.2 m^2 m^{-2} [*Thomas and Foken*, 2007] and an average canopy height of 19 m. The experiment site Waldstein/Weidenbrunnen (GE1-Wei) is part of the FLUXNET network and is located in the Fichtelgebirge Mountains in Germany (50°08'31" N, 11°52'01" E, 775 m a.s.l.) on slightly sloping terrain (2°). A detailed description of the site can be found in *Gerstberger et al.* [2004] and *Staudt and Foken* [2007]. The REA sample inlet was installed on a tower at 33 m just below the sonic anemometer used for continuous EC measurements of the atmospheric CO_2 exchange at the site. A vertical profile air sampling system with 8 inlets was used to continuously monitor CO_2 concentration changes in the air below 33 m, i.e. above canopy, in the canopy space, in the sub-canopy space and close to the forest floor. The same system was also used to collect whole-air samples during nighttime and three times during the day for isotope analysis. Results of a three day intensive isotope measurement campaign are discussed in Appendix 3 [*Ruppert et al.*, 2008a] and Appendix 4 [*Ruppert et al.*, 2008b]. The data of this period was selected because significant isotopic differences in updraft and downdraft air samples could be observed after a period of several days with rainfall. A comprehensive strategy for the evaluation of the continuous EC CO_2 data collected at Waldstein/Weidenbrunnen for the determination of the

annual sum of the net ecosystem exchange (NEE) is presented in Appendix 2 [*Ruppert et al.*, 2006a].

4.5. Additional experimental data

Turbulence data obtained above three different surface types (grassland, cotton and spruce forest) was analyzed in order to study the effect on the characteristics of the turbulent exchange of different scalar quantities. Similar such characteristics, i.e. scalar similarity, are a basic assumption for the application of conditional sampling flux measurement methods like the REA and HREA method. Data from the GRASATEM-2003 and WALDATEM-2003 experiments was supplemented with data from turbulence measurements over a cotton plantation in California obtained during the EBEX-2000 field experiment [*Bruckmeier et al.*, 2001; *Oncley et al.*, 2000]. These sets of high resolution turbulence data were analyzed for the similarity of the turbulent exchange of different scalars and relative flux errors determined from simulation of REA and HREA sampling. The results of this analysis are discussed in Appendix 1 [*Ruppert et al.*, 2006b] and summarized in the following section.

5. Assessment of scalar similarity in the turbulent exchange

The results of simulation of conditional sampling on data from the EBEX-2000 experiment over cotton indicated the risk of errors in flux measurements by the HREA method [*Ruppert*, 2002]. The errors were assumed to result from a lack of similarity in the turbulent exchange of different scalars (scalar similarity) [*Ruppert et al.*, 2002; *Wichura et al.*, 2004], and gave some indication for a systematic component of errors in conditional sampling methods. A literature study showed that there was one research paper in which scalar similarity was assessed based on analysis of high resolution time series of different scalar concentrations with respect to ozon flux measurements [*Pearson et al.*, 1998]. Apart from that and studies on similarity theory for the flux-gradient method with a focus on energy and latent heat fluxes, there was a lack of fundamental literature on scalar similarity in the turbulent exchange of gases. Testing the hypothesis of HREA flux errors due to a lack of scalar similarity required the definition of a general indicator for its critical assessment. Scalar-scalar correlation coefficients $r_{c,c\,proxy}$ (Appendix 1, Equation 4, SS-7) for three scalars (temperature, water vapor and carbon dioxide) were therefore analyzed with respect to (i) their temporal variability, (ii) their relation to exchange event characteristics in the frequency domain and (iii) their relation to errors in the REA and HREA method. This study was based on additional simulations and data from three sites with different vegetation height, i.e. grass, cotton and spruce forest. It indicated the risk of systematic underestimation of fluxes by HREA in times of a lack in scalar similarity between the scalar of interest and the proxy scalar. Data of a proxy scalar is required for the HREA sampling and evaluation scheme. The publication presented in Appendix 1 [*Ruppert et al.*, 2006b] closed a gap of fundamental research literature on scalar similarity with respect to conditional sampling techniques. It demonstrates the diurnal variability of the scalar similarity in the CO_2, sensible heat and latent heat flux and the link of scalar similarity to the exchange in events with durations longer than 60 s (Appendix 1, Figure 3, SS-13). Furthermore, the implications for conditional sampling flux measurement methods like REA and HREA are discussed.

The definition of the research problem and the data displayed in Figures 1c, 4a and 4b originated from simulations performed with EBEX-2000 data in the framework of a diploma

thesis [*Ruppert*, 2002]. The calculation of wavelet variances was performed by Christoph Thomas, who also contributed section 4.3 to the manuscript presented in Appendix 1 [*Ruppert et al.*, 2006b]. All further analysis, especially all correlation analysis, and the preparation of the manuscript were done by myself. This included the selection of the scalar-scalar correlation coefficient $r_{c,c\ proxy}$ as principle parameter of scalar similarity, which provides the link to time domain wavelet analysis. I performed a detailed visual analysis of a large set of wavelet variance spectra. Based on this analysis, I suggested a further correlation parameter, i.e. the spectral correlation coefficient r_s (Appendix 1, Equation 8, SS-8). Its calculation from the different wavelet variance spectra was performed by Christoph Thomas. After decreasing scatter in this data by applying moving window averaging, the comparison of both kinds of correlation coefficients showed that the diurnal variation observed in the scalar-scalar correlation coefficients could be attributed to events with durations longer than 60 s, which predominantly control the scalar similarity in the turbulent exchange. This finding would allow the analysis of scalar similarity by data from slow sensors. I hypothesized that the observed diurnal variation of scalar similarity is related to changes in the source or sink strength, which would mean that plant physiological processes, like e.g. afternoon stomata closure, can significantly affect scalar similarity, which is an prerequisite for the application of conditional sampling methods, as discussed in Appendix 3, [*Ruppert et al.*, 2008a].

6. Gap-filling of CO_2 net ecosystem exchange (NEE) data

The derivation of annual sums of the CO_2 net ecosystem exchange (NEE) from eddy covariance (EC) measurements requires careful assessment of the collected data including criteria for rejecting invalid data and gap-filling strategies to replace rejected and missing data. Standardized methodologies are proposed for most of the necessary corrections to eddy-covariance data [*Aubinet et al.*, 2000; *Aubinet et al.*, 2003]. However, strategies for gap-filling are still subject to discussion within the research community [*Falge et al.*, 2001; *Gu et al.*, 2005; *Hui et al.*, 2004]. The comparison of different methods (mean diurnal variation, look-up tables, nonlinear regression) showed small differences in the accuracy of the gap-filling method itself but that the accuracy is sensitive to the criteria applied to rate the data quality and reject certain data [*Falge et al.*, 2001]. The quality assessment must effectively check for instrument failures and for the fulfillment of the prerequisites of the EC method. The highest potential for systematic errors in the annual sum of the NEE and for flux partitioning methods based on respiration models is normally found for nighttime data [*Goulden et al.*, 1996; *Massman and Lee*, 2002; *Moncrieff et al.*, 1996; *Morgenstern et al.*, 2004; *Stoy et al.*, 2006].

The objective of the research paper presented in Appendix 2 [*Ruppert et al.*, 2006a] was to establish a comprehensive method for the evaluation of CO_2 EC flux measurements for the derivation of annual sums of NEE (Appendix 2, Figure 1, GF-26) based on a set of criteria including fundamental quality criteria presented by *Foken and Wichura* [1996] and *Foken, et al.* [2004] in order to minimize potential systematic errors. The complete evaluation scheme was applied to data recorded above the spruce forest at the FLUXNET station Waldstein/Weidenbrunnen (GE1-Wei) in 2003. The applied criteria were able to increase the number of available high quality nighttime data especially in summer, when respiration and assimilation rates are relatively high. Even more important, they were able to reduce the systematic distribution of gaps in comparison to commonly applied criteria based on the friction velocity u_* (Appendix 2, Figure 6, GF-31). The complete evaluation scheme and set of criteria are presented in Appendix 2 [*Ruppert et al.*, 2006a] including a detailed discussion of the results. These included the determination of the annual sum of the CO_2 NEE at

Waldstein/Weidenbrunnen for the year 2003. During periods with high temperatures and drought stress in the summer of 2003 [*Granier et al.*, 2007; *Reichstein et al.*, 2007], decreased CO_2 assimilation was observed [*Ruppert and Foken*, 2005; *Ruppert et al.*, 2006a], which most likely was related to afternoon stomata closure.

Large parts of the EC data were collected by Christoph Thomas and additional environmental data was collected in collaboration with colleagues from the Department of Micrometeorology. Matthias Mauder processed the EC data with the software TK2 [*Mauder and Foken*, 2004] and contributed section 2.2 to the manuscript presented in Appendix 2 [*Ruppert et al.*, 2006a]. The development of the comprehensive gap-filling strategy, including the definition of additional quality criteria and the assessment of their effects, was performed by myself. I refined the principle concept for the parameterization scheme that was applied in earlier studies by *Rebmann* [2003] and *Rebmann, et al.* [2004]. All figures and the manuscript were prepared by myself. A more detailed analysis for an objective seasonal segregation based on average temperatures was tested in collaboration with Johannes Lüers, but excluded from the manuscript during the review process due to its small effect on the results. The parameterization of the nighttime respiration model was subsequently used for estimating the daytime respiration flux F_R in Appendix 4 [*Ruppert et al.*, 2008b].

7. Whole-air relaxed eddy accumulation (REA) isotope flux measurements

The measurement of isotopic flux densities (isofluxes) requires high precision during the sampling process and subsequent isotope analysis. Isoflux measurements are especially challenging above tall vegetation because normally only relatively small concentration and isotopic gradients can be observed above the ecosystem. With a lack of fast and precise sensors for EC measurements, conditional sampling methods, like the REA can be applied. The development of a REA instrument for the collection of whole-air samples and isoflux measurements was outlined in section 3 of this synopsis. It required the application of thorough quality control for the instrument development, during the sampling procedure and for the evaluation of the experimental data obtained from a three-day intensive measuring campaign during the experiment WALDATEM-2003. The methods for quality control and assessment are discussed in detail in Appendix 3 [*Ruppert et al.*, 2008a]. In this study we were able to validate the sampling process (i) by comparing the diurnal change of isotope ratios in above canopy air samples of two independent sampling systems, i.e. the whole-air REA system and the isotope and trace-gas profile air sampling system (Appendix 3, Figure 5, REA-29), and (ii) by comparing simulated and observed updraft and downdraft CO_2 mixing ratio differences (Appendix 3, Figure 7, REA-31). Detailed axis rotation procedures were implemented for the conditional sampling process by performing online planar-fit corrections according to the method presented by *Wilczak, et al.* [2001], which originally was developed for the post-processing of EC data. An increase of concentration differences by 63% was achieved by applying the hyperbolic relaxed eddy accumulation method (HREA) [*Bowling et al.*, 1999b] (Appendix 3, Table 1, REA-24). Our study demonstrates the feasibility of isotopic flux measurements above a forest ecosystem not only for $^{13}CO_2$ isotopes but also for $CO^{18}O$ isotopes. The scalar similarity was assessed as fundamental prerequisite for the application of conditional sampling methods and the EC/flask method [*Bowling et al.*, 1999a; *Bowling et al.*, 2001] based on the correlation of isotope ratios and CO_2 mixing ratios. Different timescales were comprised in this analysis, i.e. timescales of several minutes represented in vertical profile air samples and relatively short timescales of the turbulent exchange represented in HREA

updraft and downdraft air samples. The linear regression analysis showed good scalar correlations, which supports the assumption of scalar similarity. However, different slopes were found in HREA and profile samples from early morning transition periods (Appendix 3, Figure 6, REA-30). This effect was likely caused by isotopically depleted air above the canopy from respiratory built up during the night in combination with high photosynthetic discrimination in the top canopy in the morning. Consequently, temporal and spatial scales of the isotopic exchange should be considered carefully, especially for the application of the EC/flask method. A comprehensive assessment of the impact of scalar similarity on isotopic flux measurement methods like demonstrated in Appendix 1 [*Ruppert et al.*, 2006b] would however require continuous and high resolution time series from EC isoflux measurements, which are currently not feasible for forest ecosystems.

The instrument development and the experimental work were supported by a number of people (see Acknowledgments). The isotope ratio mass spectrometry (IRMS) analysis of air samples was supervised by Willi A. Brand, who also provided parts of section 3.6 of the manuscript. The analysis of the results obtained from the laboratory and field experiments, their validation by simulations, their interpretation and the preparation of the manuscript presented in Appendix 3, [*Ruppert et al.*, 2008a], were performed by myself.

8. Flux weighted isotopic signatures and discrimination in the ecosystem gas exchange

The high precision isotope analysis of updraft and downdraft HREA air samples provided the basis for further evaluating $^{13}CO_2$ and $CO^{18}O$ isotopic mass balances and isotopic signatures of the atmospheric exchange of the spruce forest at Waldstein/Weidenbrunnen. The manuscript presented in Appendix 4 [*Ruppert et al.*, 2008b] demonstrates that truly flux weighted isotopic signatures and the ecosystem discrimination Δ_e and net ecosystem discrimination Δ_E can be determined directly from whole-air updraft and downdraft air samples. By HREA sampling above the ecosystem, these parameters integrate fluxes and small scale heterogeneity at the ecosystem level and are determined at half-hourly timescales, which are typical for EC flux measurements. Such measurements can therefore be used to investigate the diurnal variability of isotopic signatures and discrimination and can contribute to close the gap between isotope measurements at the leaf and branch scale to isotope mass balances and modeling studies at the regional and global scale. The isotopic signature δ_c of the turbulent atmospheric exchange can be read as the slope of the line connecting updraft and downdraft air sample data in a so called Miller-Tan plot (Appendix 4, Equation 9, ED-6). δ_c conceptually corresponds to the flux weighted derivative of the isotopic mixing line at measurement height. The display of updraft and downdraft data in Miller-Tan plots visualized key processes of the atmospheric CO_2 exchange of the ecosystem (Appendix 4, Figure 3, ED-39). This form of display could therefore be a useful method for analyzing continuous isotope data, which potentially can be obtained by tunable diode laser (TDL) isotope measurements. The observed diurnal variability of isotopic signatures of the turbulent exchange demonstrates that no general isotopic mixing relation can be assumed, e.g. for the application of the EC/flask method [*Bowling et al.*, 1999a; *Bowling et al.*, 2001] (Appendix 4, Figure 6, ED-42). Instead, the determination of isofluxes requires regularly updating of the isotopic mixing relation based on measurement methods that assure flux weighting instead of concentration weighting. The isotopic signatures and the ecosystem isotope discrimination (Appendix 4, Equation 16 and 17, ED-9) were determined directly from

isotopic flux measurements by HREA on half-hourly timescales in our study. They could be used for validating soil-vegetation-atmosphere transfer models for the isotopic exchange at the ecosystem scale [e.g. *Chen et al.*, 2006; *Ogée et al.*, 2003]. Isotopic mass balance analysis at large scale could be further constrained based on repeated measurements, which take account of the observed diurnal and additional presumed seasonal variability.

9. Potential and requirements of the isotopic flux partitioning method

For the application of the isotopic flux partitioning method independently measured or modeled values for the flux weighted and canopy integrated isotope discrimination Δ_{canopy} of the assimilation flux are indispensable [*Bowling et al.*, 2003a; *Zobitz et al.*, 2008]. In Appendix 4 [*Ruppert et al.*, 2008b] we inversed the flux partitioning method by assuming the respiration flux according to the parameterization presented in Appendix 2 [*Ruppert et al.*, 2006a], (Equation 5, GF-9). We were thereby able to estimate the integrated canopy isotope discrimination from the isotopic flux measurements performed above the ecosystem and to indicate its diurnal variability (Appendix 4, Figure 7, ED-43). In order to avoid potential systematic errors in the flux partitioning, instead of the commonly used simplified definition, a more precise definition of the canopy isotope discrimination Δ'_{canopy} should be used (Appendix 4, Equation 19, ED-10), for either assuming or validating independently measured or modeled data.

We demonstrate, that the success of the isotopic flux partitioning method is highly sensitive to the precision of flux weighted isotopic signatures (Appendix 4, section 4.8, ED-21ff). Their determination at the ecosystem scale should therefore apply high precision analysis of isotopic signatures of the turbulent exchange. These have to be combined with precise measurements of the bulk CO_2 mixing ratios as demonstrated by whole-air REA measurements in Appendix 3 [*Ruppert et al.*, 2008a]. While isotope analysis by tunable diode lasers (TDL) provides valuable continuous information on isotopic signatures, its precision is currently not sufficient to resolve the small isotopic gradients and updraft–downdraft isotopic differences observed above the spruce forest at Waldstein/Weidenbrunnen.

The mass balances that form the basis for the isotopic flux partitioning method assume well-mixed air below the measurement level above the canopy. It is therefore important to investigate the mixing conditions, which was done by analyzing organized air motion and CO_2 mixing ratio changes in a vertical profile throughout the canopy (Appendix 4, Figure 4, ED-40).

Furthermore, the isotopic flux partitioning requires the existence of significant disequilibrium between the isotopic signatures δ_A of the assimilation flux and δ_R of the respiration flux. The observed diurnal variability of δ_R demonstrated that daytime values cannot be inferred from nighttime vertical profile measurements but should be determined from profile measurements during daytime (Appendix 4, Figure 8, ED-44). In tall vegetation like forests, the analysis for daytime δ_R should be restricted to the sub-canopy space in order to avoid bias (Appendix 4, Table 1, ED-35), which results from the photosynthetic uptake and consequential isotopic enrichment in the canopy space (Appendix 4, Figure 2, ED-38).

At the beginning of the intensive measurement campaign, we observed isotopic disequilibria $\mathcal{D}^{13}C$ and $\mathcal{D}^{18}O$, which were opposite in sign (Appendix 4, Figure 8, ED-44). Two days past the end of a prolonged rain period, both disequilibria disappeared. The observed fast equilibration may limit the time periods for the successful application of the isotopic flux partitioning method. An independent and meaningful estimate of the assimilation flux F_A and the respiration flux F_R by isotopic flux partitioning of the NEE would require independently measured or

validated modeled data on the canopy isotope discrimination Δ'_{canopy}, which must reflect its diurnal variability.

The methods proposed in Appendix 4 [*Ruppert et al.*, 2008b] were my idea. I performed the corresponding analysis and prepared the entire manuscript. The data predominately originated from the isotope flux and profile measurements presented in Appendix 3 [*Ruppert et al.*, 2008a]. Johannes Lüers provided refined meteorological data presented in Figure 4a and 4b. Christoph Thomas contributed the results on the status of coupling as presented in Figure 4d.

10. Conclusion

The quantification of CO_2 net ecosystem exchange (NEE) using the eddy-covariance (EC) method has become an important tool for investigating the carbon balance of terrestrial ecosystems. The derivation of annual sums of the NEE requires careful assessment of the collected data including criteria for rejecting invalid data and gap-filling strategies to replace rejected and missing data.

The application of a set of quality criteria on the fundamental prerequisites of the eddy-covariance method and the meteorological conditions is able to increase the availability of high quality flux data especially during summer nights. This results in a less systematic distribution of data gaps that need to be filled compared to the use of a u_* threshold criterion. The u_* criterion is not sufficient for the assessment of the prerequisites of the EC method. Especially above forest ecosystems, any further rejection of data related to the dependence of nighttime NEE on turbulent mixing or decoupling within the canopy should use more specific information than u_* measured above the canopy in order to prevent the risk of double accounting of respiratory fluxes and potential systematic error.

The determination of temperature dependent light response functions for the parameterization of daytime NEE and gap-filling integrates information on seasonality so that further segregation of data into seasonal classes did not significantly improve the parameterization scheme applied to data of the spruce forest site at Waldstein/Weidenbrunnen of the year 2003.

The partitioning of the NEE into its gross flux components, i.e. the assimilation flux as a sink and the respiration flux as a source of CO_2, allows investigating the sensitivity of the carbon balance of terrestrial ecosystems. The isotopic flux partitioning method requires determining flux weighted isotopic signatures of the turbulent exchange above the ecosystem and of the component fluxes. However, currently no fast sensors for EC isoflux measurements are available, that would be able to sufficiently resolve relatively small isotopic gradients observed above forest ecosystem.

Alternatively, conditional sampling methods provide the basis for isotopic flux measurements also above tall vegetation as accumulated air samples can be analyzed with high precision by isotope ratio mass spectrometry (IRMS) in the laboratory. Its combination with the hyperbolic relaxed eddy accumulation method (HREA) and with whole-air sampling allows for quantifying the isotopic flux densities (isofluxes) of $^{13}CO_2$ and $CO^{18}O$. Samples from above the spruce forest and the canopy top at Waldstein/Weidenbrunnen, which were collected during a three-day intensive measuring campaign, demonstrated that high precision can be achieved. For the determination of isofluxes, a measurement uncertainty in the order of 10−20% is estimated. Sufficient precision for $CO^{18}O$ isotope analysis requires efficient drying during the sampling process and before sample storage.

The application of conditional sampling methods requires the assumption of similarity in the turbulent exchange of different scalar quantities. Scalar similarity between carbon dioxide, sonic

temperature and water vapor showed distinct diurnal changes. It is predominantly controlled by events on longer time scales (event durations > 60 s), which most likely represent changes in the source/sink strength or convective or advective processes. This finding suggests that firstly plant physiological processes, like e.g. afternoon stomata closure, can have a major effect on the diurnal pattern of scalar similarity. Secondly, sampling with slow sensors may be suitable to assess the scalar similarity, e.g. by tunable diode laser (TDL) measurements for CO_2 and $^{13}CO_2$ isotopes. Poor scalar-scalar correlations indicate the risk of systematic underestimation of fluxes measured by HREA. As required for the flux determination in the REA or HREA method, scalar similarity is assumed by defining the proportionality factor *b* from a proxy scalar. Based on the analysis of CO_2 HREA data, it is concluded that *b*-factors should be determined for each sampling period and from measurements of the proxy scalar in whole-air samples. The determination of *b*-factors from HREA simulations should be validated by measurements in order to assess the sampling process and prevent systematic errors.

While there is some evidence for good scalar similarity and a generally linear relation between bulk CO_2 and its isotopic signatures in the turbulent exchange, the slope of that relation changes temporarily, e.g. during morning transition periods. In the HREA method the slope of the mixing line is determined by precisely measuring the average isotopic and mixing ratio differences in updraft and downdraft air. Compared to the EC/flask method, these measurements incorporate important additional information on the turbulent exchange of isotopes on small timescales into the HREA isoflux evaluation scheme. For the regression analysis of the EC/flask method, scalar similarity of the isotopic exchange and temporal and spatial scales represented in flask samples must carefully be considered.

HREA measurements have a footprint similar to the footprint of EC measurements and are therefore able to integrate small-scale heterogeneity in ecosystems. They allow determining ecosystem integrated and truly flux weighted isotopic signatures and ecosystem isotope discrimination Δ_e and Δ_E on half-hourly timescales. The flux weighted isotopic signature δ_c of the turbulent exchange can be determined directly from isotopic signatures and mixing ratio differences in updraft and downdraft whole-air samples. Correct flux weighting is a fundamental prerequisite for the quantitative evaluation of isotopic mass balances and the isotopic flux partitioning method. The observed diurnal variability demonstrates the need for repeated measurement of isotopic signatures at ecosystem scale and ecosystem isotope discrimination. The analysis of vertical profile air samples showed that (i) the isotopic signature δ_R of the respiration flux during daytime could not be inferred from nighttime samples and (ii) that the determination of δ_R during daytime should be restricted to sub-canopy samples because of multiple source mixing at higher levels.

The definition of the canopy integrated isotope discrimination Δ_{canopy} commonly used for isotopic partitioning of assimilation and respiration fluxes is a potential source of bias. A more precise definition (Δ'_{canopy}) is suggested. For isotopic flux partitioning, data on the canopy isotope discrimination Δ'_{canopy} from independent measurements or validated models is indispensable. Isotopic disequilibria $\mathcal{D}^{13}C$ and $\mathcal{D}^{18}O$ between the assimilation and respiration fluxes were observed to equilibrate within two days after a rain period. This fast equilibration may limit the periods for the successful application of the isotopic flux partitioning method.

Due to the general sensitivity of the isotopic flux partitioning method to the precision of isotopic signatures, there is further need to investigate the variability of truly flux weighted isotopic signatures by high precision isotope measurements at ecosystem scale. The diurnal variability of the isotope discrimination should be regarded for the evaluation of isotope mass balances of ecosystems and for the validation of models.

11. References

Aranibar, J. N., J. A. Berry, W. J. Riley, D. E. Pataki, B. E. Law, and J. R. Ehleringer (2006), Combining meteorology, eddy fluxes, isotope measurements, and modeling to understand environmental controls of carbon isotope discrimination at the canopy scale, *Global Change Biol.*, *12*, 710-730.

Aubinet, M., A. Grelle, A. Ibrom, U. Rannik, J. Moncrieff, T. Foken, A. S. Kowalski, P. H. Martin, P. Berbigier, C. Bernhofer, R. Clement, J. Elbers, A. Granier, T. Grunwald, K. Morgenstern, K. Pilegaard, C. Rebmann, W. Snijders, R. Valentini, and T. Vesala (2000), Estimates of the annual net carbon and water exchange of forests: The EUROFLUX methodology, in *Advances in Ecological Research*, edited, pp. 113-175, Academic Press, San Diego.

Aubinet, M., R. Clement, J. A. Elbers, T. Foken, A. Grelle, A. Ibrom, J. Moncrieff, K. Pilegaard, Ü. Rannik, and C. Rebmann (2003), Methodlogy for data acquisition, storage and treatment, in *Fluxes of Carbon, Water, Energy of European Forests*, edited by R. Valentini, pp. 9-35, Springer, Berlin.

Bakwin, P. S., P. P. Tans, J. W. C. White, and R. J. Andres (1998), Determination of the isotopic (C-13/C-12) discrimination by terrestrial biology from a global network of observations, *Glob. Biogeochem. Cycles*, *12*, 555-562.

Baldocchi, D., E. Falge, L. H. Gu, R. Olson, D. Hollinger, S. Running, P. Anthoni, C. Bernhofer, K. Davis, R. Evans, J. Fuentes, A. Goldstein, G. Katul, B. Law, X. H. Lee, Y. Malhi, T. Meyers, W. Munger, W. Oechel, K. T. P. U, K. Pilegaard, H. P. Schmid, R. Valentini, S. Verma, T. Vesala, K. Wilson, and S. Wofsy (2001), FLUXNET: A new tool to study the temporal and spatial variability of ecosystem-scale carbon dioxide, water vapor, and energy flux densities, *Bull. Amer. Met. Soc.*, *82*, 2415-2434.

Barbour, M. M., G. D. Farquhar, D. T. Hanson, C. P. Bickford, H. Powers, and N. G. McDowell (2007), A new measurement technique reveals temporal variation in $\delta^{18}O$ of leaf-respired CO_2, *Plant, Cell and Environment*, *30*, 456-468.

Beyrich, F., W. K. Adam, J. Bange, K. Behrens, F. H. Berger, C. Bernhofer, J. Bösenberg, H. Dier, T. Foken, M. Göckede, U. Görsdorf, J. Güldner, B. Hennemuth, C. Heret, S. Huneke, W. Kohsiek, A. Lammert, V. Lehmann, U. Leiterer, J.-P. Leps, C. Liebethal, H. Lohse, A. Lüdi, M. Mauder, W. M. L. Meijinger, H.-T. Mengelkamp, R. Queck, S. H. Richter, T. Spiess, B. Stiller, A. Tittebrand, U. Weisensee, and P. Zittel (2004), Verdunstung über einer heterogenen Landoberfläche - Das LITFASS-2003 Experiment, Ein Bericht., *Arbeitsergebnisse 79*, German Meteorological Service, Offenbach, Germany. Print, ISSN 1430-0281.

Bowling, D. R., D. D. Baldocchi, and R. K. Monson (1999a), Dynamics of isotopic exchange of carbon dioxide in a Tennessee deciduous forest, *Glob. Biogeochem. Cycles*, *13*, 903-922.

Bowling, D. R., A. C. Delany, A. A. Turnipseed, D. D. Baldocchi, and R. K. Monson (1999b), Modification of the relaxed eddy accumulation technique to maximize measured scalar mixing ratio differences in updrafts and downdrafts, *J. Geophys. Res.*, *104*, (D8), 9121-9133.

Bowling, D. R., P. P. Tans, and R. K. Monson (2001), Partitioning net ecosystem carbon exchange with isotopic fluxes of CO_2, *Global Change Biol.*, *7*, 127-145.

Bowling, D. R., D. E. Pataki, and J. R. Ehleringer (2003a), Critical evaluation of micrometeorological methods for measuring ecosystem-atmosphere isotopic exchange of CO_2, *Agric. For. Meteorol.*, *116*, 159-179.

Bowling, D. R., S. D. Sargent, B. D. Tanner, and J. R. Ehleringer (2003b), Tunable diode laser absorption spectroscopy for stable isotope sudies of ecosystem-atmosphere CO_2 exchange, *Agric. For. Meteorol.*, *118*, 1-19.

Bruckmeier, C., T. Foken, J. Gerchau, and M. Mauder (2001), Documentation of the experiment EBEX-2000 (July 20 to August 24, 2000), *Arbeitsergebnisse 13*, Universität Bayreuth, Abt. Mikrometeorologie, Bayreuth, Germany. Print, ISSN 1614-8916.

Buchmann, N., J. R. Brooks, L. B. Flanagan, and J. R. Ehleringer (1998), Carbon isotope discrimination of terrestrial ecosystems, in *Stable Isotopes and the Integration of Biological, Ecological and Geochemical Processes*, edited by H. Griffiths, et al., pp. 203-221, BIOS Scientific Publishers Ltd., Oxford.

Buchmann, N., and J. O. Kaplan (2001), Carbon isotope discrimination of terrestrial ecosystems - how well do observed and modeled results match?, in *Global biogeochemical cycles in the climate system*, edited by E. D. Schulze, et al., pp. 253-266, Academic Press, San Diego.

Businger, J. A., and S. P. Oncley (1990), Flux Measurement with conditional sampling, *J. Atmos. Ocean. Tech.*, *7*, 349-352.

Cernusak, L. A., G. D. Farquhar, S. C. Wong, and H. Stuart-Williams (2004), Measurement and interpretation of the oxygen isotope composition of carbon dioxide respired by leaves in the dark, *Plant Physiol.*, *136*, 3350-3363.

Chen, B., J. M. Chen, L. Huang, and P. P. Tans (2006), Modeling dynamics of stable carbon isotopic exchange between a boreal forest ecosystem and the atmosphere, *Global Change Biol.*, *12*, 1842-1867.

Ciais, P., P. P. Tans, J. W. C. White, M. Trolier, R. J. Francey, J. A. Berry, D. R. Randall, P. Sellers, J. G. Collatz, and D. S. Schimel (1995), Partitioning of ocean and land uptake of CO_2 as inferred by $\delta^{13}C$ measurements from NOAAA Climate Monitoring and Diagnostics Laboratory Global Air Sampling Netweork, *J. Geophys. Res.*, *100*, (D), 5051-5070.

Delany, A. C., S. P. Oncley, J. A. Businger, and E. Sievering (1991), Adapting the conditional sampling concept for a range of different chemical species, paper presented at Seventh symposium on meteorological observations and instruments, American Meteorological Society, Boston, New Orleans, La., 14-18 January 1991.

Desjardins, R. L. (1977), Description and evaluation of a sensible heat flux detector, *Boundary-Layer Meteorol.*, *11*, 147-154.

Falge, E., D. Baldocchi, R. Olson, P. Anthoni, M. Aubinet, C. Bernhofer, G. Burba, R. Ceulemans, R. Clement, H. Dolman, A. Granier, P. Gross, T. Grunwald, D. Hollinger, N. O. Jensen, G. Katul, P. Keronen, A. Kowalski, C.

T. Lai, B. E. Law, T. Meyers, H. Moncrieff, E. Moors, J. W. Munger, K. Pilegaard, U. Rannik, C. Rebmann, A. Suyker, J. Tenhunen, K. Tu, S. Verma, T. Vesala, K. Wilson, and S. Wofsy (2001), Gap filling strategies for defensible annual sums of net ecosystem exchange, *Agric. For. Meteorol.*, *107*, 43-69.

Farquhar, G. D., J. R. Ehleringer, and K. T. Hubick (1989), Carbon isotope discrimination and photosynthesis, *Annu. Rev. Plant Physiol. Plant Mol. Biol.*, *40*, 503-537.

Flanagan, L. B., S. L. Phillips, J. R. Ehleringer, J. Lloyd, and G. D. Farquhar (1994), Effect of changes in leaf water oxygen isotopic composition on discrimination against $C^{18}O^{16}O$ during photosynthetic gas-exchange, *Austr. J. Plant Physiol.*, *21*, 221-234.

Flanagan, L. B., and A. R. Ehleringer (1998), Ecosystem-atmosphere CO_2 exchange: interpreting signals of change using stable isotope ratios, *Trends Ecol. Evol.*, *13*, 10-14.

Foken, T., and B. Wichura (1996), Tools for quality assessment of surface-based flux measurements, *Agric. For. Meteorol.*, *78*, 83-105.

Foken, T., M. Göckede, M. Mauder, L. Mahrt, B. Amiro, and W. Munger (2004), Post-field data qualtiy control, in *Handbook of Micrometeorology*, edited by X. Lee, et al., pp. 181-208, Kluwer, Dordrecht.

Fung, I., C. B. Field, J. A. Berry, M. V. Thompson, J. T. Randerson, C. M. Malmstrom, P. M. Vitousek, G. J. Collatz, P. J. Sellers, D. A. Randall, A. S. Denning, F. Badeck, and J. John (1997), Carbon 13 exchanges between the atmosphere and biosphere, *Glob. Biogeochem. Cycles*, *11*, 507-533.

Gerstberger, P., T. Foken, and K. Kalbitz (2004), The Lehstenbach and Steinkreuz Catchments in NE Bavaria, Germany, in *Biogeochemistry of Forested Catchments in a Changing Environment: A German case study*, edited by E. Matzner, pp. 15-41, Springer, Berlin.

Goulden, M. L., J. W. Munger, S.-M. Fan, B. C. Daube, and S. C. Wofsy (1996), Measurements of carbon sequestration by long-term eddy covariance: Methods and a critical evaluation of accuracy, *Global Change Biol.*, *2*, 169-182.

Granier, A., M. Reichstein, N. Bréda, I. A. Janssens, E. Falge, P. Ciais, T. Grünwald, M. Aubinet, P. Berbigier, C. Bernhofer, N. Buchmann, O. Facini, G. Grassi, B. Heinesch, H. Ilvesniemi, P. Keronen, A. Knohl, B. Köstner, F. Lagergren, A. Lindroth, B. Longdoz, D. Loustau, J. Mateus, L. Montagnani, C. Nys, E. Moors, D. Papale, M. Peiffer, K. Pilegaard, G. Pita, J. Pumpanen, S. Rambal, C. Rebmann, A. Rodrigues, G. Seufert, J. Tenhunen, T. Vesala, and Q. Wang (2007), Evidence for soil water control on carbon and water dynamics in European forests during the extremely dry year: 2003, *Agric. For. Meteorol.*, *143*, 123-145.

Griffis, T. J., J. M. Baker, S. D. Sargent, B. D. Tanner, and J. Zhang (2004), Measuring field-scale isotopic CO_2 fluxes with tunable diode laser absorption spectroscopy and micrometeorological techniques, *Agric. For. Meteorol.*, *124*, 15-29.

Griffis, T. J., X. Lee, J. M. Baker, S. D. Sargent, and J. Y. King (2005), Feasibility of quantifying ecosystem-atmosphere $C^{18}O^{16}O$ exchange using laser spectroscopy and the flux-gradient method, *Agric. For. Meteorol.*, *135*, 44-60.

Gu, L., E. M. Falge, T. Boden, D. D. Baldocchi, T. A. Black, S. R. Saleska, T. Suni, S. B. Verma, T. Vesala, S. C. Wofsy, and L. Xu (2005), Objective threshold determination for nighttime eddy flux filtering, *Agric. For. Meteorol.*, *128*, 179-197.

Hui, D. F., S. Q. Wan, B. Su, G. Katul, R. Monson, and Y. Q. Luo (2004), Gap-filling missing data in eddy covariance measurements using multiple imputation (MI) for annual estimations, *Agric. For. Meteorol.*, *121*, 93-111.

IPCC (2007), *Climate Change 2007: The Physical Science Basis. Contribution of Working Group I to the Fourth Assessment Report of the IPCC*, Cambridge University Press, Cambridge, 996 pp.

Kaplan, J. O., I. C. Prentice, and N. Buchmann (2002), The stable carbon isotope composition of the terrestrial biosphere: Modeling at scales from the leaf to the globe, *Glob. Biogeochem. Cycles*, *16*, 1060, doi:10.1029/2001GB001403.

Lai, C.-T., J. R. Ehleringer, P. Tans, S. C. Wofsy, S. P. Urbanski, and D. Y. Hollinger (2004), Estimating photosynthetic ^{13}C discrimination in terrestrial CO_2 exchange from canopy to regional scales, *Glob. Biogeochem. Cycles*, *18*, GB1041, doi:10.1029/2003GB002148.

Lloyd, J., B. Kruijt, D. Y. Hollinger, J. Grace, R. J. Francey, S. C. Wong, F. M. Kelliher, A. C. Miranda, G. D. Farquhar, J. H. C. Gash, N. N. Vygodskaya, I. R. Wright, H. S. Miranda, and E. D. Schulze (1996), Vegetation effects on the isotopic composition of atmospheric CO_2 at local and regional scales: Theoretical aspects and a comparison between rain forest in Amazonia and a Boreal Forest in Siberia, *Austr. J. Plant Physiol.*, *23*, 371-399.

Massman, W. J., and X. Lee (2002), Eddy covariance flux corrections and uncertainties in long-term studies of carbon and energy exchanges, *Agric. For. Meteorol.*, *113*, 121-144.

Mauder, M., T. Foken, M. Göckede, C. Liebethal, J. Ruppert, and T. Bertolini (2003), Dokumentation des Experimentes LITFASS-2003,19.5.-20.6.2003, Dokumentation des Experimentes GRASATEM-2003, 14.5.-1.6.2003, *Arbeitsergebnisse 23*, 47 pp, Universität Bayreuth, Abt. Mikrometeorologie, Bayreuth, Germany. Print, ISSN 1614-8916.

Mauder, M., and T. Foken (2004), Documentation and instruction manual of the eddy covariance software package TK2, *Arbeitsergebnisse 26*, 45 pp, Universität Bayreuth, Abt. Mikrometeorologie, Bayreuth, Germany. Print, ISSN 1614-8916.

Miller, J. B., P. P. Tans, J. W. C. White, T. J. Conway, and B. W. Vaughn (2003), The atmospheric signal of terrestrial carbon isotopic discrimination and its implication for partitioning carbon fluxes, *Tellus, Series B: Chemical and Physical Meteorology*, *55*, 197-206.

Moncrieff, J. B., Y. Malhi, and R. Leuning (1996), The propagation of errors in long-term measurements of land-atmosphere fluxes of carbon and water, *Global Change Biol.*, *2*, 231-240.

Morgenstern, K., T. A. Black, E. R. Humphreys, T. J. Griffis, G. B. Drewitt, T. Cai, Z. Nesic, D. L. Spittlehouse, and N. J. Livingston (2004), Sensitivity and uncertainty of the carbon balance of a Pacific Northwest Douglas-fir forest during an El Niño/La Niña cycle, *Agric. For. Meteorol., 123*, 201-219.

Ogée, J., P. Peylin, P. Ciais, T. Bariac, Y. Brunet, P. Berbigier, C. Roche, P. Richard, G. Bardoux, and J. M. Bonnefond (2003), Partitioning net ecosystem carbon exchange into net assimilation and respiration using $^{13}CO_2$ measurements: A cost-effective sampling strategy, *Glob. Biogeochem. Cycles, 17*, 1070, doi:10.1029/2002GB001995.

Ogée, J., P. Peylin, M. Cuntz, T. Bariac, Y. Brunet, P. Berbigier, P. Richard, and P. Ciais (2004), Partitioning net ecosystem carbon exchange into net assimilation and respiration with canopy-scale isotopic measurements: An error propagation analysis with $^{13}CO_2$ and $CO^{18}O$ data, *Glob. Biogeochem. Cycles, 18*, GB2019, doi:10.1029/2003GB002166.

Oncley, S. P., A. C. Delany, T. W. Horst, and P. P. Tans (1993), Verification of flux measurement using relaxed eddy accumulation, *Atmos. Environ., 27A*, 2417-2426.

Oncley, S. P., T. Foken, R. Vogt, C. Bernhofer, H. P. Liu, Z. Sorbijan, A. Pitacco, D. Grantz, and L. Riberio (2000), The EBEX-2000 field experiment, paper presented at 14th Symposium on Boundary Layers and Turbulence, American Meteorological Society, Boston, Aspen, Colorado, 7th-11th August 2000.

Pattey, E., R. L. Desjardins, and P. Rochette (1993), Accuracy of the relaxed eddy-accumulation technique, evaluated using CO_2 flux measurements, *Boundary-Layer Meteorol., 66*, 341-355.

Pearson, R. J., S. P. Oncley, and A. C. Delany (1998), A scalar similarity study based on surface layer ozone measurements over cotton during the California Ozone Deposition Experiment, *J. Geophys. Res., 103*, (D15), 18919-18926.

Phillips, D. L., and J. W. Gregg (2001), Uncertainty in source partitioning using stable isotopes, *Oecologia, 127*, 171-179.

Randerson, J. T., G. J. Collatz, J. E. Fessenden, A. D. Munoz, C. J. Still, J. A. Berry, I. Y. Fung, N. Suits, and A. S. Denning (2002), A possible global covariance between terrestrial gross primary production and C-13 discrimination: Consequences for the atmospheric C-13 budget and its response to ENSO, *Glob. Biogeochem. Cycles, 16*, 1136, doi:10.1029/2001GB001845.

Rebmann, C. (2003), Kohlendioxid-, Wasserdampf und Energieaustausch eines Fichtenwaldes in Mittelgebirgslage in Nordostbayern, PhD thesis thesis, 140 pp, University of Bayreuth, Bayreuth.

Rebmann, C., P. Anthoni, E. Falge, M. Göckede, A. Mangold, J. A. Subke, C. Thomas, B. Wichura, E. D. Schulze, J. D. Tenhunen, and T. Foken (2004), Carbon budget of a spruce forest ecosystem, in *Biogeochemistry of Forested Catchments in a Changing Environment: A german case study*, edited by E. Matzner, pp. 143-159, Springer, Berlin.

Reichstein, M., A. Rey, A. Freibauer, J. Tenhunen, R. Valentini, J. Banza, P. Casals, Y. Cheng, J. M. Grünzweig, J. Irvine, R. Joffre, B. E. Law, D. Loustau, F. Miglietta, W. Oechel, J.-M. Ourcival, J. S. Pereira, A. Peressotti, F. Ponti, Y. Qi, S. Rambal, M. Rayment, J. Romanya, F. Rossi, V. Tedeschi, G. Tirone, M. Xu, and D. Yakir (2003), Modeling temporal and large-scale spatial variability of soil respiration from soil water availability, temperature and vegetation productivity indices, *Glob. Biogeochem. Cycles, 17*, 1104, doi:10.1029/2003GB002035.

Reichstein, M., E. Falge, D. Baldocchi, D. Papale, M. Aubinet, P. Berbigier, C. Bernhofer, N. Buchmann, T. Gilmanov, A. Granier, T. Grünwald, K. Havrankova, H. Ilvesniemi, D. Janous, A. Knohl, T. Laurila, A. Lohila, D. Loustau, G. Matteucci, T. Meyers, F. Miglietta, J.-M. Ourcival, J. Pumpanen, S. Rambal, E. Rotenberg, M. Sanz, J. Tenhunen, G. Seufert, F. Vaccari, T. Vesala, D. Yakir, and R. Valentini (2005), On the separation of net ecosystem exchange into assimilation and ecosystem respiration: review and improved algorithm, *Global Change Biol., 11*, 1424–1439, doi:10.1111/j.1365-2486.2005.001002.x.

Reichstein, M., P. Ciais, D. Papale, R. Valentini, S. Running, N. Viovy, W. Cramer, A. Granier, J. Ogée, V. Allard, M. Aubinet, C. Bernhofer, N. Buchmann, A. Carrara, T. Grünwald, M. Heimann, B. Heinesch, A. Knohl, W. Kutsch, D. Loustau, G. Manca, G. Matteucci, F. Miglietta, J. M. Ourcival, K. Pilegaard, J. Pumpanen, S. Rambal, S. Schaphoff, G. Seufert, J. F. Soussana, M. J. Sanz, T. Vesala, and M. Zhao (2007), Reduction of ecosystem productivity and respiration during the European summer 2003 climate anomaly: A joint flux tower, remote sensing and modelling analysis, *Global Change Biol., 13*, 634-651.

Ruppert, J. (2002), Eddy sampling methods for the measurement of trace gas fluxes, Diploma thesis, 95 pp, University of Bayreuth, Bayreuth.

Ruppert, J., B. Wichura, A. C. Delany, and T. Foken (2002), Eddy sampling methods, a comparison using simulation results, paper presented at 15th Symposium on Boundary Layers an Turbulence, American Meteorological Society, Wageningen, Netherlands, 15-19 July 2002.

Ruppert, J. (2005), ATEM software for atmospheric turbulent exchange measurements using eddy covariance and relaxed eddy accumulation systems + Bayreuth whole-air REA system setup, *Arbeitsergebnisse 28*, 29 pp, Universität Bayreuth, Abt. Mikrometeorologie, Bayreuth, Germany. Print, ISSN 1614-8916.

Ruppert, J., and T. Foken (2005), Messung turbulenter Flüsse von Kohlendioxid und stabilem Kohlenstoffisotop ^{13}C über Pflanzenbeständen mit Hilfe der Relaxed Eddy Accumulation Methode, in Klimatologische und mikrometeorologische Froschungen im Rahmen des Bayreuther Institutes für terrestrische Ökosystemforschung (BITÖK) 1998 - 2004, edited by T. Foken, *Arbeitsergebnisse 29*, 81-104, Universität Bayreuth, Abt. Mikrometeorologie, Bayreuth, Germany. Print, ISSN 1614-8916.

Ruppert, J., M. Mauder, C. Thomas, and J. Lüers (2006a), Innovative gap-filling strategy for annual sums of CO_2 net ecosystem exchange, *Agric. For. Meteorol., 138*, 5-18, doi:10.1016/j.agrformet.2006.03.003.

Ruppert, J., C. Thomas, and T. Foken (2006b), Scalar similarity for relaxed eddy accumulation methods, *Boundary-Layer Meteorol., 120*, 39-63.

Ruppert, J., W. A. Brand, N. Buchmann, and T. Foken (2008a), Whole-air relaxed eddy accumulation for the measurement of isotope and trace-gas fluxes, *J. Geophys. Res.*, prepared manuscript.

Ruppert, J., C. Thomas, J. Lüers, T. Foken, and N. Buchmann (2008b), Ecosystem $^{13}CO_2$ and $CO^{18}O$ isotope discrimination measured by hyperbolic relaxed eddy accumulation, *Glob. Biogeochem. Cycles*, prepared manuscript.

Saleska, S. R., J. H. Shorter, S. Herndon, R. Jiménez, J. B. McManus, J. W. Munger, D. D. Nelson, and M. S. Zahniser (2006), What are the instrumentation requirements for measuring the isotopic composition of net ecosystem exchange of CO_2 using eddy covariance methods?, *Isotopes in Environmental and Health Studies*, *42*, 115-133.

Seibt, U., L. Wingate, J. A. Berry, and J. Lloyd (2006), Non-steady state effects in diurnal ^{18}O discrimination by Picea sitchensis branches in the field, *Plant, Cell and Environment*, *29*, 928-939.

Staudt, K., and T. Foken (2007), Documentation of reference data for the experimental areas of the Bayreuth Centre for Ecology and Environmental Research (BayCEER) at the Waldstein site, *Arbeitsergebnisse 35*, 37 pp, Universität Bayreuth, Abt. Mikrometeorologie, Bayreuth, Germany. Print, ISSN 1614-8916.

Stoy, P. C., G. G. Katul, M. B. S. Siqueira, J. Y. Juang, K. A. Novick, J. M. Uebelherr, and R. Oren (2006), An evaluation of models for partitioning eddy covariance-measured net ecosystem exchange into photosynthesis and respiration, *Agric. For. Meteorol.*, *141*, 2-18.

Thomas, C., J. Ruppert, J. Lüers, J. Schröter, J. C. Mayer, and T. Bertolini (2004), Documentation of the WALDATEM-2003 experiment, 28.4.-3.8.2003, *Arbeitsergebnisse 24*, 59 pp, Universität Bayreuth, Abt. Mikrometeorologie, Bayreuth, Germany. Print, ISSN 1614-8916.

Thomas, C., and T. Foken (2007), Organised Motion in a Tall Spruce Canopy: Temporal Scales, Structure Spacing and Terrain Effects, *Boundary-Layer Meteorol.*, *122*, 123-147.

Thomas, C., J. G. Martin, M. Göckede, M. B. Siqueira, T. Foken, B. E. Law, H. W. Loescher, and G. Katul (2008), Estimating daytime ecosystem respiration from conditional sampling methods applied to multi-scalar high frequency turbulence time series, *Agric. For. Meteorol.*, *148*, 1210-1229, doi:10.1016/j.agrformet.2008.03.002.

Wichura, B., N. Buchmann, and T. Foken (2000), Fluxes of the stable carbon isotope ^{13}C above a spruce forest measured by hyperbolic relaxed eddy accumulation method, paper presented at 14th Symposium on Boundary Layers and Turbulence, American Meteorological Society, Boston, Aspen, Colorado, 7-11 August 2000.

Wichura, B., N. Buchmann, T. Foken, A. Mangold, G. Heinz, and C. Rebmann (2001), Pools und Flüsse des stabilen Kohlenstoffisotopes ^{13}C zwischen Boden, Vegetation und Atmosphäre in verschiedenen Planzengemeinschaften des Fichtelgebirges, *Bayreuther Forum Ökologie (bfö)*, *84*, 123-153.

Wichura, B., J. Ruppert, A. C. Delany, N. Buchmann, and T. Foken (2004), Structure of carbon dioxide exchange processes above a spruce forest, in *Biogeochemistry of Forested Catchments in a Changing Environment: A german case study*, edited by E. Matzner, pp. 161-176, Springer, Berlin.

Wilczak, J. M., S. P. Oncley, and S. A. Stage (2001), Sonic anemometer tilt correction algorithms, *Boundary-Layer Meteorol.*, *99*, 127-150.

Wingate, L., U. Seibt, J. B. Moncrieff, P. G. Jarvis, and J. Lloyd (2007), Variations in ^{13}C discrimination during CO_2 exchange by Picea sitchensis branches in the field, *Plant, Cell and Environment*, *30*, 600-616.

Yakir, D., and X.-F. Wang (1996), Fluxes of CO_2 and water between terrestrial vegetation and the atmosphere estimated from isotope measurements, *Nature*, *380*, 515-517.

Yakir, D., and L. da S. L. Sternberg (2000), The use of stable isotopes to study ecosystem gas exchange, *Oecologia*, *123*, 297-311.

Zhang, J., T. J. Griffis, and J. M. Baker (2006), Using continuous stable isotope measurements to partition net ecosystem CO_2 exchange, *Plant, Cell and Environment*, *29*, 483-496.

Zobitz, J. M., S. P. Burns, M. Reichstein, and D. R. Bowling (2008), Partitioning net ecosystem carbon exchange and the carbon isotopic disequilibrium in a subalpine forest, *Global Change Biol.*, *14*, 1785–1800, doi:10.1111/j.1365-2486.2008.01609.x.

Scalar Similarity for Relaxed Eddy Accumulation Methods

Johannes Ruppert
Department of Micrometeorology, University of Bayreuth, Bayreuth, Germany
Present address: Environmental Measuring Department, Verein Deutscher Zementwerke e.V. (VDZ), Research Institute of the Cement Industry, Duesseldorf, Germany, E-mail: rj@vdz-online.de

Christoph Thomas
Department of Micrometeorology, University of Bayreuth, Bayreuth, Germany
Present address: Department of Forest Science, Oregon State University, Corvallis, OR, USA

Thomas Foken
Department of Micrometeorology, University of Bayreuth, Bayreuth, Germany

Abstract. The relaxed eddy accumulation (REA) method allows the measurement of trace gas fluxes when no fast sensors are available for eddy covariance measurements. The flux parameterisation used in REA is based on the assumption of scalar similarity, i. e. similarity of the turbulent exchange of two scalar quantities. In this study changes in scalar similarity between carbon dioxide, sonic temperature and water vapour were assessed using scalar correlation coefficients and spectral analysis. The influence on REA measurements was assessed by simulation. The evaluation is based on observations over grassland, irrigated cotton plantation and spruce forest.

Scalar similarity between carbon dioxide, sonic temperature and water vapour showed a distinct diurnal pattern and change within the day. Poor scalar similarity was found to be linked to dissimilarities in the energy contained in the low frequency part of the turbulent spectra (< 0.01 Hz).

The simulations of REA showed significant change in b-factors throughout the diurnal course. The b-factor is part of the REA parameterisation scheme and describes a relation between the concentration difference and the flux of a trace gas. The diurnal course of b-factors for carbon dioxide, sonic temperature and water vapour matched well. Relative flux errors induced in REA by varying scalar similarity were generally below ± 10 %. Systematic underestimation of the flux of up to -40 % was found for the use of REA applying a hyperbolic deadband (HREA). This underestimation was related to poor scalar similarity between the scalar of interest and the scalar used as proxy for the deadband definition.

Keywords: Conditional Sampling, Relaxed Eddy Accumulation, Scalar Similarity, Spectral Analysis, Trace Gas Flux

Article published in Boundary-Layer Meteorology, 120, 39-63,
doi:10.1007/s10546-005-9043-3. Published online: 5 August 2006,
www.springer.com/geosciences/meteorology/journal/10546

1. Introduction

In recent years growing interest was developed to measure the turbulent exchange of various trace gases in the surface layer in order to investigate biogeochemical processes. The relaxed eddy accumulation method (REA, Businger and Oncley, 1990) allows flux measurements for many scalar quantities with air analysis in a laboratory when no fast sensors are available for eddy covariance (EC) measurements. In REA the trace gas flux is calculated using a parametrization applying flux-variance similarity (Obukhov, 1960; Wyngaard et al., 1971) and scalar similarity, i. e. similarity in the characteristics of the turbulent exchange. Scalar similarity is defined as similarity in the scalar time series throughout the scalar spectra (Kaimal et al., 1972; Pearson et al., 1998). Scalar similarity requires that scalar quantities are transported with similar efficiency in eddies of different size and shape.

Differences in the turbulent exchange of scalar quantities and therefore in scalar similarity must be expected when sources and sinks are distributed differently within the ecosystem, e. g. within tall vegetation, or when they show significant changes in their source/sink strength (Katul et al., 1995; Andreas et al., 1998a; Simpson et al., 1998; Katul et al., 1999). Scalar quantities such as carbon dioxide, temperature and water vapour have different sources and sinks within a plant canopy and exhibit differences in their turbulent exchange. While canopy top surfaces are the main source for heating of air during the day, carbon dioxide and water vapour are consumed and respectively released mainly within the canopy. Temperature and to some degree also water vapour actively influence turbulent exchange and are therefore called active scalars, whereas carbon dioxide does not effect buoyancy and is regarded as passive scalar quantity (Katul et al., 1996; Pearson et al., 1998).

In particular for the REA method scalar similarity is needed for the derivation of b-factors (Oncley et al., 1993 and Section 2). This parameterisation requires similarity in the shape of the joint frequency distribution (JFD) of the scalar of interest and a scalar quantity for which the flux can be determined independently, e. g. with EC (Wyngaard and Moeng, 1992; Katul et al., 1996). Information on the vertical wind speed in the JFDs for two scalar quantities is identical. The only difference in the shape of the JFDs results from differences in the scalar time series. Scalar similarity needed for REA therefore can be analyzed by directly comparing the scalar time series and the shape of their frequency distribution or spectra (Kaimal et al., 1972; Pearson et al., 1998).

In this paper we investigate the degree of scalar similarity between three different scalar quantities (carbon dioxide, sonic temperature and water vapour) throughout the diurnal cycle. The analysis is done on the basis of high-frequency time series recorded during field experiments over grassland, an irrigated cotton plantation and a spruce forest. The study (i) characterizes typical changes of scalar similarity during the diurnal cycle for the three surface types. (ii) Wavelet variance spectra are used to test the influence of coherent structures on the turbulent transport and to identify the time scales on which the lack of scalar similarity in the transport of scalars appears. (iii) Finally we evaluate the error that is introduced in flux measurements with REA methods due to lack in scalar similarity. Effects from scalar similarity on flux measurements using REA methods are investigated by simulation.

In the analysis we compare classical REA with those modifications of the REA method, that are able to significantly increase concentration differences of the scalar quantities in updraft and downdraft samples by introducing hyperbolic deadbands (hyperbolic relaxed eddy accumulation, HREA, Bowling et al., 1999b, see Section 2). HREA can increase the concentration difference above critical limits of sensor resolution, e.g. for isotope flux measurements. At the same time the restriction on few samples for flux determination representing strong updrafts and downdrafts increases their vulnerability to the lack of scalar similarity.

2. Theory

The eddy covariance method relies on Reynolds decomposition of the turbulent signals of vertical wind speed w and the scalar of interest c ($w = \overline{w} + w'$, $c = \overline{c} + c'$). The overbar denotes temporal averaging for a typical measurement period of 30 min. Primes denote the fluctuation of a quantity around its average value. A zero mean vertical wind speed is assumed ($\overline{w} = 0$). The turbulent flux is determined by $\overline{w'c'}$. This method of direct flux measurement is the basis and reference for the relaxed eddy accumulation method.

2.1. Relaxed Eddy Accumulation (REA)

REA measurements rely on conditional sampling (Desjardins, 1972; Hicks and McMillen, 1984) of the scalar of interest into reservoirs for updraft and downdraft air samples. The temporal averaging of scalar samples occurs physically within the two reservoirs. The 'relaxation' means that samples are taken with a constant flow rate and are not weighted according to the vertical wind speed (Foken et al., 1995). The sample consequently lacks information on the vertical wind speed. This lack is compensated by relying on flux-variance similarity and the parametrisation of the proportionality factor b, resulting in the basic Equation (1) for the flux determination in REA (Businger and Oncley, 1990).

$$\overline{w'c'} = b\,\sigma_w(\overline{c_\uparrow} - \overline{c_\downarrow}) \tag{1}$$

σ_w is the standard deviation of the vertical wind speed. $\overline{c_\uparrow}$ and $\overline{c_\downarrow}$ are the average scalar values for updrafts and downdrafts. The b-factor is well defined with a value of 0.627 for an ideal Gaussian joint frequency distribution (JFD) of w and c (Baker et al., 1992; Wyngaard and Moeng, 1992). However, turbulent transport especially over rough surfaces often violates the underlying assumption of a linear relationship between w and c (Katul et al., 1996). Excursions from the linear relation occur due to skewness in the JFD and result in smaller b-factors from parameterisation (Milne et al., 2001). Gao (1995) found this effect to be most pronounced close to the canopy top and suggested a scaling of the b-factors with measurement height. b exhibits a relative independence from stability due to the characteristics of σ_w and σ_c (Foken et al., 1995). For many experimental data b was found to range from 0.54 to 0.60 on average. However, Andreas et al. (1998b) and Ammann and Meixner (2002)

found an increase of average b-factors under stable conditions in the surface layer. The b-factors can vary also significantly for individual 30 min integration intervals (Businger and Oncley, 1990; Baker et al., 1992; Oncley et al., 1993; Pattey et al., 1993; Beverland et al., 1996; Katul et al., 1996; Bowling et al., 1999a; Ammann and Meixner, 2002), which restricts the use of a fixed b-factor.

2.2. Wind-Deadband

The above mentioned values for b were determined for REA without the use of a deadband in which all updraft and downdraft samples are collected. However, normally a wind-deadband is defined by an upper and lower threshold for vertical wind speed around zero vertical wind speed (w_0). All samples within this wind-deadband, which fall between the upper and lower threshold values, are rejected during REA sampling for technical reasons (Oncley et al., 1993; Foken et al., 1995). The wind-deadband H_w is normally scaled with the standard deviation of the vertical wind speed σ_w, Equation (2).

$$\left| \frac{w'}{\sigma_w} \right| \leq H_w \tag{2}$$

The use of a wind-deadband changes the definition of what is regarded as updraft ($\uparrow$: $w'/\sigma_w > H_w$) and downdraft ($\downarrow$: $w'/\sigma_w < -H_w$) during REA sampling. The advantage for technical realization of REA is, that the use of a deadband firstly reduces the frequency of valve switching for sample segregation significantly. Secondly, the use of a deadband increases the scalar difference ($\overline{c_\uparrow} - \overline{c_\downarrow}$) and thereby reduces errors in the chemical analysis. Increased scalar differences decrease corresponding b-factors according to Equation (1). A functional dependency of average b-factors on wind-deadband size was determined for the necessary adjustment ($b_{(H_w)}$, Businger and Oncley, 1990, Pattey et al., 1993, Katul et al., 1996, Ammann and Meixner, 2002). Nevertheless, the potential for variation of individual b-factors around adjusted average values for b persists. The use of b-factors individually determined from a proxy scalar may be able to better reflect the correct b-factor for a certain measurement period and thereby minimize REA flux errors. This determination of individual b-factors requires good scalar similarity between the scalar of interest and the proxy scalar.

2.3. Hyperbolic Relaxed Eddy Accumulation (HREA)

Application of a deadband with hyperbolas as thresholds does not exclude samples with small fluctuations of the vertical wind speed w' only, but also samples with small fluctuations of the scalar quantity c' are excluded (Bowling et al., 1999b; Wichura et al., 2000; Bowling et al., 2001; Bowling et al., 2003). Thereby HREA increases scalar differences in the reservoirs even more. The hyperbolic criteria (Wallace et al., 1972; Lu and Willmarth, 1973; Shaw et al., 1983; Shaw, 1985) means rating individual samples by their contribution to the EC flux $\overline{w'c'}$. All samples below a certain threshold of 'importance' (H_h) are not collected into the reservoirs. The hyperbolic deadband is defined as

$$\left| \frac{w'c'}{\sigma_w \sigma_c} \right| \leq H_h. \tag{3}$$

The additional increase of the scalar differences in HREA is important when measurement precision for the scalar of interest is limited. Then HREA can significantly increase the signal to noise ratio for the flux measurement of a scalar (Bowling et al., 1999b).

Poor scalar similarity has the potential to induce error in the estimate of b-factors for the scalar of interest from the b-factors determined using data of a proxy scalar. From Equation (1) it is obvious, that any error present in the b-factors will transfer linearly into errors in the fluxes determined by REA or HREA. The use of a deadband in REA or HREA concentrates sampling towards strong updrafts and downdrafts, which increases the effect of non-linearity in the JFD on b-factors (Katul et al., 1996). Deadbands thereby have the potential to increase dissimilarity of b-factors due to poor scalar similarity. HREA uses the assumption of scalar similarity not only when inferring the b-factor from a proxy scalar. In addition scalar similarity is assumed when defining the hyperbolic deadbands during the measurement process from fast measurements of the proxy scalar (Bowling et al., 1999b). Therefore, the validity of scalar similarity is even more essential for HREA methods than for classical REA.

3. Experimental Data

Turbulence data with high time resolution from three field experiments over different surfaces were selected for this analysis.

Measurements of the experiment GRASATEM-2003 (Grassland Atmospheric Turbulent Exchange Measurements 2003) were performed over short cut grassland (canopy height $h_c = 0.12\,\mathrm{m}$) during the LITFASS-2003 experiment (Beyrich et al., 2004) at the Falkenberg experimental site of the German Meteorological Service (Meteorological Observatory Lindenberg), Germany ($52^o10'$ N, $14^o07'$ E, 71 m a.s.l.). A sonic anemometer (USA-1, METEK, Meteorologische Messtechnik GmbH, Elsmhorn, Germany) was used to obtain wind vector and sonic temperature and an open path sensor (LI-7500, LI-COR Inc., Lincoln, NE, USA) measured water vapour and carbon dioxide density at 2.25 m above ground. The flux source areas (footprints) of the data used in this analysis showed good homogeneity regarding the grass canopy height with some variability in soil humidity.

The EBEX-2000 (Energy Balance Experiment 2000, Oncley et al., 2002) data set was acquired in the San Joaquin Valley, CA, USA ($36^o06'$ N, $119^o56'$ W, 67 m a.s.l.). The experimental site was located in the middle of an extended irrigated cotton plantation on flat terrain. Canopy height was about 0.9 m. A sonic anemometer (CSAT-3, Campbell Scientific Ltd., Logan, UT, USA) measured 3 dimensional wind vectors and sonic temperature T_s. An open path analyzer (LI-7500) was used to measure water vapour and carbon dioxide density. The sampling rate was 20 Hz. Instruments were installed on a tower at a height of 4.7 m above ground.

During the WALDATEM-2003 (Wavelet Detection and Atmospheric Turbulent Exchange Measurements 2003) experiment a set of micrometeorological measurements was performed on a 33 m high tower over a spruce forest (*Picea abies, L.*). This study uses data from a sonic anemometer (R3-50, Gill Instruments Ltd., Lymington, UK) and an open path analyzer (LI-7500) installed at 33 m. The forest has a mean canopy height of 19 m with a plant area index (PAI) of 5.2. Understory vegetation is sparse and consists of small shrubs and grasses. The site Waldstein/Weidenbrunnen (GE1-Wei) is part of the FLUXNET network and is located in the Fichtelgebirge mountains in Germany ($50^o08'$ N, $11^o52'$ E, 775 m a.s.l.) on a slope of 2^o (Rebmann et al., 2005; Thomas and Foken, 2005). A detailed description of the site can be found in Gerstberger et al. (2004). One of the objectives of the GRASATEM-2003 and WALDATEM-2003 experiments was the determination of ^{13}C and ^{18}O isotope fluxes using the HREA method.

4. Method of Analysis

For our study we selected carbon dioxide to be the scalar of interest, for which a flux measurement with REA or HREA shall be performed. Sonic temperature T_s and water vapour density ρ_{H2O} serve as proxy scalars which are tested for sufficient similarity in their turbulent exchange compared to carbon dioxide density ρ_{CO_2}.

4.1. Data selection and preparation

Daytime periods of the three experiment days (GRASATEM-2003: May 24, 2003, EBEX-2000: August 20, 2000, WALDATEM-2003: July 8, 2003) representing different surface types (shortcut grassland, irrigated cotton, spruce forest) were selected for the analysis in this paper after assessing the quality of the flux measurements. This assessment was based on a quality check of the turbulent time series according to Foken et al. (2004) with a test on stationarity and developed turbulent conditions. The three days represent typical diurnal cycles of exchange patterns found during the experiments and provide a continuous high quality data record throughout the diurnal cycle. During the selected days only few data from the early morning (EBEX-2000) and late afternoon (GRASATEM-2003 and EBEX-2000) did not meet the quality criterion. Data from these periods were therefore not included in the analysis. The wind vectors derived from the sonic anemometer measurements were rotated using the planar fit method (Wilczak et al., 2001). Outliers in the scalar data were removed by applying a 5σ criteria ($\mu \pm 5\sigma$). In order to correct time lags between the different sensors each time series was shifted according to the maximum cross-correlation with the vertical wind speed. All subsequent analysis were performed on 30 min subsets of the data.

4.2. Scalar similarity

As a simple measure of scalar similarity we use the scalar correlation coefficient $r_{c,c_{proxy}}$ calculated from the fluctuations in the time series of the scalar of interest c and the proxy scalar c_{proxy}.

$$r_{c,c_{proxy}} = \frac{\overline{c' c'_{proxy}}}{\sigma_c \sigma_{c_{proxy}}} \tag{4}$$

The scalar correlation coefficient integrates similarity and dissimilarity over the whole frequency range of the time series. In studies by Gao (1995) and Katul and Hsieh (1999) scalar correlation coefficients were already used to discuss similarity between the turbulent exchange of temperature and water vapour.

4.3. Spectral analysis

Here, the method for spectral analysis using wavelet functions will be outlined briefly. More details can be found in Thomas and Foken (2005). First, any missing data and outliers detected were filled using an interpolation (Akima, 1970). All time series were block averaged to 2 Hz significantly reducing computation time for the wavelet analysis. Scalar time series were normalized to c'/σ_c. Vertical wind speed w was normalised to w/σ_w. In a second step, time series were low-pass filtered by a wavelet filter decomposing and recomposing the time series using the biorthogonal set of wavelets BIOR5.5. The use of this set of wavelet functions is preferred as their localisation in frequency is better than e. g. that of the HAAR wavelet (Kumar and Foufoula-Georgiou, 1994). This filter discards all fluctuations with event durations $D < D_c$, where D_c is the critical event duration chosen according to the spectral gap between high-frequency turbulence and low-frequency coherent structures. A default value of D_c=6.2 s was chosen for all datasets, which is in close agreement to other authors using similar values, e. g. D_c=5 s (Lykossov and Wamser, 1995), D_c=7 s (Brunet and Collineau, 1994) or D_c=5.7 s (Chen and Hu, 2003).

A continuous wavelet transform (Grossmann and Morlet, 1984; Grossmann et al., 1989; Kronland-Martinet et al., 1987) of the prepared and zero-padded time series f(t) was performed using the complex Morlet wavelet as analysing wavelet function $\Psi(t)$,

$$T_p(a,b) = \frac{1}{a^p} \int_{-\infty}^{+\infty} f(t) \Psi \left(\frac{t - b_t}{a} \right) dt \tag{5}$$

where $T_p(a,b)$ are the wavelet coefficients, a the dilation scale, b_t the translation parameter and the normalisation factor $p = 1$ in our case. The complex Morlet wavelet function is located best in frequency domain and thus found appropriate to extract the intended information about large scale flux contributions e. g. from coherent structures (Thomas and Foken, 2005). The dilation scales a used to calculate the continuous wavelet transform represent event durations D ranging from 6 s to 240 s. The event duration D can be linked to the dilation scale a of the wavelet transform by (e. g. Collineau and Brunet, 1993)

$$D = \frac{1}{2} f^{-1} = \frac{a\,\pi}{f_s\,\omega^0_{\Psi_{1,1,0}}}, \tag{6}$$

where f is the frequency corresponding to the event duration, f_s the sampling frequency of the time series and $\omega^0_{\Psi_{1,1,0}}$ the center frequency of the mother wavelet

function. For a sine function, the event duration D is half the length of a period. The minimum of analysed event durations was chosen according to the critical event duration D_c of the low-pass filter. The wavelet variance spectrum was then determined by

$$W_p(a) = \int_{-\infty}^{+\infty} |T_p(a,b)|^2 db. \tag{7}$$

Wavelet variance spectra $W_p(a)$ were multiplied by the angle frequency ω. The correlation coefficient of the wavelet variance spectra for the different scalar quantities $r_s(\rho_{CO_2}, c_{proxy})$ was calculated as objective measure of similarity in the distribution of energy in the frequency range (Equation (8)).

$$r_s(\rho_{CO_2}, c_{proxy}) = \frac{\overline{W(D)_{\rho_{CO_2}} W(D)_{c_{proxy}}}}{\sigma_{W(D)_{\rho_{CO_2}}} \sigma_{W(D)_{c_{proxy}}}}. \tag{8}$$

$W(D)$ denotes the wavelet variance, i. e. the spectral density at event duration, σ the standard deviation and the overbar depicts the phase mean over the fluctuations. The spectral correlation in the scalar time series is evaluated for two ranges of event durations, short event durations of 6 s to 60 s and long event durations of 60 s to 240 s.

4.4. REA and HREA simulation

REA and HREA sampling was simulated using the high resolution time series data for the vertical wind speed fluctuation w' and the scalar quantities (T_s, ρ_{H2O}, ρ_{CO_2}). Time series were sampled and segregated into updrafts, deadband and downdrafts according to the deadband definition (wind-deadband H_w, Equation (2), or hyperbolic deadband H_h, Equation (3)) and the sign of the vertical wind speed fluctuation w'. Updrafts and downdrafts were averaged to yield the scalar difference ($\overline{c_\uparrow} - \overline{c_\downarrow}$). The b-factors were calculated by rearranging Equation (1) yielding

$$b = \frac{\overline{w'c'}}{\sigma_w(\overline{c_\uparrow} - \overline{c_\downarrow})}. \tag{9}$$

Comparison of b-factors calculated for the scalar of interest (b) and a proxy scalar (b_{proxy}) directly yields the relative flux errors ε due to the linear relationship in Equation (1).

$$\varepsilon = \frac{b_{proxy} - b}{b} \tag{10}$$

In the simulation any error resulting from the instrumentation used for REA or HREA sampling in the field is avoided. For the deadband definitions the simulation is based on statistics of turbulent time series from the complete 30 min sampling interval. This means $\overline{w}$, σ_w and for HREA also $\overline{c}$ and σ_c of the proxy scalar are well known. These parameters must be estimated online during field sampling with REA or HREA, when only previously recorded data is available. Therefore the analysis of these simulations focuses on the methodological error of REA and HREA.

5. Results and Discussion

5.1. Scalar correlation coefficients

Absolute values of scalar correlation coefficients $r_{CO_2,Ts}$ and r_{CO_2,H_2O} for three days are presented in Figure 1a, Figure 1c and Figure 1e as a measure for scalar similarity. For most cases the maximal absolute correlation coefficients are in the order of 0.9. Smaller values and significant changes in the scalar correlation within the diurnal cycle are found for all three surface types (grassland, irrigated cotton and spruce forest) for many days. The varying scalar similarity is pronounced on the exemplary days presented in Figure 1 which were selected for this study because of their continuous data record. Within the diurnal pattern three cases could be distinguished, which will be used for the discussion of changes in scalar correlation as well as spectral correlation (Section 5.2). The definition of these cases is supported by the analysis of the difference of the absolute correlation coefficients ($\Delta_{|r|-|r|}$=$|r_{CO_2,Ts}|$-$|r_{CO_2,H_2O}|$) presented as average for distinct periods in Figure 1b, Figure 1d and Figure 1f.

- Case 1: During the morning hours up to about 0900-1000 local time on all three days high scalar correlation of $r_{CO_2,Ts}$ indicates better scalar similarity compared to r_{CO_2,H_2O}. In the WALDATEM-2003 data this situation persists for most of the day. Very early morning data in EBEX-2000 did not meet the quality criteria (see Section 3) and were therefore not included in the analysis. The large confidence interval for the first value in Figure 1d results from the small number of high quality data remaining for the analysis of Case 1 in the morning.
- Case 2 describes a situation in which both $r_{CO_2,Ts}$ and r_{CO_2,H_2O} show high scalar correlation. This situation can be found in some of the midday periods in the WALDATEM-2003 data and before noon in EBEX-2000 data. If we take taking into account that $r_{CO_2,Ts}$ of about 0.9 is already indicating high scalar correlation, it it is also found during the early afternoon in the EBEX-2000 data.
- Case 3 denotes situations in which $r_{CO_2,Ts}$ shows low scalar correlation compared to r_{CO_2,H_2O}. Such situations are visible in the late afternoon hours (∼1600 local time) in the GRASATEM-2003, EBEX-2000 and WALDATEM-2003 datasets. These afternoon periods were characterized by diminishing buoyancy fluxes, near neutral or even slightly stable stratification and persistent latent heat fluxes.

The loss of scalar correlation in $r_{CO_2,Ts}$ between 1015 to 1300 local time in the GRASATEM-2003 data (Figrue 1a and Figure 1b) corresponds to a period with significantly reduced global radiation due to cirrus clouds. A large confidence interval for the last value in Figure 1b results from the small number of data within the represented period. Nevertheless, the corresponding level of statistical significance for a difference between $r_{CO_2,Ts}$ and r_{CO_2,H_2O} for this period is $p = 0.064$. The scalar correlation during the three days approximately follows the change from Case 1 in the morning, Case 2 for some periods around noon or during the early afternoon

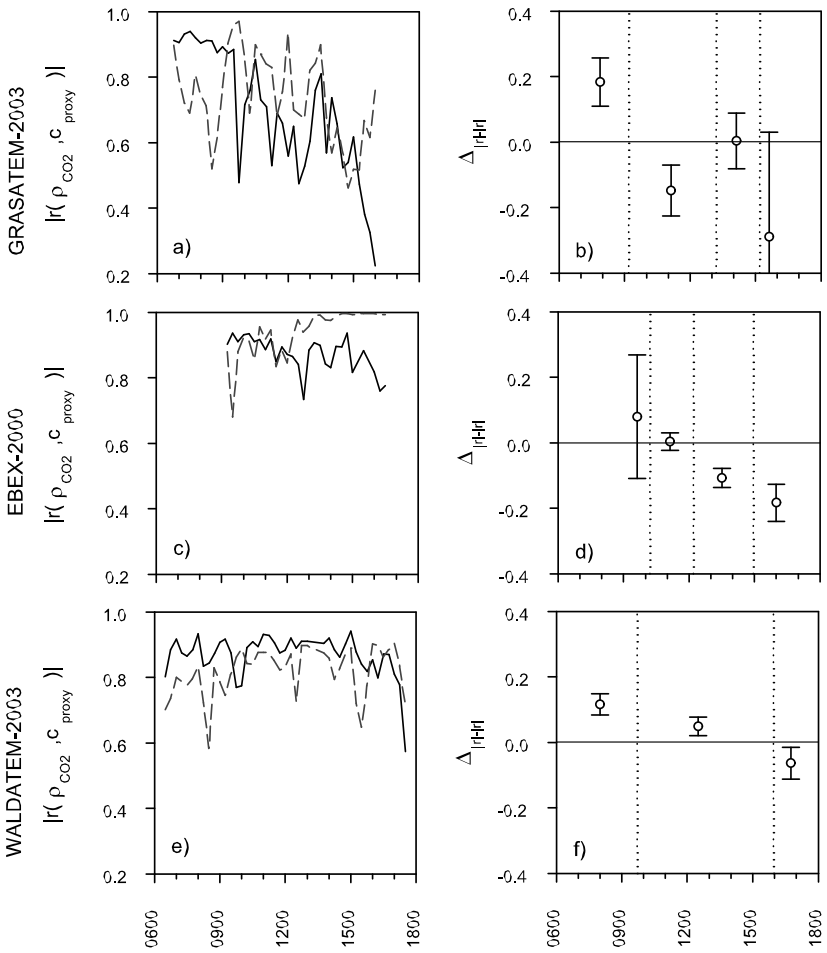

Figure 1. Diurnal course of scalar correlation coefficients (absolute values) calculated from carbon dioxide density ρ_{CO_2} and sonic temperature T_s (solid lines) or water vapour density ρ_{H2O} (dashed lines) for the three datasets from GRASATEM-2003 (a), EBEX-2000 (c) and WALDATEM-2003 (e). The averaged difference of the absolute scalar correlation coefficients $\Delta_{|r|-|r|}$ for distinct periods is given in (b), (d) and (f) correspondingly. The dotted lines indicate the segregation of these periods. Error bars represent the 95% confidence interval of the average differences calculated for each period. The averaged difference between the absolute correlation coefficients is statistically significant ($p < 0.05$) if the confidence interval does not include zero. Time is indicated as local time.

and Case 3 in the late afternoon or early evening. This pattern is exhibited very clearly in the EBEX-2000 data, which represent an ideal diurnal cycle of global radiation.

Results presented in Figure 1 show that significant temporal changes in scalar similarity linked to source and sink strength must be expected even over short vegetation, where sources and sinks are located close together in the vertical profile.

5.2. Spectral analysis

In order to identify possible reasons for the lack of scalar similarity we analyzed wavelet variance spectra computed from the scalar time series. The comparison of these spectra allows to identify on which temporal scales the characteristics of turbulent transport correspond or differ. The frequency range was selected to cover typical frequencies of coherent structures commonly found in turbulent time series from the roughness sublayer (Thomas and Foken, 2005) in order to assess their contribution to changes in scalar similarity.

Figure 2 shows three exemplary wavelet variance spectra $W_p(a) \cdot \omega$ for the cases distinguished in the previous section based on the scalar correlation coefficients (Figure 1). All three spectra show very good similarity for the three scalars T_s, ρ_{H_2O} and ρ_{CO_2} in short temporal scales. Major deviations are only found for ρ_{H_2O} in Figure 2a (Case 1) and for T_s in Figure 2c (Case 3) in the longer time scales (D >60 s and D >40 s). The spectra in Figure 2b reveal a very good match of all three scalars (Case 2) over the complete range of event durations (6 s to 240 s). The visual assessment of the match in the spectra throughout the complete diurnal course for the EBEX-2000 data corresponded to the findings for scalar similarity based on the scalar correlation coefficients i.e. poor similarity between ρ_{H_2O} and ρ_{CO_2} in the morning (Figure 2a) and poor similarity between T_s and ρ_{CO_2} in the late afternoon (Figure 2c). Differences in the spectra occurred solely in the longer time scales with the exemption of spectra after 1600. After 1600 differences were present also in shorter event durations due to the diminishing buoyancy flux which reduces the energy throughout the spectra.

As objective measure for spectral correlation the spectral correlation coefficient, Equation (8), is presented in Figure 3. In order to validate the finding from the visual assessment of wavelet variance spectra, spectral correlation was calculated separately for shorter (6 s to 60 s) and longer (60 s to 240 s) event durations. High values for the spectral correlation in Figure 3a, Figure 3c and Figure 3e confirm that scalar similarity is good for the range of short event durations over all three surface types. However, the spectral correlation for long event durations (Figure 3b, Figure 3d and Figure 3f) shows significant fluctuations. Poor scalar similarity measured with the scalar correlation coefficients must therefor be attributed primarily to processes on larger temporal scales (event durations > 60 s or frequencies < 0.01 Hz). Dissimilarity on these scales can arise from temporal changes of source/sink strength or due to convective or advective processes. A high degree of scatter is present in the spectral correlation calculated for individual 30 min periods. After smoothing the time series of spectral correlation with a running average (lines), the diurnal changes in similarity in the longer timescales correspond approximately to the scalar

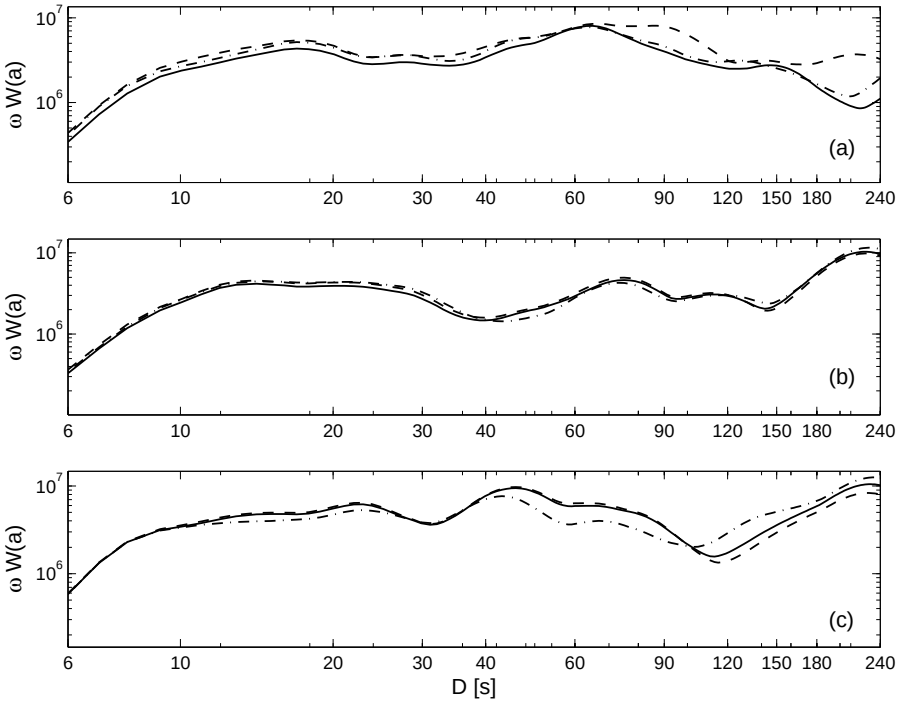

Figure 2. Spectra of the normalised wavelet variance ωW versus event duration D of the carbon dioxide ρ_{CO_2} (solid line), sonic temperature T_s(dashed line) and water vapour ρ_{H_2O} (dash-dotted line)based on data from the EBEX-2000 experiment on August 20, 0915 to 0945 (a), 1430 to 1500 (b) and 1545 to 1615 (c) local time.

correlation (Figure 1) and the results for spectral correlation can be compared to the findings in Section 5.1 for the three cases distinguished there:

Case 1 is found correspondingly to the results on scalar correlation for all three surface types in the morning hours and for the entire afternoon in the WALDATEM-2003 data. Case 2 is found between 1300 and 1500 in the EBEX-2000 data and around noon in the WALDATEM-2003 data. The GRASATEM-2003 data shows poor spectral correlation for the rest of the day after a cloud cover appeared at 10 h. Case 3 is only visible clearly in the spectral correlation calculated from the EBEX-2000 data of the late afternoon. The general features of scalar similarity between the three scalar quantities distinguished with the Cases 1 and 2 are well reflected in the spectral correlation for the long time scales. Dissimilarity in periods with diminishing buoyancy fluxes seems to be reflected less adequately by the spectral correlation for long event durations.

Pearson et al. (1998) studied scalar similarity by comparing non-dimensional power spectra and found good agreement in frequency ranges above 0.01 Hz for temperature, water vapour and ozone. Results presented in Figure 2 and Figure 3 affirm that scalar similarity is relatively good for short event durations. However, we

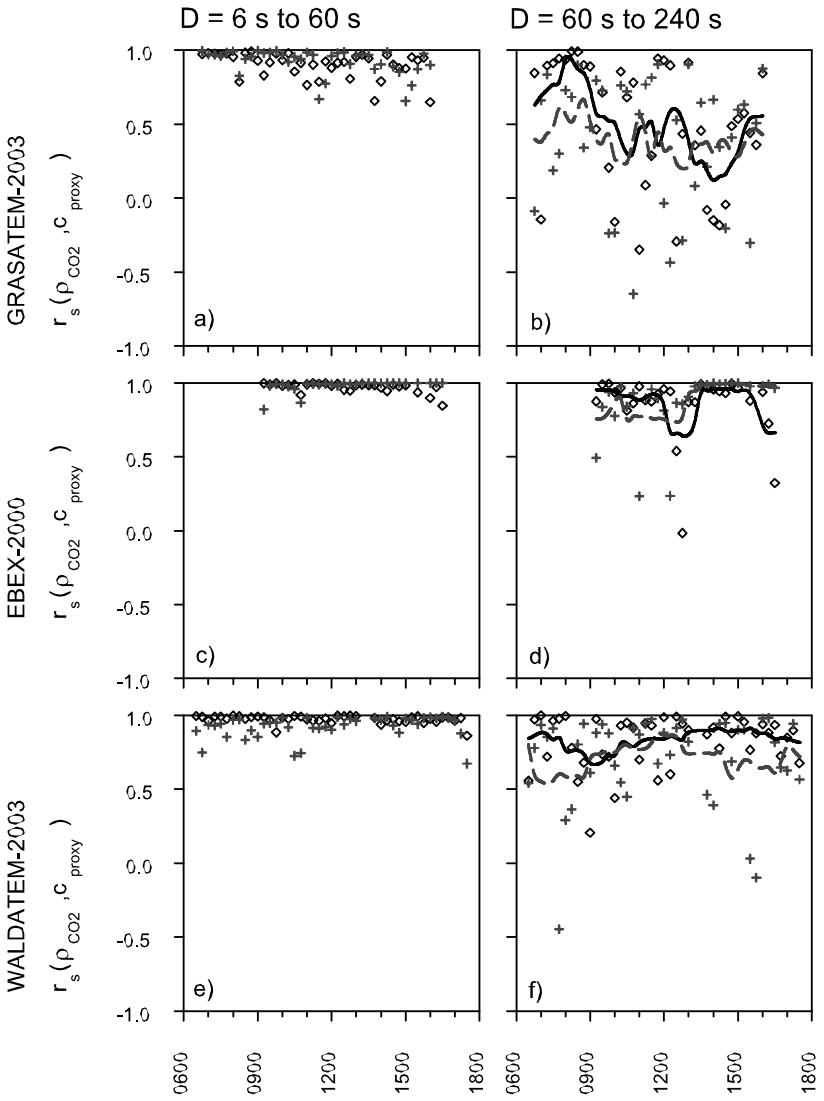

Figure 3. Spectral correlation between ρ_{CO_2} and T_s (diamonds, solid line) and ρ_{CO_2} and ρ_{H_2O} (crosses, dashed line). Lines represent the running average of the time series of spectral correlation for individual 30 min periods (symbols). (a), (c) and (e) show the correlation coefficients for short event durations D from 6 to 60 s. (b), (d) and (f) show the correlation coefficients for long event durations D from 60 to 240 s.

find that longer event durations ($D > 60\,\mathrm{s}$ corresponding to frequencies $< 0.01\,\mathrm{Hz}$) have to be included in the assessment of scalar similarity. McNaughton and Laubach (1998) showed that unsteadiness in the mean wind and internal boundary layers induced dissimilarity between eddy diffusivities for temperature and water vapour. Gao (1995), Katul et al. (1996) and Andreas et al. (1998b) relate differences in the shape of organized (coherent) structures in the turbulent exchange of scalar quantities to differences in b-factors used in REA. From our spectral analysis most of the variability in scalar similarity has to be attributed to event durations that are even larger ($D > 60\,\mathrm{s}$) than typical event durations of mechanically induced coherent structures in the roughness sublayer.

Combined with the notion, that spectral correlation was predominantly high for the short event durations, we have confidence, that observations of scalar fluctuations on long time scales with slow instruments can already deliver most of the information needed for the assessment of scalar similarity. This is of importance for REA or HREA measurements, when no fast sensor is available for the scalar of interest. In such a situation no data can be generated for the determination of scalar correlation, Equation (4), or the spectral correlation, Equation (8) for short event durations. The use of slow sensors would allow one to assess scalar similarity for long event durations for many different trace gases. Similarity in event durations of longer than 60 s could also be investigated by air sampling in flasks and subsequent laboratory analysis.

For an application of this method of assessment of scalar similarity, additional care has to be taken, when fluxes of the proxy scalar become very small, because poor similarity may not be reflected adequately in the spectral correlation, e. g. diminishing buoyancy fluxes in the late afternoon (Case 3). An analysis of scalar similarity by spectral analysis on more extended time scales was reported by Watanabe et al. (2000) for the assessment of the 'Bandpass Eddy Covariance method' (e. g. Hicks and McMillen, 1988, Horst and Oncley, 1995). While achieving relatively good latent heat flux results using fast temperature measurements for the spectral correction of a slow humidity sensor, flux errors became large during times with small sensible heat fluxes, which confirms our finding for Case 3.

5.3. b-FACTORS FROM REA AND HREA SIMULATION

b-factors from simulations of REA with a wind-deadband of $H_w = 0.6$ (classical REA, abbreviated with REA 0.6 here after) on average met the values predicted from models (e.g. Pattey et al., 1993: $b_{(H_w=0.6)} = 0.394$) during all three days. However, results for the EBEX-2000 data (Figure 4a and 4b) show a diurnal variation of b-factors in the range of 0.36 to 0.41 with maximum values shortly after noon. This means that the use of the fixed average b-factor would result in flux errors with a systematic diurnal course. The diurnal course does not originate from a change in σ_w, which remains relatively constant for the EBEX-2000 data (0.31 ± 0.02). At the same time there is good agreement in the diurnal course of b-factors calculated for carbon dioxide, sonic temperature and water vapour. The use of a variable b-factors determined from a proxy scalar can therefore reduce REA flux errors.

Figure 4c and 4d display a similar diurnal trend of b-factors for HREA with a hyperbolic deadband size of $H_h = 1.0$ (abbreviated with HREA 1.0 here after). Values in the range of 0.15-0.27 correspond to the range of 0.22 ± 0.05 found

by Bowling et al. (1999b). The ratio of b-factors for REA 0.6 and HREA 1.0 is proportional to the increase in scalar difference ($\overline{c_\uparrow} - \overline{c_\downarrow}$, Equation (1)) that can be achieved by changing to HREA 1.0 when σ_w is more or less constant. For the EBEX-2000 data the increase in scalar difference for HREA 1.0 compared to REA 0.6 averages to 1.65±0.13. b-factors for the proxy scalars T_s and ρ_{H_2O} (Figure 4c and 4d, unfilled symbols) are the result of segregating c_{proxy} time series into updrafts and downdrafts with a hyperbolic deadband definition based on the same c_{proxy} data. If we would apply hyperbolic deadbands defined on the carbon dioxide record for the simulation of HREA 1.0 for carbon dioxide (our scalar of interest) the match between b-factors would be similar to the match found for REA 0.6 (Figure 4a and 4b). However, we have to rely on a deadband definition from fast measurements of the proxy scalar during HREA sampling of the scalar of interest in the field. In order to give realistic results of the methodological error in HREA we used either T_s (Figure 4c) or ρ_{H_2O} (Figure 4d) as proxy scalar for the deadband definition in the simulation of HREA 1.0 for carbon dioxide (filled triangles).

Besides the diurnal trend we see an offset in the b-factors for most sampling periods with higher b-factors for the scalar of interest ρ_{CO_2} than for the proxy scalars. The increased b-factors are a result of decreased scalar differences ($\overline{c_\uparrow} - \overline{c_\downarrow}$) according to Equation (1) because Flux $\overline{w'c'}$ and σ_w stay the same for one sampling period of 30 min. The reduction in scalar difference can be explained by small dissimilarities between scalar of interest and proxy scalar. A hyperbolic deadband definition with a mismatch of the JFDs leads to some inefficiency in the selection of large positive and negative scalar fluctuations. The small inefficiency in correctly sampling the extreme scalar fluctuations causes decreased scalar difference and results in the observed offset of b-factors.

5.4. Relative flux errors in REA and HREA

The difference in b-factors is the basis for the determination of relative flux errors ε, Equation (10). Our results show small relative flux errors for REA 0.6 when using a proxy scalar for the determination of b-factors instead of using a fixed b-factor. Scatter in ε, i. e. the risk of error in the flux, increases slightly with decreasing scalar correlation, but generally stays below ±10 % except for very few outliers (Figure 5a to 5d). ε does not show signs of significant systematic underestimation or overestimation of fluxes, so that classical REA 0.6 can be regarded as relatively robust against the changes in scalar similarity.

This is in agreement with studies finding a relative stability for the b-factor and small errors in REA when using a wind-deadband size H_w of 0.6 to 0.8 (Oncley et al., 1993; Foken et al., 1995; Ammann and Meixner, 2002). Nevertheless, the scaling of the scatter in ε indicates, that the scalar correlation coefficient is an appropriate measure for the description of scalar similarity required for REA methods.

A significant influence of scalar similarity on ε in HREA is visible in Figure 6. The systematic underestimation of the flux correlates with scalar correlation and linear regressions lead to similar coefficients of determination (r^2) for the use of either of the two proxy scalars. A larger degree of scatter in the relative flux errors found for the GRASATEM-2003 data (Figure 6a and Figure 6b) and consequently a reduced coefficient of determination in Figure 6b are the result of small absolute fluxes during

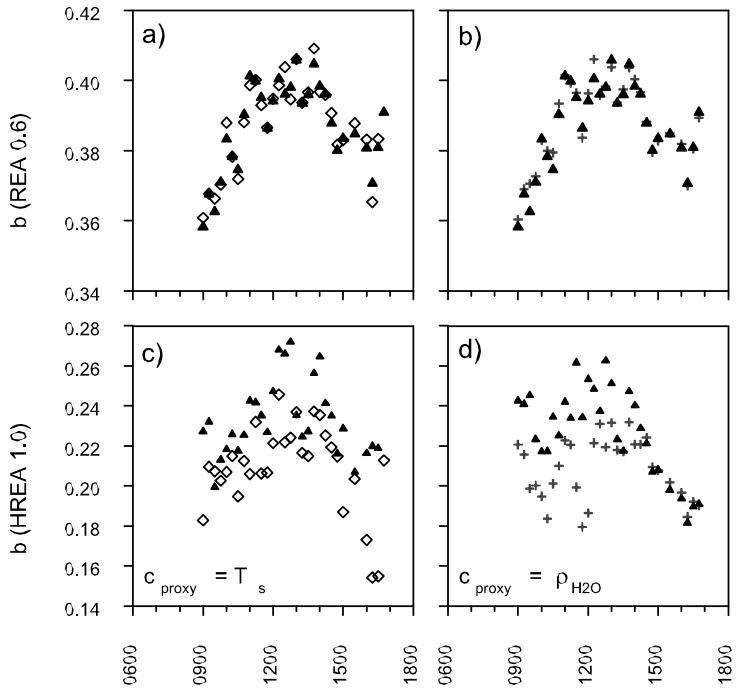

Figure 4. *b*-factors from simulation of REA 0.6 (a, b) and HREA 1.0 (c, d) sampling. The results are based on high resolution time series from the EBEX-2000 dataset. Filled triangles represent *b*-factors for carbon dioxide density ρ_{CO_2}, dimonds for sonic temperature T_s and crosses for water vapour density ρ_{H_2O}. The difference between *b*-factors for HREA of carbon dioxide (filled triangles in c and d) originates from the use of T_s (c) or ρ_{H_2O} (d) as proxy scalar for the definition of the hyperbolic deadband.

and after the period with cloud cover (Section 5.1). Errors remain in the order of ±10 % for high scalar correlations for all three surface types. Simulation results indicate systematic underestimation of the flux of about -40 % for periods with poor scalar similarity. Only for the WALDATEM-2003 data systematic underestimation was smaller on average when using T_s as proxy scalar compared to using ρ_{H_2O} as proxy scalar, which is in agreement with higher scalar correlation (Figure 6e) and spectral correlation (Figure 3f).

The results presented in Figure 6 clearly show that high scalar similarity between the scalar of interest and the proxy scalar is essential to avoid systematic underestimation of fluxes determined with the HREA method. Therefore, great care has to be taken in the selection of an appropriate proxy scalar. Diurnal changes in scalar similarity may require a change of the proxy scalar in order to avoid large errors in the flux measurements using HREA.

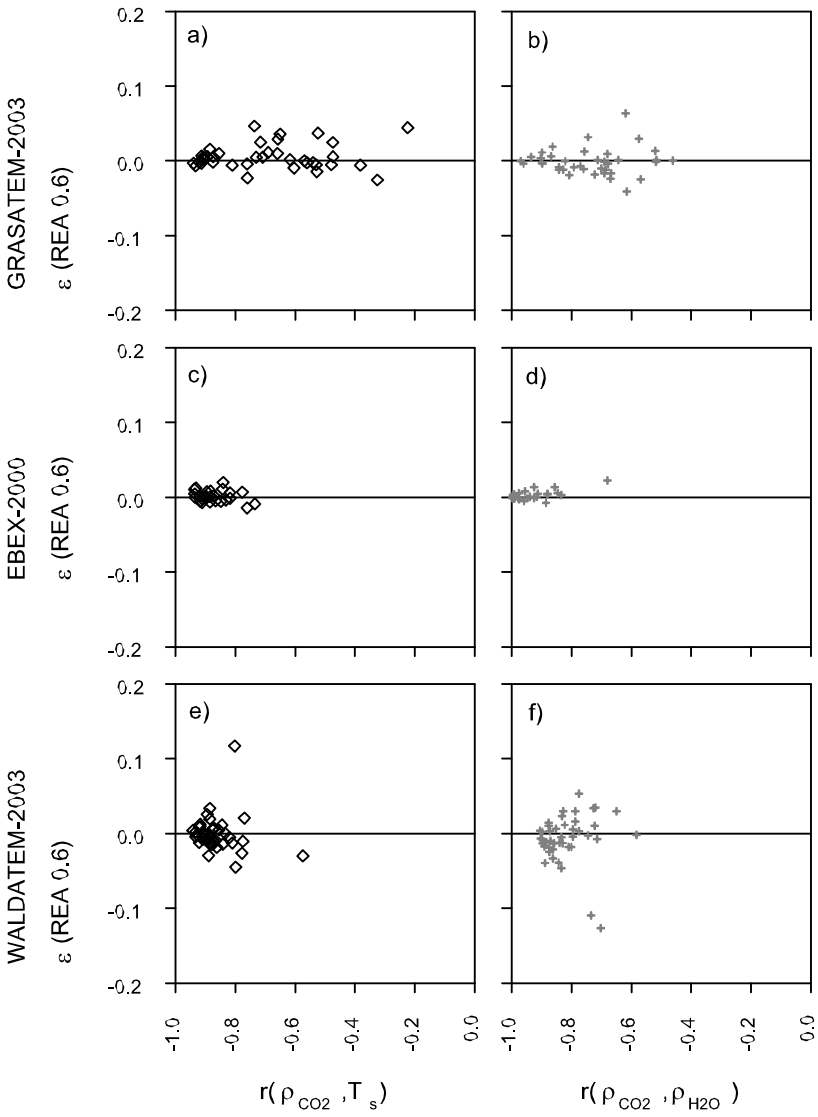

Figure 5. Relative flux error ε for carbon dioxide flux from REA 0.6 simulations in relation to the scalar correlation coefficient r (absolute values). In (a), (c) and (e)(diamonds) sonic temperature T_s was used as proxy scalar, whereas in (b), (d) and (f)(crosses) water vapour density ρ_{H_2O} was used as proxy scalar.

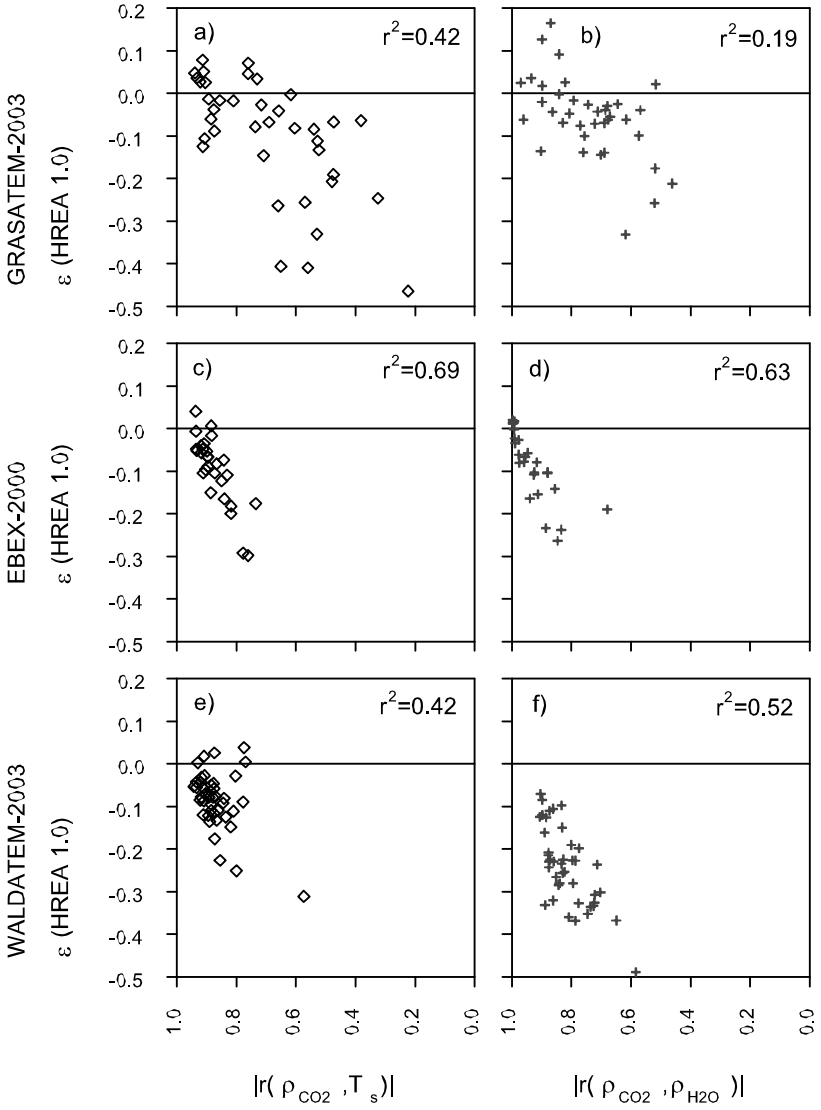

Figure 6. Relative flux error ε for carbon dioxide flux from HREA 1.0 simulations in relation to the scalar correlation coefficient r (absolute values). In (a), (c) and (e)(diamonds) sonic temperature T_s was used as proxy scalar, whereas in (b), (d) and (f)(crosses) water vapour density ρ_{H_2O} was used as proxy scalar. The coefficient of determination r^2 of a linear regression indicates to which degree scalar correlation can explain the variation in the relative flux error. Note the difference in scale for ε when comparing to Figure 5.

The scaling of scatter in ε for REA 0.6 and the scaling of systematic underestimation of fluxes in HREA 1.0 show that the scalar correlation coefficient is an efficient measure for the description of scalar similarity needed in REA or HREA methods. Further investigations of the behavior of the scalar correlation may lead to better understanding of the diurnal changes (Case 1, 2, 3) and processes controlling scalar similarity. However, the assessment of suitable proxy scalars especially for flux measurements applying the HREA method can normally only be based on measurements using slow sensors. The spectral analysis presented in this study as well as investigations on the 'Bandwidth Eddy Covariance' method (Watanabe et al., 2000) give confidence, that enough information on scalar similarity is contained in such slow sensor measurements.

6. Conclusions

Changes in scalar similarity between carbon dioxide, sonic temperature and water vapour were analysed with the scalar correlation coefficient. This evaluation used high quality flux data from experiments over grassland, an irrigated cotton plantation and spruce forest.

Significant changes of scalar similarity were observed over all three surface types within the diurnal cycle. We therefore conclude that differences in scalar similarity have to be expected even if sources and sinks are located close together within the vertical profile (short cut grassland).

Spectral analysis showed consistently good scalar correlation in the higher frequency range (event durations of 6 s to 60 s), which is in agreement with findings by Pearson et al. (1998). Scalar similarity is predominantly controlled by events on longer time scales (event durations > 60 s), which most likely represent changes in the source/sink strength, convective or advective processes. This finding suggests that sampling with slow sensors may be sufficient as alternate strategy for the assessment of scalar similarity required for REA methods when the scalar of interest can not be measured with a fast sensors.

The scaling of scatter in REA flux errors and scaling of systematic underestimation of fluxes in HREA confirm that the scalar correlation coefficient is an efficient measure for the assessment of scalar similarity needed for REA and HREA methods. The effects of changing scalar similarity on REA flux measurement errors were relatively small ($\varepsilon < \pm 10\,\%$). A diurnal course of the b-factors was found for the EBEX-2000 dataset, so that the use of a b-factor determined from a proxy scalar is recommended compared to the use of a fixed b-factor in order to reduce relative flux errors in classical REA.

Poor similarity between the scalar of interest and the proxy scalar leads to systematic underestimation of fluxes determined with HREA (up to -40 %). Therefore great care has to be taken for the selection of a suitable proxy scalar. In the absence of fast recorded time series for the scalar of interest, a slow sensor could generate appropriate data for subsequent assessment of HREA measurements or more detailed investigations on the general behavior of scalar similarity. Diurnal changes in the scalar similarity may require to change the proxy scalar within the

diurnal cycle accordingly in order to correctly measure trace gas fluxes. From the results presented in this study, the use of sonic temperature as proxy for carbon dioxide seems favorable during the morning. However, scalar similarity was poor during situations with diminishing buoyancy fluxes in the late afternoon or during a period with cloud shading during the day.

A preliminary interpretation can be given for the diurnal pattern of scalar correlation. The good scalar similarity between carbon dioxide and sonic temperature found before 0900-1000 local time for all three surface types (Case 1) could be due to processes of carbon dioxide consumption (assimilation) and heat production that start rapidly and simultaneously with increasing global radiation in the morning. In contrast, the atmospheric sink for water vapour, i. e. water vapour deficit, gains strength more slowly throughout the day with the warming of the surface layer. More experimental results on scalar correlation from other sites and flux profile measurements, as outlined in Pearson et al. (1998) would be needed to check this hypothesis further. The link to source/sink strength suggests that also plant physiological processes, like e. g. afternoon stomata closure, can have a major effect on the diurnal pattern of scalar similarity, when there is a difference of the effect on source/sink strength of the two scalars.

Acknowledgements

The authors wish to acknowledge the help and technical support performed by the staff of the Bayreuth Institute for Terrestrial Ecosystem Research (BITÖK) of the University of Bayreuth. We want to thank the participants of the EBEX-2000 experiment of the Department of Micrometeorology, University of Bayreuth, for providing data. This study was supported by the German Federal Ministry of Education and Research (PT BEO51-0339476 D).

References

Akima, H.: 1970, 'A new method of interpolation and smooth curve fitting based on local procedures'. *J. Assc. Comp. Mach.* **17**, 589–602.

Ammann, C. and F. X. Meixner: 2002, 'Stability dependence of the relaxed eddy accumulation coefficient for various scalar quantities'. *J. Geophys. Res.* **107(D8)**, 4071.

Andreas, E. L., R. Hill, J. R. Gosz, D. Moore, W. Otto, and A. Sarma: 1998a, 'Statistics of Surface Layer Turbulence over Terrain with Meter-Scale Heterogeneity'. *Boundary-Layer Meteorol.* **86**, 379–409.

Andreas, E. L., R. J. Hill, J. R. Gosz, D. I. Moore, W. D. Otto, and A. D. Sarma: 1998b, 'Stability dependence of the eddy-accumulation coefficients for momentum and scalars'. *Boundary-Layer Meteorol.* **86**, 409–420.

Baker, J. M., J. M. Norman, and W. L. Bland: 1992, 'Field-scale application of flux measurement by conditional sampling'. *Agric. For. Meteorol.* **62**, 31–52.

Beverland, I. J., R. Milne, C. Boissard, D. H. O'Neill, J. B. Moncrieff, and C. N. Hewitt: 1996, 'Measurements of carbon dioxide and hydrocarbon fluxes from a

sitka spruce using micrometeorological techniques'. *J. Geophys. Res.* **101(D17)**, 22807–22815.

Beyrich, F., W. Adam, J. Bange, K. Behrens, F. H. Berger, C. Bernhofer, J. Bösenberg, H. Dier, T. Foken, M. Göckede, U. Görsdorf, J. Güldner, B. Hennemuth, C. Heret, S. Huneke, W. Kohsiek, A. Lammert, V. Lehmann, U. Leiterer, J.-P. Leps, C. Liebethal, H. Lohse, A. Lüdi, M. Mauder, W. Meijinger, H.-T. Mengelkamp, R. Queck, S. Richter, T. Spiess, B. Stiller, A. Tittebrand, U. Weisensee, and P. Zittel: 2004, 'Verdunstung über einer heterogenen Landoberfläche - Das LITFASS-2003 Experiment, Ein Bericht.'. Technical Report Arbeitsergebnisse Nr. 79, German Meteorological Service, Offenbach, Germany. ISSN 1430-0281.

Bowling, D. R., D. D. Baldocchi, and R. K. Monson: 1999a, 'Dynamics of isotopic exchange of carbon dioxide in a Tennessee deciduous forest'. *Global Biogeochemical Cycles* **13**, 903–922.

Bowling, D. R., A. C. Delany, A. A. Turnipseed, D. D. Baldocchi, and R. K. Monson: 1999b, 'Modification of the relaxed eddy accumulation technique to maximize measured scalar mixing ratio differences in updrafts and downdrafts'. *J. Geophys. Res.* **104(D8)**, 9121–9133.

Bowling, D. R., D. E. Pataki, and J. R. Ehleringer: 2003, 'Critical evaluation of micrometeorological methods for measuring ecosystem-atmosphere isotopic exchange of CO2'. *Agric. For. Meteorol.* **116**, 159–179.

Bowling, D. R., P. P. Tans, and R. K. Monson: 2001, 'Partitioning net ecosystem carbon exchange with isotopic fluxes of CO2'. *Global Change Biol.* **7**, 127–145.

Brunet, Y. and S. Collineau: 1994, 'Wavelet analysis of diurnal and nocturnal turbulence above a maize canopy'. In: E. Foufoula-Georgiou and P. Kumar (eds.): *Wavelets in Geophysics*, Vol. 4 of *Wavelet analysis and its applications*. Academic Press, San Diego, USA, pp. 129–150.

Businger, J. A. and S. P. Oncley: 1990, 'Flux Measurement with Conditional Sampling'. *J. Atmos. Ocean. Tech.* **7**, 349–352.

Chen, J. and F. Hu: 2003, 'Coherent structures detected in atmospheric boundary-layer turbulence using wavelet transforms at Huaihe River Basin, China'. *Boundary-Layer Meteorol.* **107**, 429–444.

Collineau, S. and Y. Brunet: 1993, 'Detection of turbulent coherent motions in a forest canopy. Part I: Wavelet analysis'. *Boundary-Layer Meteorol.* **65**, 357–379.

Desjardins, R. L.: 1972, 'A Study of Carbon Dioxide and Sensible Heat Fluxes using the Eddy Correlation Techinique'. Ph.d., Cornell University.

Foken, T., R. Dlugi, and G. Kramm: 1995, 'On the determination of dry deposition and emission of gaseous compounds at the biosphere-atmosphere interface'. *Meteorol. Z.* **4**, 91–118.

Foken, T., M. Göckede, M. Mauder, L. Mahrt, B. Amiro, and W. Munger: 2004, 'Post-Field data Qualtiy Control'. In: X. e. a. Lee (ed.): *Handbook of Micrometeorology*. Kluwer, Dordrecht, The Netherlands, pp. 181–208.

Gao, W.: 1995, 'The vertical change of coefficient b , used in the relaxed eddy accumulation method for flux measurement above and within a forest canopy'. *Atmos. Environ.* **29**, 2339–2347.

Gerstberger, P., T. Foken, and K. Kalbitz: 2004, 'The Lehstenbach and Steinkreuz 'Catchments in NE Bavaria, Germany'. In: E. Matzner (ed.): *Biogeochemistry of Forested Catchments in a Changing Environment: A german case study*, Vol. 172 of *Ecological Studies*. Springer, Heidelberg, Germany, pp. 15–41.

Grossmann, A., R. Kronland-Martinet, and J. Morlet: 1989, 'Reading and Understanding Continous Wavelet Transforms'. In: J. Combes, A. Grossmann, and

P. Tchamitchian (eds.): *Wavelets: Time-Frequency Methods and Phase Space*. Springer, New York, USA, pp. 2–20.

Grossmann, A. and J. Morlet: 1984, 'Decomposition of Hardy Functions into Square Integrable Wavelets of Constant Shape'. *J. Math. Anal* **15**, 723–736.

Hicks, B. B. and R. T. McMillen: 1984, 'A simulation of the eddy accumulation method for measuring pollutant fluxes'. *J. Climate Appl. Meteorol.* **23**, 637–643.

Hicks, B. B. and R. T. McMillen: 1988, 'On the measurement of Dry Deposition Using Imperfect Sensors and in Non-Ideal Terrain'. *Boundary-Layer Meteorol.* **42**, 79–94.

Horst, T. W. and S. P. Oncley: 1995, 'Flux-PAM Measurement of Scalar Fluxes Using Cospectral Similarity'. In: *Proc. 9th Symp. on Meteorological Observations and Instumentation*, Vol. Conference Preprint. Charlotte, North Carolina, American Meteorological Society, Boston, USA. pp. 495-500.

Kaimal, J. C., J. C. Wyngaard, Y. Izumi, and O. R. Coté: 1972, 'Spectral characteristics of surface-layer turbulence'. *Quart. J. Roy. Meteorol. Soc.* **98**, 563–589.

Katul, G., C. I. Hsieh, D. Bowling, K. Clark, N. Shurpali, A. Turnipseed, J. Albertson, K. Tu, D. Hollinger, B. Evans, B. Offerle, D. Anderson, D. Ellsworth, C. Vogel, and R. Oren: 1999, 'Spatial variability of turbulent fluxes in the roughness sublayer of an even-aged pine forest'. *Boundary-Layer Meteorol.* **93**, 1–28.

Katul, G. G., P. L. Finkelstein, J. F. Clarke, and T. G. Ellestad: 1996, 'An investigation of the conditional sampling method used to estimate fluxes of active, reactive, and passive scalars'. *J. Appl. Meteorol.* **35**, 1835–1845.

Katul, G. G., S. M. Goltz, C. I. Hsieh, Y. Cheng, F. Mowry, and J. Sigmon: 1995, 'Estimation of Surface Heat and Momentum Fluxes Using the Flux-Variance Method above Univorm and Non-Uniform Terrain'. *Boundary-Layer Meteorol.* **80**, 249–282.

Katul, G. G. and C. I. Hsieh: 1999, 'A note on the flux-variance similarity relationships for heat and water vapour in the unstable atmospheric surface layer'. *Boundary-Layer Meteorol.* **90**, 327–338.

Kronland-Martinet, R., J. Morlet, and A. Grossmann: 1987, 'Analysis of Sound Patterns Through Wavelet Transforms'. *Int. J. Pattern Recognition and Artificial Intelligence* **1**, 273–302.

Kumar, P. and E. Foufoula-Georgiou: 1994, 'Wavelet analysis in Geophysics: An Introduction'. In: E. Foufoula-Georgiou and P. Kumar (eds.): *Wavelets in Geophysics*, Vol. 4 of *Wavelet analysis and its applications*. Academic Press, San Diego, USA, pp. 1–43.

Lu, S. S. and W. W. Willmarth: 1973, 'Measurements of the structure of Reynolds stress in a turbulent boundary layer'. *J. Fluid. Mech.* **60**, 481–512.

Lykossov, V. and C. Wamser: 1995, 'Turbulence Intermittency in the Atmospheric Surface Layer over Snow-Covered Sites'. *Boundary-Layer Meteorol.* **72**, 393–409.

McNaughton, K. G. and J. Laubach: 1998, 'Unsteadiness as a cause of non-equality of eddy diffusivities for heat and vapour at the base of an advective inversion'. *Boundary-Layer Meteorol.* **88**, 479–504.

Milne, R., A. Mennim, and K. Hargreaves: 2001, 'The value of the beta coefficient in the relaxed eddy accumulation method in terms of fourth-order moments'. *Boundary-Layer Meteorol.* **101**, 359–373.

Obukhov, A. M.: 1960, 'O strukture temperaturnogo polja i polja skorostej v uslovijach konvekcii'. *Izvestia AN SSSR, seria Geofizika* pp. 1392–1396.

Oncley, S., T. Foken, R. Vogt, C. Bernhofer, W. Kohsiek, H. P. Liu, A. Pitacco, D. Grantz, and L. Riberio: 2002, 'The Energy Balance Experiment EBEX-2000'.

In: *15th Conference on Boundary Layer and Turbulence*. Wageningen University, Wageningen, Netherlands, American Meteorological Society, Boston, USA. pp. 1-4.

Oncley, S. P., A. C. Delany, T. W. Horst, and P. P. Tans: 1993, 'Verification of flux measurement using relaxed eddy accumulation'. *Atmos. Environ.* **27A**, 2417–2426.

Pattey, E., R. L. Desjardins, and P. Rochette: 1993, 'Accuracy of the relaxed eddy-accumulation technique, evaluated using CO2 flux measurements'. *Boundary-Layer Meteorol.* **66**, 341–355.

Pearson, R. J., S. P. Oncley, and A. C. Delany: 1998, 'A scalar similarity study based on surface layer ozone measurements over cotton during the California Ozone Deposition Experiment'. *J. Geophys. Res.* **103(D15)**, 18919–18926.

Rebmann, C., M. Göckede, T. Foken, M. Aubinet, M. Aurela, P. Berbigier, C. Bernhofer, N. Buchmann, A. Carrara, A. Cescatti, R. Ceulemans, R. Clement, J. Elbers, A. Granier, T. Grünwald, D. Guyon, K. Havrankova, B. Heinesch, A. Knohl, T. Laurila, B. Longdoz, B. Marcolla, T. Markkanen, F. Miglietta, H. Moncrieff, L. Montagnani, E. Moors, M. Nardino, J.-M. Ourcvial, S. Rambal, U. Rannik, E. Rotenberg, P. Sedlak, G. Unterhuber, T. Vesala, and D. Yakir: 2005, 'Quality analysis applied on eddy covariance measurements at complex forest sites using footprint modelling'. *Theor. App. Climatol.* pp. DOI: 10.1007/s00704–004–0095–y.

Shaw, R. H.: 1985, 'On diffusive and dispersive fluxes in forest canopies'. In: B. A. Hutchinson and B. B. Hicks (eds.): *The Forest-Atmosphere Interaction*. D. Reidel, Norwell, USA, pp. 407–419.

Shaw, R. H., J. Tavangar, and D. P. Ward: 1983, 'Structure of the Reynolds stress in a canopy layer'. *J. Climate Appl. Meteorol.* **22**, 1922–1931.

Simpson, I. J., G. W. Thurtell, H. H. Neumann, G. Den Hartog, and G. C. Edwards: 1998, 'The validity of similarity theory in the roughness sublayer above forests'. *Boundary-Layer Meteorol.* **87**, 69–99.

Thomas, C. and T. Foken: 2005, 'Detection of Long-term Coherent Exchange over Spruce Forest Using Wavelet Analysis'. *Theor. App. Climatol.* **80**, 91–104.

Wallace, J. M., H. Eckelmann, and R. S. Brodkey: 1972, 'The wall region in turbulent shear flow'. *J. Fluid. Mech.* **54**, 39–48.

Watanabe, T., K. Yamanoi, and Y. Yasuda: 2000, 'Testing of the bandpass eddy covariance method for a long-term measurement of water vapour flux over a forest'. *Boundary-Layer Meteorol.* **96**, 473–491.

Wichura, B., N. Buchmann, and T. Foken: 2000, 'Fluxes of the stable carbon isotope 13C above a spruce forest measured by hyperbolic relaxed eddy accumulation method'. In: *14th Symposium on Boundary Layers and Turbulence*, Vol. Conference Preprint. Aspen, Colorado, American Meteorological Society, Boston, USA. pp. 559-562.

Wilczak, J. M., S. P. Oncley, and S. A. Stage: 2001, 'Sonic anemometer tilt correction algorithms'. *Boundary-Layer Meteorol.* **99**, 127–150.

Wyngaard, J. C., O. R. Coté, and Y. Izumi: 1971, 'Local free convection, similarity and the budgets of shear stress and heat flux'. *J. Atmos. Sci.* **28**, 1171–1182.

Wyngaard, J. C. and C.-H. Moeng: 1992, 'Parameterizing turbulent diffusion through the joint probability density'. *Boundary-Layer Meteorol.* **60**, 1–13.

Innovative gap-filling strategy for annual sums of CO_2 net ecosystem exchange

J. Ruppert [a,b,*] M. Mauder [a] C. Thomas [a,c] J. Lüers [a]

[a] *University of Bayreuth, Department of Micrometeorology, Universitätsstrasse 30, 95440 Bayreuth, Germany*

[b] *now Research Institute of the Cement Industry, German Cement Works Association, Environmental Measuring Department, Tannenstrasse 2, 40476 Düsseldorf, Germany*

[c] *now Oregon State University, Department of Forest Science, 321 Richardson Hall, Corvallis, OR, 97331, USA*

Abstract

The determination of carbon dioxide net ecosystem exchange (NEE) using the eddy-covariance (EC) method has become a fundamental tool for the investigation of the carbon balance of terrestrial ecosystems. This study presents a strategy for the processing, subsequent quality control and gap-filling of carbon dioxide eddy-covariance flux measurements for the derivation of annual sums of NEE. A set of criteria is used for quality assessment and to identify periods with instrumental or methodological failures. The complete evaluation scheme was applied to data recorded above a spruce forest at the FLUXNET-station Waldstein-Weidenbrunnen (DE-Wei) in 2003. Comparison of this new evaluation scheme to the use of a friction velocity (u_*) threshold criterion of $0.3\,\mathrm{m\,s^{-1}}$ indicates less systematic distribution of data gaps. The number of available high quality night-time measurements increased. This effect was most pronounced during summer, when data is essential for a robust parameterisation of respiratory fluxes. Non-linear regression analysis showed that air temperature and global radiation explain most of the variability of NEE and further seasonal segregation of the data based on an objective method did not significantly improve predictions at this evergreen forest site.

Key words: Net ecosystem exchange, Carbon dioxide exchange, Eddy-covariance, Data filling, Quality control

Article published in Agricultural and Forest Meteorology, 138, 5-18, doi:10.1016/j.agrformet.2006.03.003. accepted 2 March 2006, www.elsevier.com/locate/agrformet

* Corresponding author. *E-mail address:* rj@vdz-online.de

Nomenclature

symbol	description, unit
a	ecosystem quantum yield, [mmol m^{-2} s^{-1}]
d	displacement height, [m]
E_0	parameter of *Lloyd-Taylor* function which describes temperature sensitivity, [K]
f	Coriolis parameter [s^{-1}]
F_C	CO_2 net ecosystem exchange (NEE), [mmol m^{-2} s^{-1}]
$F_{C,day}$	CO_2 net ecosystem exchange at day-time, [mmol m^{-2} s^{-1}]
$F_{C,sat}$	CO_2 net ecosystem exchange at light saturation, [mmol m^{-2} s^{-1}]
F_E	corrected CO_2 eddy flux, [mmol m^{-2} s^{-1}]
$F_{R,10}$	ecosystem respiration rate at 10 °C, [mmol m^{-2} s^{-1}]
$F_{R,eco}$	ecosystem respiration rate at night-time, [mmol m^{-2} s^{-1}]
F_S	CO_2 storage flux, [mmol m^{-2} s^{-1}]
I_σ	relative deviation of the integral turbulence characteristic
L	Obukhov length, [m]
R_g	global radiation, [W m^{-2}]
R^2	coefficient of determination
S_{xy}	standard error of linear regression, here in [mmol m^{-3}]
t	time, [s]
T	air temperature, [K]
T_0	parameter of *Lloyd-Taylor* function, [K]
T_p	air temperature, measured with a platinum wire thermometer, [°C]
T_s	sonic air temperature, measured with a sonic anemometer, [°C]
u_*	friction velocity, [m s^{-1}]
z_+	normalising factor with the value of 1 m
z_m	measurement height, [m]
ζ	stability parameter
$\overline{\rho_C}$	mean CO_2 density, [mmol m^{-3}]
σ_w	standard deviation of the vertical wind velocity, [m s^{-1}]

Abbreviations	
AGC-value	diagnostic value which indicates if the optical path of the LI-7500 is obstructed, [%]
CET	Central European Time
De-Wei	FLUXNET-station Waldstein-Weidenbrunnen, Fichtelgebirge, Germany
NEE	net ecosystem exchange, [$\mathrm{mmol\,m^{-2}\,s^{-1}}$]
PAI	plant area index, [$\mathrm{m^2\,m^{-2}}$]
PAR	photosynthetic active radiation
PWD	present weather detector
TK2	Turbulence Knight 2 evaluation software

1 Introduction

Carbon dioxide exchange of ecosystems with the atmosphere is investigated worldwide at many stations by directly measuring turbulent fluxes applying the eddy-covariance method (Baldocchi et al., 2001). The derivation of annual sums of the CO_2 net ecosystem exchange (NEE) requires careful assessment of the collected data including criteria for rejecting invalid data and gap-filling strategies to replace rejected and missing data. Standardised methodologies are proposed for most of the necessary corrections to eddy-covariance data (Aubinet et al., 2000, 2003a). However, strategies for gap-filling are still subject to discussion within the research community (Falge et al., 2001; Hui et al., 2004; Gu et al., 2005). The comparison of different methods (mean diurnal variation, look-up tables, nonlinear regression) showed small differences in the accuracy of the gap-filling method itself but that the accuracy is sensitive to the criteria applied to rate the data quality and reject certain data (Falge et al., 2001). The quality assessment must effectively check for instrument failures and for the fulfilment of the prerequisites of the eddy-covariance method.

Especially the selection and treatment of night-time flux data bares the potential for *selective systematic error* in annual sums of NEE due to underestimation or double accounting of respiratory fluxes (Goulden et al., 1996; Moncrieff et al., 1996; Massman and Lee, 2002). Often the validity of night-time flux data is rated according to the friction velocity u_*. Data are rejected based on an absolute threshold of u_* in order to exclude situations with weak turbulent mixing in which (i) often stationarity and development of turbulence are not sufficient for the eddy-covariance method and (ii) the measured NEE seems to underestimate respiratory fluxes and there is a chance for decoupling of exchange processes within the vegetation canopy

(Aubinet et al., 2003a,b). CO_2 is then suspected to leave the ecosystem by ways that are not adequately accounted for by the eddy-covariance measurements and modelled respiration rates are used instead. This method requires the objective determination of a critical u_* threshold (Gu et al., 2005), which can not be found at all sites. The use of a fixed u_* threshold often rejects a large proportion of flux measurement data during summer nights. It is, however, especially during summer nights when respiratory CO_2 fluxes show the highest rates due to their positive correlation with temperature. Therefore the correct representation of summer night fluxes is essential for the derivation of the annual sum of CO_2 exchange.

Many studies show that the rejection of periods with low u_* values results in systematic decrease of annual sums of NEE in the order of 50-100 $\mathrm{gC\,m^{-2}\,a^{-1}}$ (Goulden et al., 1996; Falge et al., 2001; Carrara et al., 2003; Hui et al., 2004) scaling with the value of the u_* threshold criterion. Therefore, the use of absolute thresholds in u_* as data rejection criterion must be questioned as long as there is no direct evidence for CO_2 leaving the ecosystem by ways that are not adequately accounted for during periods with low u_*. Consequently, more precise criteria are needed to assess the quality of the flux data especially under low turbulence conditions.

This study presents a strategy for the processing, subsequent quality control and gap-filling of CO_2 eddy-covariance flux measurements for the derivation of annual sums of net ecosystem exchange (NEE). It applies methods for quality control and assurance proposed by Foken and Wichura (1996) and updated by Foken et al. (2004). Instead of using absolute thresholds for a certain parameter of turbulence, these methods assess the degree of stationarity in the flux data and the degree to which the development of turbulence agrees with basic flux-variance similarity. Both criteria represent fundamental prerequisites for the eddy-covariance method. The evaluation scheme is tested with data from the FLUXNET-Station Waldstein-Weidenbrunnen (DE-Wei). We analyse how the quality assessment influences the distribution of gaps in the NEE dataset. Special attention is given to the availability of measured data during summer nights for the determination of the night-time respiratory fluxes and how the quality assessment relates to the use of a u_* filter criterion.

2 Method

2.1 Experimental data

The FLUXNET-Station Waldstein-Weidenbrunnen (DE-Wei) is located in the Fichtelgebirge Mountains in Germany ($50^o08'$ N, $11^o52'$ E,) at a forested mountain ridge at 775 m a.s.l. The CO_2-Flux measurements are performed on a 33 m tall tower over spruce forest (*Picea abies*) using a sonic anemometer (R2 until 19 May 2003, since then R3-50, Gill Instruments Ltd., Lymington, UK) and an open path gas

analyser for CO_2 and H_2O (LI-7500, LI-COR Inc., Lincoln, NE, USA). The forest has a mean canopy height of 19 m and a plant area index (PAI) of 5.2 (Thomas and Foken, 2006a) and the terrain has a slope of 2^o (Rebmann et al., 2005). Understorey vegetation is sparse and consists of small shrubs and grasses. Further description of the research site can be found in Gerstberger et al. (2004). The synoptic weather code (WMO-code 4680, WMO, 1995) and visibility were obtained with a present weather detector (PWD) and allowed for an exact determination of rain and fog periods. Temperature was measured by a vertical profile of psychrometers and soil temperature probes. Long and shortwave radiation was measured at the tower top. A locally developed profile system measuring CO_2 mixing ratios at eight levels from 0.03 m to 33 m allowed determining the storage flux more precisely in summer during the intensive experiment campaign WALDATEM-2003 (Wavelet Detection and Atmospheric Turbulent Exchange Measurements 2003, Thomas et al., 2004).

2.2 Flux determination and flux corrections

Eddy-covariance measurements of turbulent fluxes are the basis for the annual NEE estimation. In general, turbulent fluxes are calculated as the covariance between the two high frequency time series of vertical wind velocity and a scalar, e.g. carbon dioxide density, which are measured at one point. Inherent to these atmospheric measurements are deficiencies which cause more or less important violations of assumptions to the underlying theory. Therefore, quality tests of the raw data, several corrections of the covariances as well as quality tests for the resulting turbulent fluxes are necessary. For the analysis of the turbulence data set from the Waldstein-Weidenbrunnen site recorded in 2003 the comprehensive software package TK2 was used, which was developed at the University of Bayreuth (Mauder and Foken, 2004). It is capable of performing the whole post-processing of turbulence measurements and producing quality assessed turbulent flux estimates. The data analysis scheme of the TK2 software package implements the current state of science including recommendations of an AMERIFLUX workshop covering methodological aspects of eddy-covariance measurements (Lee et al., 2004). It consists of the following major components:

- Detection of spikes after Vickers and Mahrt (1997) based on Højstrup (1993).
- Determination of the time delay between sensors (e.g. LI-7500 gas analyser and sonic) using cross correlations analysis.
- Cross wind correction of the sonic temperature after Liu et al. (2001), if not already implemented in sensor software (e.g. necessary for Gill Solent-R2, redundant for Gill Solent R3-50 or Campbell CSAT3).
- Planar Fit method for coordinate transformation (Wilczak et al., 2001).
- Spectral corrections after Moore (1986) using the spectral models by Kaimal et al. (1972) and Højstrup (1981).

- Conversion of fluctuations of the sonic temperature into fluctuations of the actual temperature after Schotanus et al. (1983).
- Density correction for scalar fluxes of H_2O and CO_2 and correction for mean vertical mass flow after Webb et al. (1980).
- Iteration of the correction steps because of their interdependence.
- Quality assessment, applying tests for steady state conditions and well-developed turbulence (integral turbulence characteristics) after Foken and Wichura (1996) in the version proposed by Foken et al. (2004).

Additional to the built-in functions of the software package we rejected invalid CO_2 measurements due to sensor saturation or electrical problems by applying a site specific maximum threshold to the absolute mean CO_2 density $\overline{\rho_C}$ of 17 mmol m^{-3} and rejecting half-hour periods with extremely low variance in the CO_2 density ($<$0.02 μmol m^{-3}). Few missing data in the radiation and temperature measurements (about 4 days in 2003) were filled by calculating average diurnal cycles from a 14 day period. Corresponding flux data was not included in the regression analysis (Section 2.5). Further processing of the corrected CO_2 eddy flux data (F_E), the application of the quality criteria as well as the parameterisation and gap-filling procedures are summarised in Fig. 1 and are explained in more detail in the following sections.

2.3 Flux data quality assessment

2.3.1 Environmental conditions

Environmental conditions at the FLUXNET-Station Waldstein-Weidenbrunnen are harsh especially during winter time. Under humid conditions measurements with the sonic anemometer and the open path CO_2 sensor are frequently disturbed by fog or ice formation at tower and instrument structures. Such disturbance does not necessarily result in missing values so that data has to be carefully selected during post processing, to eliminate all periods in which measurements of the CO_2 flux are not trustworthy.

The PWD allowed efficient identification of periods with any form of precipitation or fog (criterion 1, Fig. 1). We found that rain gauge measurements were not sufficiently precise in the identification of light precipitation events, which already disturb sonic anemometer and open path gas analyser measurements. When using an LI-7500, an alternative way for identifying fog periods is recording the 'AGC value' from the digital output, which indicates disturbances within the measurement path. We allowed a time of 30 min after every precipitation or fog event for drying of the instrument windows.

The combination of humid and freezing conditions leads to ice formation on the instruments in winter time. These situations were identified by comparing the sonic temperature (T_s) of the sonic anemometer with air temperature measured at the tower top with a platinum wire thermometer of a ventilated psychrometer (T_p). From Fig. 2 it is obvious that (i) the relation must be determined individually for every sonic anemometer and (ii) large deviations occur only below or close to the freezing point. Data for which the measurement of T_s is significantly disturbed could be identified and flagged as bad quality (criterion 2, Fig. 1) by defining a confidence interval from a linear regression of values above 0 ^{o}C. Even when extrapolating this regression line to -10 ^{o}C its statistical uncertainty (p=0.05) is below measurement precision (0.1 K) due to the strong correlation and the large number of data. We therefore used the linear regression line of positive temperature measurements $\pm 4\sigma$ as confidence interval for all measurements. Consequently, disturbed measurements at negative temperatures, which are likely the result of ice blocking the measurement path or the transducers of the sonic anemometer, are excluded.

2.3.2 Stationarity and developed turbulence

The tests for stationarity and developed turbulence which form the basis for criteria 3 and 4 (Fig. 1) in this study were suggested by Foken and Wichura (1996) and are discussed in detail in Foken et al. (2004). The stationarity test compares the covariance calculated for a 30 min interval of turbulence measurements to covariances calculated from 5 min subsets of this data. The flux measurement is then rated according to the relative difference by assigning quality flags. In this study only data with relative differences of less than 30% were accepted as high quality measurements (quality flag 1 or 2 after Foken et al., 2004).

The test on developed turbulence is based on the analysis of integral turbulence characteristics. These test parameters are based on the flux-variance similarity and are fundamental characteristics of atmospheric turbulence in the surface layer (Obukhov, 1960; Wyngaard et al., 1971). Integral turbulence characteristics are the ratio of the standard deviation of a turbulent parameter and its turbulent flux, e.g. σ_w/u_*. These are assumed to be nearly constant or a function of certain scaling parameters under the conditions of fully developed and unperturbed turbulence. They can be parameterised empirically as a function of stability (Panofsky et al., 1977; Foken et al., 1991) but also the Coriolis parameter f is discussed as scaling parameter (Yaglom, 1979; Tennekes, 1982; Högström, 1990). While the test on developed turbulence can be performed on a routine basis for the wind components, the integral turbulence characteristics of scalars have extremely high values under near neutral conditions. Therefore, we restricted the quality assessment for developed turbulence on the vertical wind component in this study. The empirical models for normalised standard deviations that we used for the test on developed turbulence are parameterisations presented in Foken et al. (2004) (see Table 1).

Similar to the test on stationarity, the development of turbulence is rated according

to the relative difference between observed (o) and modelled (m) integral turbulence characteristic (1):

$$I_\sigma = \left| \frac{(\sigma_\mathrm{w}/u_*)_\mathrm{m} - (\sigma_\mathrm{w}/u_*)_\mathrm{o}}{(\sigma_\mathrm{w}/u_*)_\mathrm{m}} \right|. \quad (1)$$

Only data from periods with well developed turbulence (criterion 4) in which the deviation was within 30 %, i.e. $I_\sigma < 0.3$, were accepted as high quality in this study (quality flag 1 or 2 after Foken et al., 2004).

2.4 CO_2 storage flux

A simple method for estimating the CO_2 storage flux F_S from one point CO_2 measurements was suggested by Hollinger et al. (1994). It assumes the same mean CO_2 density $\overline{\rho_\mathrm{C}}$ for the entire air column below measurement height (z_m):

$$F_{\mathrm{S(i)}} = \frac{\overline{\rho_{\mathrm{C(i+1)}}} - \overline{\rho_{\mathrm{C(i-1)}}}}{t_{\mathrm{(i+1)}} - t_{\mathrm{(i-1)}}}\, z_\mathrm{m}, \quad (2)$$

where i denotes a certain measurement interval and t the time reference of a measurement interval. A comparison of eight level CO_2 profile measurements during summer 2003 at the flux tower as well as studies by Rebmann (2003) showed that this method is able to reflect changes in the canopy storage generally well. The analysis of the storage flux data indicated that outliers were related to situations in which the open path gas analyser signal showed sudden and unrealistic changes and that these were often related to periods after rain events when the window of the sensor was not yet dried completely. We therefore developed an additional criterion (criterion 5 in Fig. 1) in order to remove spikes in the storage flux. We analysed the standard error S_xy related to the derivation of the storage flux from the linear regression of three subsequent half-hourly CO_2 density measurements:

$$S_\mathrm{xy} = \sqrt{\frac{1}{n(n-2)}\left[n\sum y^2 - (\sum y)^2 - \frac{[n\sum xy - (\sum x)(\sum y)]^2}{n\sum x^2 - (\sum x)^2}\right]}, \quad (3)$$

where x in this case is the time reference of the measurement periods t and y is the average CO_2 density $\overline{\rho_\mathrm{C}}$. Unlike the coefficient of determination R^2 the standard error S_xy is not adjusted to the variability of the CO_2 data. It gives a measure for the residuals expressed in absolute CO_2 density and indicates periods, in which the storage flux is uncertain because it is calculated from highly fluctuating $\overline{\rho_\mathrm{C}}$ with the lack of a clear trend. Such situations occur when one of the half-hourly measurements of $\overline{\rho_\mathrm{C}}$ is disturbed by measurement failures. Fig. 3 shows that very large values for the storage flux were related to high standard errors. We applied a site specific absolute limit ($S_\mathrm{xy} < 0.1784\,\mathrm{mmol\,m^{-3}} = 4\sigma$) in order to mark these

data as bad quality (criterion 5, Fig. 1). Only after removing these data we were able to also identify upper and lower limits of the absolute storage flux ($|F_S| < 0.0053\,\mathrm{mmol\,m^{-2}\,s^{-1}} = 4\sigma$) for the identification and rejection of few remaining outliers.

Valid measurements for the NEE (F_C) exist when both components (F_E and F_S) are high quality data. By convention all CO_2 fluxes into the atmosphere (upward) and storage increase have a positive sign, while fluxes from the atmosphere into the ecosystem (downward) or storage decrease have a negative sign. A final visual control of the data was performed during the parameterisation procedure, when data is grouped and plotted together with the functional dependencies on global radiation and temperature.

2.5 Parameterisation and gap-filling

The regression analysis used as parameterisation scheme for the modelling of NEE and subsequent gap-filling of the measured NEE dataset requires segregating day-time from night-time data. This segregation was done on the basis of (i) calculating astronomical sunrise and sunset for the measurement site and (ii) evaluating measurements of global radiation R_g (Fig. 1). Only when both criteria indicated night-time situation (between astronomical sunset and sunrise and $R_g < 10\,\mathrm{W\,m^{-2}}$) measured data was used for the night-time respiration regression. Time periods during dawn and dusk were grouped with the day-time values, because the light response regression is able to also represent values with low global radiation.

We used *Michaelis-Menten* functions (Michaelis and Menton, 1913; Hollinger et al., 1999; Falge et al., 2001) for the light response regression:

$$F_{C,day} = \frac{a\,R_g\,F_{C,sat}}{a\,R_g + F_{C,sat}} + F_{R,day}. \tag{4}$$

$F_{C,day}$ is the NEE during day-time, $F_{C,sat}$ the saturated NEE rate at $R_g = \infty$ and a is the initial slope of the function. The offset of the function $F_{R,day}$ represents the respiration rate during day-time. The measured NEE data was grouped in temperature classes and individual light response functions were determined for each class (Rebmann, 2003), in order to reflect temperature dependencies present in the rate of respiration and photosynthesis.

The *Lloyd-Taylor* function (Lloyd and Taylor, 1994; Falge et al., 2001) was used for the regression analysis of night-time ecosystem respiratory flux rates $F_{R,eco}$:

$$F_{R,eco} = F_{R,10}\ \mathrm{e}^{E_0[(1/(283.15-T_0))-(1/(T-T_0))]} \tag{5}$$

Parameters were determined for $F_{R,10}$, the respiration rate at 10 °C (283.15 K), and

E_0, which describes the temperature sensitivity of respiratory fluxes, while T_0 was kept constant with a value of 227.13 K as in Lloyd and Taylor (1994). Because the temperature dependency is represented in the function, data was not segregated into temperature classes for the night respiration regression.

In addition, data can be segregated into temporal classes in order to represent different seasonal and phenological stages more accurately. We tested a method based on the thermal seasons after Rapp and Schönwiese (1994) and Rapp (2000) to objectively split the data according to the annual cycle of air temperature. To smooth the daily variability in air temperature without eliminating the characteristic weather episodes of the year a low pass filter using a Gaussian weighting function was applied with a filter length of 60 days. The seasonal segregation can be integrated into the parameterisation scheme at the position indicated with a '*' symbol in Fig. 1.

The modelled NEE is calculated from the meteorological data on global radiation and air temperature and the functional dependencies described by the set of parameters. Similar to the measured NEE data, the parameterisations as well as the resulting modelled NEE data should undergo a final visual control in order to detect inconsistent data which may result from undetected spikes in the meteorological data or calculation errors during parameterisation or modelling. The complete set of gap-filled NEE data consists of the high quality measured NEE data and the modelled NEE data from periods with poor data quality (Fig. 1).

3 Results and discussion

All data rated as high quality according to the criteria 1 to 5 (Fig. 1) were used for the non-linear regression analysis of the light response of photosynthesis and night-time ecosystem respiration. The night-time NEE data shows large scatter (Fig. 4) similar to results presented by Goulden et al. (1996). Consequently the coefficient of determination R^2 of the least square regression is relatively small when half-hourly data is used for the regression analysis of night-time respiration (Tab. 2). Only after aggregating and averaging half-hourly data in temperature classes the functional dependency is clearly visible and R^2 significantly increases, which corresponds to results by Hollinger et al. (1994). We furthermore found for the aggregated and also the individual half-hourly data that (i) the Lloyd-Taylor function resulted in better regressions when not only the $F_{R,10}$ parameter but also the temperature sensitivity parameter E_0 was fitted (Tab. 2). Reichstein et al. (2003) suggest that E_0 depends on soil water availability, which may explain the need for its adjustment for a specific site. And (ii) R^2 values were slightly higher when using the air temperature measured at 2 m height for the regression analysis compared to using soil temperature measured at 0.05 m depth, which was also found for data from previous years (Rebmann, 2003). While the use of aggregated data leads to a good fit, it may represent the data less accurately, as each temperature class contains different numbers of

data. We therefore preferred to firstly identify a suitable functional dependency for the regression analysis based on the aggregated data, i.e. Eq. (5) using aggregated NEE and 2 m air temperature data leaving out the bordering classes which contain only very few data (Fig. 4 white circles). The resulting coefficients of determination R^2 (0.86 compared to 0.45, Tab. 2) suggest to adjust the E_0 parameter to local sites conditions. Secondly, the final values for the function parameters $F_{R,10}$ and E_0 were determined from the least square regression with half-hourly data (Fig. 4 grey line). The difference between large R^2 values of aggregated data and small R^2 values of half-hourly data shows, that (i) temperature is a principle driver of the net ecosystem exchange, but (ii) that other factors contribute to the large scatter observed especially at higher temperatures. Therefore further refinement of the functional dependency by including other ecological drivers like e.g. soil moisture (Reichstein et al., 2003) may lead to more precise modelling of ecosystem respiration rates.

The regression analysis showed a distinct dependence of NEE day-time light response on air temperature, which justifies determination of individual *Michaelis-Menten* functions for different temperature classes (Fig. 5). The parameterisation scheme was tested with 1 K, 2 K and 4 K air temperature classes. The 1 K air temperature classes resulted in increased scatter in the temperature dependence of NEE light response due to small numbers of data in the individual classes. The representation of the temperature dependence by 4 K air temperature classes is relatively coarse. Grouping in 2 K air temperature classes was therefore chosen in order to most precisely represent the temperature dependence. The coefficient of determination R^2 of the least square regression indicate that a large degree of the variation in NEE is explained by the *Michaelis-Menten* functions (Tab. 3). Reduced R^2 for temperature classes from -6 to 0 ^oC correspond to larger scatter and smaller numbers of available high quality NEE data under freezing conditions.

Additional segregation of data into seasonal classes (Section 2.5) did not result in significantly different functional dependencies during the regression analysis. This unexpected result may be explained by two reasons: (i) the temperature information included in both the night respiration regression and in the light response regression by determining individual functions for 2 K temperature classes already contain a certain degree of information on seasonality (Kramer and Kozlowski, 1979; Hollinger et al., 1999; Suni et al., 2003), which therefore is incorporated in the regression analysis indirectly, (ii) the evergreen spruce forest lacks a distinct additional pattern of seasonality, which is often found e.g. for deciduous forest due to plant physiological processes. We therefore did not use additional seasonal segregation within the parameterisation scheme for the determination of the annual NEE at the Waldstein-Weidenbrunnen site. As confirmation, an analysis of the residual NEE, i.e. the difference between measured NEE and NEE modelled based on the parameterisation scheme without seasonal classes, did not show distinct seasonal dependencies. Temporal segregation may be required for other sites in order to represent seasonal changes and variability of other ecological factors correctly (Falge et al., 2001, 2002; Reichstein et al., 2003). The segregation can then be integrated at the beginning of the parameterisation scheme marked with a '*' symbol in Fig.

1. Other environmental variables controlling NEE, e.g. soil water availability, could potentially be used like described in Section 2.5 in order to objectively define seasons or periods. However, with temporal segregation the regression analysis, especially for the night-time respiration, can lack statistical robustness due to the large scatter in half-hourly NEE data, limited temperature ranges and the reduced number of data in each seasonal class.

3.1 Flux data quality assessment

A large number of measured high quality data is desired in general for the determination of the annual sum of NEE and the parameterisations used for gap-filling. For the assessment of the scheme of quality control we compared the application of the criteria 3 and 4 (stationarity and developed turbulence) to filtering the dataset with a threshold criterion of $u_* > 0.3\,\mathrm{m\,s^{-1}}$ for low turbulent conditions. This threshold value is intermediate of threshold values commonly applied to respiration measurements at forest sites (Goulden et al., 1996; Greco and Baldocchi, 1996; Lindroth et al., 1998; Carrara et al., 2003; Griffis et al., 2003; Rebmann et al., 2004; Gu et al., 2005). Fig. 6 clearly shows that the data availability for night-time measurements significantly differs in its pattern. Criteria 3 and 4 tend to reject data in the early morning and late afternoon hours during which frequently extremely non-stationary conditions are observed. Data gaps during night-time and day-time show less systematic scatter and significant numbers of data are rated as high quality also during night-time. Compared to this pattern, the rejection of data by the u_* threshold criterion is much more systematic. Large proportions of the available night-time data fall below the u_* threshold criterion. This pattern increases the chance for *selective systematic error* in the annual sum of NEE (Moncrieff et al., 1996). At the same time, the availability of night-time data is much more limited with the use of the u_* threshold criterion. The selection of high quality data based on the tests of stationarity and developed turbulence as prerequisites for the eddy-covariance method (criteria 3 and 4) increases overall night-time data availability by +9 % throughout the year. This effect is even more pronounced during the summer, +26 %, when nights are shorter, respiration rates are higher and robust data is especially needed. Only when the u_* threshold value is decreased to $0.16\,\mathrm{m\,s^{-1}}$, similar amounts of data from summer night-time measurements become available.

The frequency distribution of overall quality flags after Foken et al. (2004) ranging from 1 high quality to 9 low quality in dependence of u_* is presented in Fig. 7. The quality flag is derived by combining the test on stationarity and developed turbulence. The definitions of the criteria 3 and 4 (Section 2.3.2) correspond to accepting data with quality flag 1 or 2 as high quality. A correlation of low and medium quality ratings with low u_* is apparent for half-hourly flux data at u_* below $0.25\,\mathrm{m\,s^{-1}}$. However, only at a u_* of $\leq 0.15\,\mathrm{m\,s^{-1}}$ more than 50 % of the data is rated as medium or low quality (quality flag ≥ 3) because the criteria 3 or 4 are not met. All data of medium and poor quality were rejected and gap-filled in

this study. There is also a significant number of half-hourly periods, which exhibit instationarity in fluxes or poorly developed or disturbed turbulent conditions, in combination with fairly high values of u_* (Fig. 8a and 8b). During these periods, u_* seems to be insufficient for rating the quality of the flux measurements. High values of u_* can occur under the presence of gravity waves. Gravity waves often result in strong correlation of scalar values and vertical wind velocity, which is not related to significant turbulent exchange (Foken and Wichura, 1996; Thomas and Foken, 2006b). Consequently, the calculated covariances are often unrealistically high. The covariances during these periods tend to show extreme instationarity and the ratio of σ_w/u_*, i.e. the integral turbulence characteristic, is increased. The tests on instationarity and developed turbulence (criteria 3 and 4) therefore provide means to reject periods with the presence of gravity waves and to check for the prerequisites of the eddy-covariance method more precisely than the use of a u_* threshold criterion. The analysis of the Waldstein-Weidenbrunnen data from 2003 shows that in general the u_* threshold criterion is not sufficient to detect all periods, in which the prerequisites for the eddy-covariance method are violated. Only for the summer night-time measurements (Fig. 8c), the use of a very low u_* threshold criterion of $0.15\,\mathrm{m\,s^{-1}}$ could potentially indicate poor data quality in a manner comparable to the criteria 3 and 4. The use of data down to relatively low values of u_* during summer ($\leq 0.16\,\mathrm{m\,s^{-1}}$) is in general supported by an analysis applying objective methods for the determination of critical u_* thresholds (Gu et al., 2005). The determination of a critical threshold of u_* would require a well defined plateau in NEE plotted against u_* (Goulden et al., 1996; Gu et al., 2005), which is analysed in the following section.

3.2 Systematic dependence of night-time NEE on u_*

Another reason for the use of a u_* threshold criterion in many studies is the observation of systematically reduced flux rates measured above canopy under conditions of low turbulent mixing. Generally, a systematic scaling of CO_2 fluxes with u_* should be expected from K-theory (Massman and Lee, 2002). However, biological source strength during night-time is assumed to be independent of turbulent mixing (Goulden et al., 1996). The deficit should then be explained either by storage accumulation below measurement hight or CO_2 leaving the forest in ways that are not adequately accounted for, e.g. by advection. In order to assess the relationship between u_* and night-time NEE after rejection of medium and low quality data (criteria 1 to 5), remaining summer night-time eddy-covariance flux F_E data was plotted in dependence of u_* aggregated in $0.05\,\mathrm{m\,s^{-1}}$ bins (Fig. 9a, dashed line). It shows the expected scaling of CO_2 fluxes with u_*. The storage flux F_S (dash-dotted line) used for the derivation of NEE, F_C (solid line) in Fig. 9a and normalised NEE Fig. 9b (dots) is calculated from measurements performed with the eight point profile system (0.03 m to 33 m a.g.l.). Therefore it represents the canopy storage changes more accurately than the storage flux derived from the CO_2 measurements at tower top (Section 2.4). The NEE data in Fig. 9b was normalised by NEE modelled with

parameters from the night-time regression analysis with air temperature.

From the 2003 data (Fig. 9a) as well as from previous years data (Station Bayreuth data presented in Aubinet et al., 2000) there is no indication of systematic accumulation of CO_2 in the forest canopy during conditions with low turbulent mixing. Consequently, also for storage corrected night-time NEE a typical scaling with u_* measured above canopy is found at the FLUXNET-station Waldstein-Weidenbrunnen. Fig. 9a and Fig. 9b show the lack of a plateau in NEE. The levelling of bin aggregated NEE (Fig. 9a) is rather an effect of significantly reduced numbers of representative data left above a value of $u_* = 0.6\ \mathrm{m\,s^{-1}}$ (Fig. 8c) than of saturation in NEE. Therefore, the use of a critical u_* threshold lacks justification also during summer nights. For the summer night-time data (Fig. 9a) we can not attribute the pattern to inadequate vertical profile resolution within the canopy space like suggested in Gu et al. (2005). However, measurements at 0.03 m and 0.30 m indicated a moderate accumulation of CO_2 very close to the forest floor in periods with very low u_*. These measurements represent only a very small volume of the canopy air so that this accumulation does not compensate the reduction of the CO_2 flux observed above canopy at low values of u_*. Still, they indicate, that respired CO_2 is accumulated at the forest floor and likely even more within the litter and top soil. Adequate representation of such storage components below the canopy space would require to (i) extent CO_2 mixing ratio measurements into the forest floor (Rayment and Jarvis, 2000; Tang et al., 2003) and to (ii) assure sufficient horizontal representation of these measurements in order to reduce effects of small scale heterogeneity in the ecosystem (Buchmann, 2000; Gu et al., 2005).

The lack of any significant CO_2 storage accumulation in the overall forest canopy measured with an eight point profile system during low turbulent conditions (Fig. 9a) could be explained either by significantly reduced CO_2 release from the soil or very efficient horizontal transport. The latter was tested by measurements of horizontal CO_2 gradients, which were performed during the WALDATEM-2003 experiment. The exemplary analysis of CO_2 gradients in very stable nights with very low u_* which showed downhill katabatic air flows did not indicate significant horizontal advection which could explain the reduced values in NEE.

Patterns similar to those found for absolute NEE data in Fig. 9a and for normalised half-hourly NEE data in Fig. 9b from the FLUXNET-Station Waldstein-Weidenbrunnen were reported for other sites by Massman and Lee (2002) and Gu et al. (2005). These were named as examples for situations in which no critical threshold in u_* exists and in which likely the effect of 'pressure pumping' is contributing to the observed pattern. Pressure pumping means, that the release of CO_2 from the soil into the canopy air-space is controlled to a large extend by strong exchange events like coherent structures which penetrate the forest canopy and change the pressure field at the soil surface. Presuming the existence of pressure pumping, the systematic rejection of low NEE values at low values of u_* would most likely introduce 'double accounting' of respiratory fluxes into the annual sum of NEE (Aubinet et al., 2000), because night-time respired CO_2 is then released from the soil

predominantly during periods of vigorous turbulence in which normally the prerequisites for eddy-covariance measurements are given. The corresponding night-time respiration of CO_2 is then adequately accounted for later during the morning.

Especially for flux measurements above tall vegetation, any systematic rejection of data beyond the assessment of flux measurement quality (criteria 1 to 5) should therefore be justified by more precise measurements or parameters describing the complex exchange processes. There should be clear evidence for CO_2 leaving the forest by ways that are not accounted for by the eddy-covariance system in order to prevent the risk of double accounting of fluxes from systematic rejection. Based on the relation between summer night-time NEE and u_* we decided not to apply a u_* threshold criterion additional to the criteria 1 to 5. The application of criteria 3 and 4 makes the use of u_* for the assessment of the quality of the turbulent flux measurements by the eddy-covariance method obsolete.

The annual sum of NEE calculated by applying the complete data processing scheme presented in Fig. 1 and using the criteria 1 to 5 for the quality assessment was determined with -398 $\mathrm{gC\,m^{-2}}$. Likewise for many other flux stations we find that the use of a u_* threshold criterion would significantly change the annual sum of NEE. The change amounted to +51 $\mathrm{gC\,m^{-2}}$ (annual sum of NEE: -347 $\mathrm{gC\,m^{-2}}$) when rejecting all measured data with $u_* < 0.3\,\mathrm{m\,s^{-1}}$.

4 Conclusions

The combination of data quality criteria presented in this study provides means to efficiently select high quality flux data based on the fundamental prerequisites of the eddy-covariance method (criteria 3 and 4) and on meteorological conditions (criteria 1 and 2). The data selection forms the basis for subsequent parameterisation and gap-filling of NEE measurements for the derivation of annual sums of NEE.

Flux data quality assessment with tests on stationarity of fluxes and on developed turbulence (criteria 3 and 4) lead to a less systematic distribution of data gaps compared to the use of a u_* threshold criterion of $0.3\,\mathrm{m\,s^{-1}}$. It may therefore help to reduce the risk of *selective systematic error* in the annual sum of NEE. At the same time it significantly increased the number of available high quality night-time measurements, especially during summer, giving a more robust basis for the parameterisation of respiratory fluxes and for the derivation of the annual sum. Data rated as low quality at higher values of u_* indicate, that the u_* criterion is not sufficient for the assessment of the prerequisites of the eddy-covariance method. Especially above forest sites, any further rejection of data related to the dependence of night-time NEE on turbulent mixing or decoupling within the canopy should use more specific information than u_* measured above the canopy in order to prevent the risk of double accounting of respiratory fluxes. Extended CO_2 concentration measurements at the forest floor could provide more detailed insight into characteristic

patterns of CO_2 exchange from below the canopy.

The determination of temperature dependent light response functions integrates information on seasonality so that further segregation of data into seasonal classes did not significantly improve the parameterisation scheme applied to data from the evergreen forest site Waldstein-Weidenbrunnen.

5 Acknowledgments

The authors wish to thank Thomas Foken head of the Department of Micrometeorology and Eva Falge from the Department of Plant Ecology, both University of Bayreuth, Germany, for helpful comments and discussions. We acknowledge the help and technical support performed by the staff of the Bayreuth Institute for Terrestrial Ecosystem Research (BITÖK) of the University of Bayreuth. This study was supported by the German Federal Ministry of Education and Research (PT BEO51-0339476 D) and CarboEurope-IP.

References

Aubinet, M., Clement, R., Elbers, J. A., Foken, T., Grelle, A., Ibrom, A., Moncrieff, J., Pilegaard, K., Rannik, U., Rebmann, C., 2003a. Methodology for data acquisition, storage and treatment. In: Valentini, R. (Ed.), Fluxes of Carbon, Water, Energy of European Forests. Vol. 163 of Ecological Studies. Springer, Heidelberg, pp. 9–35.

Aubinet, M., Grelle, A., Ibrom, A., Rannik, U., Moncrieff, J., Foken, T., Kowalski, A. S., Martin, P. H., Berbigier, P., Bernhofer, C., Clement, R., Elbers, J., Granier, A., Grunwald, T., Morgenstern, K., Pilegaard, K., Rebmann, C., Snijders, W., Valentini, R., Vesala, T., 2000. Estimates of the annual net carbon and water exchange of forests: The EUROFLUX methodology. In: Advances in Ecological Research. Vol. 30. Academic Press, San Diego, pp. 113–175.

Aubinet, M., Heinesch, B., Yernaux, M., 2003b. Horizontal and vertical CO_2 advection in a sloping forest. Boundary-Layer Meteorol. 108, 397–417.

Baldocchi, D., Falge, E., Gu, L. H., Olson, R., Hollinger, D., Running, S., Anthoni, P., Bernhofer, C., Davis, K., Evans, R., Fuentes, J., Goldstein, A., Katul, G., Law, B., Lee, X. H., Malhi, Y., Meyers, T., Munger, W., Oechel, W., U, K. T. P., Pilegaard, K., Schmid, H. P., Valentini, R., Verma, S., Vesala, T., Wilson, K., Wofsy, S., 2001. FLUXNET: A new tool to study the temporal and spatial variability of ecosystem-scale carbon dioxide, water vapor, and energy flux densities. Bull. Amer. Met. Soc. 82, 2415–2434.

Buchmann, N., 2000. Biotic and abiotic factors controlling soil respiration rates in Picea abies stands. Soil Biol. Biochem. 32, 1625–1635.

Carrara, A., Kowalski, A. S., Neirynck, J., Janssens, I. A., Yuste, J. C., Ceulemans, R., 2003. Net ecosystem CO_2 exchange of mixed forest in Belgium over 5 years. Agric. For. Meteorol. 119, 209–227.

Falge, E., Baldocchi, D., Olson, R., Anthoni, P., Aubinet, M., Bernhofer, C., Burba, G., Ceulemans, R., Clement, R., Dolman, H., Granier, A., Gross, P., Grunwald, T., Hollinger, D., Jensen, N. O., Katul, G., Keronen, P., Kowalski, A., Lai, C. T., Law, B. E., Meyers, T., Moncrieff, H., Moors, E., Munger, J. W., Pilegaard, K., Rannik, U., Rebmann, C., Suyker, A., Tenhunen, J., Tu, K., Verma, S., Vesala, T., Wilson, K., Wofsy, S., 2001. Gap filling strategies for defensible annual sums of net ecosystem exchange. Agric. For. Meteorol. 107, 43–69.

Falge, E., Baldocchi, D., Tenhunen, J., Aubinet, M., Bakwin, P., Berbigier, P., Bernhofer, C., Burba, G., Clement, R., Davis, K. J., Elbers, J. A., Goldstein, A. H., Grelle, A., Granier, A., Guomundsson, J., Hollinger, D., Kowalski, A. S., Katul, G., Law, B. E., Malhi, Y., Meyers, T., Monson, R. K., Munger, J. W., Oechel, W., Paw, K. T., Pilegaard, K., Rannik, U., Rebmann, C., Suyker, A., Valentini, R., Wilson, K., Wofsy, S., 2002. Seasonality of ecosystem respiration and gross primary production as derived from fluxnet measurements. Agric. For. Meteorol. 113, 53–74.

Foken, T., Göckede, M., Mauder, M., Mahrt, L., Amiro, B., Munger, W., 2004. Post-field data qualtiy control. In: Lee, X., Massman, W., Law, B. E. (Eds.), Handbook of Micrometeorology. Kluwer, Dordrecht, pp. 181–208.

Foken, T., Skeib, G., Richter, S., 1991. Dependence of the integral turbulence characteristics on the stability of stratification and their use for doppler- sodar measurements. Z. Meteorol. 41, 311– 315.

Foken, T., Wichura, B., 1996. Tools for quality assessment of surface-based flux measurements. Agric. For. Meteorol. 78, 83–105.

Gerstberger, P., Foken, T., Kalbitz, K., 2004. The Lehstenbach and Steinkreuz catchments in NE Bavaria, Germany. In: Matzner, E. (Ed.), Biogeochemistry of Forested Catchments in a Changing Environment: A German case study. Vol. 172 of Ecological Studies. Springer, Heidelberg, pp. 15–41.

Goulden, M. L., Munger, J. W., Fan, S.-M., Daube, B. C., Wofsy, S. C., 1996. Measurements of carbon sequestration by long-term eddy covariance: Methods and a critical evaluation of accuracy. Global Change Biol. 2, 169–182.

Greco, S., Baldocchi, D., 1996. Seasonal variations of CO_2 and water vapour exchange rates over a temperate deciduous forest. Global Change Biol. 2, 183–197.

Griffis, T. J., Black, T. A., Morgenstern, K., Barr, A. G., Nesic, Z., Drewitt, G. B., Gaumont-Guay, D., McCaughey, J. H., 2003. Ecophysiological controls on the carbon balances of three southern boreal forests. Agric. For. Meteorol. 117, 53–71.

Gu, L., Falge, E. M., Boden, T., Baldocchi, D. D., Black, T., Saleska, S. R., Suni, T., Verma, S. B., Vesala, T., Wofsy, S. C., Xu, L., 2005. Objective threshold determination for nighttime eddy flux filtering. Agric. For. Meteorol. 128, 179–197.

Högström, U., 1990. Analysis of turbulence structure in the surface layer with a modified similarity formulation for near neutral conditions. J. Atm. Sci. 47, 1949–

1972.

Højstrup, J., 1981. A simple model for the adjustment of velocity spectra in unstable conditions downstream of an abrupt change in roughness and heat flux. Boundary-Layer Meteorol. 21, 341–356.

Højstrup, J., 1993. A statistical data screening procedure. Measuring Science Technology 4, 153–157.

Hollinger, D. Y., Goltz, S. M., Davidson, E. A., Lee, J. T., Tu, K., Valentine, H. T., 1999. Seasonal patterns and environmental control of carbon dioxide and water vapour exchange in an ecotonal boreal forest. Global Change Biol. 5, 891–902.

Hollinger, D. Y., Kelliher, F. M., Byers, J. N., Hunt, J. E., McSeveny, T. M., Weir, P. L., 1994. Carbon dioxide exchange between an undisturbed old-growth temperate forest and the atmosphere. Ecology 75, 134–150.

Hui, D. F., Wan, S. Q., Su, B., Katul, G., Monson, R., Luo, Y. Q., 2004. Gap-filling missing data in eddy covariance measurements using multiple imputation (MI) for annual estimations. Agric. For. Meteorol. 121, 93–111.

Kaimal, J. C., Wyngaard, J. C., Izumi, Y., Coté, O. R., 1972. Spectral characteristics of surface-layer turbulence. Quart. J. Roy. Meteor. Soc. 98, 563–589.

Kramer, P., Kozlowski, T., 1979. Enzymes, energetics, and respiration. In: Physiology of Woody Plants. Academic Press, New York, pp. 223–257.

Lee, X., Massman, W., Law, B. E. (Eds.), 2004. Handbook of micrometeorology. A guide for surface flux measurement and analysis. Kluwer, Dordrecht.

Lindroth, A., Grelle, A., Moren, A.-S. a., 1998. Long-term measurements of boreal forest carbon balance reveal large temperature sensitivity. Global Change Biol. 4, 443–450.

Liu, H. P., Peters, G., Foken, T., 2001. New equations for sonic temperature variance and buoyancy heat flux with an omnidirectional sonic anemometer. Boundary-Layer Meteorol. 100, 459–468.

Lloyd, J., Taylor, J., 1994. On the temperature dependence of soil respiration. Funct. Ecol. 8, 315–323.

Massman, W. J., Lee, X., 2002. Eddy covariance flux corrections and uncertainties in long-term studies of carbon and energy exchanges. Agric. For. Meteorol. 113, 121–144.

Mauder, M., Foken, T., 2004. Documentation and instruction manual of the eddy covariance software package TK2. Arbeitsergebnisse 26, Universität Bayreuth, Abt. Mikrometeorologie, Bayreuth, Germany. Print, ISSN 1614-8916.

Michaelis, L., Menton, M. L., 1913. Die Kinetik der Invertinwirkung, Kinetics of the invertin reaction. Biochem. Z. 49, 333.

Moncrieff, J. B., Malhi, Y., Leuning, R., 1996. The propagation of errors in long-term measurements of land-atmosphere fluxes of carbon and water. Global Change Biol. 2, 231–240.

Moore, C. J., 1986. Frequency response corrections for eddy correlation systems. Boundary-Layer Meteorol. 37, 17–35.

Obukhov, A. M., 1960. O strukture temperaturnogo polja i polja skorostej v uslovijach konvekcii, Structure of the temperature and velocity fields under conditions of free convection. Izvestia AN SSSR, seria Geofizika, 1392–1396.

Panofsky, H. A., Tennekes, H., Lenschow, D. H., Wyngaard, J. C., 1977. The characteristics of turbulent velocity components in the surface layer under convective conditions. Boundary-Layer Meteorol. 11, 355–361.

Rapp, J., 2000. Konzeption, Problematik und Ergebnisse klimatologischer Trendanalysen für Eruopa und Deutschland, Concept, problems and results of climatological trend analysis for Europe and Germany. Berichte des Deutschen Wetterdienstes Nr. 212. Tech. rep., German Meteorological Service, Offenbach a. M., Germany.

Rapp, J., Schönwiese, C.-D., 1994. Thermische Jahreszeiten als anschauliche Charakteristik klimatischer Trends, Thermal Seasons as descriptive characteristic of climatological trends. Meteorol. Z. 3, 91–94.

Rayment, M. B., Jarvis, P. G., 2000. Temporal and spatial variation of soil CO_2 efflux in a Canadian boreal forest. Soil Biol. Biochem. 32, 35–45.

Rebmann, C., 2003. Kohlendioxid-, Wasserdampf und Energieaustausch eines Fichtenwaldes in Mittelgebirgslage in Nordostbayern, Carbon dioxide, water vapor and energy exchange of a spruce forest in midrange mountains in North-East Bavaria. Phd thesis, University of Bayreuth.

Rebmann, C., Anthoni, P., Falge, E., Göckede, M., Mangold, A., Subke, J. A., Thomas, C., Wichura, B., Schulze, E. D., Tenhunen, J. D., Foken, T., 2004. Carbon budget of a spruce forest ecosystem. In: Matzner, E. (Ed.), Biogeochemistry of Forested Catchments in a Changing Environment: A german case study. Vol. 172 of Ecological Studies. Springer, Heidelberg, pp. 143–159.

Rebmann, C., Göckede, M., Foken, T., Aubinet, M., Aurela, M., Berbigier, P., Bernhofer, C., Buchmann, N., Carrara, A., Cescatti, A., Ceulemans, R., Clement, R., Elbers, J., Granier, A., Grünwald, T., Guyon, D., Havrankova, K., Heinesch, B., Knohl, A., Laurila, T., Longdoz, B., Marcolla, B., Markkanen, T., Miglietta, F., Moncrieff, H., Montagnani, L., Moors, E., Nardino, M., Ourcvial, J.-M., Rambal, S., Rannik, U., Rotenberg, E., Sedlak, P., Unterhuber, G., Vesala, T., Yakir, D., 2005. Quality analysis applied on eddy covariance measurements at complex forest sites using footprint modelling. Theor. Appl. Climatol. 80, 121–141.

Reichstein, M., Rey, A., Freibauer, A., Tenhunen, J., Valentini, R., Banza, J., Casals, P., Cheng, Y., Grünzweig, J. M., Irvine, J., Joffre, R., Law, B. E., Loustau, D., Miglietta, F., Oechel, W., Ourcival, J.-M., Pereira, J. S., Peressotti, A., Ponti, F., Qi, Y., Rambal, S., Rayment, M., Romanya, J., Rossi, F., Tedeschi, V., Tirone, G., Xu, M., Yakir, D., 2003. Modeling temporal and large-scale spatial variability of soil respiration from soil water availability, temperature and vegetation productivity indices. Global Biogeochemical Cycles 17, 1104, doi:10.1029/2003GB002035.

Schotanus, P., Nieuwstadt, F. T. M., DeBruin, H. A. R., 1983. Temperature measurement with a sonic anemometer and its application to heat and moisture fluctuations. Boundary-Layer Meteorol. 26, 81–93.

Suni, T., Berninger, F., Vesala, T., Markkanen, T., Hari, P., Makela, A., Ilvesniemi, H., Hanninen, H., Nikinmaa, E., Huttula, T., Laurila, T., Aurela, M., Grelle, A., Lindroth, A., Arneth, A., Shibistova, O., Lloyd, J., 2003. Air temperature triggers the recovery of evergreen boreal forest photosynthesis in spring. Global Change Biol. 9, 1410–1426.

Tang, J. W., Baldocchi, D. D., Qi, Y., Xu, L. K., 2003. Assessing soil CO_2 efflux using continuous measurements of CO_2 profiles in soils with small solid-state sensors. Agric. For. Meteorol. 118, 207–220.

Tennekes, H., 1982. Similarity relations, scaling laws and spectral dynamics. In: Nieuwstadt, F., Van Dop, H. (Eds.), Atmospheric turbulence and air pollution modelling. D. Reidel Publishing Company, Dordrecht, Boston, London, pp. 37–68.

Thomas, C., Foken, T., 2002. Re-evaluation of integral turbulence characteristics and their parameterisations. In: 15th Symposium on Boundary Layers and Turbulence. Am.Meteorol.Soc., Wageningen, The Netherlands, pp. 129–132.

Thomas, C., Foken, T., 2006a. Coherent structures in a tall spruce canopy: temporal scales, structure spacing and terrain effects. Boundary-Layer Meteorol., in press.

Thomas, C., Foken, T., 2006b. Flux contribution of coherent structures and its implications for the exchange of energy and matter in a tall spruce canopy. Boundary-Layer Meteorol., submitted for publication.

Thomas, C., Ruppert, J., Lüers, J., Schröter, J., Mayer, J., Bertolini, T., 2004. Documentation of the WALDATEM-2003 Experiment, 28.4.-3.8.2003. Arbeitsergebnisse 24, Universität Bayreuth, Abt. Mikrometeorologie, Bayreuth, Germany. Print, ISSN 1614-8916.

Vickers, D., Mahrt, L., 1997. Quality control and flux sampling problems for tower and aircraft data. J. Atmos. Ocean. Tech. 14, 512–526.

Webb, E. K., Pearman, G. I., Leuning, R., 1980. Correction of flux measurements for density effects due to heat and water vapour transfer. Quart. J. Roy. Meteor. Soc. 106, 85–100.

Wilczak, J. M., Oncley, S. P., Stage, S. A., 2001. Sonic anemometer tilt correction algorithms. Boundary-Layer Meteorol. 99, 127–150.

WMO, 1995. Manual on codes - International codes VOLUME I.1, Annex II to WMO technical regulations, Part A - Alphanumeric codes. WMO-No. 306, World Meteorological Organization, Geneve.

Wyngaard, J. C., Coté, O. R., Izumi, Y., 1971. Local free convection, similarity and the budgets of shear stress and heat flux. J. Atmos. Sci. 28, 1171–1182.

Yaglom, A., 1979. Similarity laws for constant-pressure and pressure-gradient turbulent wall flows. Annu. Rev. Fluid Mech. 11, 505– 540.

6 Tables

Table 1
Recommended parameterisations for the integral turbulence characteristics of the vertical wind component σ_w/u_* (Thomas and Foken, 2002; Foken et al., 2004).

Integral turbulence	stability ranges		
characteristic	$\zeta <$ -0.2	-0.2 $< \zeta <$ 0.4	$\zeta >$ 0.4
σ_w/u_*	$2.0(\zeta)^{1/8}$	$0.21\ln((z_+f)/(u_*)) + 3.1$	$1.3(\zeta)$

ζ, stability parameter $((z_m - d)/L)$; z_+, normalising factor with a value of 1 m; f, Coriolis parameter.

Table 2
Coefficients of determination R^2 from night respiration regressions with fixed or fitted temperature sensitivity parameter E_0.

	E_0=308.56	E_0 fitted
R^2 (half-hourly data)	0.10	0.18
R^2 (2 K bin aggregated data)	0.45	0.86

Table 3
Coefficients of determination R^2 from light response regressions and high quality NEE data availability for 2 K air temperature classes.

2 K air temperature classes:	-6 to 0 ^{o}C	2 to 28 ^{o}C
range of R^2	0.17 to 0.42	0.42 to 0.74
average R^2	0.28	0.61
average number of data	99	267

7 Figures

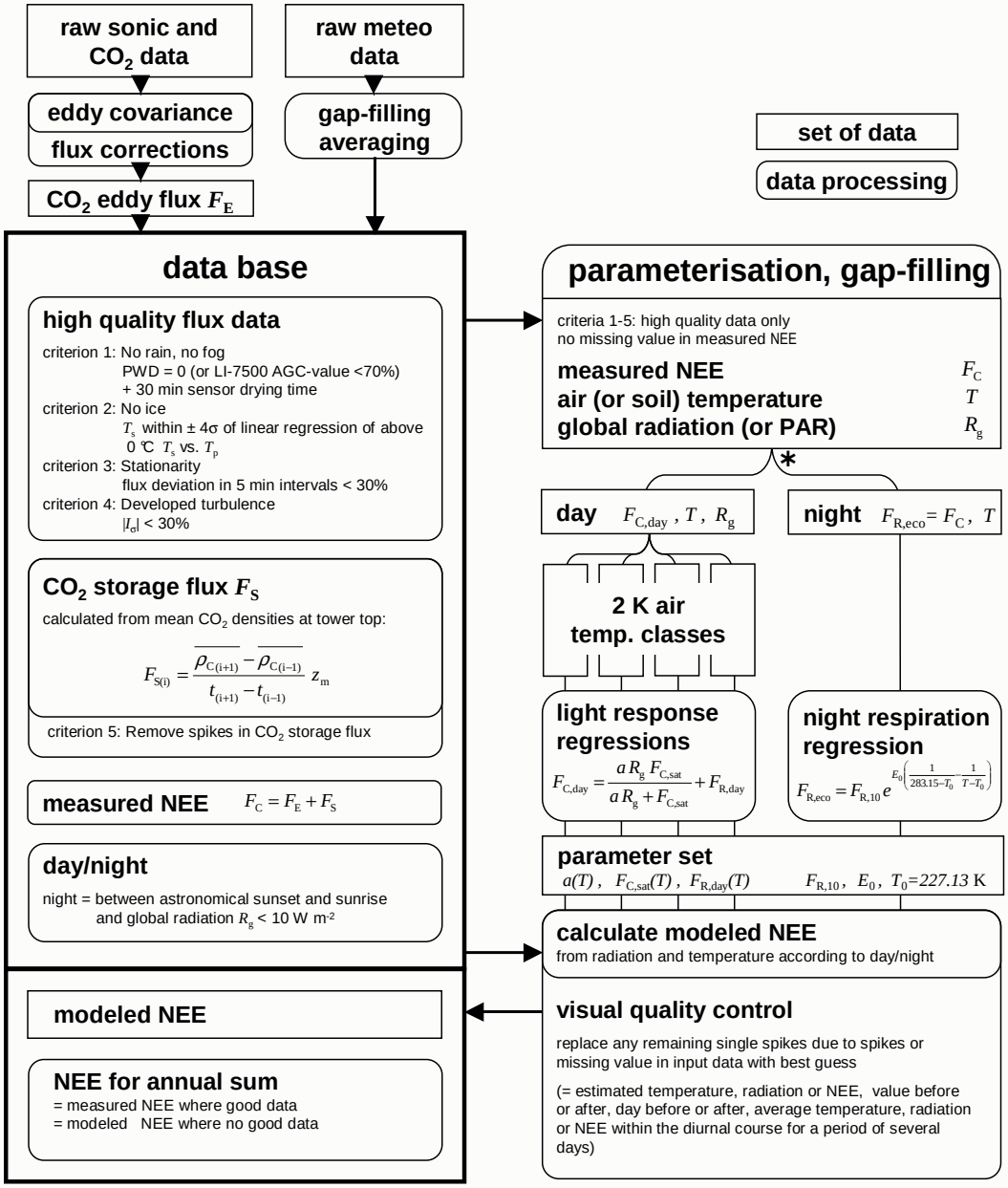

Fig. 1. Scheme of the step by step data handling and processing for the calculation of annual sums of NEE. Rectangular boxes represent sets of data. Rounded boxes represent steps in data processing. For an explanation of symbols and abbreviations refer to the Nomenclature at the beginning of the paper. Temporal segregation can be included into the evaluation scheme at the position marked with a '*' symbol.

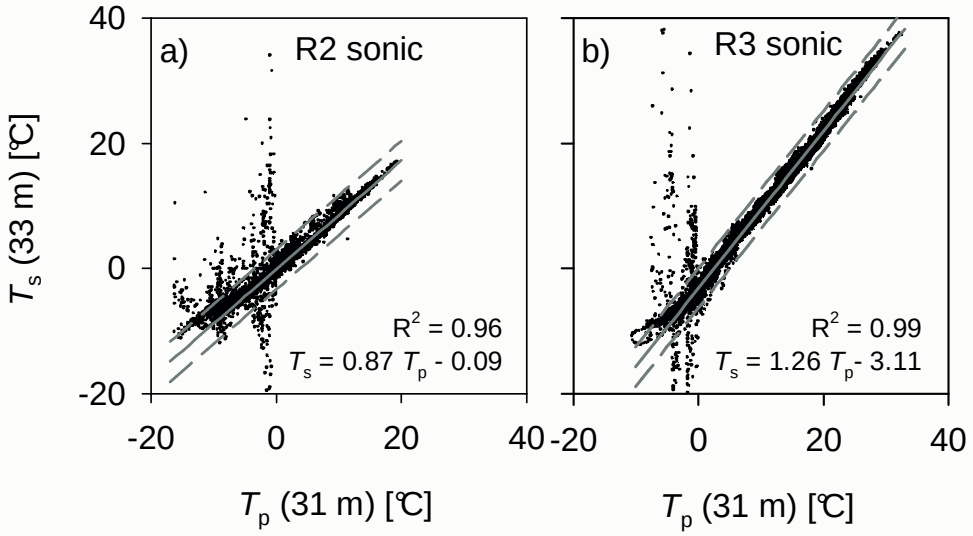

Fig. 2. Air temperature T_p measured at 31 m above ground compared to the sonic temperature T_s recorded with (a) a R2 or (b) R3 sonic anemometer at the FLUXNET-Station Waldstein-Weidenbrunnen in 2003 (dots). The solid lines represent a linear least square regression based on all data above 0 °C. Dashed lines indicate residuals of plus or minus four standard deviations from the linear regression.

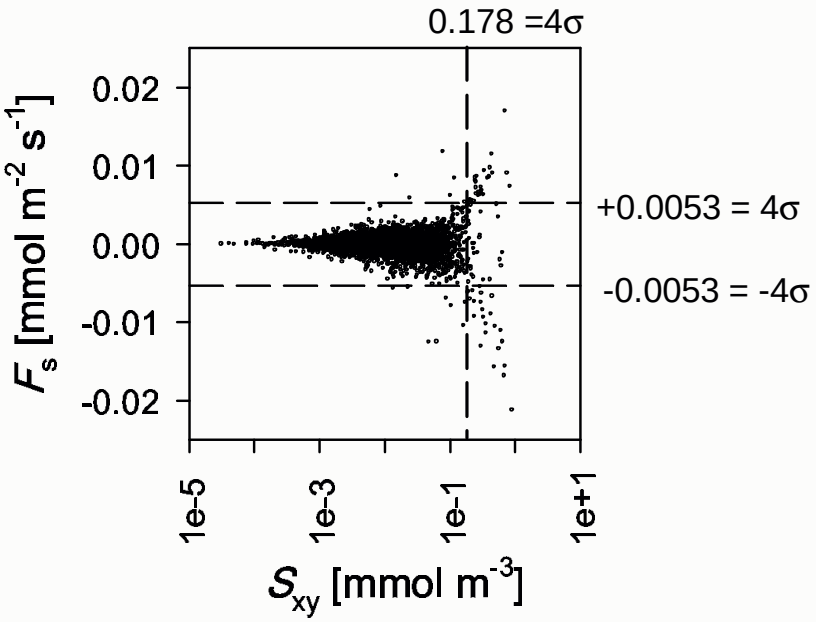

Fig. 3. The storage flux, F_S plotted against the standard error, S_{xy} of the linear regressions are the basis for the criterion 5 (Fig. 1) in which a limit of 4 standard deviations (dashed lines) was used in order to flag outliers. Data was recorded at the FLUXNET-Station Waldstein-Weidenbrunnen in 2003.

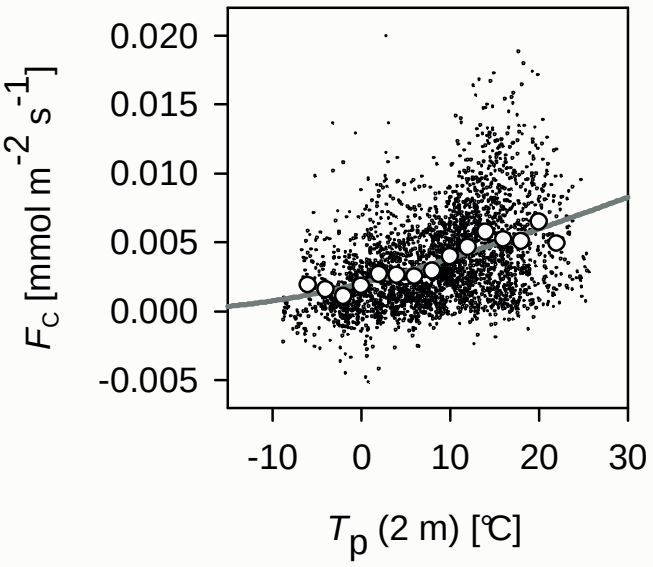

Fig. 4. Regression of night-time net ecosystem exchange, F_C against air temperature, T_p at 2 m above ground for all high quality half-hourly data (dots) and 2 K bin aggregated data (circles). The grey line indicates the least square fit of the exponential equation proposed by Lloyd and Taylor (1994) to the half-hourly data with variable $F_{R,10}$ and E_0 and fixed $T_0 = 227.13$.

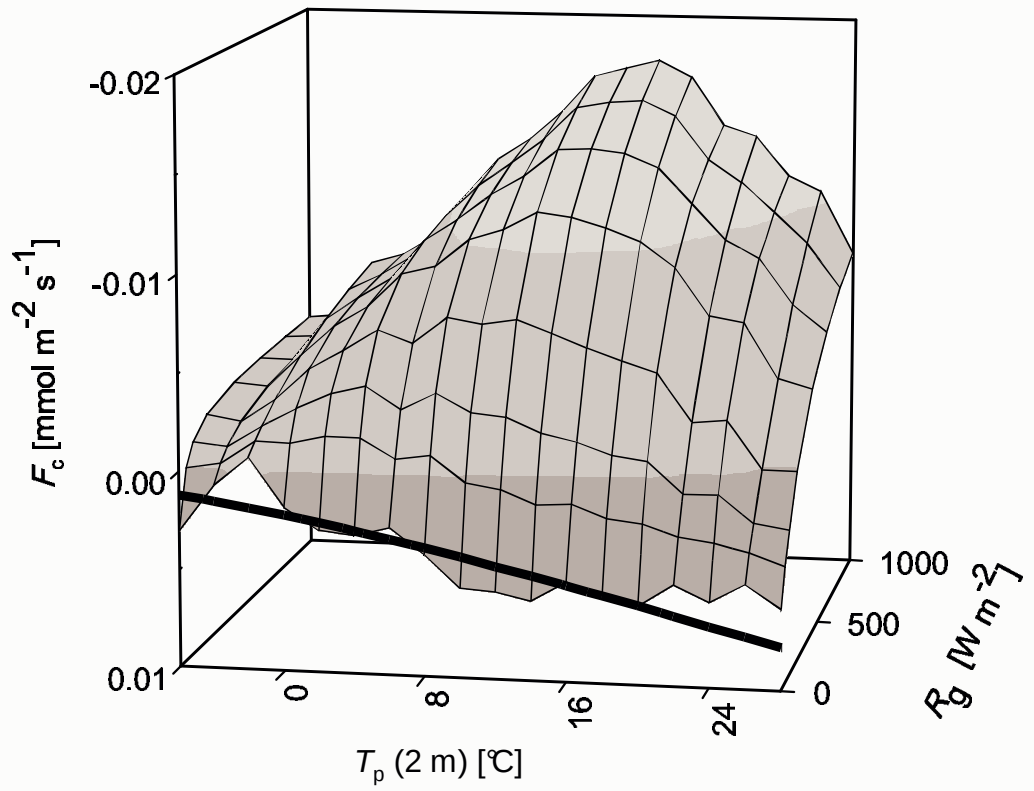

Fig. 5. Dependence of day-time net ecosystem exchange, NEE, F_C (surface) and night-time NEE (black line) measured at the FLUXNET-Station Waldstein-Weidenbrunnen on air temperature T_p (2 m a.g.l.) and global radiation R_g modelled with parameters from the regression analysis using *Michaelis-Menten* functions (1913) for the light response regression and the *Lloyd-Taylor* function (1994) for the regression of night-time ecosystem respiratory fluxes.

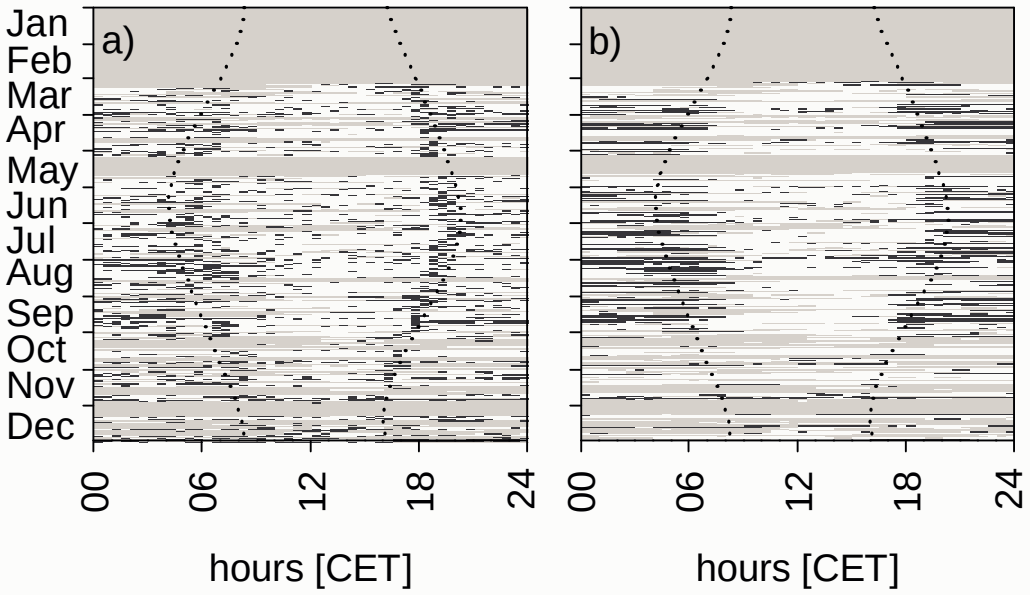

Fig. 6. Distribution of quality data by day and hour through 2003 obtained at FLUXNET-Station Waldstein-Weidenbrunnen using criteria based on (a) stationarity and integral turbulence characteristic tests (criteria 3 and 4) and (b) friction velocity, $u_* < 0.3\,\mathrm{m\,s^{-1}}$. White areas indicate accepted and black areas rejected data with grey areas indicating missing data due to rain, fog, ice (criteria 1 and 2) or instrumental failures. The dotted lines indicate astronomical sunrise and sunset.

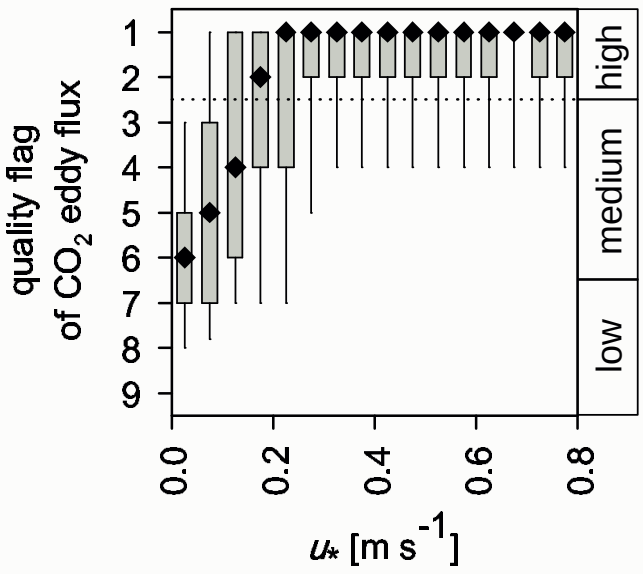

Fig. 7. Dependence of frequency distributions of quality flags after Foken et al. (2004) for the CO_2 eddy flux data at the FLUXNET-station Waldstein-Weidenbrunnen on friction velocity, u_* aggregated in $0.05\,\mathrm{m\,s^{-1}}$ bins. Diamonds indicate the median, box boarders the 25 % and 75 % percentile and lines the 10 % and 90 % percentile.

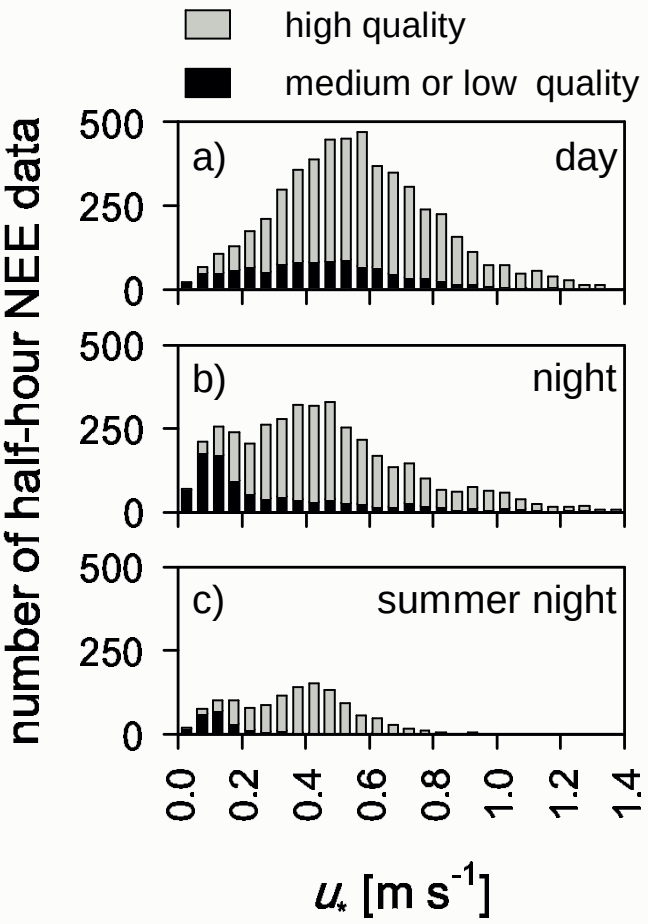

Fig. 8. Histograms of (a) day-time half-hourly net ecosystem exchange, NEE and (b) and (c) night-time half-hourly NEE measured at the FLUXNET-station Waldstein-Weidenbrunnen for $0.05\,\mathrm{m\,s^{-1}}$ bins of friction velocity, u_* - (b) all nights and (c) summer nights only. The grey part of the bars represents data rated as high quality according to the criteria 1-5 (Fig. 1), while the black part of the bar represents medium or poor quality data.

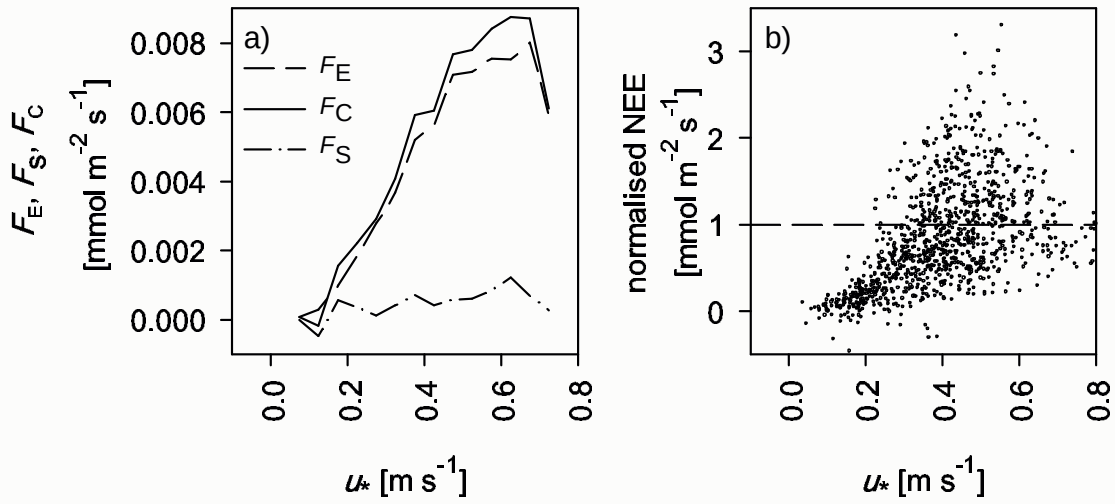

Fig. 9. Dependence of (a) CO_2 eddy flux, F_E, storage flux, F_S and net ecosystem exchange, NEE, F_C and (b) normalised NEE on friction velocity, u_* measured at the FLUXNET-Station Waldstein-Weidenbrunnen during summer 2003 (June, July, August).

Whole-air relaxed eddy accumulation for the measurement of isotope and trace-gas fluxes

J. Ruppert[1,2*], W. A. Brand[3], N. Buchmann[4], T. Foken[1]

[1]Department of Micrometeorology, University of Bayreuth, Germany

[2]now: Research Institute of the Cement Industry, Verein Deutscher Zementwerke, Düsseldorf, Germany

[3]Max Planck Institute for Biogeochemistry, Jena, Germany

[4]Institute of Plant Science, ETH Zürich, Switzerland

*Corresponding author: Johannes Ruppert, Research Institute of the Cement Industry, Environment and Plant Technology Department, Verein Deutscher Zementwerke, Tannenstrasse 2, 40476 Düsseldorf, Germany.
E-mail: rj@vdz-online.de, Telephone: +49-211-4578-275, Fax: +49-211-4578-256.

Abstract

Measuring the isotopic composition of trace gas fluxes can provide additional information on ecosystem gas exchange, when ecosystem processes, like assimilation, discriminate against heavier isotopes. In the case of CO_2 exchange, different mass-balances for bulk CO_2 and its $^{13}CO_2$ or $CO^{18}O$ isotopes can be used to separate respiration from photosynthetic assimilation. Up to now, detectors for direct isotope measurements in the field lack the precision needed for fast eddy covariance (EC) flux measurements. The collection of updraft and downdraft whole-air samples using the relaxed eddy accumulation technique (REA) allows simultaneously determining trace gas concentrations and isotope ratios by high precision laboratory analysis. At the same time whole-air REA relaxes several of the technical problems related to REA sampling on traps.

In tests using air from a tank the complete whole-air REA sampling system and its foil balloon bag reservoirs showed no signs of contamination after cleaning. The standard deviations of $\delta^{13}C$ and $\delta^{18}O$ isotope ratios were only slightly higher than the precision specified for the laboratory analysis procedure. Results from a field experiment above a spruce forest showed (i) a good match of samples taken with the whole-air REA system and an independent vertical profile air sampling system and (ii) that isotopic differences (updrafts−downdrafts) were large enough to yield signal to noise ratios greater than five when applying hyperbolic deadbands during REA sampling (HREA). The performance of the instrument and the HREA sampling method are investigated by simulation of the sampling process for bulk CO_2, which serves as proxy scalar.

Measurements by whole-air HREA in combination with high precision isotope analysis can quantify the isofluxes of $^{13}CO_2$ and $CO^{18}O$. Furthermore, additional information is collected on the scalar correlation of bulk CO_2 and its stable isotopes, which represents the relatively short timescale of updrafts and downdrafts in the turbulent exchange above the canopy. This information is essential to check the scalar similarity assumptions made in the HREA and EC/flask method for the quantification of isofluxes.

Index terms:

0315 Biosphere/atmosphere interactions (0426, 1610)
0394 Instruments and techniques
0454 Isotopic composition and chemistry (1041, 4870)
0490 Trace gases
0428 Carbon cycling (4806)

Keywords: Relaxed eddy accumulation, Isotope, Trace-gas flux, Trace-gas sampling, Carbon flux

Manuscript prepared for submission to Journal of Geophysical Research – D: Atmospheres

1. Introduction

In recent years, a special interest was to quantify the isotopic composition of CO_2 flux densities above different ecosystems [*Bowling et al.*, 2003a; *Ehleringer et al.*, 2002; *Yakir and da S. L. Sternberg*, 2000]. Such measurements provide means for identifying the individual contributions of sources and sinks with different isotopic signature to the CO_2 net ecosystem exchange (NEE) and the rate of internal recycling of CO_2, e.g. in the canopy space of forests [*Lloyd and Farquhar*, 1994; *Lloyd et al.*, 1996; *Yakir and Wang*, 1996]. Two different mass-balances for bulk CO_2 and its isotopes can be used to separate respiration from assimilation, which discriminates against $^{13}CO_2$ and $CO^{18}O$ [*Bowling et al.*, 2001; *Wichura et al.*, 2000].

Different eddy sampling methods like relaxed eddy accumulation (REA) [*Businger and Oncley*, 1990] are commonly used to measure trace gas fluxes in the boundary layer when fast high precision chemical sensors are not available for eddy covariance (EC) flux measurements. Eddy sampling methods are passive in the sense that they do not modify the turbulent gas exchange of the ecosystem. Therefore such measurements are complementary to measurements with enclosures e.g. on individual parts of the ecosystem and can be used for their validation. Measurements of the turbulent exchange above an ecosystem provide information with a spatial integration that can close a gap of scale between isotope studies at leaf or branch scale and atmospheric isotope studies and large scale modeling approaches [*Canadell et al.*, 2000; *Kaplan et al.*, 2002; *Yakir and da S. L. Sternberg*, 2000]. This is especially important for the investigation of carbon budgets of forests, because in tall vegetation complex gas exchange processes exist.

The ability to analyze the isotopic signature of the turbulent exchange is mainly limited by the measurement uncertainty regarding the CO_2 isotope ratios at small differences of bulk CO_2 mixing ratios [*Bowling et al.*, 1999a; *Bowling et al.*, 1999b; *Bowling et al.*, 2003b; *Zobitz et al.*, 2006]. Most studies on isotope flux measurements above the canopy focus on the evaluation of the ^{13}C-isotope signatures. In general, the difference of isotope signatures in the CO_2 exchange during the day is expected to be larger for ^{18}O-isotopes, because the ^{18}O-isotope signature of CO_2 can equilibrate with ^{18}O-depleted soil water and ^{18}O-enriched leaf water pools [*Yakir and da S. L. Sternberg*, 2000]. $CO^{18}O$ isotope fluxes could therefore yield more independent information on assimilation and respiration. However, measurement results presented by *Bowling et al.* [1999a] were less uniform, which might reflect higher temporal and spatial variability of the water pools.

The aim of this study is to present a method for the measurement of $^{13}CO_2$ and $CO^{18}O$ isotope fluxes based on the hyperbolic relaxed eddy accumulation method (HREA) and whole-air sampling. The application of the hyperbolic sampling criteria maximizes scalar concentration differences [*Bowling et al.*, 1999b]. Whole-air sampling allows subsequent high precision isotope analysis in a laboratory directly from the accumulated updraft and downdraft air samples [*Bowling et al.*, 2003a]. With the construction of a new sampling system we aimed at further improving the accuracy of isotope sampling especially for ^{18}O isotopes. Sample volumes were increased in order to also allow direct and precise analysis of the corresponding bulk CO_2 mixing ratios. The integrity of isotope samples and sampling accuracy was thoroughly tested in the laboratory and in the field by comparison with independent measurements above a spruce forest during the experiment WALDATEM-2003.

The combined information of CO_2 isotope ratios and mixing ratios in updraft and downdraft air samples is used to analyze the scalar correlation, which is a basic assumption in the HREA and EC/flask methods [*Bowling et al.*, 2003a]. Based on the measured bulk CO_2, the HREA

sampling procedure and flux determination method are validated as requested by *Bowling et al.* [1999a] and *Kramm et al.* [1999]. The methodological performance of HREA is investigated by simulation of the sampling process. However, the effective sampling efficiencies determined from measured bulk CO_2 data are taken into account for the determination of turbulent isofluxes.

2. Theory

In the conditional sampling or relaxed eddy accumulation method (REA) [*Businger and Oncley*, 1990] the turbulent flux density is determined from the concentration difference measured in updraft and downdraft air samples. This concentration difference is scaled with the intensity of turbulent vertical mixing measured by the standard deviation of the vertical wind speed σ_w based on the assumption of flux-variance similarity. Because air sampling is not proportional to the vertical wind speed, it is referred to as relaxed sampling. Consequently, REA is an indirect method for flux measurements. It relies on a parameterization in which the so called *b*-factor is determined from a second scalar quantity (proxy scalar) which shows similarity in its atmospheric transport (scalar similarity, [*Ruppert et al.*, 2006b; *Wyngaard and Moeng*, 1992]) and for which the fluctuations of its concentration can be measured in the field with high temporal resolution:

$$F_c = b\sigma_w \rho_a \left(\overline{c_\uparrow} - \overline{c_\downarrow}\right). \tag{1}$$

F_c is the turbulent flux density of the scalar c. ρ_a is the dry air density. $\overline{c_\uparrow}$ and $\overline{c_\downarrow}$ are the average scalar concentrations respectively in updraft and downdraft air samples expressed as dry air mixing ratios.

For the proxy scalar normally F_c is determined by eddy covariance (EC) measurements ($F_c=\overline{w'c'}$), where w' and c' are the fluctuations of the vertical wind speed w and scalar concentration c around their average values. The over bar denotes Reynolds averaging. The proportionality factor b can then be determined for the proxy scalar by rearranging (1) either based on (i) simulation of REA sampling on high frequency scalar time series and its resulting concentration difference $\overline{c_\uparrow} - \overline{c_\downarrow}$ or based on (ii) measured concentration difference from real REA air sampling for the proxy scalar:

.

$$b = \frac{\overline{w'c'}}{\rho_a \sigma_w \left(\overline{c_\uparrow} - \overline{c_\downarrow}\right)} \tag{2}$$

Many studies demonstrate the relative stability of average *b*-factors in unstable and moderately stable conditions [*Ammann and Meixner*, 2002; *Baker et al.*, 1992; *Beverland et al.*, 1996a; *Foken et al.*, 1995]. Nevertheless, significant variability of *b*-factors for individual 30 min periods is observed, and different factors are discussed [*Gao*, 1995; *Guenther et al.*, 1996; *Oncley et al.*, 1993; *Pattey et al.*, 1993; *Ruppert et al.*, 2006b]. Several studies point out, that skewness in the joint frequency distribution (JFD) of w' and c' and structures in the turbulent exchange are causing changes in *b*-factors [*Fotiadi et al.*, 2005; *Katul et al.*, 1996; *Milne et al.*, 2001; *Ruppert et al.*, 2006b]. The study by *Ruppert et al.* [2006b] attributes observed variation in the scalar exchange to events at time scales >60 s. This limits the use of a unique *b*-factor for all times and asks for the determination of individual *b*-factors for each sampling period. Under the assumption of scalar similarity, the *b*-factor determined for a proxy scalar by (2) is used to

derive the turbulent flux density of the scalar of interest from its measured average concentration difference between updraft and downdraft REA samples $\overline{c}_{\uparrow} - \overline{c}_{\downarrow}$ by solving (1).

Application of a wind deadband for small vertical wind speeds, in which no samples are taken, increases the concentration difference between the updraft and downdraft air accumulation reservoirs and thereby the certainty of the flux measurement, especially if chemical sensor resolution is a limiting factor [*Businger and Delany*, 1990; *Delany et al.*, 1991]. At the same time, the *b*-factor decreases with the size of the deadband. The wind deadband size H_w is normally defined in reference to the normalized vertical wind speed fluctuations:

$$\left| \frac{w'}{\sigma_w} \right| \leq H_w . \tag{3}$$

In the hyperbolic relaxed eddy accumulation method (HREA) the deadband rejects not only samples with small fluctuations of the vertical wind speed *w*' but also samples with small deviations from the mean scalar concentration, which further increases the concentration difference $\overline{c}_{\uparrow} - \overline{c}_{\downarrow}$ [*Bowling et al.*, 1999b; *Bowling et al.*, 2003a]:

$$\left| \frac{w'c'}{\sigma_w \sigma_c} \right| \leq H_h . \tag{4}$$

The hyperbolic deadband with the size H_h must be determined online from a proxy scalar measured with high temporal resolution, which again assumes scalar similarity. A deadband reduces the frequency of valve switching during sampling and at the same time, the number of samples used for flux calculation. It also reduce the sensitivity of REA methods to uncertain definition of the mean vertical wind speed *w* needed for segregating samples in the up and down reservoirs [*Businger and Oncley*, 1990; *Pattey et al.*, 1993]. Details on the sampling method and procedures used in this study are described in Section 3. A comparison of general characteristics of eddy sampling methods like REA and HREA and different sources of error for flux determination are presented in a paper by *Ruppert et al.* [2002].

3. Methods and Material

The design of the whole-air REA system goes back to the principles ideas for conditional sampling of trace gases [*Businger and Oncley*, 1990; *Delany et al.*, 1991; *Desjardins*, 1977; *Oncley et al.*, 1993; *Pattey et al.*, 1993] and is based on a design presented by *Bowling et al.* [2003a] in which foil balloon bags serve as intermediate storage for updraft and downdraft air samples at ambient pressure.

3.1. Scalar similarity

The determination of *b*-factors in the REA method and the online definition of a hyperbolic deadband (i.e. in the HREA method) requires the selection of a proxy scalar, which shows good scalar similarity with the scalars of interest. For this study the bulk CO_2 density signal (ρ_{CO2}) of an open path gas analyzer was selected as proxy scalar for the estimation of the scalar intensity of ^{13}C and ^{18}O isotopes[1] of CO_2. The assumption is, that bulk CO_2 density shows sufficient

[1] ^{13}C and ^{18}O isotope ratios in this study refer to the isotope composition of CO_2, i.e. the ratio of $^{13}CO_2$ or $CO^{18}O$ to bulk CO_2. The isotope ratio is expressed in δ-notation. All $\delta^{13}C$ and $\delta^{18}O$ values are reported relative to ^{13}C and ^{18}O

scalar similarity with the unknown fast fluctuations of the CO_2 isotopic composition. A detailed discussion of the effects of scalar similarity in REA flux measurements is presented by *Ruppert et al.* [2006b].

We are confident, that the assumption is justified at least for the efficient selection of the strong up- and downdrafts by a hyperbolic deadband, as all CO_2 isotope turbulent exchange is part of the bulk CO_2 turbulent exchange. Also, linear relationships between the $\delta^{13}C$ isotope ratio and bulk CO_2 mixing ratio of whole-air samples collected at timescales down to 500 ms and of REA samples are reported by *Bowling et al.* [1999a; 2001]. Nevertheless, if considering the location of sources and sinks in the ecosystem individually for bulk CO_2, $^{13}CO_2$ and $CO^{18}O$, some difference in the scalar exchange should be expected, which might also affect scalar similarity. Less scalar similarity would introduce some error in HREA flux results with a tendency for underestimating the flux [*Ruppert et al.*, 2006b]. The assumption of scalar similarity made here is therefore tested by investigating the $\delta^{13}C/CO_2$ and $\delta^{18}O/CO_2$ relations (Section 4.4).

The following sections describe the implemented online turbulence data analysis, the HREA sampling procedures, the whole-air REA system design for high precision isotope and trace-gas sampling and sample analysis.

3.2. Axis rotation and hyperbolic deadband definition

A three-dimensional planar fit rotation matrix was determined based on 1 month of wind velocity data from the sonic anemometer used for eddy covariance and REA sampling. It indicated good horizontal orientation of the sonic anemometer and that only minor planar-fit corrections were necessary for the vertical wind speed.

The determination of the turbulent CO_2 flux densities from EC measurements was performed with the TK2 software package [*Mauder and Foken*, 2004] and common corrections and quality control measures were applied as outlined by *Ruppert et al.* [2006a] including a WPL-correction for density fluctuations [*Webb et al.*, 1980] and a planar-fit rotation [*Wilczak et al.*, 2001] with a vertical wind speed offset correction of 0.032 m.

The problem of axis rotation for REA was raised by *Beverland et al.* [1996b] and *Moncrieff et al.* [1998]. We addressed this issue by applying the previously determined planar-fit correction to the vertical wind component online during HREA sampling and were thereby able to correct the vertical wind speed offset. The coordinate rotation of the planar-fit correction (<3°) was applied slightly incorrect to the online data used during HREA sampling. This was due to an unidentified azimuth rotation of 120° between the sonic anemometer raw online data and stored data. However, simulations showed, that this had only minor influence on the updraft and downdraft HREA sample segregation under the conditions of the WALDATEM-2003 experiment. The resulting relative error of the HREA concentration difference due to the erroneous online planar-fit rotation was –2(±3)%. This indicates a small underestimation of the concentration difference on average, i.e. slightly reduced efficiency in sampling the maximum concentration difference. This equally applies to the proxy scalar and the scalar of interest. Therefore, the turbulent flux densities will hardly be altered, if they are calculated from measured effective *b*-factors for the proxy scalar like in this study.

---

isotopic abundances in the international VPDB (Vienna Pee Dee Belemnite) and VPDB-CO_2 standards respectively (CG99 scale, see details in [*Werner et al.*, 2001] and [*Werner and Brand*, 2001]):
$\delta^{13}C=[[(^{13}C/^{12}C)_{sample}-(^{13}C/^{12}C)_{VPDB}]/(^{13}C/^{12}C)_{VPDB}]\cdot 1000$ (‰ VPDB).
$\delta^{18}O=[[(^{18}O/^{16}O)_{sample}-(^{18}O/^{16}O)_{VPDB\text{-}CO2}]/(^{18}O/^{16}O)_{VPDB\text{-}CO2}]\cdot 1000$ (‰ VPDB-CO_2).

In general, the problem of axis rotation and definition of the vertical wind vector for REA and HREA can be addressed. Like described above the planar-fit correction method can be applied as detailed axis rotation procedures for the correction of the vertical wind speed *w* based on fast online analysis of the 3D wind data with a computer. This can be done without time lags from filter functions as asked for by *Moncrieff et al.* [1998] as long as (i) a 3D sonic anemometer is installed long enough before REA sampling to collect a statistically meaningful amount of wind data specific to the site, sonic anemometer and its orientation and (ii) the anemometer orientation remains unchanged for REA sampling. Both criteria can easily be met when REA sampling is performed at sites with permanently installed eddy covariance measurement systems, e.g. at FLUXNET sites.

For the online definition of the hyperbolic deadband during REA sampling according to (4) the vertical wind speed fluctuations *w*' were determined from the 3D wind vector after applying the planar-fit correction. The standard deviation of the vertical wind speed as well as the average and standard deviation of the CO_2 density were continuously recalculated from the most recent 6 min of data applying a linear weighting function by which the newest data was rated three times more important than the oldest data.

3.3. Whole-air REA sampling system and sampling procedure

From close to the measurement path of a sonic anemometer air is sampled through a 1 µm filter and 5 m of Dekabon tubing with polyethylene as inner wall material with a total flow rate of 6.6 L min^{-1}, which assures predominantly turbulent flow (Reynolds number= 2433) in the inlet tube. Plumbing in the system consisted of stainless steel tubing and fittings. All steel and glass material in the system was thoroughly cleaned before assembling by threefold rinsing with Acetone:Hexane 1:1 (nanograde) and subsequent heating. Connection to the REA system and to the glass flasks is made using quick connectors and ultra-torr glass connectors. Viton® only is used as seal material also in membrane pumps and valves. The air stream is splitted into a bypass and a sub-sample of 3 L min^{-1} (Figure 1a). Only the sub-sample is used for REA sampling of updrafts and downdrafts. Constant flow rates ($\sigma \leq 0.5\%$) with minimum pressure drop as asked for by *Bowling et al.* [1998] and *Moncrieff et al.* [1998] are achieved by using low pressure drop flow meters in combination with pulse-width pump motor drivers for the adjustment of constant pump performance, instead of flow controllers. A Nafion® gas-dryer is used for pre-drying of the sample air. Two three-way valves (V1, V2) direct the sample into the vent (deadband) or the bag 1 or bag 2 reservoirs according to the sign of the vertical wind speed and the size of the deadband (updraft, downdraft). During field experiments the definition of bag 1 and bag 2 as reservoirs for REA updraft or downdraft samples was switched after each sampling interval in order to minimize any systematic influence of one sampling path. A third non-operating valve of the same kind is installed to assure the same flow restriction on all three flow paths. The time lag (7 ms) resulting from the separation of the sampling valves V1 and V2 and the selected flow rate and the valve response times (10-20 ms) are small enough in relation to a desired sampling frequency of 10 Hz (100 ms). In order to allow for larger sample volumes, each bag reservoir consists of two 45 cm diameter Mylar® foil balloons, which are equipped with stainless steel filling tubes, partially perforated, inserted through the foil valve of the balloons and joined with a T-fitting (not shown in Figure 1a and 1b). An airtight seal was achieved by wrapping strong rubber band around the filling tube and foil valve. After REA sampling and before filling into 1 L glass flasks with PCTFE stopcocks the air from the reservoirs is further dried by passing through drying traps filled with magnesium perchlorate

granulate ($Mg(ClO_4)_2$). Backpressure valves at the system outlet constantly maintain +500 hPa over ambient pressure in the drying traps and glass flasks in order to minimize potential fractionation by adsorption/desorption processes at the relatively large surfaces of the granulate and flasks.

The dead volume of the bag reservoirs, which cannot be removed by pumping, is about 20 mL. Nevertheless, all old sample in the reservoirs is removed effectively (dilution >>10000:1) prior to REA sampling by flushing the bag reservoirs two times with 10 L of dried air from sampling height through the flushing unit and emptying via the flask-fill units. During a third flushing cycle the bag reservoirs and the two flask-fill units are then conditioned with dried air from sampling height. The bag reservoirs are emptied and conditioning air remains in the drying traps and glass flasks during the next 30-40 min REA sampling procedure. Normally about 10 to 15 L of updraft and downdraft air were collected within 30-40 min of REA sampling with a hyperbolic deadband of H_h=1.0. This allowed flushing the 1 L glass flasks with 6 to 10-fold volume of sample at +500 hPa overpressure. The filling procedure is stopped shortly before one of the bag reservoirs is emptied by closing actuated two-way valves on both sides of the glass flasks and then manually closing the stopcocks of the flasks. Refer to the appendix for details on individual system components.

The complete sampling procedure is controlled by the software 'ATEM' (Atmospheric Turbulence Exchange Measurements, [*Ruppert*, 2005]), which allows online monitoring and automated detailed documentation of each sampling procedure. This software also performs the required online analysis of wind and scalar data during REA sampling for the definition of the hyperbolic deadband and corresponding segregation of updraft and downdraft air samples.

3.4. Synchronization of updraft and downdraft sample segregation

The importance and difficulty of correct synchronization of valve switching in REA and HREA to the vertical wind speed fluctuations under the presence of a unknown time lag as the result of sample flow in a tube is discussed by *Bowling et al.* [1998], *Moncrieff et al.* [1998] and *Fotiadi et al.* [2005]. We addressed this problem by performing a differential measurement of sample delay in the tube under defined sampling flow conditions before HREA sampling. The time lag was determined by cross-correlation of vertical wind speed measured at the tube inlet and CO_2 density fluctuations firstly measured at the sample tube inlet and secondly at the segregation valves V1 and V2 (Figure 1a). During HREA sampling, the same defined flow conditions were adjusted and continuously monitored and the time lag measured beforehand was set in the sampling system control software 'ATEM' for valve switching. Thereby we were able to assure correct synchronization of valve switching to the updraft and downdraft events in the turbulence data under defined sampling conditions. The 'ATEM' software also corrected a 200 ms delay of the open-path CO_2 signal due to electronic processing in the instrument. Further details on the synchronization and the online data handling are described by *Ruppert* [2005].

3.5. Whole-air sampling method, density corrections and simulations

In whole-air REA sampling the information on the volume of the sample is preserved, in contrast to sampling on traps. Therefore, the collection of whole-air samples slightly relaxes the demand for very precisely controlled volume flow rates during sampling [*Bowling et al.*, 1998]. After passing several meters of tube, updraft and downdraft samples have similar temperature at the pump and segregation valves. No density correction is needed for the measured scalar concentration differences, *b*-factors and turbulent flux densities, because air samples are dried in

the sampling process and the updraft and downdraft concentrations in whole-air samples are determined as mixing ratios by laboratory analysis [*Lee,* 2000; *Pattey et al.,* 1992; *Webb et al.,* 1980]. Because the whole-air sample collection is not component specific, different non-reactive and stable trace gas components can be analyzed from the same sample.

Relative to sampling on cryo-traps [*Bowling et al.,* 1999a; *Wichura et al.,* 2000], smaller sample volumes are sufficient for whole-air isotope sampling. Smaller sample flow rates, low pressure drop flow meters and the use of flexible Mylar® balloon bags as intermediate storage at ambient pressure minimize pressure changes at orifices in the sampling path and difficulties with fractionation processes [*Bowling et al.,* 1999a]. An important practical advantage of whole-air sampling for isotopes compared to cryo-trap sampling is, that no liquid nitrogen needs to be carried to and handled in the field.

The system design and operation presented in Section 3.4 was chosen in order to achieve larger whole-air sample volumes compared to the design presented by *Bowling et al.* [2003a] with the aim to increase the sampling accuracy and precision for high precision isotope analysis of $^{13}CO_2$ and $CO^{18}O$. Sufficient amounts of updraft and downdraft air are preserved as dried whole-air samples so that also bulk CO_2, N_2O and CH_4 could be measured. The exact bulk CO_2 mixing ratio of the updraft and downdraft samples is valuable information:

(i) Both bulk mixing ratio and isotope ratio are required for the determination of the isotope mixing ratio, which forms the basis for the calculation of the turbulent isotope flux density according to (1) formulated for the turbulent isoflux as (6) (see Section 4.7). With measured bulk CO_2 mixing ratios there is no general need to indirectly infer the mixing ratio from field instrumentation measurements and simulation of the sampling process.

(ii) Measured effective *b*-factors for CO_2 can be determined according to (2) and from the EC CO_2 flux density. Such *b*-factors integrate all aspects of the sampling process and potential errors. They are compared to *b*-factors from simulation of the ideal HREA sampling process on the CO_2 data record of the EC system in Section 4.5. The comparison of measured effective and simulated *b*-factors forms the basis for the validation of the sampling method and process.

(iii) The scalar correlation of isotope ratios and bulk CO_2 mixing ratios in updraft and downdraft air samples can be investigated with higher precision (see Section 4.4). The accumulated updraft and downdraft samples are taken during very short time intervals ranging from 100 ms to several seconds. They therefore represent turbulent exchange processes on relatively short timescales and can be compared to flask samples collected during longer time intervals. Such data allows investigating the scalar similarity assumptions of the HREA method and the so called EC/flask method [*Bowling et al.,* 1999a; *Bowling et al.,* 2001; *Bowling et al.,* 2003a] on relevant timescales.

For the simulations, the time series of the CO_2 mixing ratio (μ_{CO2}) was determined from the CO_2 density (ρ_{CO2}) record of the open path gas analyzer of the EC system and air density (ρ_a) according to the following equation based on the ideal gas law. Its applicability for simulation studies depending on the design of REA measurement systems is discussed in detail by *Ammann* [1999, p. 92] and *Leuning and Judd* [1996]:

$$\mu_{CO2} \equiv \frac{\rho_{CO2}}{\rho_a} = \frac{\rho_{CO2} T p_0}{\rho_0 T_0 p}\left(1+\mu_{H2O}\right). \quad (5)$$

Where ρ_0, T_0 and p_0 are respectively the standard dry air density, temperature and pressure. Temperature T was determined from the high frequency sonic anemometers speed of sound measurements and an instrument specific correction for the sonic temperature [*Ruppert et al.*, 2006a]. 30 min integrated pressure data from a nearby measurement station were corrected to measurement height in order to yield p. The water vapor mixing ratio (μ_{H2O}) was determined from the high frequency open path gas analyzer H_2O density (ρ_{H2O}) record after application of a similar density correction.

3.6. High precision isotope REA sampling, isotope ratio mass spectrometry (IRMS) and trace gas analysis

High precision sampling for the stable isotopes $^{13}CO_2$ and $CO^{18}O$ of CO_2 requires avoiding sample contamination by fractionation processes. A potential source for isotope sample contamination and fractionation processes are adsorption and desorption effects at large surfaces like the balloon bag reservoirs and the drying traps or related to pressure fluctuations. Such surface effects were reduced by increasing the collected and stored sample volumes and by conditioning bags and flasks before sampling with dried ambient air from sampling height. The flexible balloon bag reservoirs remain at ambient pressure levels. The automation of the conditioning and sample transfer procedures in the new system allowed to assure a constant level of pressure at +500 hPa over ambient pressure in the drying traps and glass flasks, in which the samples are stored until analysis. The automation of the REA system was also intended to improve the measurement repeatability regarding the sampling and filling procedures and to avoid exceptional errors, which might result from manual sample handling. 1 L glass flasks with PCTFE stopcocks are used for sample storage and transport into the laboratory. The large sample volume and sampling flask conditioning with dry air are required for subsequent high precision isotope and trace gas analysis [*Brand*, 2005; *Rothe et al.*, 2005; *Sturm et al.*, 2004; *Werner et al.*, 2001].

For isotope analysis, sample air from the flasks is directed into a home made trapping line ('BGC AirFlo', [*Werner et al.*, 2001] attached to a MAT 252 isotope ratio mass spectrometer (IRMS) system. The air is pumped through the cryogenic trapping system and CO_2 is frozen out at a temperature of –196 °C using a flow of 60 bml/min. The dual inlet system of the MAT 252 is used as the pumping infrastructure. Sample CO_2 is extracted from 600 mL of air and, after pumping away residual air and allowing for complete isotopic equilibration, measured directly from the sampling reservoir via the 252 changeover valve. The system is under full computer control for reliable timing and unattended operation. The isotopic analysis is performed with high level of overall precision for both $\delta^{13}C$ and $\delta^{18}O$ at about 0.013‰ vs. VPDB and 0.02% vs. VPDB-CO_2 respectively. For further details on the IRMS high precision analysis system and procedures see *Werner et al.* [2001].

The CO_2, N_2O and CH_4 mixing ratios were determined in the trace gas laboratory of the Max-Planck Institute in Jena, Germany. A chromatographic run starts with flushing sample gas from the pressurized glass flask through the two sample loops. The amount of gas is controlled by a mass flow controller. For some samples lacking pressure above ambient in the glass flask a manual injection method with a syringe was applied. The lack of pressure in these glass flasks was due to a temporal malfunctioning of a backpressure valve during the filling procedure.

After equilibration with ambient pressure the loop gases were injected onto the respective precolumn using Valco 10 port injection valves. After the analytes have passed the precolumn and entered the main GC-column the Valco 10 port valves are switched again to backflush the precolumns. Injections are made alternatingly between sample gas and one reference gas ("working standard"). The ratio of a sample analysis and the mean of the two bracketing working standard analysis are calculated for quantification. With this approach, average relative precisions of 0.02 % for CO_2 (0.08 µmol mol^{-1} at atmospheric mixing ratio levels), 0.04% for N_2O (0.13 nmol mol^{-1}) and 0.07% for CH_4 (1.3 nmol mol^{-1}) are achieved. The calibration scale for each compound is set using standard gases calibrated by the Central Calibration Laboratory (CMDL, Boulder, Colorado) as required by the World Meteorological Organization (WMO) and in compliance with recommendations of the eleventh WMO/IAEA CO_2 Experts Meeting on the CO_2 calibration scale for measurements of atmospheric samples (direct link to the WMO mole fraction scale, see recommendations in the reports by *Jordan and Brand* [2003] and *Miller* [2006]).

3.7. Field experiment

The whole-air REA system was used to collect updraft and downdraft air during the field experiment WALDATEM-2003 (Wavelet Detection and Atmospheric Turbulent Exchange Measurements 2003, [*Thomas et al.*, 2004]). Samples were collected above a spruce forest (*Picea abies, L.*) with a plant area index (PAI) of 5.2 m^2 m^{-2} [*Thomas and Foken*, 2007] and an average canopy height of 19 m. The experiment site Waldstein/Weidenbrunnen (GE1-Wei) is part of the FLUXNET network and is located in the Fichtelgebirge mountains in Germany (50°08'31" N, 11°52'01" E, 775 m a.s.l.) on a slope of 2°. A detailed description of the site can be found in *Gerstberger et al.* [2004] and *Staudt and Foken* [2007]. A sonic anemometer (R3-50, Gill Instruments Ltd., Lymington, UK) and an open path CO_2 and H_2O analyzer (LI-7500) are installed on a tower at 33 m and their data is used for continuous EC measurements at the site. During the WALDATEM-2003 experiment, the EC data was used also for the HREA measurements with the whole-air REA system. The sample inlet was installed at 33 m just below the sonic anemometer and samples were directed through a Teflon® filter into the whole-air REA system as described in Section 3.3. The whole-air REA system was positioned on the tower at a platform at 28 m. Automated sample transfer procedures were used to immediately store the samples in the glass flasks and avoid uncontrolled pressure changes and any contamination in the field.

3.8. Isotope and trace gas profile system

In parallel, an isotope and trace gas profile system sampled air at eight levels from the tower top to the forest floor at 33, 22, 15, 5.25, 2.25, 0.9, 0.3 and 0.03 m. The 33 m inlet was installed close to the inlet of the whole-air REA system. From each profile height air was continuously driven at about 1.2 L min^{-1} through a 1 µm Teflon® filter and 25 m of Dekabon tubing into a 2.5 L buffer volume. Profile sample air from the buffer volumes was dried with a Nafion® gas dryer and continuously analyzed with a closed path CO_2 analyzer (LI-820). Whole-air samples for high precision isotope and trace gas analysis in the laboratory were taken from the buffer volumes during nighttime and several times during the day within 15 to 30 min, dried with $Mg(ClO_4)_2$ and sampled into glass flasks. The design of the isotope and trace gas profile system followed the principles of the whole-air REA system design especially regarding the treatment and use of materials.

4. Results and Discussion

4.1. Foil balloon bag tests

The importance of the material selection and treatment for air sample isotope analysis is highlighted by tests results presented by *Schauer et al.* [2003] in which heated stainless steel tubing, Viton® seals and polyethylene (PE) were found not to contaminate CO_2 isotope samples. The isotopic integrity regarding $\delta^{13}C$ of whole-air samples during storage of up to 60 min in Mylar® foil balloon bags with PE as inner wall material was demonstrated by *Bowling et al.* [2003a]. However, a bias was found for residence times longer than 60 min and for $\delta^{18}O$. We therefore performed similar tests with the same kind of foil balloon bags. Air sampled from one pressurized air tank was analyzed after varying residence time in the balloon bags by high precision IRMS. A first test with brand new balloons flushed three times with air from the tank showed significant contamination of the air samples with heavier isotopes (Figure 2) depending on time after flushing. The contamination presumably is the result of the release of substances with fossil origin from the balloon inner wall material PE.

For a second test, we treated the balloons by flushing them for about 4 days with nitrogen and dried air and by exposing them to intense direct sunlight. Afterwards, 9 balloon bags were first filled and emptied three times in the morning of the second test and then filled consecutively with air form a tank during the day, allowing different sample residence times up to 2 h before analysis. Only after the treatment, the balloon bags lacked signs of significant contamination (Figure 3). The standard deviation for both $\delta^{13}C$ and $\delta^{18}O$ isotope ratios from the 9 samples were acceptably low and the average value of the balloon bag samples compared well with an air sample taken directly from the tank and stored in a glass flask. These results demonstrate the general suitability of foil balloon bags for both ^{13}C and ^{18}O isotope air sampling and intermediate storage, which is normally restricted to 30-40 min in REA.

4.2. Whole-air REA system tests

We repeated the tests with the complete whole-air REA system described in Section 3. Beforehand, small leaks in the REA system were located by performing leak tests with high-vacuum and removed. In a third test for isotopic integrity (no figure), samples were directed through different parts of the system (REA sampling unit, flushing unit, flask fill unit, see Figure 1a). Small standard deviations of $\delta^{13}C$ (0.022‰) and $\delta^{18}O$ (0.021‰) isotopic ratios in 15 samples assured, that the surfaces of other materials in the system which contact the sample (glass, stainless steel, aluminum, Viton® seals, Nafion®, $Mg(ClO_4)_2$ granulate) were clean and no source of sample contamination.

In a fourth test we operated the complete whole-air REA system in the same way as for field sampling with automated sampling procedures after threefold flushing of the balloon bags, drying traps and glass flasks (see Section 3.3) but by drawing sample air and air for flushing and conditioning from a tank. The samples were stored for about 30 min in the balloon bags and filled into glass flasks for later analysis. The standard deviation of $\delta^{13}C$ (0.014‰) and $\delta^{18}O$ (0.019‰) in 19 samples were close to the measurement precision of the mass spectrometer and the average isotopic ratios matched well with an air sample from the tank stored in a glass flask (Figrue 4).

Before producing the sample J585, the complete REA system, balloon bags and glass flasks were contaminated with room air (dotted line), which presumably had isotopic ratios depleted by human breath compared to the pressurized air tank. The isotopic ratios of samples produced

afterwards show no systematic deviation from the average, which indicates, that the threefold flushing procedure is effective in removing old sample air.

The test results with the treated balloon bags (9 samples) and the complete whole-air REA system with the automated field sampling procedure (19 samples) demonstrate the isotopic integrity of samples taken with the system and the systems suitability for high precision isotope sampling. Nevertheless, the sample air residence time in the balloon bags should be restricted to the minimum needed for REA sampling (30-40 min) and the samples should then be transferred to glass flasks for the transport from the field to the laboratory.

4.3. Field experiment results

The CO_2 concentrations and isotope ratios measured in updraft, downdraft and profile air sampled above the canopy at 33 m reflect the effects of high rates of photosynthesis during days with changing cloud cover and periodically intense sunlight after several days with rainfall until noon of the 187th day of the year (doy) (Figure 5). The air above the canopy is enriched with heavier ^{13}C and ^{18}O isotopes, while bulk CO_2 is consumed. This trend is stopped (doy 188) or even reversed (doy 189) later in the afternoon.

The analysis of the sampling procedure and outliers in the REA updraft and downdraft samples revealed (i) that the CO_2 measurement accuracy was poor for one sample with low pressurization in the glass flask. The isotope ratios of this sample were not deviant. Poor CO_2 measurement accuracy was therefore related to insufficient sample extraction for the gas analysis with a GC-MS system. (ii) Two times the flask filling procedure in the field was not stopped early enough, so that erroneously underpressure was applied to the downdraft balloon reservoirs during flask filling. This seemed to influence the ^{18}O and in the first case also the ^{13}C isotope ratios, but not the CO_2 mixing ratios. (iii) One downdraft sample was contaminated due to poor valve sealing of the glass flask. These data were omitted from the plot in Figure 5 and from further evaluations.

The accuracy of the field measurements performed with the whole-air REA system can be validated with independent field measurements performed with the isotope and trace gas profile system. Profile samples were not taken exactly in the same time interval like REA samples. Nevertheless, samples from the top profile inlet at 33 m should represent the air composition above the forest close to the downdraft air composition or an intermediate composition as result of the mixture of updraft and downdraft air above the forest. All results for CO_2 and $\delta^{13}C$ meet this expectation. $\delta^{18}O$ values show good agreement during the period marked with a gray bar. Before the first measurements in this period, new $Mg(ClO_4)_2$ drying traps were installed in the flask filling units of the REA system. The precise measurement of ^{18}O isotope ratios requires very effective sample drying in order to prevent exchange with ^{16}O and ^{18}O isotopes in water vapor during sample storage. The deviations visible in the $\delta^{18}O$ values on doy 187 and on doy 189 after noon most likely result from inefficient drying after sampling a large number of relatively humid air samples. Most of the other profile samples taken close to the inlet of the REA system at 33 m show a close match of the air above the forest to either canopy air (updraft) or atmospheric boundary layer air (downdraft). Despite small differences in the sampling time, CO_2 mixing ratios of seven REA downdraft samples and the corresponding profile samples from 33 m match well with absolute deviations of 0.17 to 0.89 µmol mol^{-1}. The deviations in the $\delta^{13}C$ and $\delta^{18}O$ values for three comparable sampling periods for which sufficient drying in the REA system is guaranteed fall within a range of 0.012‰ to 0.033‰ ($\delta^{13}C$ REA updraft−profile 33 m) and –0.021‰ to –0.029‰ ($\delta^{18}O$ REA downdraft−profile 33 m). The

match of the $\delta^{13}C$ values of REA updraft samples and three available profile samples from the canopy top (15 m or 22 m) is even closer with absolute deviations in the range of 0.015 to 0.018‰. This close match of isotope ratios found in air samples from the two independent sampling systems despite small mismatches in the sample collection time confirms, that also during the field experiment high measurement accuracy could be achieved by sampling with the whole-air REA system.

4.4. Scalar correlation as basis for the HREA and EC/flask method

For the validation of the scalar similarity assumption and for comparison with results presented by *Bowling et al.* [1999a; 2003a] we analyzed the relation of ^{13}C and ^{18}O isotope ratios and bulk CO_2 mixing ratios in HREA and profile samples (Figure 6). The relation itself is explained by the mixing of air with different isotopic signatures from the atmosphere and the ecosystem, which is similar to the assumption of two sources mixing in classical keeling plots. Such plots of mixing relations can be used to check the integrity of air samples. Logically consistent, $\delta^{18}O$ values of samples, which presumably were not effectively dried before storage, showed up as extreme outliers from the relation, and were omitted from Figure 6b.

Despite a relatively small range of bulk CO_2 mixing ratios in the samples, the relation found for ^{13}C isotope ratios and the slope of a linear regression (m=−0.034, R^2=0.71) for all samples shown in Figure 6a closely correspond to results presented by *Bowling et al.* [2001; 2003a]. In contrast to results presented in the work of *Bowling et al.* [1999a], also the relation for ^{18}O isotope ratios shows little scatter and a linear regression results in an slope (m=−0.034, R^2=0.75), which is identical to the one found for ^{13}C isotope ratios.

The generation of these results required the collection of whole-air samples, from which precise measurements of both isotope ratios and bulk CO_2 mixing ratios could be accomplished. The results presented in Figure 6b demonstrate that also the $\delta^{18}O/CO_2$ relations in up- and downdraft samples can readily be investigated. Good scalar correlations were achieved even at relatively small ranges of CO_2 mixing ratios from HREA whole-air samples collected in foil balloon bags as intermediate reservoirs**.** It is however essential that foil balloons are pretreated as described in Section 4.2 and that samples are dried efficiently before storing in glass flasks for high precision analysis.

The analysis of scalar correlations in the heat, latent heat and carbon dioxide exchange showed that scalar similarity is controlled primarily by exchange events on time scales longer than 60 s [*Ruppert et al.*, 2006b]. However, scalar similarity between CO_2 and its isotopes ultimately can only be proven when instruments for isotope flux measurements become available, that can resolve the small fluctuation fast enough (> 1 Hz) with sufficient precision.

For both ^{13}C and ^{18}O isotope ratios (scalars of interest) the generally good correlations with bulk CO_2 mixing ratios (proxy scalar) in samples that represent relatively short timescales of updrafts and downdrafts as well as on longer timescales in the profile samples suggest good scalar similarity, and support the validity of the HREA method.

In the data presented here for $\delta^{13}C$ and $\delta^{18}O$ like in data presented in the work of *Bowling et al.* [2003a] for $\delta^{13}C$, HREA samples from the morning transition periods (encircled triangles in Figure 6a and 6b) indicate a systematically different slope in the relations to bulk CO_2 mixing ratios and seem not to fall on a common regression line with HREA samples from other periods. In the WALDATEM-2003 experiment, this result could be further validated by the relation in profile samples from the canopy top and above collected during these transition periods (encircled circles in Figure 6a and 6b). The WALDATEM-2003 results therefore confirm the

systematic difference of early morning samples collected above the canopy as observed by *Bowling et al.* [1999a; 2003a, Figure 4]. Furthermore, the match of HREA and profile samples from these transition periods supports the hypothesis that the systematic difference is caused by isotopically very negative air above the canopy from respiratory built up during night in combination with high photosynthetic discrimination in the top canopy in the morning.

For the determination of fluxes by the HREA method and the assumption of scalar similarity, such a good correlation of the scalar of interest and the proxy scalar at different time scales is essential. The actual slope of the linear regression is less important. The scalar difference between updraft and downdraft air samples is measured by high precision laboratory analysis. Although this information is not fully independent of the scalar similarity assumption, it incorporates additional information on the variance of the isotopic ratio and the turbulent isotopic exchange above the canopy into the HREA evaluation scheme. At the moment HREA is the only method which allows determining the turbulent isotopic flux density based on turbulent exchange measurements and a 'one-and-a-half order' closure scheme [*Bowling et al.*, 2003a; *Kramm et al.*, 1999]. The measured scalar difference characterizes those parts of the JFD of the isotope ratio and the vertical wind speed, in which the most significant contributions to the turbulent air exchange are found.

Linear relations between ^{13}C and ^{18}O isotope ratios and bulk CO_2 mixing ratios in flask samples were suggested as basis for the so called EC/flask method for the derivation of isotope fluxes from CO_2 EC measurements [*Bowling et al.*, 1999a; *Bowling et al.*, 2001; *Bowling et al.*, 2003a].

For the EC/flask method, in contrast, only variance data of the turbulent exchange of the proxy scalar is evaluated. The slope of the linear regression is the scaling factor, which determines the flux density of the scalar of interest. The observed temporal change of the slope limits the chance to precisely define a unique regression line based on a series of whole-air samples for the application of the EC/flask method. The linear regression function used to infer isotope ratio fluctuations from bulk CO_2 mixing ratio fluctuations must therefore be updated regularly within the diurnal cycle. This consequently would require taking a very large number of samples in order to assure sufficient accuracy of the linear regression. If the samples that are used for the regression represent different temporal or spatial scales, they most likely will fail to correctly represent the turbulent exchange process above the canopy. This complication must be considered especially above tall vegetation, where complex exchange mechanisms in the canopy space, like counter gradient fluxes, storage changes and exchange in coherent structures may be important factors. In such conditions, the combination of keeling plot information from vertical sub-canopy to above canopy profiles with the EC/flask method are not suitable to correctly quantify isotope fluxes.

4.5. HREA simulation and *b*-factors

In order to check the efficiency of the updraft and downdraft sample segregation HREA sampling was simulated for each sampling interval using the actual valve switching record from the field experiment to segregate and virtually accumulate updraft and downdraft samples of the μ_{CO2} time series determined by (5).

The simulated average updraft and downdraft mixing ratios are compared to average updraft and downdraft CO_2 mixing ratios measured in the whole-air samples in Figure 7. The least square linear regression for updraft and downdraft samples is well defined (R^2=0.93) and results in a slope very close to one. This is a proof for correct instrument performance regarding the

HREA sample segregation and accumulation process. The average offset of the measured values of +0.26 µmol mol^{-1} indicates good calibration of field instruments.

Effective *b*-factors were determined from the measured updraft and downdraft CO_2 mixing ratio difference $\overline{C_\uparrow} - \overline{C_\downarrow}$ and the turbulent CO_2 flux density measured by EC according to (2). The effective *b*-factors can be compared to *b*-factors derived from the simulated mixing ratio differences (Figure 8). The simulated *b*-factors are very sensitive to the applied density correction (5), because of small mixing ratio differences relative to the absolute values of the mixing ratio. Simulations with simplified density corrections for the CO_2 mixing ratio data resulted in significant mismatches between the measured and simulated updraft and downdraft absolute CO_2 mixing ratios and consequently less correlation between measured and simulated *b*-factors.

Both measured and simulated values of the *b*-factors show the variability that must be expected for HREA as well as for REA from the skewness in the JFD of the vertical wind speed and the scalar and from sampling effects which depend on the eddy reversal frequency [*Baker et al.*, 1992]. Like in other studies, which compare measured effective *b*-factors to simulated *b*-factors [*Baker et al.*, 1992; *Beverland et al.*, 1996b; *McInnes et al.*, 1998], we find, that simulated values tend to underestimate measured values especially at higher *b*-factors. High *b*-factors were related to high turbulent flux density (R^2=0.42) and reduced sampling efficiency, (R^2=0.78), i.e. sampled concentration difference per turbulent flux density. The observed underestimation is the result of some inefficiency of the physical sampling process in separating updraft and downdraft samples compared to the virtual 'digital' sampling in HREA simulations [*Baker et al.*, 1992; *Beverland et al.*, 1996b; *Lenschow and Raupach*, 1991; *Massman*, 1991; *McInnes et al.*, 1998; *Moncrieff et al.*, 1998]. Measured effective *b*-factors resulting from the real physical sampling process integrate such deficiencies. In order to calculate REA turbulent flux densities from measured concentration differences by (1), measured effective *b*-factors should therefore be preferred in comparison to simulated *b*-factors.

Virtual sampling results in a slightly higher concentration differences and consequently lower simulated *b*-factors according to (2). Simulated *b*-factors therefore require validation when used to replace effective *b*-factors that could not be measured, and an instrument and experiment specific correction needs to be found [*Beverland et al.*, 1996a; *McInnes et al.*, 1998], e.g. based on a least square linear regression function like shown in Figure 8. The overestimation of concentration differences from virtual 'digital' sampling of a proxy scalar in REA simulations evaluated for the *b*-factors without correction according to (2) can cause systematic underestimation of flux densities according to (1).

The size of the residuals of the measured *b*-factors in Figure 8, quantified with 0.03 by the corresponding standard error, related to their range of absolute values of 0.15 to 0.35 provides an estimate of the average uncertainty of CO_2 fluxes measured by HREA with a hyperbolic deadband of H_h=1.0 of about 10 to 20%. This quantifies the measurement uncertainty of the sampling system and method in reference to EC flux measurements for a component for which sufficient analytical precision is available during sample analysis (signal/noise ratio >10, Section 4.6).

4.6. Maximum concentration difference by HREA for isotope analysis

The application of REA with hyperbolic deadbands, i.e. the HREA method [*Bowling et al.*, 1999b], is intended to maximize the concentration difference of the scalar of interest, so that it can be resolved with sufficient precision by laboratory analysis. Simulations of REA (H_w=0.6)

and HREA (H_h=1.0) with the WALDATEM-2003 data showed an concentration difference increase by a factor of 1.78 (Table 1), which is comparable to the factor of 1.84 derived from results presented by *Bowling et al.* [1999b]. The factor reduces to 1.73 for the WALDATEM-2003 data or 1.65 in the work of *Ruppert et al.* [2006b], if imperfect scalar similarity between the scalar of interest and the proxy scalar is considered. However, all factors reported above are the result of simulations with an ideal definition of the hyperbolic deadband based on scalar data from the complete sampling interval (lines in Figure 9).

During the real sampling process, only historic scalar data is available. The mean scalar value is defined based on a filter function and the center of the hyperbolic deadband moves up and down along the scalar axis. This leads to less rigorous rejection of samples with average scalar values (see dots close to the center of Figure 9). Consequently, the average scalar concentration difference between updrafts and downdrafts is slightly decreased, e.g. the CO_2 mixing ratio difference $\overline{c}_{\uparrow} - \overline{c}_{\downarrow}$ in Figure 9. The application of a wind-deadband (REA) instead of a hyperbolic deadband (HREA) would incorporate even more air with average CO_2 mixing ratios (e.g. around 360 µmol mol^{-1} in Figure 9) in updraft and downdraft air samples and thereby further decrease the mixing ratio difference. Simulations based on the recorded valve switching from the WALDATEM-2003 experiment showed, that the realistic concentration difference increase between REA (H_w=0.6) and HREA (H_h=1.0) is only 1.63 (Table 1). The corresponding expected CO_2 mixing ratio difference from HREA simulations based on the effective sample segregation during the experiment with a hyperbolic deadband of H_h=1.0 is 2.4(±0.5) µmol mol^{-1}. The observed mixing ratio differences were only slightly smaller, (2.3(±0.6) µmol mol^{-1}, Table 1, Figure 10a), reflecting also the physical air sampling effects discussed in Section 4.6. However, these also affect REA sampling with a wind-deadband and an effective relative concentration difference increase close to 1.63 can be assumed.

We avoided increasing the hyperbolic deadband size H_h further, because in contrast to results of ideal simulations, no significant additional concentration difference increase could be expected with larger hyperbolic deadbands when acknowledging the realistic sampling process. Also, the representativness of updraft and downdraft samples for the JFD would be further decreased if larger deadbands would be applied.

During the WALDATEM-2003 experiment, the overall proportions of evaluated samples in each sampling interval were 14.7(±3.0)% updrafts and 9.1(±2.6)% downdrafts. The difference in the number of updraft and downdraft samples results from skewness in the JFD and was discussed by *Bowling et al.* [1999b]. The authors suggest an optimum deadband size at H_h=1.1 and an asymmetric adjustment of the hyperbolas. We decided not to adjust the symmetric shape of the hyperbolic deadband, in order to prevent artifacts that could result from changing shapes of the JFD, which have to be considered above tall vegetation.

CO_2 mixing ratio differences of whole-air HREA updraft and downdraft samples in the range of –1.3 to –3.9 µmol mol^{-1} exceeded the tenfold measurement precision. Two samples marked with a '+' in Figure 5a showed relatively small sample proportions. Their representativness in respect to the JFD remains questionable. Furthermore, reduced precision of the CO_2 mixing ratio difference can result from the transfer of relatively small amounts of sample air. Therefore, only simulated and corrected *b*-factors were used for the estimation of the isotope fluxes of these two samples in Figure 10b and 10c.

The ^{13}C and ^{18}O isotopic differences, i.e. the difference of the isotope ratios of updraft and downdraft air samples, observed by the HREA measurements during WALDATEM-2003 were on average 0.11(±0.03)‰ for $\delta^{13}C$ and 0.11(±0.02)‰ for $\delta^{18}O$ during the time with sufficient sample drying (Table 1). Most values lie between the fivefold and tenfold standard deviations

found in the whole-air REA system tests (dashed lines in Figure 10b and 10c, compare Figure 4). Similar $\delta^{13}C$ differences were reported for many samples by *Bowling et al.* [1999a]. Nevertheless, the small differences of the isotope ratios ask for high precision in the sample analysis. Based on the comparison of the isotopic differences and the precision determined in the whole-air REA system tests a measurement uncertainty due to the resolution of the isotopic differences of 10% to 20% can be estimated.

The mixing ratio differences observed for CH_4 and N_2O in daytime samples taken above the spruce forest at Waldstein/Weidenbrunnen during the WALDATEM-2003 experiment ranged from −2.9 to 1.6 nmol mol^{-1} for CH_4 and −0.37 to 0.49 nmol mol^{-1} for N_2O. Most mixing ratio differences were in the order of measurement precision (1.3 nmol mol^{-1} for CH_4 and 0.13 nmol mol^{-1} for N_2O) and consequently too small to be resolved by HREA sampling and whole-air analysis without pre-concentration on a trap. The indication of negative concentration differences and downward direction of CH_4 and N_2O fluxes on average of the daytime samples was not significant (Table 1).

4.7. $^{13}CO_2$ and $CO^{18}O$ turbulent isofluxes measured by HREA

The turbulent CO_2 flux density determined by EC in intervals of 5 minutes from 30 minutes of turbulence data from noon of the 187th to the end of 189th day of the year during the WALDATEM-2003 experiment is shown as solid line in Figure 11a**.** It reflects intense photosynthetic activity and CO_2 uptake during daytime after a rainy period. CO_2 release into the atmosphere during nighttime is inhibited during the second night and at the beginning of the third night by very stable stratification of the air in the forest canopy ([*Foken et al.*, 2004b; *Ruppert and Foken*, 2005], $(z_m-d)/L$= +0.4 to +1.2, z_m: measurement height, d: displacement height, L: Obukhov length) in combination with low horizontal wind velocities, which results in minimal CO_2 flux densities and rejection of some data (gaps in the solid line) due to poor flux data quality. The flux data quality was evaluated according to test criteria described by *Foken et al.* [2004a] and *Ruppert et al.* [2006a]. Quality flags of 1 or 3 for the CO_2 EC flux indicate, that the fundamental prerequisites for the EC and REA method regarding stationarity and turbulence characteristics were fulfilled during all sampling periods at daytime. Variation in the CO_2 EC flux are during daytime is caused by variable global radiation due to changing cloud cover.

$^{13}CO_2$ and $CO^{18}O$ turbulent isotope flux densities (diamonds in Figure 11b and 11c), measured by HREA at 33 m were determined from the measured isotopic differences and bulk CO_2 data and measured effective b_{CO2}-factors according to (1) expressed for turbulent isofluxes $\delta_c F_c$ of CO_2 [*Bowling et al.*, 2003a]:

$$\delta_c F_c = b\sigma_w \rho_a \left(\overline{\delta_\uparrow}\,\overline{C_\uparrow} - \overline{\delta_\downarrow}\,\overline{C_\downarrow}\right). \qquad (6)$$

Circles in Figure 11b and 11c were derived from the measured isotopic differences but simulated updraft and downdraft bulk CO_2 values and *b*-factors that were corrected according to the linear regression between measured and simulated *b*-factors.

Downward turbulent transport of CO_2 (negative CO_2 flux density by convention) correlates with isotopic enrichment of the canopy air (Figure 5) due to assimilation of CO_2 and linked discrimination of the heavier isotopes and positive turbulent isofluxes (Figure 11b and 11c). The positive sign of the isoflux results from its calculation from isotope ratios in reference to the international standard VPDB according to (6) [*Bowling et al.*, 2003a]. The maximum turbulent isofluxes were observed shortly before noon on day of the year 188 and 189. The influence of

isotopic enrichment is reflected in the positive trend of isotope ratios observed in REA and Profile whole-air samples from above the canopy on the day of the year 188 and in the morning of the day of the year 189 in Figure 5. In the ^{13}C data this trend reverses after noon on day of the year 189. Nevertheless, the maintained positive isotopic differences in Figure 5 and consequently positive turbulent isofluxes in Figure 11b indicate that turbulent air exchange between the boundary layer and the canopy air continues to enrich boundary layer air with heavier isotopes. Also ^{13}C isotope ratios in profile samples from 33 m seem to be more closely linked to boundary layer air in the afternoon of doy 189. We therefore hypothesize that advective processes in the boundary layer are dominating the air composition change during this period.

5. Conclusion

Lab experiments with foil balloon bags and the complete whole-air REA system demonstrate their suitability for high precision isotope sampling for both ^{13}C and ^{18}O isotopes of CO_2. High measurement accuracy was also achieved during a field experiment above a spruce forest. This was indicated by a close match of isotope ratios found in air samples from two independent sampling systems. We therefore conclude, that foil balloons are suitable flexible air collection containers for intermediate storage after cleaning as described in Section 4.1. Large whole-air sample volumes, precise flow and pressure control, careful material selection and treatment and effective sample drying helped to increase the sampling accuracy of the complete whole-air REA system especially for ^{18}O isotopes.

$\delta^{13}C/CO_2$ and also $\delta^{18}O/CO_2$ correlations can therefore readily be investigated even at relatively small ranges of CO_2 mixing ratios. The linear regression analysis showed good scalar correlations in HREA updraft and downdraft and in profile samples, which supports the assumption of scalar similarity at different temporal scales. However, different slopes were found in HREA and profile samples from early morning transition periods. This effect is very likely caused by isotopically depleted air above the canopy from respiratory built up during the night in combination with high photosynthetic discrimination in the top canopy in the morning. Consequently, temporal and spatial scales of the isotopic exchange must be considered carefully for the regression analysis of the EC/flask method especially above tall vegetation. HREA measurements provide additional information on the scalar variation and on the most significant events in the turbulent isotopic exchange above the canopy for the determination of isofluxes.

The comparison of measurement results and simulations of HREA sampling for bulk CO_2 confirmed good instrument performance and indicated 10 to 20% uncertainty for the quantification of fluxes due to the sampling method. The measured effective *b*-factors should be preferred for flux determination. Simulated *b*-factors require validation and potentially correction in order to prevent the risk of systematic underestimation of fluxes. Detailed axis rotation procedures for REA and HREA sampling without a time lag [*Beverland et al.*, 1996b; *McInnes et al.*, 1998; *Moncrieff et al.*, 1998] can be implemented by evaluating the 3D wind vector and performing online planar-fit corrections [*Wilczak et al.*, 2001]. The precise synchronization of REA segregation valve switching can be achieved under defined sample flow conditions by differential cross-correlation measurements as outlined in Section 3.4. A concentration difference increase of 63% was achieved by applying the HREA sampling method instead of classical REA. Nevertheless, relatively small isotopic differences in updraft and downdraft samples collected during the WALDATEM-2003 experiment above spruce forest required high precision isotope analysis. The measurement uncertainty due to the chemical resolution of the isotope ratio differences was estimated at 10 to 20%.

Whole-air HREA in combination with high precision isotope analysis can quantify the isofluxes of $^{13}CO_2$ and $CO^{18}O$ and collect additional information on the scalar correlation to bulk CO_2, representing the relatively short timescale of updrafts and downdrafts in the turbulent exchange above the canopy.

6. Acknowledgments

The authors wish to thank Anthony C. Delany and Dave R. Bowling for helpful comments and discussions on the realization of the isotope REA technique by using whole-air balloon bag reservoirs. We acknowledge the support during the field experiments by Christoph Thomas, Matthias Mauder, Teresa Bertolini, Johannes Olesch, Johannes Lüers and the technical support performed by the staff of the Bayreuth Institute for Terrestrial Ecosystem Research (BITÖK) of the University of Bayreuth. The high precision laboratory analysis was performed by Michael Rothe and Armin Jordan in the Isotope- and Gas laboratory of the Max-Planck Institute in Jena. This study was supported by the German Federal Ministry of Education and Research (PT BEO51-0339476 D).

7. References

Ammann, C. (1999), *On the applicability of relaxed eddy accumulation and common methods for measuring trace gas fluxes*, Geographisches Institut der ETH Zürich ed., ETH Zürich, Zürich, 230 pp.

Ammann, C., and F. X. Meixner (2002), Stability dependence of the relaxed eddy accumulation coefficient for various scalar quantities, *J. Geophys. Res., 107*, (D8), 4071, doi:10.1029/2001JD000649.

Baker, J. M., J. M. Norman, and W. L. Bland (1992), Field-scale application of flux measurement by conditional sampling, *Agric. For. Meteorol., 62*, 31-52.

Beverland, I. J., J. B. Moncrieff, D. H. O'Neill, K. J. Hargreaves, and R. Milne (1996a), Measurements of methane and carbon dioxide fluxes from peatland ecosystems by the conditional-sampling technique, *Quart. J. Roy. Meteor. Soc., 122*, 819-838.

Beverland, I. J., D. H. Oneill, S. L. Scott, and J. B. Moncrieff (1996b), Design, construction and operation of flux measurement systems using the conditional sampling technique, *Atmos. Environ., 30*, 3209-3220.

Bowling, D. R., A. A. Turnipseed, A. C. Delany, D. D. Baldocchi, J. P. Greenberg, and R. K. Monson (1998), The use of relaxed eddy accumulation to measure biosphere-atmosphere exchange of isoprene and other biological trace gases, *Oecologia, 116*, 306-315.

Bowling, D. R., D. D. Baldocchi, and R. K. Monson (1999a), Dynamics of isotopic exchange of carbon dioxide in a Tennessee deciduous forest, *Glob. Biogeochem. Cycles, 13*, 903-922.

Bowling, D. R., A. C. Delany, A. A. Turnipseed, D. D. Baldocchi, and R. K. Monson (1999b), Modification of the relaxed eddy accumulation technique to maximize measured scalar mixing ratio differences in updrafts and downdrafts, *J. Geophys. Res., 104*, (D8), 9121-9133.

Bowling, D. R., P. P. Tans, and R. K. Monson (2001), Partitioning net ecosystem carbon exchange with isotopic fluxes of CO_2, *Global Change Biol., 7*, 127-145.

Bowling, D. R., D. E. Pataki, and J. R. Ehleringer (2003a), Critical evaluation of micrometeorological methods for measuring ecosystem-atmosphere isotopic exchange of CO_2, *Agric. For. Meteorol., 116*, 159-179.

Bowling, D. R., S. D. Sargent, B. D. Tanner, and J. R. Ehleringer (2003b), Tunable diode laser absorption spectroscopy for stable isotope sudies of ecosystem-atmosphere CO_2 exchange, *Agric. For. Meteorol., 118*, 1-19.

Brand, W. A. (2005), O_2/N_2 Storage Aspects and Open Split Mass Spectrometric Determination, in *Proceedings of the 12th WMO/IAEA Meeting of Expert on Carbon Dioxide Concentration and Related Tracers Measurements Techniques, Toronto, Canada, Sept. 2003, WMO-GAW Report 161*, edited by D. Worthy and L. Huang, pp. 146-151.

Businger, J. A., and A. C. Delany (1990), Chemical sensor resolution required for measuring surface fluxes by three common micrometeorological techniques, *J. Atmos. Chem., 10*, 399-410.

Businger, J. A., and S. P. Oncley (1990), Flux Measurement with conditional sampling, *J. Atmos. Ocean. Tech., 7*, 349-352.

Canadell, J. G., H. A. Mooney, D. D. Baldocchi, J. A. Berry, J. R. Ehleringer, C. B. Field, S. T. Gower, D. Y. Hollinger, J. E. Hunt, R. B. Jackson, S. W. Running, G. R. Shaver, W. Steffen, S. E. Trumbore, R. Valentini, and B. Y. Bond (2000), Carbon metabolism of the terrestrial biosphere: A multitechnique approach for improved understanding, *Ecosystems, 3*, 115-130.

Delany, A. C., S. P. Oncley, J. A. Businger, and E. Sievering (1991), Adapting the conditional sampling concept for a range of different chemical species, paper presented at Seventh symposium on meteorological observations and instruments, American Meteorological Society, Boston, New Orleans, La., 14-18 January 1991.

Desjardins, R. L. (1977), Description and evaluation of a sensible heat flux detector, *Boundary-Layer Meteorol., 11*, 147-154.

Ehleringer, J. R., D. R. Bowling, L. B. Flanagan, J. Fessenden, B. Helliker, L. A. Martinelli, and J. P. Ometto (2002), Stable isotopes and carbon cycle processes in forests and grasslands, *Plant Biology, 4*, 181-189.

Foken, T., R. Dlugi, and G. Kramm (1995), On the determination of dry deposition and emission of gaseous compounds at the biosphere-atmosphere interface, *Meteorol. Z., 4*, 91-118.

Foken, T., M. Göckede, M. Mauder, L. Mahrt, B. Amiro, and W. Munger (2004a), Post-field data qualtiy control, in *Handbook of Micrometeorology*, edited by X. Lee, et al., pp. 181-208, Kluwer, Dordrecht.

Foken, T., C. Thomas, J. Ruppert, J. Lüers, and M. Göckede (2004b), Turbulent exchange processes in and above tall vegetation, paper presented at 16th Symposium on Boundary Layers and Turbulence, American Meteorological Society, Portland, ME, USA, 8-13 August 2004.

Fotiadi, A. K., F. Lohou, A. Druilhet, D. Serca, Y. Brunet, and R. Delmas (2005), Methodological development of the conditional sampling method. Part I: Sensitivity to statistical and technical characteristics, *Boundary-Layer Meteorol., 114*, 615-640.

Gao, W. (1995), The vertical change of coefficient b, used in the relaxed eddy accumulation method for flux measurement above and within a forest canopy, *Atmos. Environ., 29*, 2339-2347.

Gerstberger, P., T. Foken, and K. Kalbitz (2004), The Lehstenbach and Steinkreuz Catchments in NE Bavaria, Germany, in *Biogeochemistry of Forested Catchments in a Changing Environment: A German case study*, edited by E. Matzner, pp. 15-41, Springer, Berlin.

Guenther, A., W. Baugh, K. Davis, G. Hampton, P. Harley, L. Klinger, L. Vierling, P. Zimmerman, E. Allwine, S. Dilts, B. Lamb, H. Westberg, D. Baldocchi, G. Geron, and T. Pierce (1996), Isoprene fluxes measured by enclosure, relaxed eddy accumulation, surface layer gradient, mixed layer gradient, and mixed layer mass balance techniques, *J. Geophys. Res., 101*, (D13), 18555–18568.

Jordan, A., and W. A. Brand (2003), Technical Report: MPI-BGC, Germany, in *Report of the Eleventh WMO/IAEA Meeting of Experts on Carbon Dioxide Concentration and Related Tracer Measurement Techniques, Tokyo, Japan, Sept. 2001, WMO-GAW Report 148*, edited by S. Toru and S. Kazuto, pp. 149-153.

Kaplan, J. O., I. C. Prentice, and N. Buchmann (2002), The stable carbon isotope composition of the terrestrial biosphere: Modeling at scales from the leaf to the globe, *Glob. Biogeochem. Cycles, 16*, 1060, doi:10.1029/2001GB001403.

Katul, G. G., P. L. Finkelstein, J. F. Clarke, and T. G. Ellestad (1996), An investigation of the conditional sampling method used to estimate fluxes of active, reactive, and passive scalars, *J. Appl. Meteor., 35*, 1835-1845.

Kramm, G., N. Beier, R. Dlugi, and H. Muller (1999), Evaluation of conditional sampling methods, *Contr. Atmos. Phys., 72*, 161-172.

Lee, X. (2000), Water vapor density effect on measurements of trace gas mixing ratio and flux with a massflow controller, *J. Geophys. Res., 105*, (D14), 17807-17810.

Lenschow, D. H., and M. R. Raupach (1991), The attenuation of fluctuatations in scalar concentrations through sampling tubes, *J. Geophys. Res., 96*, (D8), 15259-15268.

Leuning, R., and M. J. Judd (1996), The relative merits of open- and closed-path analysers for measurement of eddy fluxes, *Global Change Biol., 2*, 241-253.

Lloyd, J., and G. D. Farquhar (1994), ^{13}C discrimination during CO_2 assimilation by the terrestrial biosphere, *Oecologia, 99*, 201-215.

Lloyd, J., B. Kruijt, D. Y. Hollinger, J. Grace, R. J. Francey, S. C. Wong, F. M. Kelliher, A. C. Miranda, G. D. Farquhar, J. H. C. Gash, N. N. Vygodskaya, I. R. Wright, H. S. Miranda, and E. D. Schulze (1996), Vegetation effects on the isotopic composition of atmospheric CO_2 at local and regional scales: Theoretical aspects and a comparison between rain forest in Amazonia and a Boreal Forest in Siberia, *Austr. J. Plant Physiol., 23*, 371-399.

Massman, W. J. (1991), The attenuation of concentration fluctuations in turbulent flow through a tube, *J. Geophys. Res., 96*, (D8), 15269-15273.

Mauder, M., and T. Foken (2004), Documentation and instruction manual of the eddy covariance software package TK2, *Arbeitsergebnisse 26*, 45 pp, Universität Bayreuth, Abt. Mikrometeorologie, Bayreuth, Germany. Print, ISSN 1614-8916.

McInnes, K. J., C. S. Campbell, and J. L. Heilman (1998), Separation and dispersion of conditionally sampled eddies through an intake tube, *Agron. J., 90*, 845-850.

Miller, J. B. (Ed.) (2006), *13th WMO/IAEA Meeting of Experts on Carbone Dioxide Concentration and Related Tracers Measurement Techniques, Boulder, Colorado, USA, Sept. 2005, WMO-GAW Report 168*, 201 pp.

Milne, R., A. Mennim, and K. Hargreaves (2001), The value of the beta coefficient in the relaxed eddy accumulation method in terms of fourth-order moments, *Boundary-Layer Meteorol., 101*, 359-373.

Moncrieff, J. B., I. J. Beverland, D. H. O'Neill, and F. D. Cropley (1998), Controls on trace gas exchange observed by a conditional sampling method, *Atmos. Environ., 32*, 3265-3274.

Oncley, S. P., A. C. Delany, T. W. Horst, and P. P. Tans (1993), Verification of flux measurement using relaxed eddy accumulation, *Atmos. Environ., 27A*, 2417-2426.

Pattey, E., R. L. Desjardins, F. Boudreau, and P. Rochette (1992), Impact of density fluctuations on flux measurements of trace gases: implications for the relaxed eddy accumulation technique, *Boundary-Layer Meteorol., 59*, 195-203.

Pattey, E., R. L. Desjardins, and P. Rochette (1993), Accuracy of the relaxed eddy-accumulation technique, evaluated using CO_2 flux measurements, *Boundary-Layer Meteorol., 66*, 341-355.

Rothe, M., A. Jordan, and W. A. Brand (2005), Trace gases, $\delta^{13}C$ and $\delta^{18}O$ of CO_2-in-air samples: Storage in glass flasks using PCTFE seals and other effects, in *Proceedings of the 12th WMO/IAEA Meeting of Expert on Carbon Dioxide Concentration and Related Tracers Measurements Techniques, Toronto, Canada, Sept. 2003, WMO-GAW Report 161*, edited by D. Worthy and L. Huang, pp. 64-70.

Ruppert, J., B. Wichura, A. C. Delany, and T. Foken (2002), Eddy sampling methods, a comparison using simulation results, paper presented at 15th Symposium on Boundary Layers an Turbulence, American Meteorological Society, Wageningen, Netherlands, 15-19 July 2002.

Ruppert, J. (2005), ATEM software for atmospheric turbulent exchange measurements using eddy covariance and relaxed eddy accumulation systems + Bayreuth whole-air REA system setup, *Arbeitsergebnisse 28*, 29 pp, Universität Bayreuth, Abt. Mikrometeorologie, Bayreuth, Germany. Print, ISSN 1614-8916.

Ruppert, J., and T. Foken (2005), Messung turbulenter Flüsse von Kohlendioxid und stabilem Kohlenstoffisotop ^{13}C über Pflanzenbeständen mit Hilfe der Relaxed Eddy Accumulation Methode, in Klimatologische und mikrometeorologische Froschungen im Rahmen des Bayreuther Institutes für terrestrische Ökosystemforschung (BITÖK) 1998 - 2004, edited by T. Foken, *Arbeitsergebnisse 29*, 81-104, Universität Bayreuth, Abt. Mikrometeorologie, Bayreuth, Germany. Print, ISSN 1614-8916.

Ruppert, J., M. Mauder, C. Thomas, and J. Lüers (2006a), Innovative gap-filling strategy for annual sums of CO_2 net ecosystem exchange, *Agric. For. Meteorol., 138*, 5-18, doi:10.1016/j.agrformet.2006.03.003.

Ruppert, J., C. Thomas, and T. Foken (2006b), Scalar similarity for relaxed eddy accumulation methods, *Boundary-Layer Meteorol., 120*, 39-63, doi:10.1007/s10546-005-9043-3.

Schauer, A. J., C. T. Lai, D. R. Bowling, and J. R. Ehleringer (2003), An automated sampler for collection of atmospheric trace gas samples for stable isotope analyses, *Agric. For. Meteorol., 118*, 113-124, doi:10.1016/S0168-1923(03)00065-0.

Staudt, K., and T. Foken (2007), Documentation of reference data for the experimental areas of the Bayreuth Centre for Ecology and Environmental Research (BayCEER) at the Waldstein site, *Arbeitsergebnisse 35*, 37 pp, Universität Bayreuth, Abt. Mikrometeorologie, Bayreuth, Germany. Print, ISSN 1614-8916.

Sturm, P., M. Leuenberger, C. Sirignano, R. E. M. Neubert, H. A. J. Meijer, R. Langenfelds, W. A. Brand, and Y. Tohjima (2004), Permeation of atmospheric gases through polymer O-rings used in flasks for air sampling, *J. Geophys. Res., 109*, D04309, doi:10.1029/2003JD004073.

Thomas, C., J. Ruppert, J. Lüers, J. Schröter, J. C. Mayer, and T. Bertolini (2004), Documentation of the WALDATEM-2003 experiment, 28.4.-3.8.2003, *Arbeitsergebnisse 24*, 59 pp, Universität Bayreuth, Abt. Mikrometeorologie, Bayreuth, Germany. Print, ISSN 1614-8916.

Thomas, C., and T. Foken (2007), Organised Motion in a Tall Spruce Canopy: Temporal Scales, Structure Spacing and Terrain Effects, *Boundary-Layer Meteorol., 122*, 123-147, doi:10.1007/s10546-006-9087-z.

Webb, E. K., G. I. Pearman, and R. Leuning (1980), Correction of flux measurements for density effects due to heat and water vapour transfer, *Quart. J. Roy. Meteor. Soc., 106*, 85-100.

Werner, R. A., and W. A. Brand (2001), Referencing strategies and techniques in stable isotope ratio analysis, *Rapid Commun. Mass Spectrom., 15*, 501-519.

Werner, R. A., M. Rothe, and W. A. Brand (2001), Extraction of CO_2 from air samples for isotopic analysis and limits to ultra high precision delta O-18 determination in CO_2 gas, *Rapid Commun. Mass Spectrom., 15*, 2152-2167.

Wichura, B., N. Buchmann, and T. Foken (2000), Fluxes of the stable carbon isotope ^{13}C above a spruce forest measured by hyperbolic relaxed eddy accumulation method, paper presented at 14th Symposium on Boundary Layers and Turbulence, American Meteorological Society, Boston, Aspen, Colorado, 7-11 August 2000.

Wilczak, J. M., S. P. Oncley, and S. A. Stage (2001), Sonic anemometer tilt correction algorithms, *Boundary-Layer Meteorol., 99*, 127-150.

Wyngaard, J. C., and C.-H. Moeng (1992), Cospectral similarity in the atmospheric surface layer, *Quart. J. Roy. Meteor. Soc., 98*, 590-603.

Yakir, D., and X.-F. Wang (1996), Fluxes of CO_2 and water between terrestrial vegetation and the atmosphere estimated from isotope measurements, *Nature, 380*, 515-517.

Yakir, D., and L. da S. L. Sternberg (2000), The use of stable isotopes to study ecosystem gas exchange, *Oecologia, 123*, 297-311.

Zobitz, J. M., J. P. Keener, H. Schnyder, and D. R. Bowling (2006), Sensitivity analysis and quantification of uncertainty for isotopic mixing relationships in carbon cycle research, *Agric. For. Meteorol., 136*, 56-75, doi:10.1016/j.agrformet.2006.01.003.

8. Appendix – Whole-air REA System components

Component	Company	Type
Filters	Gelman Sciences Inc., Ann Arbor, MI, USA	ACRO 50, 1.0 µm, Teflon® (PTFE)
Inlet tubing	SERTO jacob GmbH, Fuldabrück, Germany	SERTOflex-6, 6 mm OD (Dekabon tubing, PE as inner wall material)
Tubing in REA system		Stainless steel, 6 mm OD, cleaned and heated
Connectors	Swagelock, Solon, OH, USA	Stainless steel fittings, quick connects and ultra torr connectors, seals: Viton® (FPM)
Connectors	University of Bayreuth, Germany	Stainless steel fittings, seals: Viton® (FPM)
Mass flow meters (MFM1, MFM2)	Bronkhorst Hi-Tec B. V., Ruurlo, Netherlands	F-111C-HA-33-V, 6 ln/min. (low pressure drop)
Pumps (P1, P3, P4)	KNF Neuberger GmbH, Freiburg, Germany	N 86 AVDC, aluminum, Viton® (FPM)
Pumps (P2 bypass, P5 flushing unit)	KNF Neuberger GmbH, Freiburg, Germany	N 86 KVDC, Ryton®, Viton® (FPM)
Pump (P6 drying air)	FÜRGUT, Aichstetten, Germany	DC24/80S
Pump motor drivers (P1, P2)	Conrad, Hirschau, Germany	192287, pulse-width dc motor driver
Nafion® gas-dryer	Perma Pure Inc., Toms River, NJ, USA	MD-110-48S-4, stainless steel, Nafion® (FPM)
Sampling valves (V1, V2 and dummy)	Bürkert, Ingelfingen, Germany	0330, 3/2 way solenoid valve, 3 mm orifice, stainless steel, Viton® (FPM)
Valves (V3, V4, V5, V6, V7, V8)	Bürkert, Ingelfingen, Germany	6011A, 2/2 way solenoid valve, 2.4 mm orifice, version for analytical applications, stainless steel, Viton® (FPM)
Bag 1, bag 2 (intermediate sample reservoirs)	Anagram International, Inc., Eden Prairie, MN, USA	Mylar® foil balloons, 45 cm, circle shape, (one bag reservoir consists of two balloons which fill with about 14 L each to allow increased sample volumes)
Drying traps	University of Bayreuth, Germany	Magnesium perchlorate granulate, $Mg(ClO_4)_2$, in 200 mm x 20 mm ID glass tubes and glass wool cleaned and heated and Viton® (FPM) seals
Glass flasks	Max-Planck-Institute for Biogeochemistry, Jena, Germany and QVF AG, Ilmenau, Germany	1 L borosilicate glass flasks with PCTFE stopcocks
Pressure sensor (installed at the outlet of one flask filling unit)	Suchy Messtechnik, Lichtenau, Germany	SD-30, -1000…+1500 hPa, stainless steel
Backpressure valves	Riegler & Co. KG, Bad Urach, Germany	Sicherheitsventile DN 8, +500 hPa, brass, Viton® (FPM)

9. Tables

Table 1. Concentration difference increase achieved by HREA sampling during the WALDATEM-2003 experiment and comparable data.

Scenario	Concentration difference increase HREA (H_h=1.0) / REA (H_w=0.6)	Average scalar concentration differences HREA (H_h=1.0)
Simulation, ideal	1.78 this study, 1.84 [*Bowling et al.*, 1999b]	CO_2: 4.9(±2.4) µmol mol^{-1} [*Bowling et al.*, 1999b] based on data from Eastern USA deciduous forest
Simulation, imperfect scalar similarity	1.73 this study, 1.65 [*Ruppert et al.*, 2006b]	
Simulation, proxy scalar and σ_w statistics defined from previous data and filter function	1.63 this study	CO_2: 2.4(±0.5) µmol mol^{-1} this study
Measured, including physical sampling effects		CO_2: 2.3(±0.6) µmol mol^{-1} $\delta^{13}C$: 0.11(±0.03) ‰ VPDB $\delta^{18}O$: 0.11(±0.02) ‰ VPDB-CO_2 CH_4: −0.4(±1.2) nmol mol^{-1} N_2O: −0.02(±0.26) nmol mol^{-1}

10. Figures and Figure captions

a)

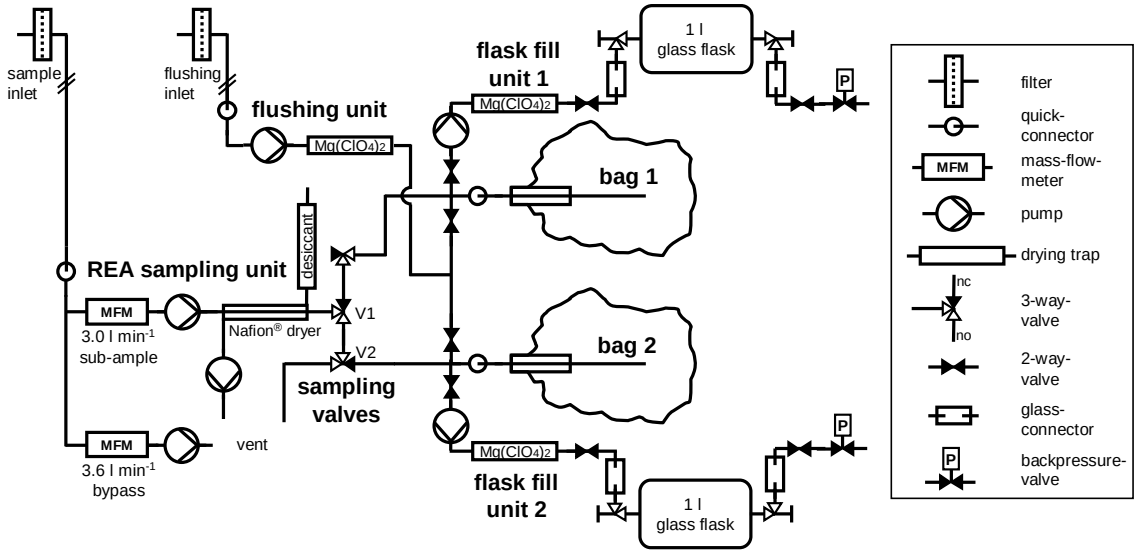

b)

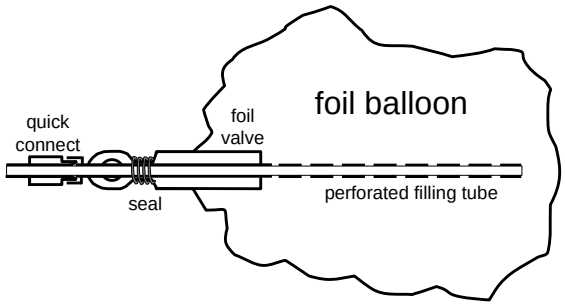

Figure 1. Design of the whole-air REA system (a) for isotope flux measurements with foil balloon bags as intermediate reservoirs (b). The perforated filling tube is inserted into the foil valve of the balloon and tightly sealed with a strong rubber band. Refer to Table A1 in the Appendix for details on individual components in (a).

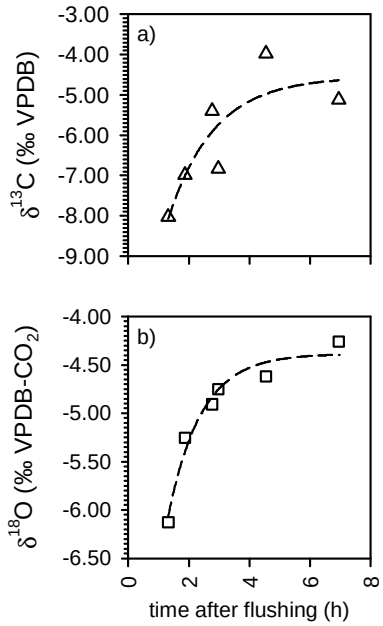

Figure 2. Foil balloon bag test for ^{13}C (a) and ^{18}O (b) isotope sampling before cleaning. The symbols represent the measured isotope ratios in 6 individual balloon bags. Each bag was flushed 3 times with sample air from one air tank on its first usage. Dashed lines indicate the progressive contamination of the air with heavier isotopes after the flushing procedure.

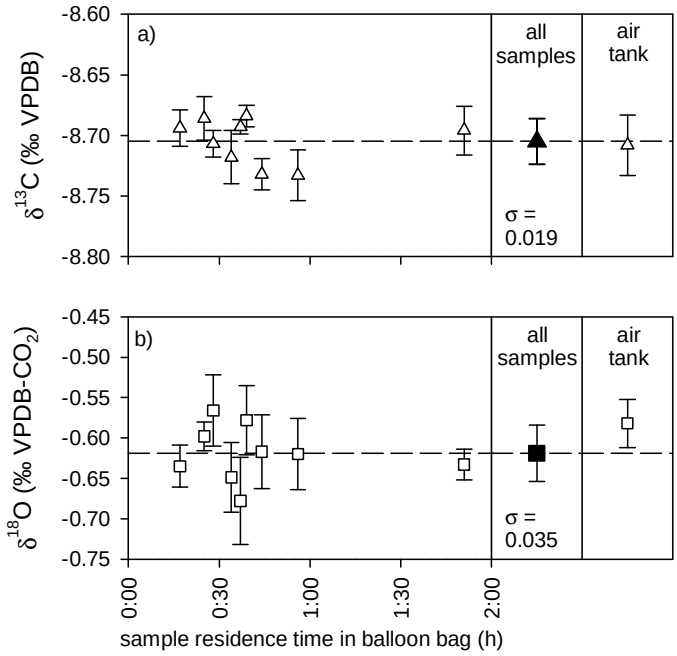

Figure 3. Foil balloon bag test for ^{13}C (a) and ^{18}O (b) isotope sampling after bag cleaning. Symbols in the leftmost section of the figure represent isotope ratios measured in air sampled from one tank after different residence times in 9 different balloon bags. Error bars indicate the standard deviation of up to 12 repeated measurements on the same air sample, which form the basis for the specification of its isotope ratio with high precision. Dashed lines and the solid symbol in the right section of the figure represent the average isotope ratio measured in the 9 balloon bags. The corresponding error bar indicates the standard deviation of the 9 specified isotope ratios from the balloon bag samples. As reference, the rightmost section of the figure shows the isotopic ratio of air sampled from the air tank into a glass flask without residence in a balloon bag. Note the difference in scales when comparing to Figure 2.

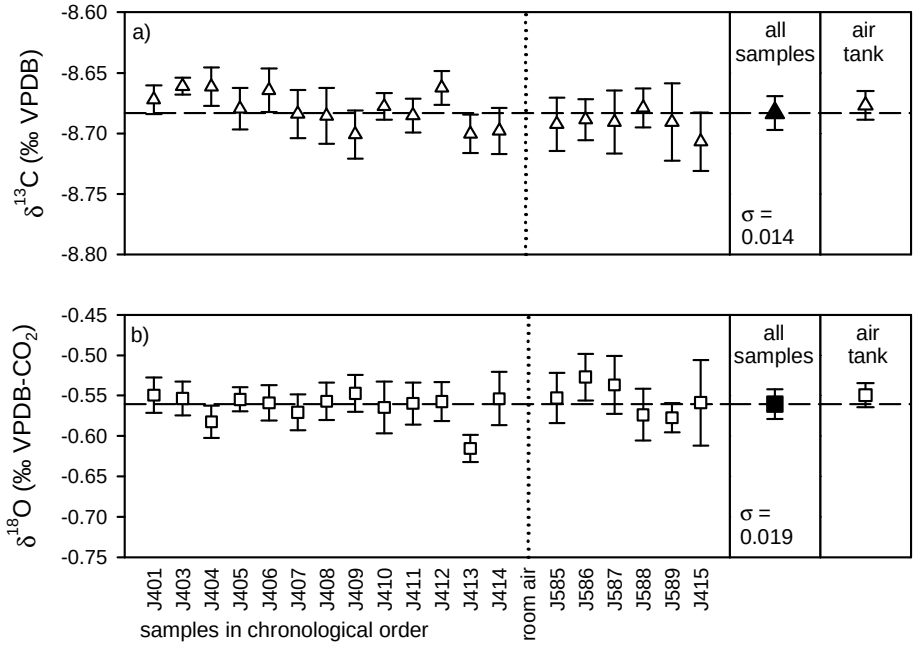

Figure 4. Test of the complete whole-air REA system for ^{13}C (a) and ^{18}O (b) isotope sampling. The usage of the symbols and lines follows the logic of Figure 3. Air from the tank was used for threefold flushing and directed through the REA sampling system, stored in the balloon bags and sampled into glass flasks in the same manner as required for REA sampling in the field. Subsequently, the ^{13}C and ^{18}O isotope ratios of CO_2 sampled into the glass flasks were measured.

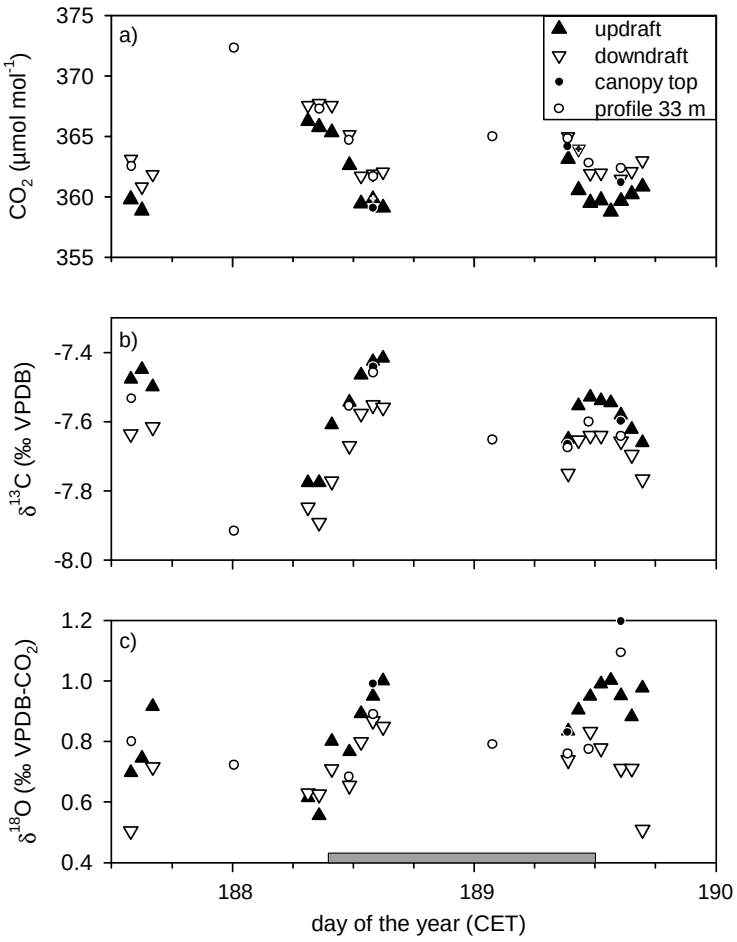

Figure 5. CO_2 mixing ratios (a) and ^{13}C (b) and ^{18}O (c) isotope ratios of updraft and downdraft air samples taken above a spruce forest at 33 m above ground (FLUXNET Station Waldstein/Weidenbrunnen, GE1-Wei) during the WALDATEM-2003 experiment by applying a hyperbolic deadband of H_h= 1.0 (HREA). Solid upward triangles = updraft air samples, unfilled downward triangles = downdraft air samples. Unfilled circles represent air samples taken simultaneously with an isotope- and trace-gas profile system also at 33 m. Solid circles represent profile samples from the canopy top at 15 m or 22 m. The gray bar marks samples, which (i) were taken after refreshing the drying traps in the whole-air REA system and the period, in which (ii) ^{18}O isotope ratios in REA and profile system air samples show the expected agreement. Two HREA samples consisted of relatively small amounts of sample air and are marked with a '+' in plot (a).

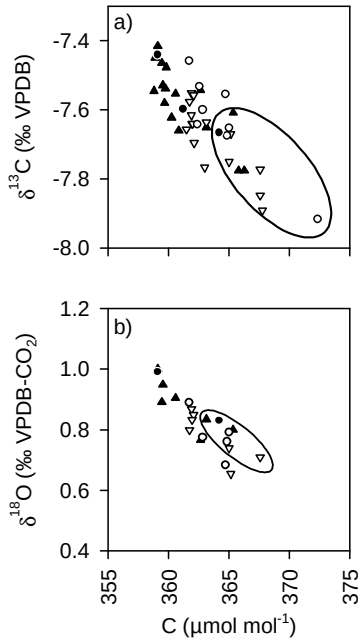

Figure 6. Scalar correlation between the ^{13}C (a) and ^{18}O (b) isotope ratios and the CO_2 mixing ratio in updraft and downdraft air samples and profile samples taken above a spruce forest at 33 m and in profile samples taken at the canopy top at 15 m or 22 m. Symbol usage corresponds to Figure 5. Figure 6b contains only samples from the period for which effective sample drying was assured. The encircled samples were collected during nighttime or morning transition periods.

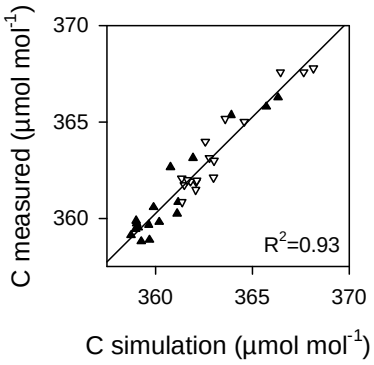

Figure 7. Measured updraft and downdraft CO_2 mixing ratios in HREA whole-air samples plotted against CO_2 mixing ratios from simulation of HREA sampling based on the EC CO_2 time series (updraft solid and downdraft unfilled triangles) with their least square linear regression (line).

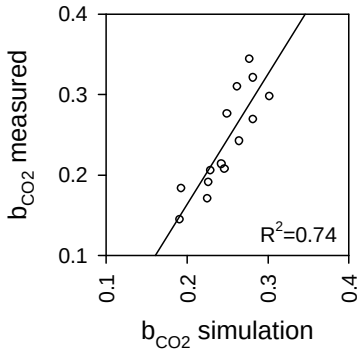

Figure 8. Effective *b*-factors derived from measured CO_2 mixing ratios in HREA whole-air samples in relation to simulated *b*-factors (circles) and their least square linear regression (line).

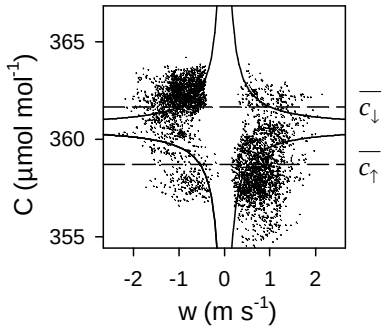

Figure 9. Plot of the effective hyperbolic sample selection for a 30 min sampling interval (dots) regarding vertical wind speed w and the open path CO_2 mixing ratio data C from the WALDATEM-2003 experiment, day of the year 188, 12:00-12:30. The sample selection is based on the original HREA valve switching record. Both axes are scaled to the 30 min average ±4 standard deviations. The solid lines indicate the ideal hyperbolic deadband with the size H_h=1.0 in respect to the 30 min statistics. The dashed lines indicate the average CO_2 mixing ratios of updraft ($\overline{c_{\uparrow}}$: w>0) and downdraft ($\overline{c_{\downarrow}}$: w<0) air samples, resulting from the effective hyperbolic sample selection.

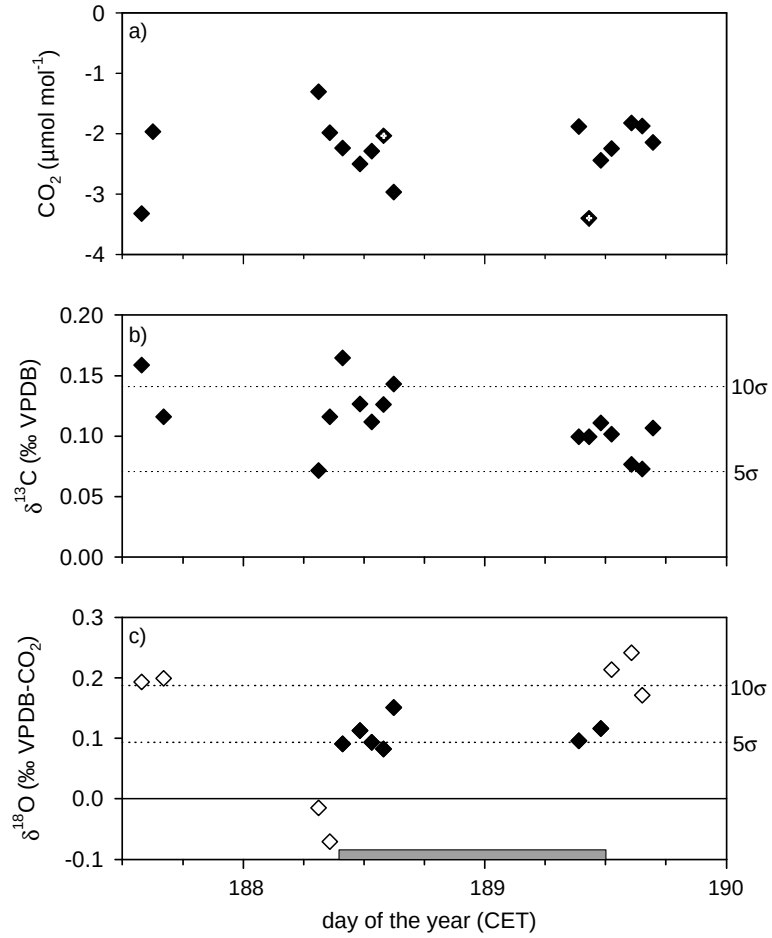

Figure 10. CO_2 mixing ratio differences (a) and ^{13}C (b) and ^{18}O (c) isotope ratio differences in updraft and downdraft REA air samples (solid diamonds). ^{18}O isotope ratio differences presumably influenced by incomplete drying out of the period marked with a gray bar are indicated as unfilled diamonds. Dotted lines indicate the fivefold and tenfold standard deviations specified in Section 4.2 and Figure 4 in order to assess the measurement precision for the isotope samples.

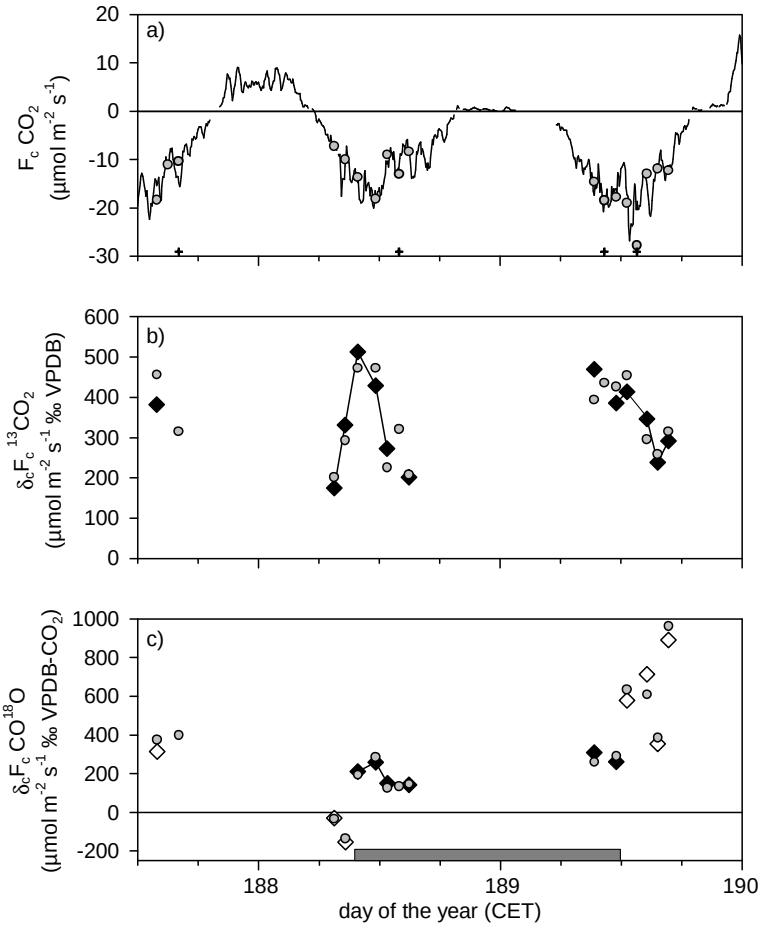

Figure 11. Turbulent CO_2 flux density (a) and $^{13}CO_2$ (b) and $CO^{18}O$ (c) turbulent isofluxes determined from whole-air HREA measurements. The solid line in (a) indicates the turbulent CO_2 flux density continuously measured with the EC system as reference. Measured b_{CO2}-factors were used for the turbulent isofluxes determined by HREA (diamonds in b and c). ^{18}O turbulent isofluxes presumably influenced by incomplete drying out of the period marked with a gray bar are indicated as unfilled diamonds in (c). Gray circles represent HREA turbulent flux densities calculated from measured concentration and isotopic differences and simulated b_{CO2}-factors, which were corrected according to the linear regression of *b*-factors in Figure 6. Either updraft or downdraft CO_2 mixing ratios of four samples marked with '+' at the bottom of plot (a) showed insufficient accuracy and were therefore replaced by simulated values. Consequently, for these samples turbulent isofluxes in plot (b) and (c) could only be determined based on simulated b_{CO2}-factors (gray circles).

Ecosystem $^{13}CO_2$ and $CO^{18}O$ isotope discrimination measured by hyperbolic relaxed eddy accumulation

J. Ruppert[1,2*], C. Thomas[1,3], J. Lüers[1], T. Foken[1], N. Buchmann[4]

[1]Department of Micrometeorology, University of Bayreuth, Germany

[2]now: Research Institute of the Cement Industry, Verein Deutscher Zementwerke, Düsseldorf, Germany

[3]now: Department of Forest Science, Oregon State University, Corvallis, OR, USA

[4]Institute of Plant Science, ETH Zürich, Switzerland

*Corresponding author: Johannes Ruppert, Research Institute of the Cement Industry, Environment and Plant Technology Department, Verein Deutscher Zementwerke, Tannenstrasse 2, 40476 Düsseldorf, Germany.
E-mail: rj@vdz-online.de, Telephone: +49-211-4578-275, Fax: +49-211-4578-256.

Abstract

The ecosystem isotope discrimination Δ_e and the flux weighted isotopic signature δ_c of the atmospheric CO_2 exchange of ecosystems are important parameters for global scale modeling of the carbon balance. Their measurement is also the basis for the isotopic flux partitioning method applied for the determination of gross flux components at ecosystem scale. The objective of this study is to demonstrate how these parameters and their diurnal variability can be determined by hyperbolic relaxed eddy accumulation (HREA) and whole-air sampling of the turbulent exchange of CO_2, $^{13}CO_2$ and $CO^{18}O$ isotopes. Additionally, the isotopic signatures of the assimilation flux and the respiration flux are analyzed in order to assess the potential for the application of the isotopic flux partitioning method. The sampling was performed above a spruce forest at the FLUXNET station Waldstein/Weidenbrunnen in Germany during a three-day intensive measurement campaign of the experiment WALDATEM-2003 (Wavelet Detection and Atmospheric Turbulent Exchange Measurements 2003). The flux weighted isotopic signature δ_c of the atmospheric turbulent exchange was determined directly from high precision analysis of updraft and downdraft air samples. Their display and geometrical interpretation in so called Miller-Tan plots visualized key processes influencing the CO_2 exchange. Based on the HREA measurements, the ecosystem isotope discrimination Δ_e and net ecosystem isotope discrimination Δ_E could be determined on half-hourly timescales with a footprint similar to that of eddy covariance (EC) measurements. The observed diurnal variability of isotopic signatures and ecosystem isotope discrimination demonstrates the need for their repeated measurement for the evaluation of isotopic mass balances at ecosystem scale. The analysis of vertical profile air samples showed that (i) the isotopic signature δ_R of the respiration flux during daytime could not be inferred from nighttime samples and (ii) that the determination of δ_R during daytime should be restricted to sub-canopy samples because of multiple source mixing at higher levels. The definition of the canopy integrated isotope discrimination Δ_{canopy} commonly used for isotopic partitioning of assimilation and respiration fluxes is a potential source of bias. An alternative definition (Δ'_{canopy}) is suggested, which yielded estimates of $\Delta^{13}C'_{canopy}$=17.7(±2.6)‰ and $\Delta^{18}O'_{canopy}$=17.8(±2.1)‰ on average. However, half-hourly values were subject to diurnal variability and data from independent measurements or validated models, which should reflect this variability, is indispensable for the isotopic partitioning of the assimilation and respiration fluxes. At the beginning of the intensive measurement campaign, their isotopic disequilibria $\mathcal{D}^{13}C$ and $\mathcal{D}^{18}O$ were opposite in sign. Two days past the end of a prolonged rain period, both disequilibria disappeared. The observed fast equilibration may limit the periods for the successful application of the isotopic flux partitioning method. Due to its general sensitivity to the precision of isotopic signatures, there is further need to investigate the variability of truly flux weighted isotopic signatures by high precision isotope measurements at ecosystem scale. The diurnal variability of the isotope discrimination should be regarded for the evaluation of isotope mass balances and for the validation of models.

Index terms: 0315 Biosphere/atmosphere interactions (0426, 1610), 0414 Biogeochemical cycles, processes, and modeling (0412, 0793, 1615, 4805, 4912), 0454 Isotopic composition and chemistry (1041, 4870), 0490 Trace gases, 0428 Carbon cycling (4806)

Keywords: Isotope discrimination, Isotopic signature, Net ecosystem exchange, Flux partitioning, Trace-gas flux, Relaxed eddy accumulation, Conditional sampling

Manuscript prepared for submission to Global Biogeochemical Cycles

1. Introduction

The carbon balance of terrestrial ecosystems and its atmospheric flux components can be investigated by relating the bulk[1] CO_2 mass balance to mass balances of the stable isotopes $^{13}CO_2$ and $CO^{18}O$ on ecosystem up to global scale [*Ciais et al.*, 1995a; *Ciais et al.*, 1995b; *Yakir and Wang*, 1996; *Yakir and da S. L. Sternberg*, 2000]. Due to discrimination of heavier isotopes during photosynthetic uptake of CO_2 in ecosystems [*Farquhar et al.*, 1989] the combination of the mass balances can be used for isotopic flux partitioning. This method requires the precise determination of isotopic signatures of the atmospheric gas exchange or of the ecosystem isotope discrimination [*Buchmann et al.*, 1998]. With appropriate temporal and spatial integration, the ecosystem isotope discrimination forms the basis for modeling of the $^{13}CO_2$ isotope and bulk CO_2 balance at global scale [*Bakwin et al.*, 1998; *Baldocchi and Bowling*, 2003; *Buchmann and Kaplan*, 2001; *Fung et al.*, 1997; *Kaplan et al.*, 2002; *Miller et al.*, 2003; *Randerson et al.*, 2002]. At the ecosystem scale, the isotopic flux partitioning method is applied in order to quantify the assimilation and respiration gross flux components based on micrometeorological isotope flux measurements above the ecosystem [*Bowling et al.*, 2001; *Lloyd et al.*, 1996; *Wichura et al.*, 2000; *Zhang et al.*, 2006]. The difference of their absolute contributions determines the relatively small net ecosystem exchange (NEE). The success of the isotopic flux partitioning method depends on (i) the difference of isotopic signatures of the component fluxes and (ii) the corresponding measurement precision [*Phillips and Gregg*, 2001]. Several studies point out that the achieved measurement precision of the $\delta^{13}C$ and $\delta^{18}O$ isotopic signatures[2] of the atmospheric turbulent exchange is the most critical parameter for the isotopic flux partitioning method applied at the ecosystem scale [*Bowling et al.*, 1999a; *Bowling et al.*, 2003a; *Zobitz et al.*, 2006; *Zobitz et al.*, 2007]. It is difficult to measure especially above tall vegetation where due to the required measurement position with sufficient relative distance to the canopy (i) concentration and isotopic differences are relatively small and (ii) the flux gradient method cannot be applied. High demand for increased measurement precision of the $\delta^{13}C$ and $\delta^{18}O$ isotopic signatures of atmospheric turbulent CO_2 exchange and the ecosystem isotope discrimination and for the investigation of their temporal variability is expressed in a number of recent studies on the measurement of isotope fluxes by tunable diode laser (TDL) [*Bowling et al.*, 2003b; *Griffis et al.*, 2004; *Griffis et al.*, 2005; *Saleska et al.*, 2006; *Zhang et al.*, 2006] and on modeling of ecosystem/atmosphere isotope exchange [*Aranibar et al.*, 2006; *Chen et al.*, 2006; *Fung et al.*, 1997; *Lai et al.*, 2004; *Ogée et al.*, 2003; *Ogée et al.*, 2004]. Isotopic signatures are often determined from Keeling plots of vertical profile air samples [*Pataki et al.*, 2003]. Their evaluation depends on the observed isotope ratio and concentration differences. The size of different flux contributions may not be accounted correctly. However, truly flux weighted isotopic signatures are required for the correct evaluation of isotopic mass balances. Also the relevant temporal variability and spatial scales, i.e. the measurement footprints, have to be considered carefully in order to avoid biased results [*Göckede et al.*, 2008; *Miller and Tans*, 2003; *Zobitz et al.*, 2007]. *Ruppert et al.* [2008] demonstrated that sufficient precision for the

---

[1] The term 'bulk CO_2' is used to refer to the sum of $^{12}C^{16}O^{16}O$, $^{13}C^{16}O^{16}O$, $^{12}C^{16}O^{18}O$ and all other CO_2 isotopes.

[2] All results reported for ^{13}C and ^{18}O isotope ratios in this study refer to the isotope composition of CO_2, i.e. the isotope ratio of $^{13}CO_2$ or $CO^{18}O$ to bulk CO_2. The isotope ratios are expressed as isotopic signatures in δ-notation. All $\delta^{13}C$ and $\delta^{18}O$ isotopic signatures are reported relative to ^{13}C and ^{18}O isotopic abundances in the international standards VPDB (Vienna Pee Dee Belemnite) and VPDB-CO_2 respectively (CG99 scale, see details in [*Werner et al.*, 2001] and [*Werner and Brand*, 2001]):
$\delta^{13}C=[[(^{13}C/^{12}C)_{sample}-(^{13}C/^{12}C)_{VPDB}]/(^{13}C/^{12}C)_{VPDB}]\cdot 1000$ (‰ VPDB).
$\delta^{18}O=[[(^{18}O/^{16}O)_{sample}-(^{18}O/^{16}O)_{VPDB\text{-}CO2}]/(^{18}O/^{16}O)_{VPDB\text{-}CO2}]\cdot 1000$ (‰ VPDB-CO_2).

measurement of the isotopic flux density (isoflux, [*Bowling et al.*, 2001; *Bowling et al.*, 2003a]) above a forest at half-hourly timescales can be achieved by combining the hyperbolic relaxed eddy accumulation method (HREA, [*Bowling et al.*, 1999b]) with whole-air sample collection and high precision isotope analysis in a laboratory [*Werner et al.*, 2001].

In this paper we suggest directly determining the flux weighted isotopic signature of atmospheric turbulent exchange from bulk CO_2 mixing ratios and ^{13}C and ^{18}O isotope ratios measured in updraft and downdraft HREA whole-air samples. Results from a three-day intensive measurement campaign in a spruce forest are presented and the achievable measurement precision is discussed.

From these results, the ecosystem discrimination is determined at half-hourly timescales, which allows investigating its variability in the diurnal cycle. By roughly estimating the daytime respiration flux based on a nighttime NEE temperature regression also the isotopic signature of the assimilation flux and the canopy isotope discrimination are determined. We discuss the sensitivity of the isotopic flux partitioning method and the potential for bias resulting from the definition of the canopy isotope discrimination.

Keeling plots and Miller-Tan plots of vertical profile air samples, commonly used for the determination of the isotopic signature δ_R of the respiration flux, are analyzed to test their inherent assumption of two source mixing during daytime. By analysis of the temporal traces of HREA updraft and downdraft air samples in Miller-Tan plots we combine and visualize information on key factors for the ecosystem CO_2 exchange, i.e. (i) assimilation and respiration of the ecosystem and (ii) release and recycling of CO_2 respired during nighttime, (iii) changes in the isotopic signature of canopy air and (iv) coupling and decoupling of certain layers in the ecosystem from the air exchange. In parallel, vertical CO_2 profile and turbulence profile measurements are analyzed for indication of temporal decoupling of the canopy and the sub-canopy space from the atmospheric exchange.

2. Theory

2.1. Isotopic signatures and mixing lines

The mixing of air from two sources with different isotope ratios δ_1 and δ_2 can be described by two simple mass balances,

$$C_a = C_1 + C_2 , \tag{1}$$

$$\delta_a C_a = \delta_1 C_1 + \delta_2 C_2 , \tag{2}$$

in which C_1 and C_2 are the dry air bulk CO_2 mixing ratios of the two sources. δ_a and C_a are the isotope ratio and bulk CO_2 mixing ratio of the mixed air, respectively. The so called 'Keeling plot' of the isotope ratios δ_a versus the inverse of the CO_2 mixing ratios $1/C_a$ of mixed air samples results in a 'mixing line' that indicates the isotopic signature of one of the sources [*Keeling*, 1958]. It can be determined as the intercept of the extrapolated linear regression and is defined by combining (1) and (2):

$$\delta_a = C_1(\delta_1 - \delta_2)\frac{1}{C_a} + \delta_2 . \tag{3}$$

This method is commonly applied to identify the isotopic signature δ_R of the nighttime respiration flux F_R in ecosystems from sampling air in a vertical profile [*Pataki et al.*, 2003]. The same result can also be achieved by plotting $\delta_a C_a$ versus C_a [*Miller and Tans*, 2003]. Here the isotopic signature δ_2 is indicated by the slope of a linear regression:

$$\delta_a C_a = \delta_2 C_a + C_1(\delta_1 - \delta_2). \quad (4)$$

Both methods require precise measurement of δ_a and C_a in order to robustly establish the linear regression, especially for small ranges of mixing ratios and isotope ratios [*Phillips and Gregg*, 2001]. Both types of linear relation, i.e. the 'Keeling plot' and the 'Miller-Tan plot', yield identical results and are equally sensitive to poor measurement resolution. Because the relative measurement error is commonly higher for isotope ratios of CO_2 than for the bulk CO_2 mixing ratios, ordinary least square (OLS) linear regression should be preferred to geometric mean (GM) linear regression, which results in systematic errors at small CO_2 ranges [*Zobitz et al.*, 2006].

2.2. Eddy flux and eddy isoflux measurement methods

The turbulent atmospheric gas exchange of an ecosystem can be measured by the eddy covariance method (EC) [*Baldocchi et al.*, 1988]. It requires that fast and precise sensors are available to resolve the fluctuations of the scalar of interest c', which in combination with sonic anemometer measurements of the fluctuations of the vertical wind velocity w' above the ecosystem allow the determination of the turbulent flux density F_c as their covariance, often called eddy flux:

$$F_c = \overline{w'c'}. \quad (5)$$

The overbar denotes Reynolds averaging over a typical measurement period of 30 min. This method is commonly applied to measure the atmospheric CO_2 exchange of different ecosystems around the globe [*Aubinet et al.*, 2000; *Baldocchi et al.*, 2001]. The derivation of the turbulent flux density requires certain corrections, transformations and quality control [*Foken et al.*, 2004]. By convention, upward fluxes into the atmosphere have a positive sign.

Up to now, no sensors are available which provide sufficient temporal resolution and chemical precision for eddy covariance measurements of stable isotopes of CO_2, i.e. $^{13}CO_2$ and $CO^{18}O$. Different methods are proposed for the investigation of isotopic signatures in the CO_2 exchange and critically reviewed by *Bowling et al.* [2003a]. These include the so called EC/flask method [*Bowling et al.*, 1999a; *Bowling et al.*, 2001], which scales the high resolution time series of bulk CO_2 fluctuations by a linear function derived from the relation of the isotopic signatures and bulk CO_2 mixing ratios in air samples in order to estimate the time series of fluctuations of the isotopic signature. This method assumes a strictly linear relation on all scales of the turbulent exchange of CO_2 and $^{13}CO_2$ or $CO^{18}O$ isotopes, i.e. strictly linear scalar similarity.

Above short vegetation, the flux-gradient method [e.g. *Businger*, 1986] can be applied, which is based on concentration and isotope measurements at two different levels above the ecosystem and the assumption of flux-gradient similarity for two scalar quantities. Only for one of the scalar quantities direct flux measurements have to be performed. This method is now combined with tunable diode laser (TDL) isotope analysis, which is able to resolve typical isotopic

gradients above ecosystems with intense photosynthetic activity with sufficient precision, when allowing about 10 s of integration time [*Bowling et al.*, 2003b; *Griffis et al.*, 2004; *Griffis et al.*, 2005; *Pattey et al.*, 2006; *Saleska et al.*, 2006; *Zhang et al.*, 2006]. The assumption of flux-gradient similarity is based on certain vertical profile characteristics. Over tall vegetation, these can only be observed at greater distances from the canopy. Also, the existence of counter gradient fluxes [*Denmead and Bradley*, 1985] often limits the use of the flux gradient method.

When no fast high resolution sensors are available for EC, the conditional sampling or relaxed eddy accumulation method (REA) [*Businger and Oncley*, 1990] can be applied in order to determine the turbulent flux density from the average concentration difference measured in updraft and downdraft air samples. Air samples are typically selected on a 10 Hz basis and are accumulated for subsequent laboratory analysis by isotope ratio mass spectrometry (IRMS):

$$F_c = b\sigma_w\rho_a\left(\overline{c_\uparrow} - \overline{c_\downarrow}\right), \tag{6}$$

where ρ_a is the dry air density. $\overline{c_\uparrow}$ and $\overline{c_\downarrow}$ are the average scalar concentrations expressed as dry air mixing ratios in updraft and downdraft air samples, respectively. The concentration difference is scaled with the intensity of turbulent vertical mixing measured by the standard deviation of the vertical wind speed σ_w based on the assumption of flux-variance similarity. The proportionality factor b is determined from EC flux measurements of a proxy scalar, under the assumption of scalar similarity in the turbulent exchange by combining (5) and (6) and rearranging for b:

$$b = \frac{\overline{w'c'}}{\sigma_w\rho_a\left(\overline{c_\uparrow} - \overline{c_\downarrow}\right)}. \tag{7}$$

The REA method can be applied to determine isotope fluxes by measuring isotope and bulk CO_2 mixing ratios in updraft and downdraft air samples [*Bowling et al.*, 1999a; *Bowling et al.*, 1999b]. For the scalar similarity assumption this means $b_{13CO2}=b_{CO18O}=b_{CO2}$. Rewriting (6) for the determination of the turbulent isotopic flux density, i.e. the eddy isoflux $\delta_c F_c$, based on isotope ratios expressed in δ-notation [*Bowling et al.*, 2001; *Bowling et al.*, 2003a] yields:

$$\delta_c F_c = b\sigma_w\rho_a\left(\overline{\delta_\uparrow}\,\overline{C_\uparrow} - \overline{\delta_\downarrow}\,\overline{C_\downarrow}\right). \tag{8}$$

$\overline{\delta_\uparrow}$ and $\overline{\delta_\downarrow}$ are the average isotopic signatures in updraft and downdraft air samples, respectively. $\overline{C_\uparrow}$ and $\overline{C_\downarrow}$ are the updraft and downdraft average bulk CO_2 mixing ratios in dry air. Such measurements directly above forest ecosystems require high analytical precision in order to correctly resolve small concentration and isotopic differences. In order to increase the concentration difference and to resolve certain technical sampling problems, normally a deadband is applied during REA sampling for low vertical wind velocities at which no samples are accumulated in the updraft or downdraft reservoirs [*Businger and Oncley*, 1990; *Pattey et al.*, 1993]. *Bowling et al.* [1999b] suggested a modification of the REA method, in which a hyperbolic deadband is applied (HREA) in order to maximize the scalar difference for isotope flux measurements.

Problems with the assumption of scalar similarity for REA and HREA are discussed in *Ruppert et al.* [2006b]. A comprehensive assessment of the impact of scalar similarity on

isotopic flux measurement methods could only be performed with continuous and high resolution time series from EC isotope flux measurements. However, in comparison to the EC/flask method, the assumption of scalar similarity in HREA is significantly relaxed. Strict similarity is only assumed for sample selection, when individual samples are rated according to their flux contribution $w'c'$ to the proxy scalar turbulent exchange, i.e. when defining the hyperbolic deadband for updraft and downdraft sample segregation. While there is some evidence that the relation between bulk CO_2 and its isotopic signatures in the turbulent exchange might generally be linear [*Bowling et al.*, 2001], the slope of that relation may change temporarily, e.g. during morning transition periods [*Bowling et al.*, 2003a; *Ruppert et al.*, 2008]. In HREA the slope of the mixing line is determined by precisely measuring the average isotopic and mixing ratio differences in updrafts and downdrafts. This incorporates important additional information on the major turbulent fluctuations and the $w'c'$ joint frequency distribution of the isotopes into the flux evaluation scheme [*Ruppert et al.*, 2008].

The proxy scalar difference and appropriate *b*-factors can be determined either from simulation of HREA sampling of turbulent time series or based on measured concentration differences, e.g. in the case of whole-air sampling and multiple scalars analysis. In the latter case, the advantage is, that potential sources of error related to the current micrometeorological situation or the technical sampling procedure identically influence the concentration difference of the scalar of interest and the proxy scalar. The measured *b*-factors are then determined for each measuring period of typically 30-40 min individually. This and other issues regarding the technical performance of whole-air HREA measurements are discussed in detail by *Ruppert et al.* [2008]. If bulk CO_2 mixing ratios and $\delta^{13}C$ and/or $\delta^{18}O$ isotopic signatures are measured from the same updraft and downdraft air sample and scalar similarity is assumed as discussed above, the ratio of (8) and (6) directly determines the flux weighted isotopic signature δ_c of the turbulent atmospheric exchange of CO_2:

$$\delta_c = \frac{\delta_c F_c}{F_c} = \frac{\left(\overline{\delta_\uparrow}\,\overline{C_\uparrow} - \overline{\delta_\downarrow}\,\overline{C_\downarrow}\right)}{\left(\overline{C_\uparrow} - \overline{C_\downarrow}\right)}. \qquad (9)$$

δ_c is the key parameter that relates the eddy isoflux $\delta_c F_c$ measured by HREA to the CO_2 eddy flux F_c, which can be measured by EC (5). Consequently, the same term results from combining (8) with the definition of *b* by (7) and dividing by (5). This definition has similarity to the expressions suggested by *Lloyd et al.* [1996, Equations 14 and 15] for the determination of the isotopic content of one way fluxes. However, in the presented form and in the context of HREA whole-air sampling it allows the direct derivation of δ_c and $\delta_c F_c$ without requiring flux determinations other than the eddy flux of bulk CO_2 determined by EC according to (5). It conceptually compares to the flux-ratio methodology suggested by *Griffis et al.* [2004] for the estimation of the isotopic signature δ_R of the respiration flux from isotope flux-gradient measurements at two levels above an ecosystem with a TDL during nighttime. However, above tall vegetation flux-gradient measurements could be disturbed by counter-gradient fluxes and internal boundary layers. The definition of δ_c according to (9) in the context of HREA sampling contains information on the dynamic of the turbulent exchange, which is inherent to the updraft–downdraft differences. In this respect, three advantages of isotope HREA should be considered. Firstly, δ_c is determined in a truly flux weighted manner and represents the derivative of the isotopic mixing line of the turbulent exchange at the point or level of measurement z_m above the ecosystem. Secondly, the isotopic signature of the turbulent

exchange can be measured with a footprint that is identical or at least very similar to the footprint of EC flux measurements. Thirdly, also the typical measurement integration times of the HREA and EC measurements are well comparable.

2.3. Mass balances for the net ecosystem exchange (NEE)

Mass balances for the CO_2 exchange of ecosystems are commonly evaluated by accounting for concentration changes in the air below measurement height as storage flux F_S in order to derive the mass balance for the ecosystem/atmosphere interface under the assumption that horizontal and vertical advection terms are negligible. This allows quantifying the net ecosystem exchange (NEE) F for individual sampling periods, which can directly be related to ecosystem processes. Equally, mass balances for CO_2 isotopes at the ecosystem/atmosphere interface, i.e. the isofluxes F_δ, are defined by including the so called 'isostorage' as isoflux term $\delta_S F_S$ [*Bowling et al.*, 2001]:

$$F = F_c + F_S = F_R + F_A \,, \tag{10}$$

$$F_\delta = \delta_c F_c + \delta_S F_S = \delta_R F_R + (\delta_a - \Delta_{canopy}) F_A \,. \tag{11}$$

NEE can be partitioned into its component fluxes of assimilation F_A and respiration F_R by combining (10) and (11) [*Bowling et al.*, 2001; *Bowling et al.*, 2003a; *Lloyd et al.*, 1996; *Wichura et al.*, 2000]. According to the definition presented by *Bowling et al.* [2001], the daytime foliar respiration is excluded from the daytime respiration flux F_R and included into the assimilation flux F_A, which then represents a canopy net assimilation flux. The difference between the isotopic signature δ_a of canopy air and the integrated canopy isotope discrimination Δ_{canopy} defines the isotopic signature of the assimilation flux $\delta_A=\delta_a-\Delta_{canopy}$. The mass balances (10) and (11) and the isotopic flux partitioning method are based on the assumption of well mixed air below EC measurement height z_m [*Lloyd et al.*, 1996; *Wichura et al.*, 2004].

The isotopic disequilibrium $\mathcal{D}$ is defined as the difference in the isotopic signatures δ_R of the carbon dioxide released to the atmosphere by respiration and the isotopic signatures δ_A of the carbon dioxide consumed by assimilation:

$$\mathcal{D} = \delta_A - \delta_R \,. \tag{12}$$

The ecosystem CO_2 exchange is in a state of isotopic equilibrium if $\mathcal{D}=0$. Isotopic disequilibrium results e.g. from changes of the canopy isotope discrimination Δ_{canopy} in the assimilation flux due to changes of environmental conditions and stomata opening [*Farquhar et al.*, 1989; *Flanagan et al.*, 1994]. The isotopic flux partitioning method requires isotopic disequilibrium $\mathcal{D}\neq 0$ and the precise measurement or modeling of F_c, F_S, $\delta_c F_c$, $\delta_S F_S$, δ_R and δ_A.

A schematic overview of the mass balances established for the investigation of ecosystem-atmospheric CO_2 exchange in a forest is presented in Figure 1. The measurement height z_m (dashed line) is the level of EC flux measurements and determination of the isotopic signature δ_c of atmospheric turbulent exchanger from HREA sampling. The mass balances of bulk CO_2 and its isotopes can here be described by (5) and the product of (5) and (9). The ecosystem/atmosphere boundary (dash-dotted line and dotted line) is the interface at which the CO_2 NEE and the isoflux are determined according to (10) and (11), i.e. mass balancing after

inclusion of the storage flux terms. Additional terms of horizontal and vertical advection are neglected here.

With the same concept as for the derivation of δ_c in (9), the flux weighted isotopic signature δ_N of the NEE is defined by the ratio of (11) to (10):

$$\delta_N = \frac{F_\delta}{F} . \tag{13}$$

During daytime and well-developed turbulent exchange, the storage flux terms F_S and $\delta_S F_S$ are normally small compared to the turbulent eddy fluxes F_c and $\delta_c F_c$. Thus, the most important parameter for the determination of the isotopic signature δ_N of the NEE is δ_c, which has to be measured with high precision above the ecosystem.

In tall vegetation, complex exchange processes like CO_2 recycling Φ within the canopy or decoupling of certain air layers in the canopy or sub-canopy space can complicate flux measurements and mass balancing for the derivation of NEE as indicated in Figure 1. A dense canopy can act like a bottleneck in the vertical exchange of air from the sub-canopy space in times of less developed turbulent mixing [*Thomas and Foken*, 2007b]. This has implications for mass balances based on gas exchange measurements performed above the canopy as the ecosystem/atmosphere boundary in the canopy or sub-canopy space (dotted line) is sometimes poorly defined. A variable status of atmospheric coupling may limit the mixing of canopy air with air from the sub-canopy space. The assumption of well-mixed air below EC flux measurement height z_m, which is fundamental to the isotopic flux partitioning method, may then partially be violated. Stable stratification of canopy air and a lack of vertical air exchange are often observed during nighttime. These conditions result in a risk of systematic error for the evaluation of isotopic mass balances, as discussed likewise for the evaluation of the CO_2 NEE [e.g. *Ruppert et al.*, 2006a].

2.4. Ecosystem isotope discrimination

A general definition of isotopic discrimination Δ commonly used in the context of biological processes is presented by *Farquhar et al.* [1989]:

$$\Delta = \frac{\delta_a - \delta_p}{1 + \delta_p} . \tag{14}$$

It relates the isotopic signature δ_a of source air to the isotopic signature δ_p of the product. This relative definition makes the isotope discrimination Δ independent from the reference value of the international isotope standard Vienna Pee Dee Belemnite (VPDB).

The definition of isotope discrimination Δ_e at the ecosystem scale was suggested by *Buchmann et al.* [1998]. Δ_e is estimated on long timescales based on the difference between the isotopic signature δ_{trop} of air samples from the free troposphere and the integral ecosystem isotopic signature inferred from the isotopic signature δ_R of the respiration flux commonly measured during nighttime.

$$\Delta_e = \frac{\delta_{trop} - \delta_R}{1 + \delta_R} . \tag{15}$$

In this definition δ_R is dominated by small spatial scales represented in air samples collected close to the ground, while δ_{trop} represents the large scale background air of the free troposphere. The underlying assumption of complete mixing in the air column spanning from the ground to the free troposphere and the use of δ_R as integral ecosystem isotopic signature are only valid on long timescales. Consequently, the variability of δ_R on diurnal and seasonal timescales should be considered [*Ekblad and Högberg*, 2001; *Knohl et al.*, 2005].

As described above, two different surfaces exist for CO_2 mass balancing of ecosystem atmospheric exchange on ecosystem scale: (i) A plane at measurement height z_m and (ii) the ecosystem/atmosphere interface. The corresponding balances differ by the inclusion of the storage flux term in the mass balance for the ecosystem/atmosphere interface. For the isotopic discrimination related to a net exchange through a surface, the product is characterized by the isotopic composition of the net flux, e.g. the isotopic composition of CO_2 that remains (i) below measurement height or (ii) within the ecosystem. The corresponding isotopic signatures are described by δ_c and δ_N, respectively.

In the first case (i), the definition of ecosystem isotope discrimination describes the isotopic influence of the turbulent exchange above the ecosystem on the atmosphere, here the lower boundary layer. This concept corresponds to the definition of ecosystem discrimination Δ_e [*Buchmann et al.*, 1998; *Buchmann and Kaplan*, 2001; *Kaplan et al.*, 2002]. We here suggest that on smaller half-hourly timescales Δ_e can be defined as ecosystem isotope discrimination of the atmospheric exchange at measurement height against isotopes in the lower boundary layer air. It can be determined from the flux weighted isotopic signature δ_c of the atmospheric turbulent exchange at measurement height z_m in reference to the isotopic signature δ_B of lower boundary layer source air above measurement height.

$$\Delta_e = \frac{\delta_B - \delta_c}{1+\delta_c}. \tag{16}$$

The source air from above the measurement height is best sampled by collecting downdraft air like in the HREA sampling scheme, which for its isotopic signature implies $\delta_B=\overline{\delta}_{\downarrow}^{-}$.

In the second case (ii), the combined discrimination effect of isotopic fluxes during photosynthesis and respiration was termed net ecosystem discrimination and denoted with Δ_E by *Lloyd et al.* [1996]. It equals the ecosystem isotope discrimination of the net ecosystem exchange (NEE) in reference to the isotopic signature δ_a of canopy source air below measurement height, and can be defined as

$$\Delta_E = \frac{\delta_a - \delta_N}{1+\delta_N}. \tag{17}$$

This term is conceptually identical to the original definition [*Lloyd et al.*, 1996]. However, assumptions on the magnitude of net and one-way flux components were made there, which are not required for its definition according to (17). We want to adopt the second assumption made by *Lloyd et al.* [1996], stating that an integrated air sample of air below measurement height, is sufficiently approximated by the updraft air sampled in the HREA sampling scheme and can also be used to describe the source air at the ecosystem/atmosphere interface, i.e. $\delta_a=\overline{\delta}_{\uparrow}^{-}$ and $C_a=\overline{C}_{\uparrow}^{-}$. Support for this assumption during daytime was provided by a close agreement between

diurnally changing CO_2 mixing ratios, $\delta^{13}C$ and $\delta^{18}O$ isotopic signatures in updraft air samples and canopy air samples [*Ruppert et al.*, 2008].

2.5. Canopy isotope discrimination

The integrated canopy isotope discrimination Δ_{canopy} is commonly defined as the difference of δ_A to the isotope ratio of canopy source air by (11) [*Bowling et al.*, 2001; *Bowling et al.*, 2003a], i.e.

$$\Delta_{canopy} = \delta_a - \delta_A \,. \tag{18}$$

This definition of the discrimination in the net assimilation flux is based on an approximation, in which terms of $\delta_a\Delta_{canopy}$ and Δ_{canopy}^2 are ignored [*Bowling et al.*, 2001; *Bowling et al.*, 2003a] in order to allow for simple calculations of the flux partitioning method. Similar approximations were also used for global scale modeling [*Bakwin et al.*, 1998; *Randerson et al.*, 2002]. However, the definition of isotope discrimination from a simple difference has a systematic difference to conceptually similar definitions of isotope discrimination of ecosystem fluxes, i.e. Δ_e and Δ_E [*Buchmann et al.*, 1998; *Lloyd et al.*, 1996] and the general definition of isotope discrimination Δ [*Farquhar et al.*, 1989]. We therefore suggest an alternative definition of the canopy discrimination Δ'_{canopy} in the net assimilation flux,

$$\Delta'_{canopy} = \frac{\delta_a - \delta_A}{1 + \delta_A}, \tag{19}$$

which is compared to (18) and discussed in Section 4.6 and Section 4.8. A solution for the inclusion of (19) into the isoflux mass balance (11) is presented in Appendix B.

3. Methods and Material

3.1. Field experiment

A whole-air REA system was used to collect updraft and downdraft air during the field experiment WALDATEM-2003 (Wavelet Detection and Atmospheric Turbulent Exchange Measurements 2003, [*Thomas et al.*, 2004]). Samples were collected during the summer above a spruce forest (*Picea abies, L.*) with a plant area index (PAI) of 5.2 $m^2\ m^{-2}$ and an average canopy height of 19 m [*Thomas and Foken*, 2007a]. Understorey vegetation consists of small shrubs and grasses. The experiment site Waldstein/Weidenbrunnen (GE1-Wei) is part of the FLUXNET network and is located in the Fichtelgebirge Mountains in Germany (50°08'31" N, 11°52'01" E, 775 m a.s.l.) on a slope of 2°. A detailed description of the site can be found in publications by *Gerstberger et al.* [2004] and *Staudt and Foken* [2007].

A sonic anemometer (R3-50, Gill Instruments Ltd., Lymington, UK) and an open path CO_2- and H_2O-analyser (LI-7500) were installed on a tower at 33 m and their data was used for continuous EC measurements. The application of corrections for the derivation of the turbulent flux density and further quality control measures are discussed in detail by *Ruppert et al.* [2006a] and were equally applied to determine the sensible heat, latent heat and CO_2 flux densities presented in this study. Turbulence data from a vertical profile of 3D-sonic anemometers was evaluated by methods presented by *Thomas and Foken* [2007b] to determine the status of coupling of the turbulent exchange between the sub-canopy, canopy and above-

canopy space. Mean air temperature was measured in a vertical profile of ventilated psychrometers. Long and short-wave radiation was measured at the tower top.

During the WALDATEM-2003 experiment, the online EC data was used for the HREA measurements with the whole-air REA system. The design of the whole-air REA system goes back to the principles ideas of conditional sampling of trace gases [*Businger and Oncley*, 1990; *Delany et al.*, 1991; *Desjardins*, 1977; *Oncley et al.*, 1993; *Pattey et al.*, 1993] and is based on a design suggested by *Bowling et al.* [2003a] in which foil balloon bags serve as intermediate storage for updraft and downdraft air samples at ambient pressure. Technical details, the complete evaluation scheme and thorough quality control applied during the material selection, the construction, the measurements and their evaluation are described and discussed by *Ruppert et al.* [2008]. Only a brief summary is presented here:

The sample air inlet was installed at 33 m just below the sonic anemometer. The air samples were directed through a 1 µm Teflon® filter into the whole-air REA system positioned just below the tower top. Updraft and downdraft samples were selected according to the definition of a hyperbolic deadband defined from the proxy scalar CO_2, pre-dried in a Nafion® drier and accumulated in foil balloon bags at ambient pressure for intermediate storage. Foil balloon bags were conditioned before the first usage by exposure to direct sunlight and flushing for several days and before each sampling interval by threefold flushing with dried ambient air from measurement height. After a typical sampling period of 30-40 min, updraft and downdraft air samples were further dried by pumping them through $Mg(ClO_4)_2$ drying traps and were stored in 1 L glass flasks with PCTFE stopcocks. All air samples were analyzed in the gas- and isotope laboratories of the Max-Planck-Institute in Jena, Germany.

Thorough testing of the complete whole-air REA system with air from a pressurized air tank assured that neither the foil balloon bags during storage times up to 1 h nor the rest of the sampling system contaminated ^{13}C or ^{18}O isotope ratios. For both, $\delta^{13}C$ and $\delta^{18}O$, the overall measurement precision of the whole-air REA system was very close to the high measurement precision of the IRMS system, which was used for isotope analysis [*Werner et al.*, 2001], i.e. 0.014‰ vs. VPDB for $\delta^{13}C$ and 0.02‰ vs. VPDB-CO_2 for $\delta^{18}O$ respectively [*Ruppert et al.*, 2008]. The evaluation of measurements from the field experiment during three consecutive days from 6–8 of July 2003, day of the year (doy) 187-189, and the comparison with samples collected with an independent isotope and trace gas profile system showed a very close match of mixing ratios and isotopic signatures in updraft air samples and in profile air samples from 33 m measurement height and canopy top. This confirmed that high levels of measurement precision could be maintained for ^{13}C and ^{18}O isotope ratios and bulk CO_2 mixing ratios during the field experiment and even small isotopic differences could be resolved sufficiently. However, at the beginning and the end of the measurement period, insufficient drying due to exhausted drying traps caused artificially changed ^{18}O isotope ratios of CO_2. These values are therefore omitted from further analysis in this study. ^{13}C isotope ratios and ^{18}O isotope ratios measured after the replacement of the drying traps in the morning of doy 188 were not affected. Systematic errors from specific sampling paths in the whole-air REA system were avoided by changing the sampling path for updrafts and downdrafts after each sampling interval.

In parallel, an isotope and trace gas profile system sampled air at eight levels from the tower top to the forest floor at 33, 22, 15, 5.25, 2.25, 0.9, 0.3 and 0.03 m above the ground. The 33 m inlet was installed close to the inlet of the whole-air REA system. Inlets at 22, 15 and 5.25 m span from the top to the bottom of the canopy space, while inlets at 2.25 m and below are positioned in the sub-canopy space. Air from each height was continuously sampled at about 1.2 L min^{-1}, passed through a 1 µm Teflon® filter and 25 m of Dekabon tubing into a 2.5 L

buffer volume. Profile sample air from the buffer volumes was dried with a Nafion® gas dryer and continuously analyzed with a closed path CO_2 analyzer (LI-820). Whole-air samples were taken from the buffer volumes within 15 to 30 min during nighttime and up to three times during the day, dried with $Mg(ClO_4)_2$ and sampled into 1 L glass flasks with PCTFE stopcocks for subsequent high precision isotope and trace gas analysis in the laboratory. The whole-air profile samples allowed for improved inter-calibration by allowing for an offset correction in the continuous CO_2 profile measurements. The design of the isotope and trace gas profile system followed the design principles of the whole-air REA system, in particular with respect to the treatment and use of materials.

3.2. Estimating storage flux and isostorage from HREA updraft air samples

In our experiment, the best temporal representation of the changes in the isotopic content below measurement height can be obtained from the HREA updraft air samples, in which the signal of mixed canopy air is captured above the canopy. This signal can be used to determine storage changes with regards to the isotopic composition of CO_2, i.e. the isostorage $\delta_S F_S$. The representativness of the updraft air samples for the air column from the forest floor to measurement height z_m of 33 m was tested for bulk CO_2. The CO_2 storage fluxes F_S calculated from updraft air samples fell on a 1:1 line compared to results obtained from the continuous CO_2 mixing ratio measurements in the eight-level profile. The adoption of a 1:1 relation correctly reproduced about 85% of the variation. This finding suggests that most of the storage change below measurement height z_m can be approximated correctly by evaluating updraft air samples:

$$F_S = \int_0^{z_m} \frac{d(\rho_a C_a)}{dt} dz \approx z_m \frac{d(\rho_a \overline{C_\uparrow})}{dt}, \tag{20}$$

$$\delta_S F_S = \int_0^{z_m} \frac{d(\rho_a \delta_a C_a)}{dt} dz \approx z_m \frac{d(\rho_a \overline{\delta_\uparrow} \overline{C_\uparrow})}{dt}. \tag{21}$$

It is worth noting that the temporal integration d/dt of the storage flux calculated from the preceding and subsequent HREA updraft air samples is slightly different (~2 h) from the temporal integration of the storage flux measured with the continuous profile system (30 min) and HREA isoflux temporal integration (30-40 min). However, the absolute contribution of storage fluxes F_S to the NEE was very small during daytime when isotope fluxes were measured (Figure 5). For consistency of the data used for mass balance analysis in this study, both the bulk CO_2 storage flux F_S and isostorage $\delta_S F_S$ were approximated according to (20) and (21), respectively.

3.3. Isotopic signature δ_A of the assimilation flux and canopy discrimination Δ_{canopy}

The isotopic flux partitioning method based on equation (10) and (11) requires the determination of the isotopic signatures of the net assimilation flux δ_A and of the respiration flux δ_R. We determined δ_R from the mixing line intercept in Keeling plots of sub-canopy air samples. The reasoning for restricting the analysis to sub-canopy samples is discussed in Section 4.1. The isotopic signature δ_a of canopy source air for the net assimilation flux was determined from HREA updraft air samples by assuming $\delta_a \approx \overline{\delta_\uparrow}$. The whole canopy isotope discrimination Δ_{canopy} can be determined from models for leaf level isotope discrimination [*Farquhar et al.*, 1989] and

canopy conductance estimated from the Penman-Monteith equation [*Bowling et al.*, 2001; *Grace et al.*, 1995; *Knohl and Buchmann*, 2005]. However, for the comparison of canopy discrimination Δ_{canopy} to ecosystem discrimination values Δ_e and Δ_E we chose to inverse the partitioning approach in order to estimate Δ_{canopy} based on measured isotopic signatures of the atmospheric turbulent exchange [*Bowling et al.*, 2003a]. This requires the determination of the contribution of the respiration flux F_R to the NEE. F_R was obtained from a simple exponential temperature regression model [*Lloyd and Taylor*, 1994], which was used for gap-filling of nighttime data and derivation of the annual sum of NEE at Waldstein/Weidenbrunnen [*Ruppert et al.*, 2006a]:

$$F_R = F_{R,10}\, e^{E_0[(1/(283.15-T_0))-(1/(T-T_0))]}. \quad (22)$$

$F_{R,10}$=3.84 µmol m^{-2} s^{-1} is the respiration flux density at 10 °C, E_0=163.7 K is the temperature sensitivity parameter and T_0=227.13 K was kept constant as in the original publication of the model. The regression showed a high coefficient of determination for 2 K bin aggregated data of nighttime total ecosystem respiration (R^2=0.86). It also compared well to the intercept of a daytime temperature-light response model [*Ruppert et al.*, 2006a]. However, half-hourly nighttime total ecosystem respiration data plotted against sub-canopy air temperature at 2 m showed large scatter. Due to this scatter and the assumption that daytime soil respiration shows a similar exponential dependence on temperature, the modeled respiration flux data should be regarded as a rough estimate [*Reichstein et al.*, 2005]. Nevertheless, during daytime, normally the absolute assimilation flux is significantly higher in magnitude than the respiration flux. For estimating the isotopic signature δ_A from a combination of (10) and (11), the propagation of error in F_R scales with the relative contribution of F_R to NEE. Therefore, some confidence is provided, that during daytime valid estimates of the canopy integrated and flux weighted value of δ_A and Δ_{canopy} can be obtained. These values will depend primarily on the measured isotopic signature δ_c in the atmospheric turbulent exchange. With this calculation method, δ_A and Δ_{canopy} are independent of leaf-level model assumptions.

4. Results and discussion

The flux weighted isotopic signature δ_c of the atmospheric turbulent exchange was determined from high precision measurements of the $\delta^{13}C$ and $\delta^{18}O$ isotopic signatures and bulk CO_2 mixing ratios in whole-air HREA updraft and downdraft air samples. From δ_c as principle parameter the isotopic signature δ_N in the net ecosystem exchange and related ecosystem isotope decimation parameters Δ_e and Δ_E were determined as described in Section 2 and 3.2. The estimation of Δ_{canopy} required modeling of the respiration flux F_R (Section 3.3) and the determination of its isotopic signature δ_R from sub-canopy air samples.

4.1. Determination of δ_R from isotopic mixing relations in vertical profile air samples

Air samples from the vertical profile were evaluated by separately analyzing the isotopic mixing lines for upper canopy samples (ranging from mid to above canopy, 15-33 m) and sub-canopy samples (0.03-5.25 m). The analysis of samples from doy 175, 12:50 h (Figure 2a-e) indicated the existence of two different mixing lines. For $\delta^{13}C$, the slope of the two mixing lines was obviously different. However, the uncertainty of a mixing line for upper canopy samples is larger due to the small range of CO_2 and a small number of sampling points. Exactly the same pattern was found in three other mixing relations of midday vertical profile air samples

presented together in Figure 2f. Although the definition of the upper canopy mixing lines is poor, the common pattern clearly demonstrates that the assumption of a single mixing line often made for the evaluation of δ_R is not valid during these daytime hours.

Sampling height dependence of the isotopic signature δ_R was found in a study by *Ogée et al.* [2003] in a pine stand with a leaf area index (LAI) around 3 m^2 m^{-2}. Also *Knohl et al.* [2005] found visual indication for the existence of different mixing lines in upper and lower canopy air samples from a deciduous forest. Their analysis however did not result in statistically significant differences in Keeling plot intercepts.

From the minimum CO_2 concentrations and maximum $\delta^{13}C$ isotopic signatures at mid canopy height in Figure 2a and b it is obvious that the observed change in slope is due to photosynthesis as a sink for CO_2 leading to relative enrichment of $\delta^{13}C$ due to isotopic discrimination in the net assimilation flux. The height at which a sample will represent exactly the crossing of the two mixing lines is likely to change with photosynthetic activity and the dynamic of the atmospheric exchange. Consequently, if accepting all vertical profile samples for the determination of δ_R, any mixing line regression and slope in a Miller-Tan plot (or intercept of a Keeling plot) will highly depend on at which heights within and above the canopy samples were collected. It is likely, that with more intense vertical mixing and consequently smaller gradients or with less analytical precision, such patterns cannot be clearly identified. In Figure 2e the discussed effect seems to be even more critical for $\delta^{18}O$ than for $\delta^{13}C$. It remains unclear, how the two different isotopic mixing lines with similar slope relate to each other.

Due to the obvious existence of different isotopic mixing relations in vertical profile air samples, we restricted our analysis of δ_R to the sub-canopy air samples, for which the two source mixing assumption seems to be more appropriate and which generally showed high coefficients of determination for linear regression lines (in most cases R^2>0.99). Studies by *Pataki et al.* [2003] and *Zobitz et al.* [2006] suggested the use of the standard error of the regression coefficients as measure for the uncertainty of δ_R. The corresponding results for δ_R for the HREA sampling period of doy 187-189 are summarized in Table 1. We found that most of the daytime samples showed significant differences between δ_R from sub-canopy samples only and δ_R derived from sub-canopy and upper canopy air samples. This was assessed by exceedance of the onefold or twofold standard error. A significant difference observed for $\delta^{18}O_R$ in the second nighttime profile was related to strong decoupling of the air exchange within the canopy and changing boundary layer air. The observed status of coupling, the diurnal variability of δ_R and appropriate methods for the determination of flux weighted isotopic signatures are discussed in context of Section 4.2, 4.7 and 4.9.

In conclusion, the assumption of a single mixing line for daytime vertical profiles seems problematic in forest canopies because the assumption of two source mixing is clearly violated. Dynamic processes on different height levels and with different temporal scales influence the air composition. Also, correct flux weighting of the different isotopic signatures cannot be assumed. Firstly, any combined estimate would highly depend on where samples were obtained in the vertical profile. Secondly, it would require that the two different isotopic signatures or slopes are weighted by the corresponding dynamic flux contribution [*Miller and Tans*, 2003, Equation 7] and not by the absolute span of CO_2 mixing and isotope ratios observed.

4.2. Isotopic mixing lines determined from HREA updraft and downdraft air samples

The mixing relation of HREA updraft and downdraft air samples can be analyzed in a similar way as in Figure 2 by the display in a Miller-Tan plot (Figure 3). According to (9), the slope of

the line connecting the updraft and downdraft samples equals the flux weighted isotopic signature δ_c of the atmospheric turbulent exchange measured above the canopy.

Despite variability in individual slopes and the spread of isotopic signatures especially for $\delta^{18}O$ in Figure 3d, a common direction of mixing lines and an overall mixing relation of the group of all samples in each plot is apparent. Contaminated samples, as those ^{18}O isotope samples that were subject to inefficient drying (Section 3.1), are not displayed, because they showed up as extreme outliers from this overall mixing relation either regarding their absolute updraft ($\overline{C_\uparrow}$,$\overline{\delta_\uparrow C_\uparrow}$) or downdraft ($\overline{C_\downarrow}$,$\overline{\delta_\downarrow C_\downarrow}$) values and/or the slope of their connecting line. Therefore, Miller-Tan plots of HREA samples allow efficient visual data inspection for the assessment of data with small mixing ratio and isotopic differences. Despite an overall isotopic mixing relation, the diurnal variability in the data demonstrates, that the definition of one single mixing line, like tested for the application of the EC/flask method [*Bowling et al.*, 1999a; *Bowling et al.*, 2001; *Bowling et al.*, 2003a], is not a valid assumption.

The display of the HREA data in Miller-Tan plots combines information on important factors for the investigation of ecosystem CO_2 exchange. This is the bulk CO_2 consumption and release of the ecosystem and related isotope discrimination. By indicating the sequence of samples with numbers and a gray line, the development of CO_2 mixing ratios and the isotopic content of updraft canopy air and downdraft boundary layer air can be followed. This relative development contains information on the status of coupling and decoupling of the air exchange between the boundary layer, the canopy and the sub-canopy space. For example, the coupling of the sub-canopy space in the morning would be indicated by a drop of the updraft air sample to the left or below the overall isotopic mixing relation, when isotopically depleted air from nighttime respiration is transported upwards towards the HREA sampling inlet. Such influence of continued upward mixing of isotopically depleted air can be suspected in Figure 3b in the development from sample '1' to '2'. Further development from sample '2' to '3' indicates significant enrichment of heavier isotopes in the canopy because of discrimination in the net assimilation flux. The enrichment coincides with less CO_2 mixing ratio decrease than would be expected from the overall isotopic mixing relation, which causes a deviation to the top. This pattern indicates CO_2 recycling [*da S. L. O'R. Sternberg*, 1989]. At the same time it provides an explanation for the excursion of early morning samples from the overall isotopic mixing relation [*Ruppert et al.*, 2008] also observed in the study by *Bowling et al.* [2003a]. Further significant decrease of CO_2 mixing ratios in sample '4' and '5' close to the overall isotopic mixing relation was related to decreased cloud cover for about 2 hours around noon (Figure 4a) and intense assimilation in well mixed canopy air. An inclined 'S'-like pattern results for the complete diurnal course of doy 188 from the line connecting the updraft samples in Figure 3b. This pattern partly is resample in Figure 3d. However, the relative changes on the vertical axis seem to be amplified for $\delta^{18}O$ data. Figure 3c shows a different pattern. The trace of the temporal development of updraft air samples would result in an inclined oval form, if we hypothesize continued mixing of canopy air and further addition of isotopically depleted CO_2 from respiration in the evening and night (gray-dotted line in Figure 3c, nighttime δ_R=26.7‰ VPDB, Table 1). A 'S'-like pattern in the morning is assumed for the start of photosynthesis and vertical mixing similar to the pattern found in Figure 3b. Data in Figure 3b, 3c and 3d also show that even under conditions with well developed turbulent mixing in the afternoon of doy 188 and 189 (Figure 4d) the slope of the black line connecting each updraft and downdraft sample, i.e. δ_c, can be different from the mixing relation inferred from the temporal development of isotope ratios in canopy air (gray line), e.g. in Figure 3b and 3d from sample '5' via '6' to '7' or in Figure 3c from sample '6' via '7' to '8'. This demonstrates the need for dynamic updraft and

downdraft whole-air sampling instead of average whole-air sampling for the measurement of δ_c. We suspect that by the method of graphical display presented in Figure 3 and by more completely sampling the diurnal cycle (Section 4.10), typical patterns related to specific characteristics of the net ecosystem exchange of CO_2 could become visible. For the analysis of isotopic signatures from updraft and downdraft samples the assessment of deviations from an overall isotopic mixing relation in Miller-Tan plots has methodological similarity to a geometrical interpretation of conditional samples suggested by *Porporato* [1999] for the analysis of coherent structures and the dynamic in turbulent time series.

4.3. Environmental conditions and characterization of the turbulent exchange situation

Effects from the European summer drought in 2003 [*Granier et al.*, 2007; *Reichstein et al.*, 2007] were visible in the diurnal courses of NEE, which was evaluated for the derivation of the annual sum of NEE for the year 2003 [*Ruppert and Foken*, 2005; *Ruppert et al.*, 2006a]. During periods with very dry and hot weather in the beginning of June and August, decreased NEE indicated drought stress and afternoon stomata closure. However, the intensive HREA measuring campaign started in the beginning of July at noon of doy 187 after a prolonged rain period. Consequently, no signs of drought stress were detected in the diurnal course of the NEE from doy 187 to 189. Changing degrees of cloud cover were observed as indicated by the diurnal courses of global radiation R_g in Figure 4a.

During the second night, a strong temperature inversion within the canopy is apparent from the vertical temperature gradient in Figure 4b, which was most likely related to the advection of warm boundary layer air masses in the evening of doy 188. The stable stratification at night [$(z_m-d)/L>0.5$, *Ruppert and Foken*, 2005] caused a nearly complete decoupling in the atmospheric exchange, which is marked by steep CO_2 mixing ratio gradients between mid canopy air (15 m) and air sampled at 14 m above the ecosystem in Figure 4c starting at sunset at about 20:00 h CET (mark '3') and diminishing CO_2 fluxes measured above the ecosystem (Figure 5).

The maxima and minima in the trend of CO_2 mixing ratios in and above the canopy in Figure 4c are a good indicator to determine the status of exchange and coupling in the morning. On doy 188 and 189 photosynthesis starts with the first light available at sunrise. This is marked by a sudden decrease in canopy CO_2 mixing ratios (marks '1' and '4'). About 1 h later, the sudden increase of CO_2 mixing ratios in the canopy air despite of increasing global radiation suggests that the CO_2 pool, which was built up by nighttime respiration in the sub-canopy space (2.25 m), is released into the upper canopy air. The coupling of the sub-canopy space coincides with the onset of sensible and latent heat fluxes measured above the ecosystem about 1 hour after sunrise (marks '2' and '5').

Before, significantly different situations for the exchange between canopy and above canopy air are visible in the morning of doy 188 and doy 189. While in the first morning mixing ratios at 33 m closely follow canopy air mixing ratios at 15 m, on the second morning equilibration of CO_2 mixing ratios occurred only after the stable stratification ended by warming of the canopy top and the onset of sensible and latent heat fluxes (mark '5'). The observed equilibration is likely due to the parallel onset of intense vertical mixing. For the sub-canopy full coupling and upward mixing of the CO_2 pool from nighttime respiration seems to occur only after about 10:00 CET.

The status of coupling in the vertical gas exchange was also analyzed by evaluating organized motion in turbulence time series from a vertical profile of sonic anemometers in *Thomas and*

Foken [2007b]. Results from this analysis are presented in Figure 4d. They indicate complete decoupling and the existence of wavelike patterns in the time series of the second night. The complex process of stepwise enhanced coupling in the morning is reflected generally well, including the prolonged decoupling of the sub-canopy space in the morning of doy 189. In the early morning hours, the temporal resolution of the exchange and coupling status could be enhanced by the identification of maxima and minima in the CO_2 mixing ratio time series in Figure 4c.

For the HREA measurement periods during daytime, generally well-coupled conditions are indicated for the canopy space. Only for the first sampling periods in the morning of doy 188 and 189 and the last sampling period in the late afternoon of doy 189, partial decoupling of the sub-canopy space should be assumed. This is indicated by an offset of sub-canopy CO_2 mixing ratios compared to canopy air in Figure 4c and the status 'Cs' and 'Ds' in Figure 4d.

4.4. Flux partitioning (F, F_R, F_A)

Figure 5 presents an overview of the CO_2 flux components in the NEE mass balance (10). As discussed above, in the second night the atmospheric turbulent exchange F_c was inhibited by a very strong temperature inversion within the forest canopy resulting in statically stable stratification. Consequently, hardly any of the respired CO_2 left the forest by vertical exchange. Instead, wavelike motions were detected in the turbulent time series of the sonic anemometer profile (Figure 4d). Measured CO_2 exchange and modeled total ecosystem respiration (TER, F_R) disagree for the second night. The stable stratification persisted and was observed well into the morning hours. The inhibited turbulent exchange caused poor data quality of the eddy covariance flux measurements (missing data of F_c in Figure 5). Observed storage fluxes were relatively small. However, small peaks of storage increase in air below measurement height are visible at sunset.

During the first night, the respiration model for F_R seems to slightly underestimate the nighttime total ecosystem respiration (TER, at nighttime equal to NEE, i.e. $F_R=F$). On the other hand, the estimation of daytime respiration flux F_R from the temperature regression of nighttime TER involves an overestimation because of the partial inhibition of dark respiration by light [*Sharp et al.*, 1984]. Furthermore, by definition daytime foliar respiration shall be excluded from F_R for the isotopic flux partitioning method according to (11). Foliar respiration is instead assigned to the net assimilation flux F_A during daytime. Because of the general uncertainty associated with the rough estimate of the daytime respiration flux F_R from nighttime TER and temperature regression (Section 3.3) and the opposing signs of the two apparent errors discussed for the actual situation during the measurement period, we decided not to apply corrections to the estimates for daytime F_R. F_A was determined from rearranging (10), i.e. $F_A=F-F_R$.

4.5. Isotopic signatures of turbulent atmospheric exchange (δ_c) and NEE (δ_N)

The flux weighted isotopic signature δ_c of the atmospheric turbulent exchange was measured by HREA 14 m above the canopy of the spruce forest at Waldstein/Weidenbrunnen and determined according to (9) as slope of a mixing line from whole-air HREA updraft and downdraft samples (Section 4.2). Error bars on δ_c values presented in Figure 6 indicate the estimated uncertainty (standard deviation) associated with a single measurement. It was determined by error propagation in (9) based on the observed isotopic and mixing ratio differences and the measurement precision for updraft and downdraft air samples as specified by *Ruppert et al.* [2008], i.e. 0.08 µmol mol^{-1} for bulk CO_2, 0.014‰ VPDB for $\delta^{13}C$ and,

0.02‰ VPDB-CO_2 for $\delta^{18}O$. On average, the relative standard deviation of the differences in the numerator was 19% for $^{13}CO_2$ and 28% for $CO^{18}O$ compared to 5% for the bulk CO_2 mixing ratio differences in the denominator. This shows that the uncertainty of the slope of the mixing line and of δ_c is dominated by the relative measurement uncertainty of small isotopic differences. Nevertheless, combined high precision bulk CO_2 measurements are also essential. The achievement of very high precision of the measurement of isotopic ratios by IRMS or absolute abundances of isotopes by TDL in the turbulent exchange is therefore of utmost importance [*Ogée et al.*, 2004; *Phillips and Gregg*, 2001; *Saleska et al.*, 2006; *Zhang et al.*, 2006]. This finding likewise applies to HREA and any other isoflux measurement method. The inclusion of samples with an 'average' isotopic signature from within the hyperbolic deadband in the EC method or application of smaller deadband sizes would further decrease the average differences that need to be determined with high precision.

The isotopic signature δ_N in the NEE was determined according to (13), (10) and (11) by accounting for the storage and isostorage changes (Section 3.2). Diurnal variability of values of δ_N and δ_c is presented in Figure 6. The variability of consecutive measurements is smaller than expected from the mathematical propagation of measurement uncertainty. Therefore, slightly better estimates of δ_c and δ_N can be achieved from the evaluation of several consecutive measurements. We assume that most of the observed temporal variability represents real changes of the isotopic signatures. Temporal variability should be expected from the observations and diurnal changes discussed in Section 4.2. For example, a small positive offset of noon and early afternoon $\delta^{13}C_c$ and $\delta^{13}C_N$ values of doy 189 compared to values of doy 188 is apparent, which seems not to apply for $\delta^{18}O$ isotopic signatures. For $\delta^{13}C_c$ comparable values were obtained at the same spruce forest site by relation of $^{13}CO_2$ fluxes measured by HREA with a cryo-trap sampling system and EC CO_2 fluxes in 2000 doy 174 [*Wichura et al.*, 2004], which showed a larger range from –15 to –38‰ VPDB [*Wichura et al.*, 2001]. In this study, the average $\delta^{13}C_c$ of 16 samples was –26.0(±3.2)‰ VPDB (Table 2b). While this average does not reflect the diurnal and seasonal variability, it is close to a value predicted for 50° N latitude by a global scale model presented by *Suits et al.* [2005]. Because during daytime, storage and isostorage changes and the difference between δ_c and δ_N are normally small, δ_c is the principle parameter that determines also the ecosystem and net ecosystem discrimination (Δ_e and Δ_E).

4.6. Ecosystem, net ecosystem and canopy isotope discrimination (Δ_e, Δ_E, Δ_{canopy}, Δ'_{canopy})

The determination of flux weighted isotopic signatures allowed the determination of related ecosystem discrimination by referencing them to the isotope ratio of source air according to (16) for ecosystem discrimination Δ_e and (17) for net ecosystem discrimination Δ_E. The measurements provide the temporal resolution necessary to study diurnal changes in Δ_e. The canopy isotope discrimination Δ_{canopy} is commonly defined according to (18) and was determined from the estimated canopy integrated and flux weighted isotopic signature δ_A of the net assimilation flux in this study as described in Section 3.3. Results for all three parameters of isotope discrimination are presented in Figure 7. The alternative definition of canopy isotope discrimination Δ'_{canopy} (19) was omitted from display in Figure 7, because its variation closely corresponds to Δ_{canopy} with a small positive offset.

While differences between the three parameters and temporal variation were found on doy 188, less variation is observed on doy 189. Differences between Δ_e and Δ_E in the first half of the day are due to small CO_2 storage and isostorage changes. Remarkable excursions to high $^{13}CO_2$ discrimination were observed in the morning of doy 188 when $CO^{18}O$ discrimination

seemed to be unaffected. Changes in $CO^{18}O$ discrimination were observed in the afternoon of doy 188, in which $^{13}CO_2$ discrimination seemed to be unaffected. Canopy isotope discrimination Δ_{canopy} seemed to be affected to a smaller extent by these variations. The average value of all measurements of $\Delta^{13}C_e$ in this study (Table 2a) closely corresponds to values about 19‰ reported for spruce forest (*Picea mariana, Miller*) [*Buchmann et al.,* 1998; *Buchmann and Kaplan,* 2001; *Flanagan et al.,* 1996; *Flanagan et al.,* 1997a].

The strong increase in $^{13}CO_2$ discrimination in the morning of doy 188 and in the afternoon of doy 187 correlates with increasing but relatively moderate vapor pressure deficit (vpd) measured at the canopy top (Figure 4b) and the formation of a more complete cloud covers just before the two measuring periods (doy 187, 15:20 CET, cumulus 6/8, doy 188, 9:35 CET, stratocumulus 8/8). This resulted in reduced global radiation R_g (Figure 4a) but high proportions of diffuse light. Diffuse light conditions are known to allow relatively high rates of photosynthesis [*Baldocchi,* 1997; *Law et al.,* 2002], which was also observed for the two measuring periods (Figure 5). High $^{13}CO_2$ isotopic discrimination at the leaf scale is related to small vpd, while contrary effects are observed for $CO^{18}O$ discrimination [*Flanagan et al.,* 1994]. The combination of small vpd, small photosynthetic photon flux density and cloudy skies was discussed to maximize $^{13}CO_2$ discrimination at the canopy scale [*Baldocchi and Bowling,* 2003]. Based on the results of these studies, the maxima in $^{13}CO_2$ discrimination are attributed to a combined effect of increased cloud cover on radiation and photosynthesis at low levels of vpd.

The absolute values and diurnal course of $\Delta^{13}C_{canopy}$ at doy 189 are very similar to branch bag measurements performed in a spruce forest (*Picea sitchensis, Bong.*) by *Wingate et al.* [2007] and results presented by *Bowling et al.* [2003a], which were also derived from inverting the flux partitioning method but based on isofluxes determined with the EC/flask method. The results support the finding, that Δ_{canopy} varies on diel timescales in response to environmental variables [*Bowling et al.,* 2003a]. Furthermore, simulation results for a deciduous forest [*Baldocchi and Bowling,* 2003; *Bowling et al.,* 2001] suggest that the greatest canopy discrimination against $^{13}CO_2$ occurs during the early morning and late afternoon.

The canopy discrimination against $CO^{18}O$ was modelled [*Flanagan et al.,* 1997b] and measured in branch bags [*Seibt et al.,* 2006]. Both studies suggest a significant change from canopy discrimination below 20‰ until around noon and a sudden increase to higher values in the afternoon. The few measured values presented in this study seem to resample this pattern.

The determination of Δ_e by HREA allows the analysis of diurnal patterns and processes that affect Δ_e on smaller time scales as discussed in this section. Based on (9) and (16), $^{13}CO_2$ and $CO^{18}O$ ecosystem discrimination Δ_e is directly determined from HREA whole-air samples with a footprint similar to EC. These measurements require that sampling and analysis can be performed with very high precision so that isotopic and mixing ratio differences can sufficiently be resolved. Scalar similarity in the turbulent exchange is assumed so far as necessary to establish flux weighting for $^{13}CO_2$ and $CO^{18}O$ isotope updraft and downdraft samples by selection of air samples that contribute most to the bulk CO_2 flux density. The ecosystem discrimination Δ_e is defined as discrimination in the atmospheric exchange above the canopy. This definition allows for a precise measurement of the source air from downdraft air samples. Whereas the net ecosystem discrimination Δ_E is defined at the ecosystem/atmosphere interface by including storage and isostorage changes below measurement height. Δ_E allows for even closer temporal correlation with respect to ecosystem processes. However, the definition of the interface and of the source air may be less precise for Δ_E than for Δ_e (Figure 1). Principally, recycling of CO_2 below measurement height should have the same influence on both terms if

the storage and isostorage are determined correctly. Recycling was discussed as a source of potential error with respect to measurements of δ_R [*da S. L. O'R. Sternberg*, 1989; *Yakir and da S. L. Sternberg*, 2000] and the original definition of Δ_e [*Buchmann et al.*, 1998; *Kaplan et al.*, 2002]. Δ_e or Δ_E defined and measured based on (16) and flux weighted isotopic signatures should not be biased by recycling processes after sufficient temporal integration. A statistical summary of the data displayed in Figure 6 and 7 is presented in Table 2. It also contains averages of canopy isotope discrimination according to the alternative definition of Δ'_{canopy} by (19) and averages of data presented in Figure 8, which is discussed in the following Section 4.7.

Average values of $\Delta^{13}C_e$ and $\Delta^{18}O_e$ ecosystem isotope discrimination show a systematic difference of 2.8‰, and respectively of 2.5‰ for $\Delta^{13}C_E$ and $\Delta^{18}O_E$. However, average canopy isotope discrimination $\Delta^{13}C'_{canopy}$ and $\Delta^{18}O'_{canopy}$ are nearly identical and closely agree with values specified in the literature for C3 vegetation, e.g. 17.8‰ [*Lloyd and Farquhar*, 1994] and without application of a correction according to (A2) in Appendix B also 16.8‰ [*Bakwin et al.*, 1998], 16.8-17.1‰ [*Bowling et al.*, 2001] 17.9‰ [*Bowling et al.*, 2003a]. The difference between net ecosystem discrimination Δ_E and canopy discrimination Δ'_{canopy} is due to the influence of the isotopic signatures δ_R of the daytime respiration flux, which is evaluated in the following section.

The systematic difference between the two definitions of canopy discrimination Δ'_{canopy} (19) and Δ_{canopy} (18) was on average 0.45(±0.12)‰ VPDB for $^{13}CO_2$ isotopes and 0.30(±0.07)‰ VPDB-CO_2 for $CO^{18}O$ isotopes. The different size of these offsets is related to the different isotopic scales involved for canopy air $\delta^{13}C_a$ and $\delta^{18}O_a$ values. The different definition of Δ_{canopy} and Δ'_{canopy} is a potential source of systematic error for the evaluation of the isotopic flux partitioning method. Equation (11) with the simplified definition for the canopy isotope discrimination by (18) should only be used if Δ_{canopy} was calculated vice versa from the inversion of the isotopic flux partitioning method. If independent data is used e.g. from modeling [*Bowling et al.*, 2001], then a correction should be applied as outlined in Appendix B. Currently the systematic nature of the error is still covered within the overall uncertainty of measurement methods and models (Figure 6 and Section 3.3). For a successful application of the isotopic flux partitioning method it is therefore of highest importance to better constrain δ_c, δ_N, Δ'_{canopy} and δ_R by precise measurements.

4.7. Isotopic disequilibrium ($\mathcal{D}$)

The comparison of the isotopic signatures δ_R in the respiration flux (Table 1) and δ_A in the net assimilation flux in Figure 8 show the presence of isotopic disequilibrium $\mathcal{D}$ in the beginning of the measurement period and equalization of isotopic signatures on doy 189. The isotopic flux partitioning method in principle must fails in periods when no isotopic disequilibrium can be observed [*Bowling et al.*, 2003a]. Hence, its application to results of doy 189 and of late afternoon at doy 187 and 188 would likely be subject to large errors and even the sign of partitioned fluxes would be uncertain. Only samples from the morning and early afternoon of doy 188 show a clear distinction of the isotopic signatures, which could provide a basis for isotopic flux partitioning. The isotopic disequilibrium observed on doy 187 and 188 is likely the result of changing meteorological conditions after rain and low rates of photosynthesis before noon of doy 187 and relatively high rates of photosynthesis during the daytime measuring periods. In studies by *Ekblad and Högberg* [2001], *Phillips and Gregg* [2001]and *Knohl et al.* [2005] it was observed that the time lag between changes in photosynthesis and the isotopic signature of soil respiration δ_R was only several days. This could explain, why two days after

the significant weather change we observe an equalization of $\delta^{13}C$ and $\delta^{18}O$ isotopic signatures. A similar two-day time lag in the response of nighttime δ_R to stomatal conductance was found in a study by *McDowell et al.* [2004] in a pine forest (*Pinus ponderosa, Douglas ex Laws. & C. Laws.*) after passage of a cold front. The analysis of the state of vertical coupling (Figure 4d) indicated well-coupled conditions throughout the canopy during midday sampling periods. In conjunction with the results presented in Figure 8, this finding confirms that the observed equalization of the isotopic disequilibrium is not the result of changes in the vertical air exchange. However, the isotopic signature $\delta^{13}C_A$ of the assimilation flux seemed to be slightly decreased in the early morning and late afternoon of doy 189, i.e. during the first and last sampling period, which coincided with the diagnosis of a decoupled sub-canopy space. Because the determination of δ_A from the mass balance (11) is based on the assumption of effectively mixed canopy air below measurement height, the δ_A and $\mathcal{D}$ values of these two measuring periods should be regarded as uncertain.

During doy 188, $\mathcal{D}^{13}C$ and $\mathcal{D}^{18}O$ had opposite sign, which means that daytime $\delta^{13}C_R$ is isotopically enriched while $\delta^{18}O_R$ is depleted compared to new assimilate ($\delta^{13}C_A$ and $\delta^{18}O_A$). This difference is also reflected in the average δ_A and daytime δ_R isotopic signatures and doy 188 disequilibria $\mathcal{D}$ in Table 2. The use of nighttime δ_R instead of daytime δ_R values in reference to daytime δ_A values would have led to an opposite assumption for several sampling periods. This demonstrates the importance of measuring the daytime isotopic signatures of the respiration flux. Considering the negative correlation of $\Delta^{13}C_{canopy}$ and positive correlation of $\Delta^{18}O_{canopy}$ to vpd as reported for measurements at the leaf scale [*Flanagan et al.*, 1994], then the different sign of $\mathcal{D}^{13}C$ and $\mathcal{D}^{18}O$ can be related to low levels of vpd on doy 187 and 188 after a rain period, which cause opposite excursions from the state of isotopic equilibrium, i.e. opposite offset of $\delta^{13}C_A$ from daytime $\delta^{13}C_R$ compared to $\delta^{18}O_A$ from daytime $\delta^{18}O_R$.

For doy 188, results in Figure 8 show a better agreement between nighttime δ_R and early morning and late afternoon δ_A than between nighttime δ_R and daytime δ_R. This finding indicates that diurnal variability in δ_R is linked to recent photosynthetic processes as reported in studies by *Bowling et al.* [2002], *Knohl et al.* [2005] and *Ogée et al.* [2004]. The diurnal variability of δ_R values in Figure 8 clearly contradicts results obtained at a boreal spruce forest (*Picea Abies, L.*) [*Betson et al.*, 2007], in which no variation of δ_R was found despite changes in meteorological conditions. For the investigation of the isotopic signatures in the atmospheric exchange of ecosystems, it is therefore important to quantify daytime δ_R values and their variability from the analysis of sub-canopy air samples.

The whole-air HREA sampling strategy combined with high precision isotope analysis was able to resolve even small $\delta^{18}O$ isotopic differences with good precision [*Ruppert et al.*, 2008] and thereby measure $CO^{18}O$ isotope fluxes. There might be a higher potential for the application of the isotopic flux partitioning method based on $\delta^{18}O$ due to often larger $\mathcal{D}^{18}O$ isotopic disequilibrium [*Yakir and da S. L. Sternberg*, 2000]. This finding is confirmed by results presented in Figure 8b for doy 188 and a larger $\delta^{18}O$ temporal variation visible in Figure 3d. However, the evaluation based on $\delta^{18}O$ isotopic signatures could be complicated, because ^{18}O isotopes in $CO^{18}O$ exchange and equilibrate with ^{18}O isotopes in leaf and soil water [*Cernusak et al.*, 2004; *Flanagan et al.*, 1994; *Riley et al.*, 2002; *Seibt et al.*, 2006].

4.8. Sensitivity of the isotopic flux partitioning method

The canopy discrimination determines the isotopic signature $\delta_A=\delta_a-\Delta_{canopy}$ of the net assimilation flux. Any systematic error therefore directly translates into the isotopic

disequilibrium $\mathit{D}=\delta_A-\delta_R$ (18). As denominator, the isotopic disequilibrium is the most sensitive factor of the isotopic flux partitioning method [*Ogée et al.*, 2004; *Phillips and Gregg*, 2001; *Zhang et al.*, 2006; *Zobitz et al.*, 2007] as can be seen from the combination of (10) and (11) resolved for F_A and F_R:

$$F_A = \frac{F_\delta - \delta_R F}{\delta_A - \delta_R}, \tag{23}$$

$$F_R = \frac{F_\delta - \delta_A F}{\delta_R - \delta_A}. \tag{24}$$

From the data presented in Section 4.6 we estimate that for partitioning based on $\delta^{13}C$ isotopic signatures the systematic relative error in Δ_{canopy} compared to Δ'_{canopy} would amount to 22% of the assimilation flux F_A with regard to an isotopic disequilibrium of $\mathit{D}^{13}C$=2‰, which is comparable to several values of doy 188 presented in Figure 8 and the value reported by *Bowling et al.* [2003a]. For partitioning based on $\delta^{18}O$ isotopic signatures the systematic relative error would amount to 7% of the assimilation flux F_A with regard to a larger isotopic disequilibrium of $\mathit{D}^{18}O$=4‰ VPDB-CO_2 (Table 2c). Even larger relative errors would apply to normally smaller respiration fluxes F_R determined by isotopic flux partitioning during daytime and in periods with smaller isotopic disequilibrium. This discussion shows how sensitive the isotopic flux partitioning method is in general to uncertainty in the isotopic signatures. The uncertainty scales directly with the isotopic disequilibrium D, which often might be smaller than 2‰ (Figure 8).

The sensitivity to D can be demonstrated in a third form of mixing line display, which relates flux weighted isotopic signatures to the actual size of the bulk CO_2 flux and isofluxes. Due to the correct flux weighting in this form of display, it is a true geometrical interpretation of the isotopic flux partitioning method (Figure 9). For land/ocean flux-partitioning based on global scale modeling *Randerson et al.* [2002] used a similar 'vector diagram', which links annual global carbon fluxes and $^{13}CO_2$ isotope fluxes. The similarity of this method to the display of HREA updraft and downdraft samples in a Miller-Tan plot (Figure 3) can be demonstrated by considering the definition of REA fluxes in (6) and (8) and equally scaling both axes and values of $\overline{C_\uparrow}$, $\overline{C_\downarrow}$, $\overline{\delta_\uparrow}\,\overline{C_\uparrow}$ and $\overline{\delta_\downarrow}\,\overline{C_\downarrow}$ in Figure 3 by the factor $b\sigma_w\rho_a$. This factor introduces flux-variance similarity in the REA method and is assumed to equal for bulk CO_2 eddy fluxes and $^{13}CO_2$ and $CO^{18}O$ eddy isofluxes under the assumption of scalar similarity. After this proportional scaling of both axes, the lines connecting updraft and downdraft air samples would represent the eddy flux F_c and eddy isoflux $\delta_c F_c$. For updraft and downdraft samples, the display in Miller-Tan plots is therefore conceptually similar to CO_2 NEE F and $^{13}CO_2$ and $CO^{18}O$ isofluxes F_δ displayed in Figure 9 as black solid lines. The study by *Randerson et al.* [2002] showed that also modeling of the global carbon balance and isotopic ocean/land flux partitioning is highly sensitive to the precision of the ecosystem discrimination. In their study a change of 0.19‰ in ^{13}C discrimination by C3 vegetation corresponded to a 0.37 Gt C/yr shift between land and ocean sinks.

In Figure 9, the isotopic disequilibrium D is equal to the difference of slopes, i.e. the angle, between the lines representing the net assimilation flux ($\delta_A F_A/F_A$) and the respiration flux ($\delta_R F_R/F_R$). Due to the different sign of $\mathit{D}^{13}C$ and $\mathit{D}^{18}O$ in the morning of doy 188, 9:51 CET (Figure 8), the orientation of the resulting shape of net and component fluxes in Figure 9b has

opposite orientation compared to Figure 9a. Figure 9 demonstrates that, if F_R and F_A were not determined from modeling but from isotopic flux partitioning, their magnitude would be highly sensitive to the size and precision of $\mathcal{D}$.

As example, Figure 10 displays the isotopic flux partitioning based on the assumption of a constant canopy isotope discrimination Δ'_{canopy} equal to an average value of 17.8‰ found in this study (Table 2). The gross flux components F_A and F_R of the NEE F were calculated from (23) and (24). The isotopic signature δ_A of the assimilation flux was determined by

$$\delta_A = \delta_a - \Delta'_{canopy} - \delta_a \Delta'_{canopy} + \Delta'^{2}_{canopy}. \quad (25)$$

This definition is according to Appendix B and identical to the term in brackets in (A1). The isotopic signature δ_a of the canopy source air of the assimilation flux was estimated from HREA updraft air samples ($\delta_a = \overline{\delta}_{\uparrow}$, Section 2.4). The isotopic signatureδ_R of the respiration flux was either measured or estimated as shown in Figure 8. In this example, the diurnal variability of the isotope discrimination displayed in Figure 7 is explicitly ignored. Consequently, F_A values show unrealistic high assimilation rates. During the measuring periods with prevailing isotopic disequilibrium (gray bars), in one case F_A is smaller than the NEE F so that F_R becomes negative. Although F_A includes the daytime foliar respiration, it should exhibit more negative values than the NEE F and F_R should always have positive values. Results from periods with a lack of isotopic disequilibrium (unfilled symbols) should be discarded, because the isotopic flux partitioning methods must fail under such conditions. The comparison of the estimated respiration fluxes F_R presented in Figure 10 and Figure 5 indicates, that isotopic flux partitioning yields highly variable and unrealistic respiration flux rates, when the isotopic disequilibrium $\mathcal{D}$ and the isotopic signature δ_A of the assimilation flux are determined from constant canopy isotope discrimination.

In principle, the isotopic flux partitioning method therefore requires also the precise and independent determination of the variable canopy isotope discrimination Δ_{canopy} or Δ'_{canopy}. By definition it must be flux weighted and integrated over the entire canopy. It is therefore of utmost importance to better constrain Δ'_{canopy} by multiple branch or leave level measurements, e.g. by enclosures or analysis of the isotopic content of fresh assimilate. A third option is the use of validated models for the canopy isotope discrimination [*Chen et al.*, 2006]. For the validation of such models, isotope flux measurements and the inverse isotopic flux partitioning method can provide canopy integrated and flux weighted estimates of Δ'_{canopy}, as demonstrated in this study.

4.9. Flux weighting of isotopic signatures

From Figure 2 it is evident that the isotopic signature determined from the vertical profile mixing line as slope in Miller-Tan plots (or intercept Keeling plots) depends on the selection of sampling heights and is weighted relative to the absolute concentration differences. Correct flux weighting like in Figure 9 is only accomplished when the concentration difference scales with the size of the flux, e.g. by dynamically sampling updrafts and downdrafts in HREA (Figure 3) or, with restriction to low vegetation, by application of the flux-gradient method for profile measurements above the canopy. This distinction is most obvious for the different relative weighting of δ_R in Figure 2d vs. Figure 9a, which is represented by the different length of the lines determined of sub-canopy air samples and of $\delta_R F_R/F_R$, respectively. Due to the exponential increase of CO_2 mixing ratios close to the forest floor, in Figure 2d an ‘integrated’ isotopic

signature determined from all samples as overall mixing relation would significantly by biased towards δ_R. On the other hand, the determination of δ_R from all samples would be more or less biased by samples from the top canopy, which to some degree represent the influence of photosynthesis and Δ'_{canopy} depending on sampling height.

Problems with incorrect concentration weighting may be augmented by significantly different footprints associated with concentration measurements compared to flux measurements as discussed by *Griffis et al.* [2007]. It is therefore essential, that the analysis of non-dynamic vertical profile samples in Miller-Tan plots (or Keeling plots) is restricted to simple two-source-mixing problems, for which they are well defined according to (4) or (3). Such conditions can often be assumed for the analysis of δ_R from vertical profiles during nighttime. Analysis of δ_R during daytime should use only data from below the photosynthetic active canopy (Section 4.1). In any case, it would be favorable to horizontally extend the sub-canopy air sampling to multiple locations in order to address ecosystem heterogeneity and match the footprint of δ_R measured in the sub-canopy space and very close to the ground to the footprint of EC flux measurements above the canopy. The investigation of the diurnal variability of isotopic signatures in the atmospheric exchange of ecosystems, including the application of the EC/flask method, requires a foundation on flux weighted mixing lines. Flux weighted isotopic signatures can be determined at the atmosphere/ecosystem boundary above the ecosystem directly from whole-air HREA sampling of updrafts and downdrafts, which correctly accounts for the dynamic and size of fluxes.

4.10. Strategies for continuous measurements

Especially above tall vegetation, any method for $^{13}CO_2$ or $CO^{18}O$ isotope flux measurements will require very high precision for the determination of small isotopic differences (Section 4.5). Methods for isotope measurements by TDL are currently developed and will likely further improve in precision and stability [*Griffis et al.*, 2004; *Griffis et al.*, 2005; *Saleska et al.*, 2006; *Zobitz et al.*, 2006; *Zobitz et al.*, 2007]. In order to achieve sufficiently precise and continuous measurements of the isotopic signature δ_c of the atmospheric turbulent exchange of $^{13}CO_2$ and $CO^{18}O$ above tall vegetation, we suggest combining whole-air HREA air sampling methods, which maximize isotopic differences [*Ruppert et al.*, 2008] and incorporate valuable information on the dynamic of the exchange (Figure 3), with continuous and differential TDL measurements of the bulk CO_2, $^{13}CO_2$ and $CO^{18}O$ isotope content of updraft and downdraft air from the turbulent atmospheric exchange above the ecosystem. The differential measurement might have the potential to partially alleviate problems with accuracy and stability of absolute TDL measurements.

As a first option, such measurements could be accomplished by combination of a whole-air REA sampling system with foil balloon bags as intermediate storage and continuous differential TDL isotope analysis at the experiment site. This would allow for long TDL measurement times and improved precision of TDL analysis. A second option is to apply conditional sampling methods to TDL $^{13}CO_2$ and $CO^{18}O$ data as suggested by *Thomas et al.* [2008] for CO_2 turbulent exchange measurements. While the implementation of the latter seems easier, it requires very high precision and stability of TDL measurements in order to resolve small fluctuations of the isotopic composition above tall vegetation. Based on the isotopic differences observed over the spruce forest at Waldstein/Weidenbrunnen, a measurement precision of 0.02‰ vs. VPDB for $\delta^{13}C$ or VPDB-CO_2 for $\delta^{18}O$ should be aspired. This is a tenth of the measurement precision currently achieved by TDL measurements [*Barbour et al.*, 2007; *Griffis et al.*, 2005; *Saleska et*

al., 2006; *Schaeffer et al.*, 2008]. Currently, such measurement precision can only be achieved by laboratory analysis, which requires the combination of whole-air sampling and high precision laboratory analysis as demonstrated by *Ruppert et al.* [2008].

5. Conclusions

Better understanding of the dynamic and absolute values of isotopic signatures in the atmospheric exchange of ecosystems is highly needed to constrain isotope partitioning approaches on very different scales, i.e. partitioning of the ocean and terrestrial carbon sink on global scale, dissolving the mixed isotopic signal of C3 and C4 vegetation on regional scale and partitioning of the assimilation and respiration fluxes at ecosystem scale. Isotopic signatures of fluxes and isotope discrimination are commonly determined at the leaf and branch scale [e.g. *Barbour et al.*, 2007; *Cernusak et al.*, 2004; *Flanagan et al.*, 1994; *Seibt et al.*, 2006; *Wingate et al.*, 2007] and are often needed for modeling at the global scale [*Bakwin et al.*, 1998; *Buchmann and Kaplan*, 2001; *Ciais et al.*, 1995a; *Hemming et al.*, 2005; *Kaplan et al.*, 2002; *Miller and Tans*, 2003; *Miller et al.*, 2003; *Randerson et al.*, 2002].

Conditional sampling methods can provide the basis for isotopic flux measurements directly at the ecosystem scale, also above tall vegetation. They have a footprint similar to the footprint of EC measurements and are therefore able to integrate small-scale heterogeneity in ecosystems. They allow determining canopy integrated and truly flux weighted isotopic signatures and ecosystem isotope discrimination Δ_e and Δ_E of forests on half-hourly timescales. The canopy isotope discrimination Δ_{canopy} of the net assimilation flux F_A can be estimated. The commonly used definition of Δ_{canopy} ignores certain higher order terms, which bears the risk of significant systematic error for isotopic flux partitioning of ecosystem assimilation and respiration fluxes. A more precise definition of the canopy isotope discrimination Δ'_{canopy} should therefore be used for either assuming or validating values of independently measured or modeled canopy isotope discrimination, which are indispensable for the isotopic flux partitioning method.

For the determination of isotopic signatures of the atmospheric turbulent exchange above forest ecosystems, high precision isotope analysis is required, which can be achieved by HREA whole-air sampling and IRMS laboratory analysis. However, the observed fast disappearance of isotopic disequilibrium $\mathcal{D}$ after significant changes in environmental conditions could limit the periods for successful application of the isotopic flux partitioning method.

High potential for achieving continuous and sufficiently precise measurements of isotopic signatures in the turbulent exchange above forests can be expected from the combination of the HREA sampling method with tunable diode laser (TDL) analysis of bulk CO_2 and its $^{13}CO_2$ and $CO^{18}O$ isotopes. More complete diurnal cycles of the updraft and downdraft air isotopic composition should be analyzed in Miller-Tan plots for typical patterns of atmospheric gas exchange processes.

For the determination of isotopic signatures from mixing line intercepts in Keeling plots (or slopes in Miller-Tan plots), the analysis of vertical profile air samples should be restricted to two source mixing problems in order to assure appropriate flux weighting, e.g. by limiting the evaluation to air samples from below the photosynthetic active canopy during daytime.

6. Acknowledgments

The authors wish to thank Dave R. Bowling and Willi A. Brand for essential comments and discussions on the realization of the high precision isotope HREA whole-air sampling technique by using foil balloon bag reservoirs. We acknowledge the technical support performed by

Teresa Bertolini, Johannes Olesch and the staff of the former Bayreuth Institute for Terrestrial Ecosystem Research (BITÖK) of the University of Bayreuth during the field experiment and the sample analysis performed by the staff of the Isotope- and Gas-Laboratories of the Max-Planck Institute for Biogeochemistry in Jena. This study was supported by the German Federal Ministry of Education and Research (PT BEO51-0339476 D).

7. References

Aranibar, J. N., J. A. Berry, W. J. Riley, D. E. Pataki, B. E. Law, and J. R. Ehleringer (2006), Combining meteorology, eddy fluxes, isotope measurements, and modeling to understand environmental controls of carbon isotope discrimination at the canopy scale, *Global Change Biol.*, *12*, 710-730.

Aubinet, M., A. Grelle, A. Ibrom, U. Rannik, J. Moncrieff, T. Foken, A. S. Kowalski, P. H. Martin, P. Berbigier, C. Bernhofer, R. Clement, J. Elbers, A. Granier, T. Grunwald, K. Morgenstern, K. Pilegaard, C. Rebmann, W. Snijders, R. Valentini, and T. Vesala (2000), Estimates of the annual net carbon and water exchange of forests: The EUROFLUX methodology, in *Advances in Ecological Research*, edited, pp. 113-175, Academic Press, San Diego.

Bakwin, P. S., P. P. Tans, J. W. C. White, and R. J. Andres (1998), Determination of the isotopic (C-13/C-12) discrimination by terrestrial biology from a global network of observations, *Glob. Biogeochem. Cycles*, *12*, 555-562.

Baldocchi, D. (1997), Measuring and modelling carbon dioxide and water vapour exchange over a temperate broad-leaved forest during the 1995 summer drought, *Plant, Cell and Environment*, *20*, 1108-1122.

Baldocchi, D., E. Falge, L. H. Gu, R. Olson, D. Hollinger, S. Running, P. Anthoni, C. Bernhofer, K. Davis, R. Evans, J. Fuentes, A. Goldstein, G. Katul, B. Law, X. H. Lee, Y. Malhi, T. Meyers, W. Munger, W. Oechel, K. T. P. U, K. Pilegaard, H. P. Schmid, R. Valentini, S. Verma, T. Vesala, K. Wilson, and S. Wofsy (2001), FLUXNET: A new tool to study the temporal and spatial variability of ecosystem-scale carbon dioxide, water vapor, and energy flux densities, *Bull. Amer. Met. Soc.*, *82*, 2415-2434.

Baldocchi, D. D., B. B. Hicks, and T. P. Meyers (1988), Measuring biosphere-atmosphere exchanges of biologically related gases with micrometeorological methods, *Ecology*, *69*, 1331-1340.

Baldocchi, D. D., and D. R. Bowling (2003), Modelling the discrimination of $^{13}CO_2$ above and within a temperate broad-leaved forest canopy on hourly to seasonal time scales, *Plant, Cell and Environment*, *26*, 231-244.

Barbour, M. M., G. D. Farquhar, D. T. Hanson, C. P. Bickford, H. Powers, and N. G. McDowell (2007), A new measurement technique reveals temporal variation in $\delta^{18}O$ of leaf-respired CO_2, *Plant, Cell and Environment*, *30*, 456-468.

Betson, N. R., S. G. Göttlicher, M. Hall, G. Wallin, A. Richter, and P. Högberg (2007), No diurnal variation in rate or carbon isotope composition of soil respiration in a boreal forest, *Tree Physiol.*, *27*, 749-756.

Bowling, D. R., D. D. Baldocchi, and R. K. Monson (1999a), Dynamics of isotopic exchange of carbon dioxide in a Tennessee deciduous forest, *Glob. Biogeochem. Cycles*, *13*, 903-922.

Bowling, D. R., A. C. Delany, A. A. Turnipseed, D. D. Baldocchi, and R. K. Monson (1999b), Modification of the relaxed eddy accumulation technique to maximize measured scalar mixing ratio differences in updrafts and downdrafts, *J. Geophys. Res.*, *104*, (D8), 9121-9133.

Bowling, D. R., P. P. Tans, and R. K. Monson (2001), Partitioning net ecosystem carbon exchange with isotopic fluxes of CO_2, *Global Change Biol.*, *7*, 127-145.

Bowling, D. R., N. G. McDowell, B. J. Bond, B. E. Law, and J. R. Ehleringer (2002), ^{13}C content of ecosystem respiration is linked to precipitation and vapor pressure deficit, *Oecologia*, *131*, 113-124.

Bowling, D. R., D. E. Pataki, and J. R. Ehleringer (2003a), Critical evaluation of micrometeorological methods for measuring ecosystem-atmosphere isotopic exchange of CO_2, *Agric. For. Meteorol.*, *116*, 159-179.

Bowling, D. R., S. D. Sargent, B. D. Tanner, and J. R. Ehleringer (2003b), Tunable diode laser absorption spectroscopy for stable isotope sudies of ecosystem-atmosphere CO_2 exchange, *Agric. For. Meteorol.*, *118*, 1-19.

Buchmann, N., J. R. Brooks, L. B. Flanagan, and J. R. Ehleringer (1998), Carbon isotope discrimination of terrestrial ecosystems, in *Stable Isotopes and the Integration of Biological, Ecological and Geochemical Processes*, edited by H. Griffiths, et al., pp. 203-221, BIOS Scientific Publishers Ltd., Oxford.

Buchmann, N., and J. O. Kaplan (2001), Carbon isotope discrimination of terrestrial ecosystems - how well do observed and modeled results match?, in *Global biogeochemical cycles in the climate system*, edited by E. D. Schulze, et al., pp. 253-266, Academic Press, San Diego.

Businger, J. A. (1986), Evaluation of the accuracy with which dry deposition can be measured with current micrometeorological techniques, *J. Climate Appl. Meteor.*, *25*, 1100-1124.

Businger, J. A., and S. P. Oncley (1990), Flux Measurement with conditional sampling, *J. Atmos. Ocean. Tech.*, *7*, 349-352.

Cernusak, L. A., G. D. Farquhar, S. C. Wong, and H. Stuart-Williams (2004), Measurement and interpretation of the oxygen isotope composition of carbon dioxide respired by leaves in the dark, *Plant Physiol.*, *136*, 3350-3363.

Chen, B., J. M. Chen, L. Huang, and P. P. Tans (2006), Modeling dynamics of stable carbon isotopic exchange between a boreal forest ecosystem and the atmosphere, *Global Change Biol.*, *12*, 1842-1867.

Ciais, P., P. P. Tans, M. Trolier, J. W. C. White, and R. J. Francey (1995a), A Large Northern hemisphere terrestrial CO_2 sink indicated by the $^{13}C/^{12}C$ ratio of atmospheric CO_2, *Science*, *269*, 1098-1102.

Ciais, P., P. P. Tans, J. W. C. White, M. Trolier, R. J. Francey, J. A. Berry, D. R. Randall, P. Sellers, J. G. Collatz, and D. S. Schimel (1995b), Partitioning of ocean and land uptake of CO_2 as inferred by $\delta^{13}C$ measurements from NOAAA Climate Monitoring and Diagnostics Laboratory Global Air Sampling Netweork, *J. Geophys. Res.*, *100*, (D), 5051-5070.

da S. L. O'R. Sternberg, L. (1989), A model to estimate carbon dioxide recycling in forests using $^{13}C/^{12}C$ ratios and concentrations of ambient carbon dioxide, *Agricultural & Forest Meteorology*, *48*, 163-173.

Delany, A. C., S. P. Oncley, J. A. Businger, and E. Sievering (1991), Adapting the conditional sampling concept for a range of different chemical species, paper presented at Seventh symposium on meteorological observations and instruments, American Meteorological Society, Boston, New Orleans, La., 14-18 January 1991.

Denmead, O. T., and E. F. Bradley (1985), Flux-gradient relationships in a forest canopy, in *The Forest-Atmosphere Interaction*, edited by B. A. Hutchison and B. B. Hicks, pp. 421-442, D. Reidel Publ. Comp., Dordrecht, Boston, London.

Desjardins, R. L. (1977), Description and evaluation of a sensible heat flux detector, *Boundary-Layer Meteorol., 11*, 147-154.

Ekblad, A., and P. Högberg (2001), Natural abundance of C-13 in CO_2 respired from forest soils reveals speed of link between tree photosynthesis and root respiration, *Oecologia, 127*, 305-308.

Farquhar, G. D., J. R. Ehleringer, and K. T. Hubick (1989), Carbon isotope discrimination and photosynthesis, *Annu. Rev. Plant Physiol. Plant Mol. Biol., 40*, 503-537.

Flanagan, L. B., S. L. Phillips, J. R. Ehleringer, J. Lloyd, and G. D. Farquhar (1994), Effect of changes in leaf water oxygen isotopic composition on discrimination against $C^{18}O^{16}O$ during photosynthetic gas-exchange, *Austr. J. Plant Physiol., 21*, 221-234.

Flanagan, L. B., J. R. Brooks, G. T. Varney, S. C. Berry, and J. R. Ehleringer (1996), Carbon isotope discrimination during photosynthesis and the isotope ratio of respired CO_2 in boreal forest ecosystems, *Glob. Biogeochem. Cycles, 10*, 629-640.

Flanagan, L. B., J. R. Brooks, and J. R. Ehleringer (1997a), Photosynthesis and carbon isotope discrimination in boreal forest ecosystems: A comparison of functional characteristics in plants from three mature forest types, *J. Geophys. Res., 102*, (D), 28861-28869.

Flanagan, L. B., J. R. Brooks, G. T. Varney, and J. R. Ehleringer (1997b), Discrimination against $C^{18}O^{16}O$ during photosynthesis and the oxygen isotope ratio of respired CO_2 in boreal forest ecosystems, *Glob. Biogeochem. Cycles, 11*, 83-98.

Foken, T., M. Göckede, M. Mauder, L. Mahrt, B. Amiro, and W. Munger (2004), Post-field data qualtiy control, in *Handbook of Micrometeorology*, edited by X. Lee, et al., pp. 181-208, Kluwer, Dordrecht.

Fung, I., C. B. Field, J. A. Berry, M. V. Thompson, J. T. Randerson, C. M. Malmstrom, P. M. Vitousek, G. J. Collatz, P. J. Sellers, D. A. Randall, A. S. Denning, F. Badeck, and J. John (1997), Carbon 13 exchanges between the atmosphere and biosphere, *Glob. Biogeochem. Cycles, 11*, 507-533.

Gerstberger, P., T. Foken, and K. Kalbitz (2004), The Lehstenbach and Steinkreuz Catchments in NE Bavaria, Germany, in *Biogeochemistry of Forested Catchments in a Changing Environment: A German case study*, edited by E. Matzner, pp. 15-41, Springer, Berlin.

Göckede, M., T. Foken, M. Aubinet, M. Aurela, J. Banza, C. Bernhofer, J. M. Bonnefond, Y. Brunet, A. Carrara, R. Clement, E. Dellwik, J. Elbers, W. Eugster, J. Fuhrer, A. Granier, T. Grünwald, B. Heinesch, I. A. Janssens, A. Knohl, R. Koeble, T. Laurila, B. Longdoz, G. Manca, M. Marek, T. Markkanen, J. Mateus, G. Matteucci, M. Mauder, M. Migliavacca, S. Minerbi, J. Moncrieff, L. Montagnani, E. Moors, J. M. Ourcival, D. Papale, J. Pereira, K. Pilegaard, G. Pita, S. Rambal, C. Rebmann, A. Rodrigues, E. Rotenberg, M. J. Sanz, P. Sedlak, G. Seufert, L. Siebicke, J. F. Soussana, R. Valentini, T. Vesala, H. Verbeeck, and D. Yakir (2008), Quality control of CarboEurope flux data - Part 1: Coupling footprint analyses with flux data quality assessment to evaluate sites in forest ecosystems, *Biogeosciences, 5*, 433-450.

Grace, J., J. Lloyd, J. McIntyre, A. C. Miranda, P. Meir, H. S. Miranda, C. Nobre, J. Moncrieff, J. Massheder, Y. Mahli, I. Wright, and J. Gash (1995), Carbon dioxide uptake by an undisturbed tropical rain forest in southwest Amazonia, *Science, 270*, 778-780.

Granier, A., M. Reichstein, N. Bréda, I. A. Janssens, E. Falge, P. Ciais, T. Grünwald, M. Aubinet, P. Berbigier, C. Bernhofer, N. Buchmann, O. Facini, G. Grassi, B. Heinesch, H. Ilvesniemi, P. Keronen, A. Knohl, B. Köstner, F. Lagergren, A. Lindroth, B. Longdoz, D. Loustau, J. Mateus, L. Montagnani, C. Nys, E. Moors, D. Papale, M. Peiffer, K. Pilegaard, G. Pita, J. Pumpanen, S. Rambal, C. Rebmann, A. Rodrigues, G. Seufert, J. Tenhunen, T. Vesala, and Q. Wang (2007), Evidence for soil water control on carbon and water dynamics in European forests during the extremely dry year: 2003, *Agric. For. Meteorol., 143*, 123-145.

Griffis, T. J., J. M. Baker, S. D. Sargent, B. D. Tanner, and J. Zhang (2004), Measuring field-scale isotopic CO_2 fluxes with tunable diode laser absorption spectroscopy and micrometeorological techniques, *Agric. For. Meteorol., 124*, 15-29.

Griffis, T. J., X. Lee, J. M. Baker, S. D. Sargent, and J. Y. King (2005), Feasibility of quantifying ecosystem-atmosphere $C^{18}O^{16}O$ exchange using laser spectroscopy and the flux-gradient method, *Agric. For. Meteorol., 135*, 44-60.

Griffis, T. J., J. Zhang, J. M. Baker, N. Kljun, and K. Billmark (2007), Determining carbon isotope signatures from micrometeorological measurements: Implications for studying biosphere-atmosphere exchange processes, *Boundary-Layer Meteorol., 123*, 295-316.

Hemming, D., D. Yakir, P. Ambus, M. Aurela, C. Besson, K. Black, N. Buchmann, R. Burlett, A. Cescatti, R. Clement, P. Gross, A. Granier, T. Grunwald, K. Havrankova, D. Janous, I. A. Janssens, A. Knohl, B. K. Ostner, A. Kowalski, T. Laurila, C. Mata, B. Marcolla, G. Matteucci, J. Moncrieff, E. J. Moors, B. Osborne, J. S. Pereira, M. Pihlatie, K. Pilegaard, F. Ponti, Z. Rosova, F. Rossi, A. Scartazza, and T. Vesala (2005), Pan-European $\delta^{13}C$ values of air and organic matter from forest ecosystems, *Global Change Biol., 11*, 1065-1093.

Kaplan, J. O., I. C. Prentice, and N. Buchmann (2002), The stable carbon isotope composition of the terrestrial biosphere: Modeling at scales from the leaf to the globe, *Glob. Biogeochem. Cycles, 16*, 1060, doi:10.1029/2001GB001403.

Keeling, C. D. (1958), The concentration and isotopic abundances of atmospheric carbon dioxide in rural areas, *Geochim. Cosmochim. Acta, 13*, 322-334.

Knohl, A., and N. Buchmann (2005), Partitioning the net CO_2 flux of a deciduous forest into respiration and assimilation using stable carbon isotopes, *Glob. Biogeochem. Cycles*, *19*.

Knohl, A., R. A. Werner, W. A. Brand, and N. Buchmann (2005), Short-term variations in $\delta^{13}C$ of ecosystem respiration reveals link between assimilation and respiration in a deciduous forest, *Oecologia*, *142*, 70-82.

Lai, C.-T., J. R. Ehleringer, P. Tans, S. C. Wofsy, S. P. Urbanski, and D. Y. Hollinger (2004), Estimating photosynthetic ^{13}C discrimination in terrestrial CO_2 exchange from canopy to regional scales, *Glob. Biogeochem. Cycles*, *18*, GB1041, doi:10.1029/2003GB002148.

Law, B. E., E. Falge, L. Gu, D. D. Baldocchi, P. Bakwin, P. Berbigier, K. Davis, A. J. Dolman, M. Falk, J. D. Fuentes, A. Goldstein, A. Granier, A. Grelle, D. Hollinger, I. A. Janssens, P. Jarvis, N. O. Jensen, G. Katul, Y. Mahli, G. Matteucci, T. Meyers, R. Monson, W. Munger, W. Oechel, R. Olson, K. Pilegaard, K. T. Paw, H. Thorgeirsson, R. Valentini, S. Verma, T. Vesala, K. Wilson, and S. Wofsy (2002), Environmental controls over carbon dioxide and water vapor exchange of terrestrial vegetation, *Agric. For. Meteorol.*, *113*, 97-120.

Lloyd, J., and G. D. Farquhar (1994), ^{13}C discrimination during CO_2 assimilation by the terrestrial biosphere, *Oecologia*, *99*, 201-215.

Lloyd, J., and J. A. Taylor (1994), On the temperature dependence of soil respiration, *Funct. Ecol.*, *8*, 315-323.

Lloyd, J., B. Kruijt, D. Y. Hollinger, J. Grace, R. J. Francey, S. C. Wong, F. M. Kelliher, A. C. Miranda, G. D. Farquhar, J. H. C. Gash, N. N. Vygodskaya, I. R. Wright, H. S. Miranda, and E. D. Schulze (1996), Vegetation effects on the isotopic composition of atmospheric CO_2 at local and regional scales: Theoretical aspects and a comparison between rain forest in Amazonia and a Boreal Forest in Siberia, *Austr. J. Plant Physiol.*, *23*, 371-399.

McDowell, N. G., D. R. Bowling, B. J. Bond, J. Irvine, B. E. Law, P. Anthoni, and J. R. Ehleringer (2004), Response of the carbon isotopic content of ecosystem, leaf, and soil respiration to meteorological and physiological driving factors in a Pinus ponderosa ecosystem, *Glob. Biogeochem. Cycles*, *18*, GB1013, doi:10.1029/2003GB002049.

Miller, J. B., and P. P. Tans (2003), Calculating isotopic fractionation from atmospheric measurements at various scales, *Tellus, Series B: Chemical and Physical Meteorology*, *55*, 207-214.

Miller, J. B., P. P. Tans, J. W. C. White, T. J. Conway, and B. W. Vaughn (2003), The atmospheric signal of terrestrial carbon isotopic discrimination and its implication for partitioning carbon fluxes, *Tellus, Series B: Chemical and Physical Meteorology*, *55*, 197-206.

Ogée, J., P. Peylin, P. Ciais, T. Bariac, Y. Brunet, P. Berbigier, C. Roche, P. Richard, G. Bardoux, and J. M. Bonnefond (2003), Partitioning net ecosystem carbon exchange into net assimilation and respiration using $^{13}CO_2$ measurements: A cost-effective sampling strategy, *Glob. Biogeochem. Cycles*, *17*, 1070, doi:10.1029/2002GB001995.

Ogée, J., P. Peylin, M. Cuntz, T. Bariac, Y. Brunet, P. Berbigier, P. Richard, and P. Ciais (2004), Partitioning net ecosystem carbon exchange into net assimilation and respiration with canopy-scale isotopic measurements: An error propagation analysis with $^{13}CO_2$ and $CO^{18}O$ data, *Glob. Biogeochem. Cycles*, *18*, GB2019, doi:10.1029/2003GB002166.

Oncley, S. P., A. C. Delany, T. W. Horst, and P. P. Tans (1993), Verification of flux measurement using relaxed eddy accumulation, *Atmos. Environ.*, *27A*, 2417-2426.

Pataki, D. E., J. R. Ehleringer, L. B. Flanagan, D. Yakir, D. R. Bowling, C. J. Still, N. Buchmann, J. O. Kaplan, and J. A. Berry (2003), The application and interpretation of Keeling plots in terrestrial carbon cycle research, *Glob. Biogeochem. Cycles*, *17*, 1022, doi:10.1029/2001GB001850.

Pattey, E., R. L. Desjardins, and P. Rochette (1993), Accuracy of the relaxed eddy-accumulation technique, evaluated using CO_2 flux measurements, *Boundary-Layer Meteorol.*, *66*, 341-355.

Pattey, E., G. Edwards, I. B. Strachan, R. L. Desjardins, S. Kaharabata, and C. Wagner Riddle (2006), Towards standards for measuring greenhouse gas fluxes from agricultural fields using instrumented towers, *Canadian Journal of Soil Science*, *86*, 373-400.

Phillips, D. L., and J. W. Gregg (2001), Uncertainty in source partitioning using stable isotopes, *Oecologia*, *127*, 171-179.

Porporato, A. (1999), Conditional sampling and state space reconstruction, *Experiments in Fluids*, *26*, 441-450.

Randerson, J. T., G. J. Collatz, J. E. Fessenden, A. D. Munoz, C. J. Still, J. A. Berry, I. Y. Fung, N. Suits, and A. S. Denning (2002), A possible global covariance between terrestrial gross primary production and C-13 discrimination: Consequences for the atmospheric C-13 budget and its response to ENSO, *Glob. Biogeochem. Cycles*, *16*, 1136, doi:10.1029/2001GB001845.

Reichstein, M., E. Falge, D. Baldocchi, D. Papale, M. Aubinet, P. Berbigier, C. Bernhofer, N. Buchmann, T. Gilmanov, A. Granier, T. Grünwald, K. Havrankova, H. Ilvesniemi, D. Janous, A. Knohl, T. Laurila, A. Lohila, D. Loustau, G. Matteucci, T. Meyers, F. Miglietta, J.-M. Ourcival, J. Pumpanen, S. Rambal, E. Rotenberg, M. Sanz, J. Tenhunen, G. Seufert, F. Vaccari, T. Vesala, D. Yakir, and R. Valentini (2005), On the separation of net ecosystem exchange into assimilation and ecosystem respiration: review and improved algorithm, *Global Change Biol.*, *11*, 1424–1439, doi:10.1111/j.1365-2486.2005.001002.x.

Reichstein, M., P. Ciais, D. Papale, R. Valentini, S. Running, N. Viovy, W. Cramer, A. Granier, J. Ogée, V. Allard, M. Aubinet, C. Bernhofer, N. Buchmann, A. Carrara, T. Grünwald, M. Heimann, B. Heinesch, A. Knohl, W. Kutsch, D. Loustau, G. Manca, G. Matteucci, F. Miglietta, J. M. Ourcival, K. Pilegaard, J. Pumpanen, S. Rambal, S. Schaphoff, G. Seufert, J. F. Soussana, M. J. Sanz, T. Vesala, and M. Zhao (2007), Reduction of ecosystem productivity and respiration during the European summer 2003 climate anomaly: A joint flux tower, remote sensing and modelling analysis, *Global Change Biol.*, *13*, 634-651.

Riley, W. J., C. J. Still, M. S. Torn, and J. A. Berry (2002), A mechanistic model of $H_2{}^{18}O$ and $CO^{18}O$ fluxes between ecosystems and the atmosphere: Model description and sensitivity analyses, *Glob. Biogeochem. Cycles*, *16*, 1095, doi:10.1029/2002GB001878.

Ruppert, J., and T. Foken (2005), Messung turbulenter Flüsse von Kohlendioxid und stabilem Kohlenstoffisotop ^{13}C über Pflanzenbeständen mit Hilfe der Relaxed Eddy Accumulation Methode, in Klimatologische und mikrometeorologische Froschungen im Rahmen des Bayreuther Institutes für terrestrische Ökosystemforschung (BITÖK) 1998 - 2004, edited by T. Foken, *Arbeitsergebnisse 29*, 81-104, Universität Bayreuth, Abt. Mikrometeorologie, Bayreuth, Germany. Print, ISSN 1614-8916.

Ruppert, J., M. Mauder, C. Thomas, and J. Lüers (2006a), Innovative gap-filling strategy for annual sums of CO_2 net ecosystem exchange, *Agric. For. Meteorol., 138*, 5-18, doi:10.1016/j.agrformet.2006.03.003.

Ruppert, J., C. Thomas, and T. Foken (2006b), Scalar similarity for relaxed eddy accumulation methods, *Boundary-Layer Meteorol., 120*, 39-63.

Ruppert, J., W. A. Brand, N. Buchmann, and T. Foken (2008), Whole-air relaxed eddy accumulation for the measurement of isotope and trace-gas fluxes, *J. Geophys. Res.*, prepared manuscript.

Saleska, S. R., J. H. Shorter, S. Herndon, R. Jiménez, J. B. McManus, J. W. Munger, D. D. Nelson, and M. S. Zahniser (2006), What are the instrumentation requirements for measuring the isotopic composition of net ecosystem exchange of CO_2 using eddy covariance methods?, *Isotopes in Environmental and Health Studies*, *42*, 115-133.

Schaeffer, S. M., J. B. Miller, B. H. Vaughn, J. W. C. White, and D. R. Bowling (2008), Long-term field performance of a tunable diode laser absorption spectrometer for analysis of carbon isotopes of CO2 in forest air, *Atmos. Chem. Phys. Discuss., 8*, 9531-9568, SRef-ID:1680-7375/acpd/2008-8-9531.

Seibt, U., L. Wingate, J. A. Berry, and J. Lloyd (2006), Non-steady state effects in diurnal ^{18}O discrimination by Picea sitchensis branches in the field, *Plant, Cell and Environment*, *29*, 928-939.

Sharp, R., M. Matthews, and J. Boyer (1984), Kok effect and the quantum yield of photosynthesis: light partially inhibits dark respiration, *Plant Physiol., 75*, 95-101.

Staudt, K., and T. Foken (2007), Documentation of reference data for the experimental areas of the Bayreuth Centre for Ecology and Environmental Research (BayCEER) at the Waldstein site, *Arbeitsergebnisse 35*, 37 pp, Universität Bayreuth, Abt. Mikrometeorologie, Bayreuth, Germany. Print, ISSN 1614-8916.

Suits, N. S., A. S. Denning, J. A. Berry, C. J. Still, J. Kaduk, J. B. Miller, and I. T. Baker (2005), Simulation of carbon isotope discrimination of the terrestrial biosphere, *Glob. Biogeochem. Cycles*, *19*, 1-15.

Thomas, C., J. Ruppert, J. Lüers, J. Schröter, J. C. Mayer, and T. Bertolini (2004), Documentation of the WALDATEM-2003 experiment, 28.4.-3.8.2003, *Arbeitsergebnisse 24*, 59 pp, Universität Bayreuth, Abt. Mikrometeorologie, Bayreuth, Germany. Print, ISSN 1614-8916.

Thomas, C., and T. Foken (2007a), Organised Motion in a Tall Spruce Canopy: Temporal Scales, Structure Spacing and Terrain Effects, *Boundary-Layer Meteorol., 122*, 123-147.

Thomas, C., and T. Foken (2007b), Flux contribution of coherent structures and its implications for the exchange of energy and matter in a tall spruce canopy, *Boundary-Layer Meteorol., 123*, 317-337.

Thomas, C., J. G. Martin, M. Göckede, M. B. Siqueira, T. Foken, B. E. Law, H. W. Loescher, and G. Katul (2008), Estimating daytime ecosystem respiration from conditional sampling methods applied to multi-scalar high frequency turbulence time series, *Agric. For. Meteorol., 148*, 1210-1229, doi:10.1016/j.agrformet.2008.03.002.

Werner, R. A., and W. A. Brand (2001), Referencing strategies and techniques in stable isotope ratio analysis, *Rapid Commun. Mass Spectrom., 15*, 501-519.

Werner, R. A., M. Rothe, and W. A. Brand (2001), Extraction of CO_2 from air samples for isotopic analysis and limits to ultra high precision delta O-18 determination in CO_2 gas, *Rapid Commun. Mass Spectrom., 15*, 2152-2167.

Wichura, B., N. Buchmann, and T. Foken (2000), Fluxes of the stable carbon isotope ^{13}C above a spruce forest measured by hyperbolic relaxed eddy accumulation method, paper presented at 14th Symposium on Boundary Layers and Turbulence, American Meteorological Society, Boston, Aspen, Colorado, 7-11 August 2000.

Wichura, B., N. Buchmann, T. Foken, A. Mangold, G. Heinz, and C. Rebmann (2001), Pools und Flüsse des stabilen Kohlenstoffisotopes ^{13}C zwischen Boden, Vegetation und Atmosphäre in verschiedenen Planzengemeinschaften des Fichtelgebirges, *Bayreuther Forum Ökologie (bfö)*, *84*, 123-153.

Wichura, B., J. Ruppert, A. C. Delany, N. Buchmann, and T. Foken (2004), Structure of carbon dioxide exchange processes above a spruce forest, in *Biogeochemistry of Forested Catchments in a Changing Environment: A german case study*, edited by E. Matzner, pp. 161-176, Springer, Berlin.

Wingate, L., U. Seibt, J. B. Moncrieff, P. G. Jarvis, and J. Lloyd (2007), Variations in ^{13}C discrimination during CO_2 exchange by Picea sitchensis branches in the field, *Plant, Cell and Environment*, *30*, 600-616.

Yakir, D., and X.-F. Wang (1996), Fluxes of CO_2 and water between terrestrial vegetation and the atmosphere estimated from isotope measurements, *Nature*, *380*, 515-517.

Yakir, D., and L. da S. L. Sternberg (2000), The use of stable isotopes to study ecosystem gas exchange, *Oecologia*, *123*, 297-311.

Zhang, J., T. J. Griffis, and J. M. Baker (2006), Using continuous stable isotope measurements to partition net ecosystem CO_2 exchange, *Plant, Cell and Environment*, *29*, 483-496.

Zobitz, J. M., J. P. Keener, H. Schnyder, and D. R. Bowling (2006), Sensitivity analysis and quantification of uncertainty for isotopic mixing relationships in carbon cycle research, *Agric. For. Meteorol., 136*, 56-75, doi:10.1016/j.agrformet.2006.01.003.

Zobitz, J. M., S. P. Burns, J. Ogée, M. Reichstein, and D. R. Bowling (2007), Partitioning net ecosystem exchange of CO_2: A comparison of a Bayesian/isotope approach to environmental regression methods, *J. Geophys. Res., 112*, G03013, doi:10.1029/2006JG000282.

8. Appendix

8.1. Appendix A: Nomenclature and Abbreviations

Symbols	Description, unit
^{13}C	here: ^{13}C isotopes of CO_2, i.e. $^{13}CO_2$ In combination with the δ symbol ^{13}C denotes the $^{13}C/^{12}C$ isotope ratio of CO_2 in δ-notation, ‰ VPDB.
^{18}O	here: ^{18}O isotope of CO_2, i.e. $CO^{18}O$ In combination with the δ symbol ^{18}O denotes the $^{18}O/^{16}O$ isotope ratio of CO_2 in δ-notation, ‰ VPDB-CO_2.
b	proportionality factor of the REA flux equation
b_{CO2}	proportionality factor of the REA flux equation derived from CO_2 EC flux measurements and measured or modeled CO_2 concentration in REA updraft and downdraft samples
c	scalar concentration
$\overline{c_\uparrow}$	updraft air average scalar concentration
$\overline{c_\downarrow}$	downdraft air average scalar concentration
C	bulk CO_2 concentration as mixing ratio, µmol mol^{-1} The term 'bulk CO_2' is used to refer to the sum of $^{12}C^{16}O^{16}O$, $^{13}C^{16}O^{16}O$, $^{12}C^{16}O^{18}O$ and all other CO_2 isotopes.
C_a	air bulk CO_2 concentration at a certain measurement height as mixing ratio, µmol mol^{-1}
C_B	bulk CO_2 concentration of lower boundary layer air as mixing ratio, µmol mol^{-1}
$\overline{C_\uparrow}$	updraft air average CO_2 mixing ratio from REA sampling, µmol mol^{-1}
$\overline{C_\downarrow}$	downdraft air average CO_2 mixing ratio from REA sampling, µmol mol^{-1}
d	displacement height, m
$\mathcal{D}$	isotopic disequilibrium between assimilation and respiration fluxes, $\mathcal{D}=\delta_A-\delta_R$, [e.g. *Zobitz, et al.*, 2007]
F	net ecosystem exchange (NEE) at the ecosystem/atmosphere interface, i.e. flux density of CO_2, including the storage change below EC measurement height, µmol m^{-2} s^{-1} This usage of F corresponds to *Bowling et al.* [2003a] and *Zobitz, et al.* [2007]. In *Ruppert et al.* [2006b] F_C is used for NEE of CO_2 including the storage change component.
F_A	assimilation flux including daytime foliar respiration flux ("net canopy exchange")
F_R	respiration flux without daytime foliar respiration flux
F_c	eddy flux, here i.e. turbulent eddy flux density of bulk CO_2, excluding the storage change component, µmol m^{-2} s^{-1} This usage of F_c corresponds to *Bowling et al.* [2003a]. In *Ruppert et al.* [2006b] F_C is used for NEE of CO_2 including the storage change component and F_E is used for the turbulent eddy flux density.
F_S	storage flux, i.e. storage change of bulk CO_2 below measurement height expressed as storage flux density, µmol m^{-2} s^{-1}
F_δ	isoflux, i.e. net isotopic flux density including the isostorage and expressed in δ-notation, µmol m^{-2} s^{-1} ‰, see definition in *Bowling et al.* [2003a]
$F_{\delta 13C}=F_\delta\ ^{13}CO_2$	$^{13}CO_2$ isoflux in δ-notation, µmol m^{-2} s^{-1} ‰ VPDB
$F_{\delta 18O}=F_\delta\ CO^{18}O$	$CO^{18}O$ isoflux in δ-notation, µmol m^{-2} s^{-1} ‰ VPDB-CO_2
h_c	canopy height, m
H_w	wind deadband size used for sample segregation in REA, [e.g. *Ruppert et al.*, 2008]
H_h	hyperbolic deadband size used for sample segregation in HREA, [e.g. *Ruppert et al.*, 2008]
L	Obukhov length, m
p	air pressure, hPa
R	molar isotope ratio of heavy to light isotope (e.g. $^{13}C/^{12}C$)
R^2	coefficient of determination
R_cF_c	turbulent isotope flux density, excluding the storage change component, µmol m^{-2} s^{-1}, i.e. the turbulent absolute flux of a certain isotope, $R_cF_c \neq \delta_cF_c$
t	time, s

T	temperature, K or °C as specified
vpd	vapour pressure deficit, hPa
w	vertical wind velocity, m s^{-1}
z	height above ground level, m
z_m	measurement height above ground level, m

Greek symbols	Description, unit
δ	isotopic signature in δ-notation, ‰ VPDB
$\overline{\delta}_{\uparrow}$	updraft air average isotopic signature in δ-notation from REA sampling, ‰ VPDB
$\overline{\delta}_{\downarrow}$	downdraft air average isotopic signature in δ-notation from REA sampling, ‰ VPDB
$\delta^{13}C$	^{13}C isotopic signature, here i.e. $^{13}CO_2/^{12}CO_2$ isotope ratio in δ-notation, ‰ VPDB
$\delta^{13}C_R$	^{13}C isotopic signature of the respiration flux excluding the daytime foliar respiration in δ-notation, ‰ VPDB
$\delta^{18}O$	^{18}O isotopic signature, here i.e. $C^{16}O^{18}O/C^{16}O^{16}O$ isotope ratio in δ-notation, ‰ VPDB-CO_2 In this paper $\delta^{18}O$ values are exclusively reported for $^{18}O/^{16}O$ isotope ratios of CO_2 and vs. the VPDB-CO_2 standard and not vs. VSMOV.
$\delta^{18}O_R$	^{18}O isotopic signature of the respiration flux excluding the daytime foliar respiration in δ-notation, ‰ VPDB-CO_2
δ_a	isotopic signature of air at a certain measurement height in δ-notation, ‰ VPDB
δ_A	isotopic signature of the assimilation flux including the daytime foliar respiration flux in δ-notation, ‰ VPDB
δ_B	isotopic signature of the lower boundary layer air in δ-notation, ‰ VPDB
δ_c	isotopic signature of the eddy flux in δ-notation, $\delta_c=\delta_c F_c/F_c$, ‰ VPDB
$\delta_c F_c$	eddy isoflux, i.e. turbulent isotopic flux density excluding the storage change component expressed in δ-notation, µmol m^{-2} s^{-1} ‰ VPDB The definition corresponds to *Bowling et al.* [2003a] and $F_{\text{eddy-isoflux}}$ in *Zobitz, et al.* [2007].
$\delta^{13}C_cF_c$ $=\delta_c F_c$ $^{13}CO_2$	eddy isoflux of $^{13}CO_2$, µmol m^{-2} s^{-1} ‰ VPDB
$\delta^{18}O_cF_c$ $=\delta_c F_c$ $CO^{18}O$	eddy isoflux of $CO^{18}O$, µmol m^{-2} s^{-1} ‰ VPDB-CO_2
δ_N	isotopic signature of the NEE in δ-notation, $\delta_N=F_\delta/F$, ‰ VPDB. The definition corresponds to the common usage of N as subscript to refer to the NEE and *Zhang, et al.* [2006]. Note that δ_N in *Zobitz, et al.* [2007] is used to refer to the isotopic signature of the eddy flux, which here is denoted as δ_c consistent with *Bowling et al.* [2003a].
δ_p	isotopic signature of a product in δ-notation, ‰ VPDB
δ_R	isotopic signature of the respiration flux excluding the daytime foliar respiration flux in δ-notation, ‰ VPDB
δ_S	isotopic signature of the isostorage in δ-notation, ‰ VPDB
$\delta_S F_S$	isostorage, i.e. isotopic storage flux density or storage change below measurement height expressed in δ-notation, µmol m^{-2} s^{-1} ‰ VPDB, the definition corresponds to $F_{\text{isostorage}}$ in *Zobitz, et al.* [2007].
δ_{trop}	isotopic signature of air in the free troposphere in δ-notation, ‰ VPDB
Δ	isotope discrimination , ‰ see general definition of isotope discrimination in *Farquhar et al.* [1989]
$\Delta^{13}C$	^{13}C isotope discrimination, ‰
$\Delta^{18}O$	^{18}O isotope discrimination, ‰
Δ_{canopy}	canopy isotope discrimination, i.e. isotope discrimination of the net assimilation flux including daytime foliar respiration against canopy air, ‰, see definition in *Bowling et al.* [2001] and *Bowling et al.* [2003a]
Δ'_{canopy}	alternative definition of canopy isotope discrimination of the net assimilation flux including daytime foliar respiration against canopy air, ‰, see definition in Equation (18) and Appendix B in this study
Δ_e	ecosystem isotope discrimination of the atmospheric exchange against boundary layer air at measurement height, ‰, compare concept and definition in *Buchmann, et al.* [1998] and *Buchmann and Kaplan* [2001]
Δ_E	net ecosystem isotope discrimination of the net ecosystem exchange (NEE) against canopy air, i.e. the combined effect of isotopic fluxes during photosynthesis and respiration, ‰, see definition in *Lloyd, et al.* [1996]

μ_{CO2}	CO_2 mixing ratio of dry air, µmol mol^{-1}
ρ_a	dry air density, mol m^{-3}
ρ_{CO2}	CO_2 density, µmol m^{-3}
σ	standard deviation
σ_w	standard deviation of vertical wind velocity, m s^{-1}

Subscripts	Description. Subscripts are used with different symbols.
a	air, here referring to air samples from below eddy flux measurement height, i.e. air from directly above canopy, within the canopy or sub-canopy space
A	net assimilation flux including daytime foliar respiration, denoted with A or P in *Bowling et al.* [2003a]
B	lower boundary layer air
c	turbulent eddy flux of a scalar, here CO_2
e	ecosystem, e.g. ecosystem isotope discrimination of the atmospheric exchange at measurement height
E	ecosystem, e.g. net ecosystem isotope discrimination in the NEE
R	respiration flux excluding daytime foliar respiration
N	related to the net ecosystem exchange (NEE), the subscript is not used for NEE and isoflux in order to be consistent with *Bowling et al.* [2003a]
S	storage change (or flux)
δ	isoflux, i.e. the isotopic flux density expressed in δ-notation
$\uparrow$	updraft air of the turbulent exchange at measurement height
$\downarrow$	downdraft air of the turbulent exchange at measurement height

Abbreviations	Description
CET	Central European Time
doy	day of the year
EC	eddy covariance method
HREA	hyperbolic relaxed eddy accumulation method, i.e. REA with a hyperbolic deadband, which is defined by the vertical wind speed and the scalar concentration of a proxy scalar *Bowling, et al.* [1999]
GM	geometric mean (with respect to the linear regression method)
GPP	gross primary production
IFP	isotopic flux partitioning method
IRMS	isotope ratio mass spectrometry
KP	Keeling plot, see *Keeling* [1958]
LAI	leaf area index, m^2 m^{-2}
$Mg(ClO_4)_2$	magnesium perchlorate used as desiccant
MTP	Miller-Tan plot, see *Miller and Tans* [2003]
NEE	net ecosystem exchange
JFD	joint frequency distribution of the vertical wind speed and a scalar
OLS	ordinary least square (with respect to the linear regression method)
PAI	plant area index, m^2 m^{-2}
REA	relaxed eddy accumulation method, see *Businger and Oncley* [1990]
TER	total ecosystem respiration
TDL	tunable diode laser
VPDB	Vienna Pee-Dee Belemnite (=international isotope standard)
vpd	vapor pressure deficit, hPa

8.2. Appendix B: Effect of the alternative definition of Δ'_{canopy} on the isoflux mass balance

The alternative definition of Δ_{canopy} as Δ'_{canopy} according to (19) requires a mathematically less comfortable definition of the isoflux mass balance (11) for the NEE regarding the respiration and net assimilation component isofluxes $\delta_R F_R$ and $\delta_A F_A$. It would require the inclusion of terms of $\delta_a \Delta'_{canopy}$ and higher order terms of Δ'^{2}_{canopy} by an infinite series expansion, which were ignored in the definition of Δ_{canopy} presented by *Bowling et al.* [2001] and *Bowling et al.* [2003a]. In order to minimize the potential systematic error discussed in Section 4.6 and 4.8 but also provide a practical definition, we suggest including the first stage of the series expansion in the mass balance:

$$F_\delta = \delta_R F_R + (\underbrace{\delta_a - \Delta'_{canopy}}_{\text{I}} \underbrace{-\delta_a \Delta'_{canopy}}_{\text{II}} \underbrace{+\Delta'^{2}_{canopy}}_{\text{III}}) F_A . \qquad \text{(A1)}$$

Term I is similar in (11) and (A1), but not exactly identical regarding its numerical value due to the inclusion of Terms II and III in (A1). Depending on the sign and isotopic scale of the isotopic signature δ_a of canopy source air, Term II is normally positive for $\delta^{13}C$ measured on the VPDB scale and negative but small for $\delta^{18}O$ measured on the VPDB-CO_2 scale. Term III is always positive for discrimination against heavier isotopes. The remaining IV term $+\delta_A \Delta'^{2}_{canopy}$, which was not included in (A1), is truly small enough to be ignored without significant error in the context of flux partitioning methods. The inclusion of the Terms II and III is important to prevent systematic underestimation of the canopy isotope discrimination from Δ_{canopy} compared to Δ'_{canopy} (Section 4.6 and Section 4.8). The conversion between both definitions of canopy isotope discrimination is evident from the combination of (18) and (19):

$$\Delta'_{canopy} = \frac{\Delta_{canopy}}{1+\delta_A} . \qquad \text{(A2)}$$

9. Tables

Table 1. Isotopic signature δ_R of the respiration flux and the standard error of the intercept from OLS linear regressions in Keeling plots of sub-canopy air samples.

doy 2003	sampling time CET	$\delta^{13}C_R$ (±std. err.) (‰ VPDB)	$\delta^{18}O_R$ (±std. err.) (‰ VPDB-CO_2)
187	13:54	−30.9 (±0.4)**	−23.6 (±0.8)**
188	night, 00:08	−24.9 (±1.9)	−15.8 (±0.7)
188	08:35	−21.7 (±0.8)*	−20.3 (±1.4)
188	11:36	−20.6 (±0.2)**	−23.0 (±6.1)
188	13:57	−22.4 (±0.6)*	−18.9 (±0.8)*
189	night, 01:50	−26.7 (±0.3)	−13.6 (±1.3)**
189	09:19	−22.7 (±0.5)	−19.0 (±1.5)
189	11:31	−24.1 (±0.7)	−17.5 (±1.0)*
189	14:34	−24.1 (±0.3)**	−14.1 (±1.2)**

Values are marked with * or **, if the difference of the Keeling plot intercept for sub-canopy air samples only and all air samples including upper canopy air samples was larger than the onefold or twofold standard error, respectively.

Table 2. Averaged ecosystem, net ecosystem and canopy isotope discrimination Δ against $^{13}CO_2$ and $CO^{18}O$ (a), flux weighted isotopic signatures δ (b) and isotopic disequilibrium $\mathit{\Delta}$ (c) determined from daytime HREA isotope measurements above a spruce forest at Waldstein/Weidenbrunnen and estimated respiration flux. Averages and standard deviations are obtained from the statistics of the data in Figure 6, 7 and 8 and are subject to the observed diurnal variability.

a) Isotope discrimination	Equation	$\Delta^{13}C$ (±std. dev.) (‰)	$\Delta^{18}O$ (±std. dev.) (‰)
Δ_e	(16)	18.9 (±3.4)	16.1 (±2.7)
Δ_E	(17)	18.1 (±3.2)	15.6 (±2.6)
Δ_{canopy}	(18)	17.3 (±2.5)	17.5 (±2.0)
Δ'_{canopy}	(19)	17.7 (±2.6)	17.8 (±2.1)
b) Isotopic signature	**Equation**	**$\delta^{13}C$ (±std. dev.) (‰ VPDB)**	**$\delta^{18}O$ (±std. dev.) (‰ VPDB-CO_2)**
δ_c	(9)	−26.0 (±3.2)	−15.1 (±2.6)
δ_N	(13)	−25.2 (±3.1)	−14.5 (±2.5)
δ_A	(10)+(11) Section 3.3	−24.9 (±2.5)	−16.6 (±2.0)
daytime δ_R	(3)	−23.8 (±3.4)	−19.5 (±3.3)
nighttime δ_R	(3)	−25.8 (1.8)*	−14.7 (2.3)*
c) Isotopic disequilibrium	**Equation**	**$\mathit{\Delta}^{13}C$ (±std. dev.) (‰ VPDB)**	**$\mathit{\Delta}^{18}O$ (±std. dev.) (‰ VPDB-CO_2)**
doy 188** $\mathit{\Delta}$	(12)	−3.7 (±3.0)	4.3 (±0.8)
doy 189 $\mathit{\Delta}$	(12)	0.1 (±1.2)	0.3 (1.6)*

* Variation is indicated by the absolute difference of two measurements.

** Except last sample from 14:57 CET.

10. Figures and Figure captions

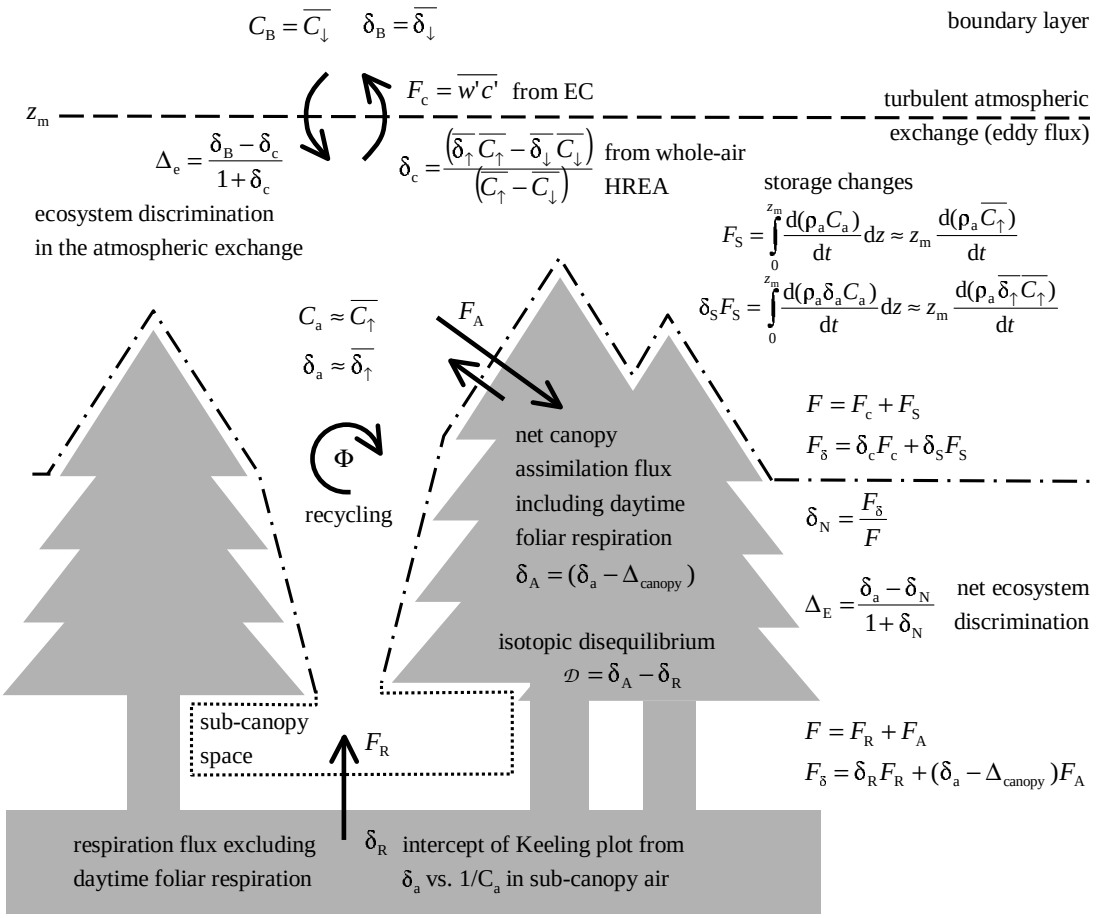

Figure 1. Carbon dioxide and isotope mass balances in a forest ecosystem. Arrows indicate the one-way flux components. The dashed line indicates the plane at EC measurement height z_m above the ecosystem. The dash-dotted and dotted line represents the ecosystem/atmosphere interface for which the NEE $F=F_c+F_S$ and the isoflux F_δ are determined. Additional terms for horizontal and vertical advection are here neglected. The mass balance equations and the definition of parameters of the isotopic exchange are described in detail in Section 2 and 3. The nomenclature of symbols is summarized in Appendix A.

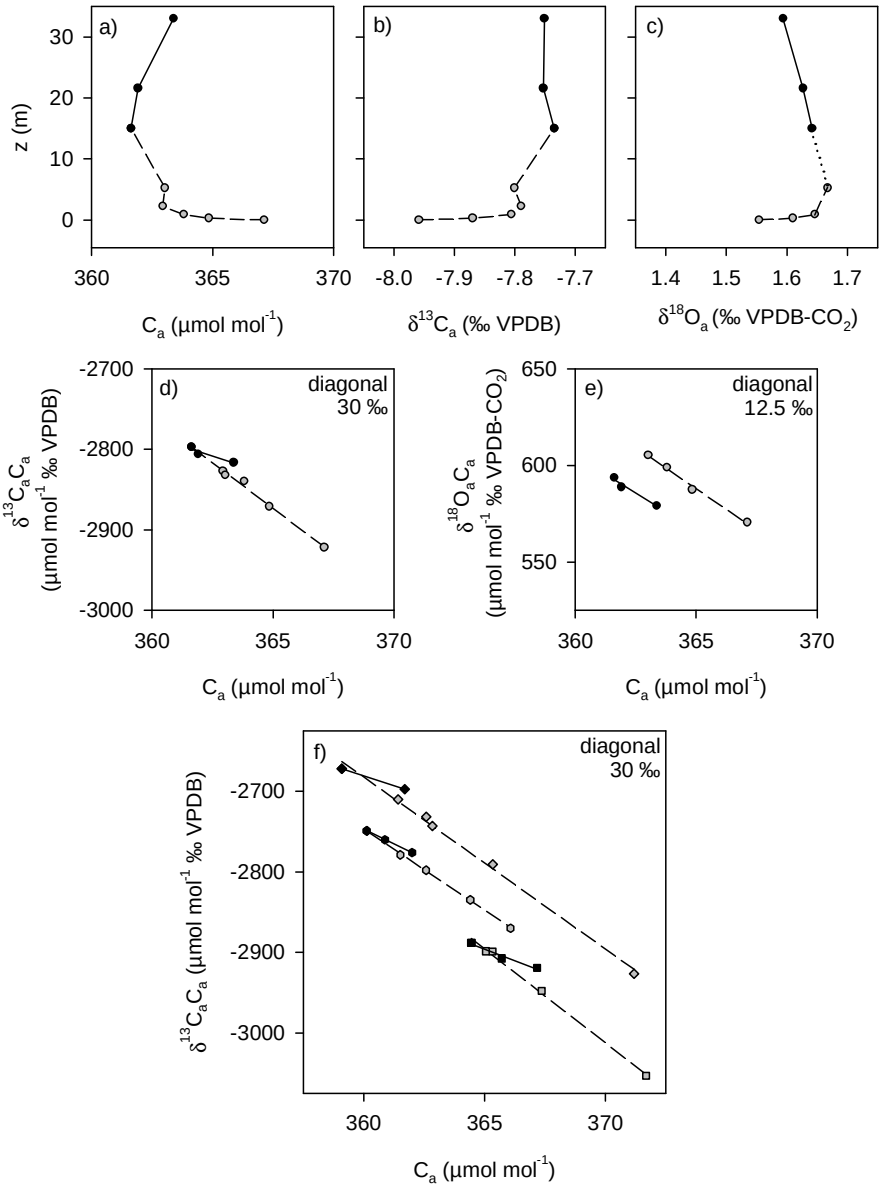

Figure 2. Vertical profiles of bulk CO_2 (a), $\delta^{13}C$ (b) and $\delta^{18}O$ (c) and the corresponding Miller-Tan plots with OLS linear regression lines for $\delta^{13}C$ (d) and $\delta^{18}O$ (e) from air samples collected on day of the year (doy) 175 at 12:50 CET. Black circles represent air samples from the upper canopy up to 33 m measurement height connected by solid lines. Grey circles represent samples from the sub-canopy space connected by dashed lines. Figure 2(f) shows corresponding Miller-Tan plots and regression lines for $\delta^{13}C$ from air samples collected at doy 188 at 13:58 (diamonds), doy 174 at 11:26 (hexagons) and doy 204 at 12:56 (squares), top to bottom. Note that in Figure 2(e) for $\delta^{18}O$ isotopic mixing lines the diagonal represents a smaller isotopic signature as specified in the plots.

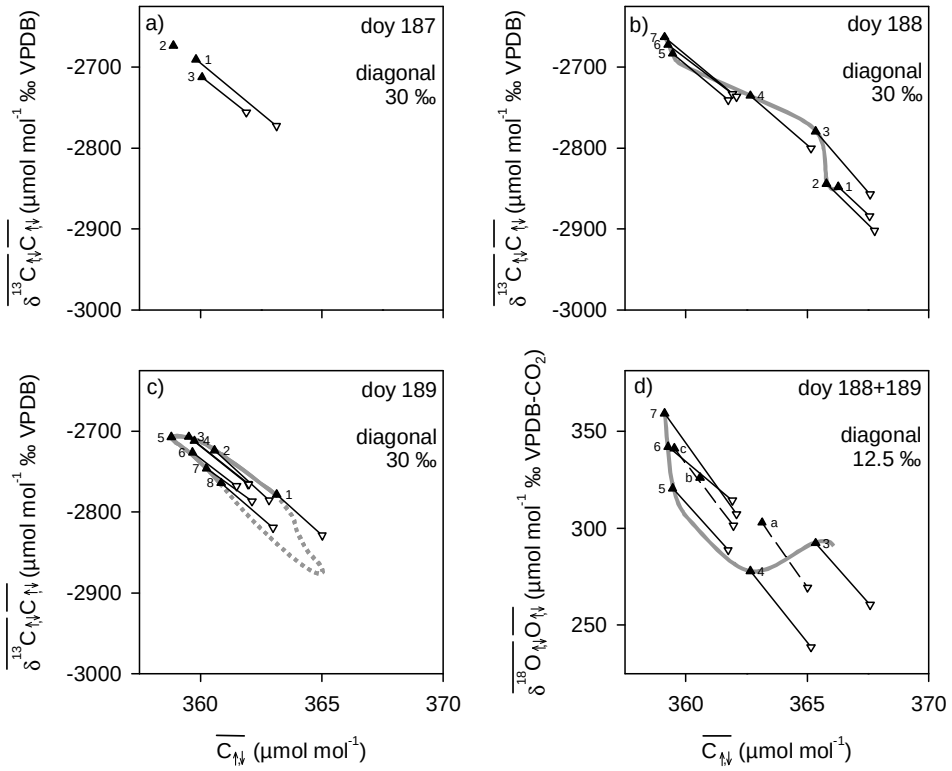

Figure 3. Miller-Tan plots displaying the slopes (black lines) resulting from the relation of updraft (black triangles) and downdraft (white triangles) whole-air samples collected by HREA with application of a hyperbolic deadband (H_h=1.0). The slope of the lines connecting the updraft and downdraft samples equals the flux weighted isotopic signature δ_c of atmospheric turbulent exchange measured above the canopy. Numbers on updraft values indicate the sequence of samples in the diurnal cycle. Samples denoted with letters a, b and c in Figure 3(d) represent morning samples 1, 2 and 3 from doy 189 connected with dashed lines. Sample 2 of doy 187, sample 5 of doy 189 and regarding $\delta^{18}O$ sample b of doy 189 lack the downdraft sample. The gray solid lines indicate the temporal change of the bulk CO_2 mixing ratio and the isotope content of updraft air samples within the diurnal cycle. The gray dotted line is hypothesized for the development of updraft air samples during nighttime in a situation with continued vertical mixing and based on the isotopic signature $\delta^{13}C_R$ of the nighttime respiration flux of –26.7‰ VPDB. Note that in Figure 3(d) for $\delta^{18}O$ isotopic mixing lines the diagonal represents a smaller isotopic signature as specified in the plots.

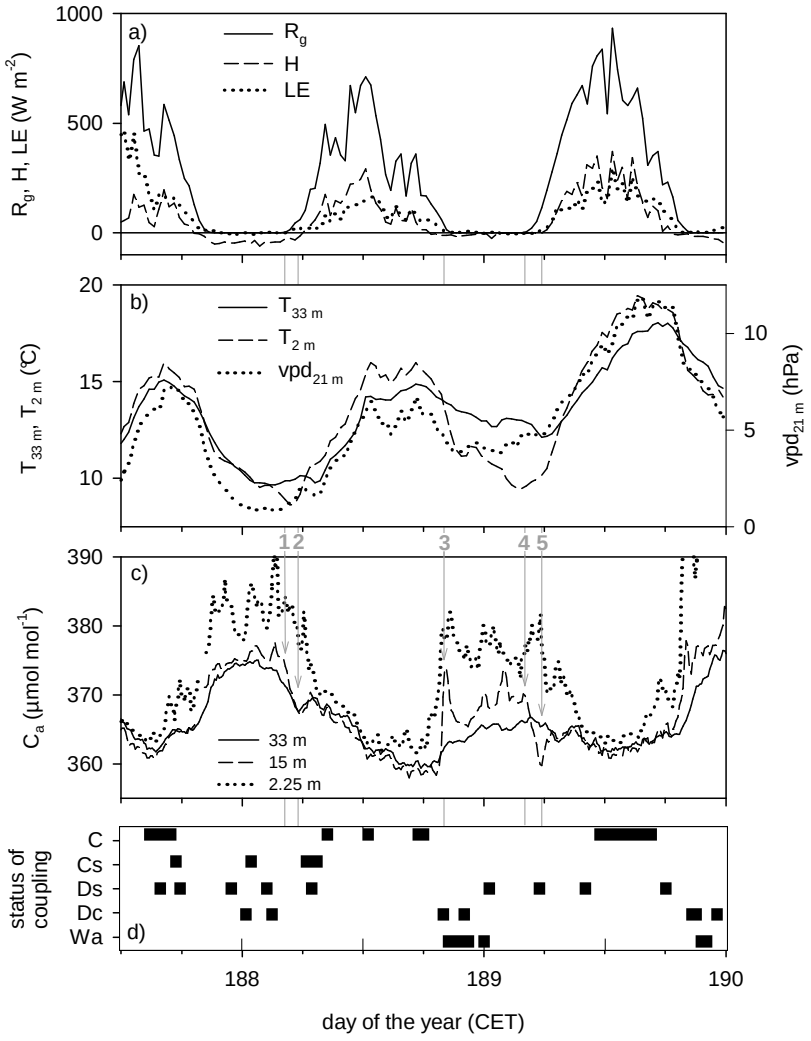

Figure 4. Time series of (a) global radiation (R_g), sensible and latent heat fluxes (H, LE), (b) above canopy and sub-canopy air temperatures ($T_{33\,m}$, $T_{2\,m}$) and vapor pressure deficit ($vpd_{21\,m}$) measured at canopy top, (c) carbon dioxide mixing ratios (C_a) above (33 m), within (15 m) and below (2.25 m) the canopy. Figure 4(d) shows the status of coupling between the atmosphere and different layers below 33 m measurement height derived from turbulence measurements within and above the canopy with following nomenclature [*Thomas and Foken*, 2007b]: 'C' coupling of the entire air column below measurement height, 'Cs' partially decoupled sub-canopy space, 'Ds' decoupled sub-canopy, 'Dc' decoupled canopy and 'Wa' for decoupled situations with wavelike motions of air layers. Gray numbers '1' to '5' mark significant changes in the CO_2 exchange as indicated from the CO_2 concentration profile and pointed out by gray arrows and lines.

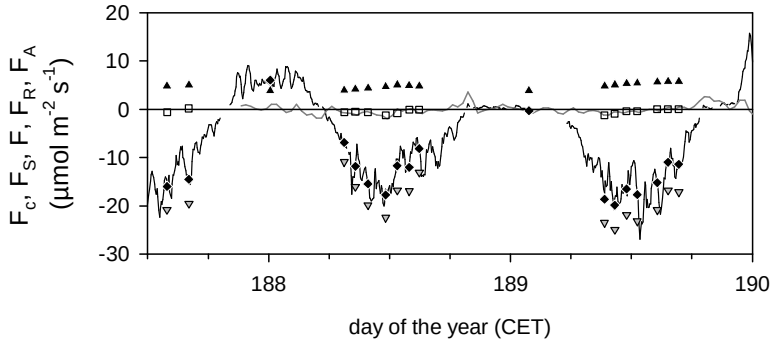

Figure 5. CO_2 net ecosystem exchange (NEE, *F*, black diamonds) and individual flux components. NEE is determined from the sum of the CO_2 eddy flux (F_c, black line) and the storage flux determined from updraft air CO_2 mixing ratios (F_S, unfilled squares). The latter is comparable to the storage flux determined from the vertical profile of continuous CO_2 measurements (gray line). The net assimilation flux (F_A, gray triangles) results from the difference of NEE and the estimated respiration flux (F_R, black triangles).

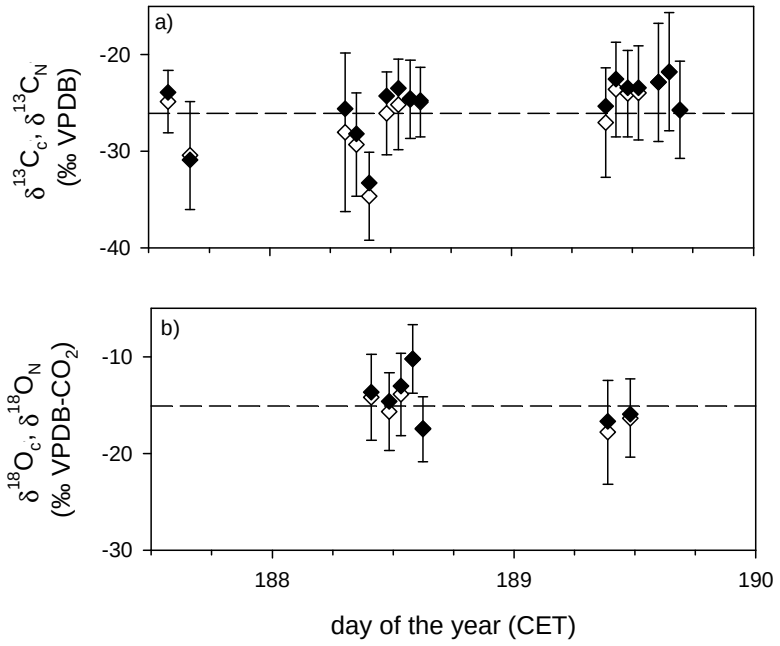

Figure 6. Flux weighted $\delta^{13}C$ (a) and $\delta^{18}O$ (b) isotopic signatures of the atmospheric turbulent exchange (δ_c, white diamonds) 14 m above the canopy of a spruce forest and of net ecosystem exchange (δ_N, black diamonds). Error bars on δ_c values indicate the estimated standard deviation for a single measurement. Dashed lines indicate the average of the isotopic signature of the atmospheric turbulent exchange, which was –26.0‰ VPDB for $\delta^{13}C_c$ and –15.1‰ VPDB-CO_2 for $\delta^{18}O_c$.

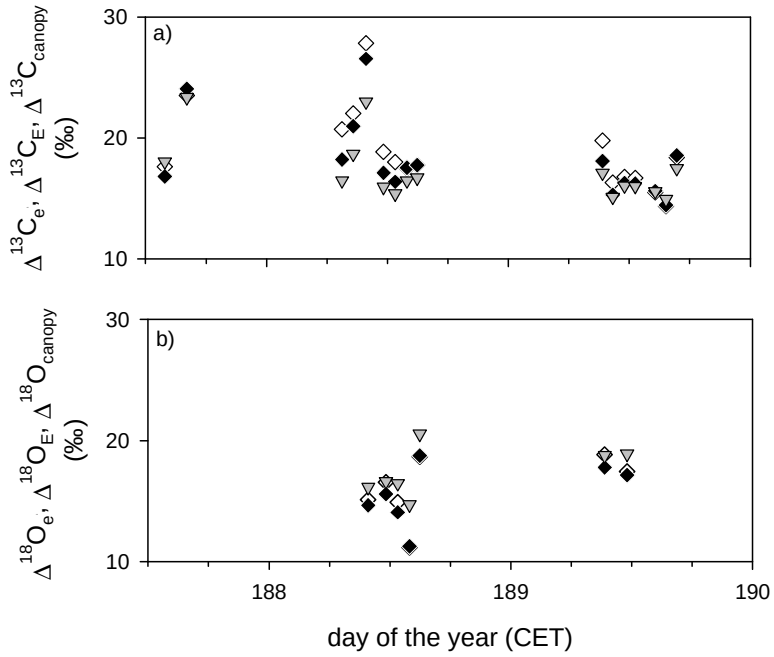

Figure 7. Synopsis of parameters for discrimination against $^{13}CO_2$ (a) and $CO^{18}O$ (b) isotopes in the atmospheric turbulent exchange, net ecosystem exchange and net assimilation flux, i.e. respectively ecosystem discrimination (Δ_e, white diamonds), net ecosystem discrimination (Δ_E, black diamonds) and canopy discrimination (Δ_{canopy}, gray triangles) estimated from modeling of the respiration flux F_R.

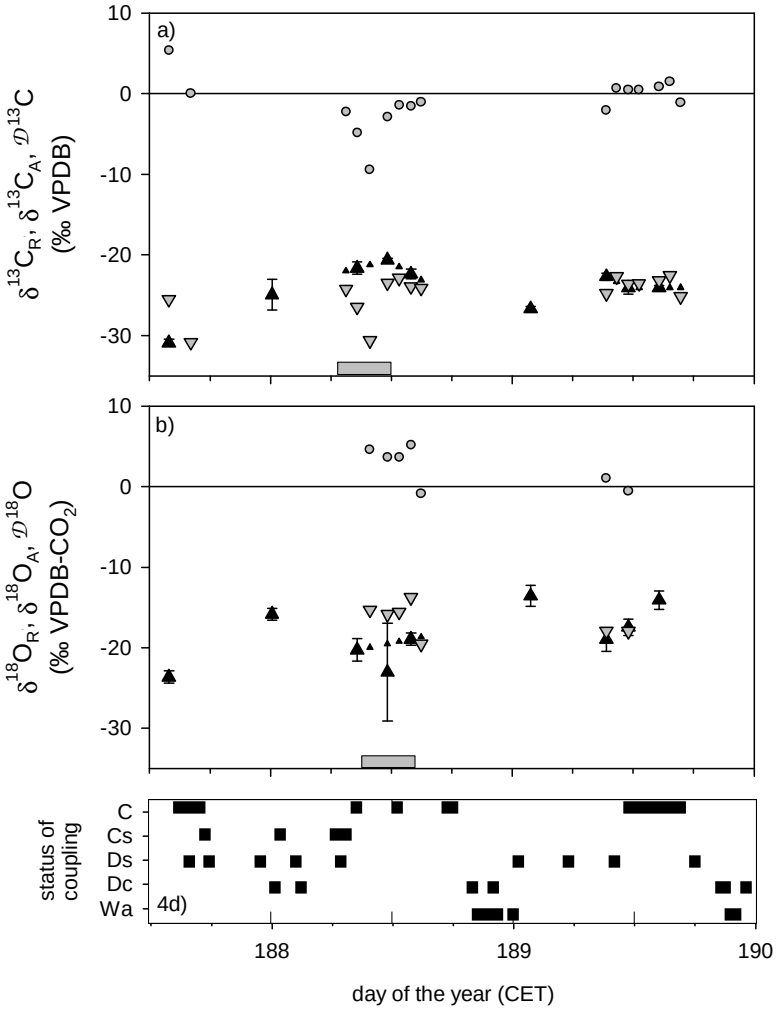

Figure 8. Isotopic disequilibrium $\mathcal{D}$ (gray circles) between the isotopic $\delta^{13}C$ (a) and $\delta^{18}O$ (b) signatures in the daytime respiration flux (δ_R, upward-black triangles) and net assimilation flux (δ_A, downward-gray triangles). The periods during which prevailing isotopic disequilibrium $\mathcal{D}$ was observed in the ecosystem exchange are marked with a gray bar. The error bars on δ_R values indicate the standard error of the intercept from an OLS linear regression in a Keeling plot of sub-canopy air samples. The small-black triangles indicate the estimated values used for δ_R for the evaluation of HREA measurements at times, in which δ_R was not measured or in one case subject to large uncertainty. For comparison, the status of coupling as presented in Figure 4d is displayed at the bottom.

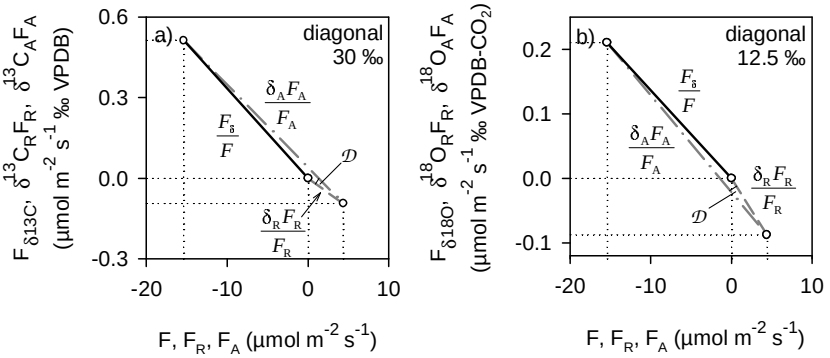

Figure 9. Geometrical interpretation of flux weighted isotopic signatures $\delta^{13}C$ (a) and $\delta^{18}O$ (b) as determined for doy 188 at 9:51 CET and flux partitioning based on the estimated respiration flux F_R. In this display, the span of the lines represents the bulk CO_2 flux density on the horizontal axis and the $\delta^{13}C$ or $\delta^{18}O$ isoflux density on the vertical axis for the net ecosystem fluxes (F_δ/F, black-solid line), the respiration fluxes ($\delta_R F_R/F_R$, gray-dashed line) and the net assimilation fluxes ($\delta_A F_A/F_A$, gray-dashed-dotted line). The slope of the lines equals the flux weighted isotopic signatures (δ_N, δ_R and δ_A) comparable to δ_c and the geometrical interpretation of HREA updraft and downdraft samples in Miller-Tan plots in Figure 3. $\mathcal{D}$ denotes the isotopic disequilibrium as the difference in slope, i.e. the angle, between δ_A and δ_R.

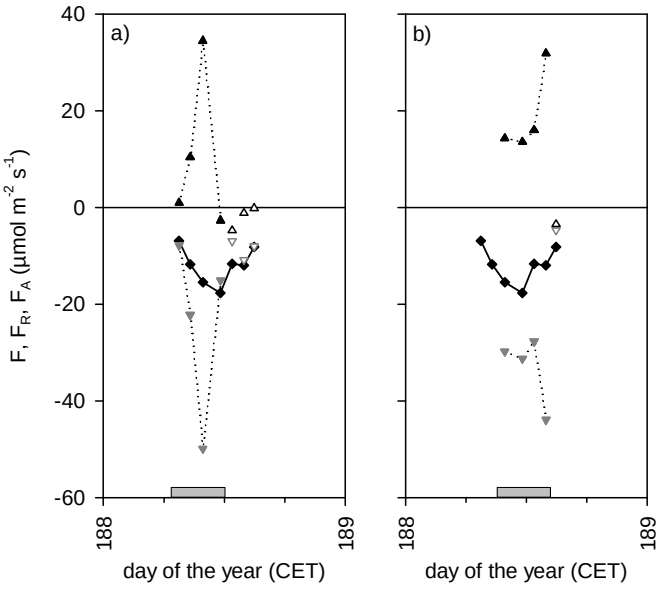

Figure 10. Isotopic flux partitioning of the NEE F (black diamonds connected by solid line) into the assimilation flux F_A (gray triangles) and respiration flux (black triangles) based on $\delta^{13}C$ (a) and $\delta^{18}O$ (b) isotopic signatures measured on doy 188 at Waldstein/Weidenbrunnen. The isotopic signature δ_A of the assimilation flux was determined based on the assumption of a constant canopy isotope discrimination Δ'_{canopy}=17.8‰. The isotopic signature δ_R of the respiration flux was determined from Keeling plot intercepts of sub-canopy air samples. Estimated values displayed in Figure 8 were used for missing δ_R values. The NEE F and isofluxes F_δ were determined from EC and HREA measurements of the CO_2 eddy flux F_c and the eddy isoflux $\delta_c F_c$, respectively, and according to (10) and (11) by adding the storage flux F_S and the isostorage $\delta_S F_S$, respectively. The gray bars and dotted lines mark the periods with prevailing isotopic disequilibrium $\mathcal{D}$. During periods with a lack of isotopic disequilibrium, the results for the component fluxes F_A and F_R are displayed as unfilled symbols.

Erklärung

Hiermit erkläre ich, dass ich die Arbeit selbstständig verfasst und keine anderen als die angegebenen Hilfsmittel verwendet habe.

Weiterhin erkläre ich, dass ich nicht anderweitig mit oder ohne Erfolg versucht habe, eine Dissertation einzureichen oder mich einer Doktorprüfung zu unterziehen.

Düsseldorf, den

Johannes Ruppert